Cape Peninsula
University of Technology

MODELING AND CONTROLLER DESIGN OF A FLOTATION COLUMN

by

NOMZAMO TSHEMESE-MVANDABA

Thesis submitted in fulfilment of the requirements for the degree

Doctor of Engineering: Electrical Engineering,

in the Faculty of Engineering and the Built Environment

at the Cape Peninsula University of Technology

Supervisor: Prof. R. Tzoneva

Co-supervisor: Dr. M.E.S Mnguni

Bellville campus

July 2022

DECLARATION

I, Nomzamo Tshemese-Mvandaba, declare that the contents of this dissertation/thesis represent my own unaided work, and that the dissertation/thesis has not previously been submitted for academic examination towards any qualification. Furthermore, it represents my own opinions and not necessarily those of the Cape Peninsula University of Technology.

July 2022

Signed **Date**

ABSTRACT

An improved technique for the design of decentralised dynamic decoupled Proportional Integral (PI) controllers to control numerous variables of column flotation is developed and implemented in this thesis. This thesis was motivated by challenges when working with Multiple Inputs Multiple Outputs (MIMO) systems that are not controllable by conventional linear feedback controllers. Conventional feedback control design consists of various drawbacks, especially with the introduction of complex industrial processes. The introduction of nonlinear controller design, decentralization, and decoupling of a system overcome these drawbacks. The reason these advanced controllers are needed is because of the complex interaction that is required by the system. Therefore, designing controllers or control systems that mitigate stability is important.

In this thesis different innovative control design methods and algorithms which are based on decentralized coupled and decentralized dynamic decoupled systems are developed. This thesis first focused on the mathematical modeling of the column flotation system. The column flotation system model and dynamic characteristics were analysed to achieve a good understanding of the system's behaviour. The system's dynamic behavior is assessed based on multiple changes in the input circumstances. The analysis of the open-loop and closed-loop systems under study was performed based on the Matlab/Simulink simulation environment. The Column Flotation process was modelled by a 2x2 and 3x3 multivariable system and simulated in Matlab/Simulink. Through several evaluations, it was noted that the most critical constraints were the maximum value of wash water (Q_w), the minimum of the froth layer height, and the minimum of the gas holdup.

The new improved decentralized controller was thoughtfully developed using single-loop parings. Relative Gain Array (RGA) method was deployed to reduce the effects of process interactions when designing the decentralized controller. The design technique adopted was using Internal Model Controller-based (IMC) PID feedback control for set-point tracking. Set-point tracking control was achieved, and the effects of various disturbances on the behaviour of the designed closed-loop systems were investigated and analysed. The developed strategies were then deployed by a special transformation process from Simulink to a Beckhoff PLC via the functional block programming language TwinCAT 3.1. Beckhoff CX5020 PLC together with TwinCAT 3 software was used for the implementation of the decentralized coupled and decentralized dynamic decoupled model-based controllers. The technique used and implemented deployed a Programmable Logic Controller (PLC) as it allows the model transformation from Matlab/Simulink to be implemented directly for industrial application purposes.

The effectiveness of set-point tracking control and disturbance rejection was assessed in this thesis. The desired variables were achieved in run-time mode using the TwinCAT 3 functional blocks module, which was then downloaded to the Beckhoff CX5020 PLC for real-time implementation. One of the reasons for using the Beckhoff PLC CX5020 as an implementation environment was motivated by the reliability of this platform and Beckhoff CX5020 that is built according to new industry standards and allowing transformation which makes it more advantageous to use more than any other Programmable Logic Controllers.

ACKNOWLEDGEMENTS

I wish to thank:

- Professor Raynitchka Tzoneva my supervisor, and mentor for her guidance, advice, and contribution throughout the thesis, I am so thankful to Prof.
- Dr. Mkhululi Elvis Siyanda Mnguni (my co-supervisor) for his contribution throughout the thesis write-up and unconditional support all these years.
- My colleagues at RTDS and CSAEMS for paying attention to the problems faced along the way, their advice, and their support.
- GOD, above everything for the strength you have granted me with. You have provided me with more than I could ever have imagined, without you Lord I am nothing.

DEDICATION

I dedicate this thesis to my husband **Mfuneko Mvandaba**, my three Children **Elethu Mvandaba**, **Snelitha Mvandaba**, and **Isiphile One Mvandaba**. Further dedication goes to my two mothers **Emelina Tshemese** and **Nowages Mvandaba**.

A special dedication goes to my mentor **Professor Raynitchka Tzoneva**, I am so thankful that I knew her. She has pushed and guided me in the right direction in life. For that, I will always be grateful. May your dear soul rest in peace **Prof!**

TABLE OF CONTENTS

LIST OF FIGURES

LIST OF TABLES

GLOSSARY

List of Abbreviations

AC	Adaptive Control
ADP	Adaptive Dynamic Programming
ANN	Artificial Neural Network
BSD	Bubble Size Distribution
ECC	Equivalent Conventional Controller
CPU	Central Processing Unit
FL	Fuzzy Logic
FPGA	Field-Programmable Gate Array
DAF	Dissolved Air Flotation
DCS	Distributed Control Systems
DNA	Direct Nyquist Array
GCS	Distributed Control System
HIL	Hardware In Loop
IEC	International Electro-technical Commission
IMC	Internal Model Controller-based
MPC	Model Predictive Control
MHE	Moving Horizon Estimator
MA	Modifier-Adaptation
MIMO	Multiple Input Multiple Output
NN	Neural Network
PI	Proportional Integral
PID	Proportional-Integral-Derivative
PLC	Programmable Logic Controllers
PCA	Principal Component Analysis
PDE	Partial Differential Equations
PLS	Partial Least Squares
RAM	Random Access Memory
ROM	Read-Only Memory (ROM),
RTO	Real-Time Optimization
RGA	Relative Gain Array
RNGA	Relative Normalised Gain Array
SISO	Single Input Single Output
SCADA	Supervisory Control and Data Acquisition
IMC	Internal Model Control
IO	Input/Output

NI	Niederlinski index
TcCOM	TwinCAT Component Object Model
TITO	Two-Input Two-Output
TwinCAT	The Windows Control Automation
XAE	Extended Automation Engineering
XAR	Extended Automation Runtime
SiL	Software-in-the-loop
HiL	Hardware in the Loop

Mathematical Notations

h	froth layer height
Q_B	bias
Q_F	feed flow
Q_T	non-floated
ρ_{fz}	froth layer density
ρ_{sl}	pulp density
ε_{gcz}	collection zone
k_{sl}	pulp conductivity
k_{sgl}	pulp-gas mixture conductivity
λ	Lambda
U_g	air valve
U_W	wash water valve
U_T	non-floated fraction
ζ	damping factor
ω_n	un-damped natural frequency

CHAPTER ONE:
INTRODUCTION

1.1 Introduction

Flotation is derived from the word float. It can be interpreted as a separation of material from other materials in a liquid or a solution based on differences in surface properties of the material to be separated. As an example, the gold flotation process aims to separate and produce a metal concentrate. In general, the column flotation process is a multivariable process with the major control goal of ensuring that the metallurgical performance conforms to the process operation and that the concentrate is classified according to the content and recovery of valuable minerals, (Yahui et al., 2018), (Yang & Fan, 2012). Mineral processing, waste-water treatment, and paper recycling all use the flotation process. This was first utilized in the mining industry, and it was considered one of the most important enabling technologies of the twentieth century. Column flotation is widely used in the concentration of low-grade ores. Its concentrate on the last product of a complex circuit, and hence control of the metallurgical performance has a direct impact on the plant performance (Núñez et al., 2010).

Over the last two decades, the use of pneumatic flotation columns in the metal, non-metal, and coal ore processing industries has spread worldwide. The column is much greater than traditional mechanical cells in the cleaning process due to its special foam operation that improves product quality. When it comes to the column flotation process, the major control objective is to improve metallurgical performance so that the column operation meets the required reference level for the intended enhanced stream extraction and location (Persechini et al., 2000). According to (Liuyuan et al., 2011), the first foundation of the flotation column was in the 1960s, the emphasis was on high productivity, high enrichment rate, low operational cost, and many other desirable characteristics. The process of flotation concentrate is widely used in the separation of coal, lead, zinc, iron, antimony, copper, molybdenum, and other metals (Zahiri et al., 2021). The detection and control of liquid level have a significant impact on the flotation column process and thus directly affects the quality of the product. Therefore, accurate detection of the liquid level plays a key role in the regulation of the input and output of the flotation column, and improves, its efficiency and product quality.

The main steps performed before the column flotation process or froth flotation process are based on grinding rock minerals, grinding ore (reduced to a smaller size) and releasing the metal for the separation process, and the preparation of the right size for the next process. The column flotation or froth flotation process consists of reagent/material flotation, mineral concentrates made using chemical modifiers,

followed by air bubbling of vigorous and agitated ore slurries to produce a rich foam concentrate. Flotation column simulation and control have progressively become a significant field of investigation/ research (Bouchard et al., 2009). This method was first used commercially many years ago, but research into the control of hydrodynamic parameters of the process and the sensors for measuring them is not yet mature (Calisaya et al., 2012).

1.2 Awareness of the problem

Froth flotation columns are mainly used in various sulfide mineral concentrators during the purifying or cleaning stage. These facilities (flotation columns) are long vertical tanks that continuously supply pulp composed of fine solid particles contained in valuable minerals and gangue (valueless material in which ore is found) solid particles. Column flotation concentration is achieved by conditioning the pulp with appropriate chemical reagents, blowing air continuously, and washing the concentrate with freshwater (Bergh & Yianatos, 2003). Figure 1.1 is used to represent a general simplified scheme of a flotation column.

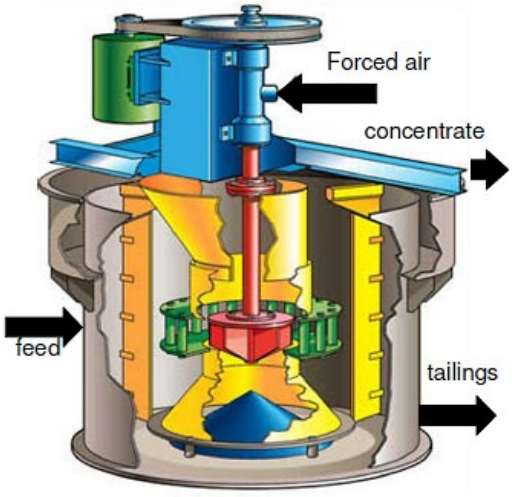

Figure 1.1: **Basic Schematic of a Flotation Cell (Blahous & Marx, 2009)**

Column flotation works on the same principle as a mechanical flotation device. Mineral separation is done with a moving (restless) or aerated water-mineral slurry. This slurry makes the surface of the selected mineral hydrophobic (water-repellent) by conditioning it with the selected reagent. However, in column flotation, there is no mechanical mechanism that causes agitation, and the separation is done in a high aspect ratio vessel. A sparer pumps air into the slurry, causing a counter-current flow of air bubbles. The research shows that proper control of the flotation column suggests many characteristics including:

- Improvement of metallurgical performance
- Less energy consumption
- Concentrated footprint
- Reduce capital requirement

The column achieves well-organized separation and high upgrading mainly by two methods. Primarily, by using wash water, entrained minerals can be washed from the froth before being passed through to the concentrate. Second, high froth levels in columns encourage draining and decrease entrainment induced by high gas rates. The manner gas bubbles are created differs between column cells as well. Air is either injected into the cell directly by using the internal spargers or is carried into the cell through a high-velocity recirculated stream of tailings. The air intake can then be adjusted based on the concentration grade or throughput. When it comes to dynamic systems that need to be controlled, the motivation for using nonlinear control is based on its characteristics. Sustainable outcomes to the problems of the flotation process require the development of appropriate information systems intended for control and supervision of the nonlinear process to be controlled.

1.3 Problem statement

Flotation columns are an important area of research for the metallurgical industry, and according to (Bouchard et al., 2009), the introduction of flotation columns in mineral processing plants caught the attention of many researchers in the last two decades. Flotation systems are nonlinear systems because the process interactions make a change in a particular manipulated variable to affect more than one controlled variable. Control strategies aimed at controlling multiple variables at the same time need to take into account the interactions between controlled and manipulated variables. Hence, this area of research is always interesting for many process control engineers.

Selecting the best combination of control and manipulated variables is the decisive factor for the success of this type of process control. The complex interactions that exist between the controlled and manipulated variables in a column flotation process require research into the development and implementation of a unique real-time optimization control strategy that accounts for the multiple-input, multiple-output (MIMO) nature of the system (Persechini et al., 2004). These problems can be divided and addressed using the following sub-problems.

1.3.1 Sub-problem 1 based on design

A comparative analysis of the existing components of the flotation process and the methods for recognition of this process operational control using linear and nonlinear control techniques are reviewed. The following were carried out:

a) Preparation of the mathematical model classified for the MIMO system.
b) Development of techniques to be used for the design of decentralized controllers' methods appropriate to the MIMO systems.
c) Development of methods to be used in the design of controllers using dynamic decoupling techniques that apply to the MIMO plant model.
d) Design of controllers, in addition to the dynamic decoupling, and decentralized for closed-loop system performance.
e) Development of the model to be used in Matlab/Simulink software and simulation of the MIMO closed-loop systems.

1.3.2 Sub-problem 2 based on the implementation

The research problem was implemented through the following steps:

a) Simulations are performed in the Matlab/Simulink environment for the designed closed-loop decentralized control system.
b) The simulations of the developed closed-loop decoupled control system are executed in Matlab/Simulink environment.
c) Transform the developed control system model from Matlab/Simulink environment to the Programmable Logic Controllers (PLC) hardware, using the standard-based TwinCAT 3 simulation software.
d) Real-time implementation of the closed-loop systems is executed using the TwinCAT PLC environment, this is done to demonstrate the usefulness of the transformations.

1.4 Aim and Objectives

1.4.1 Aim

This investigation aims to design unique controllers and implement them in the function block-based Programmable Logic Controller (PLC) environment to achieve real-time implementation of the closed-loop MIMO industrial systems.

1.4.2 Objectives:

1. To develop open-loop systems based on flotation column models.
2. To design a decentralized control, develop a closed-loop system model in Matlab/Simulink software environment and simulate it to evaluate the closed-loop system for disturbance rejection and set-point tracking control.
3. To design the decoupling controller and simulate it for set-point tracking control and disturbance rejection using Matlab/Simulink.
4. To perform a comparative analysis of the simulated results obtained from the decentralized control technique and dynamic decoupling controller design technique (Simulated in points 2 and 3).
5. Transform the results obtained in point 3 to TwinCAT 3 environment for real-time simulation purposes.
6. Program the PLC and implement closed hardware in the loop scheme.

1.5 Hypothesis

Due to many industrial processes with nonlinearity, it has been of great interest to many researchers to perform studies based on advising linear controllers, linearizing or nonlinear controller design. The development and implementation of controllers that are suitable for processes with nonlinearities need to accommodate the following in their design:

- Simulink and TwinCAT 3 software integration enables real-time implementation of linear and nonlinear controllers for MIMO processes.
- The application of PC and PLC technologies (or HIL) can produce better real-time results of the proposed process in comparison with the manual or classical control methods.

1.6 Delimitation of the Research

The proposed investigation project focuses on the design strategies and implementation of different control techniques using the Matlab/Simulink platform. It considers a Column flotation (MIMO plant) plant model with two to three controlled variables. The scope of the project is based on the decentralized control and dynamic decoupling control design that is to be implemented in Matlab/Simulink environment and the TwinCAT 3.1 environment. The use of the simulations is to validate the stability of the new proposed control systems. A comparative study is analysed and a recommendation is drawn. The implementation in Matlab/Simulink was transformed into TwinCAT 3.1 platform to accommodate real-time control implementation.

Real-time control implementation is also carried out by the transformation of the established and Matlab/Simulink closed-loop schemes into the TwinCAT 3.1 Beckhoff Automation software and Beckhoff CX-5020 Programmable Logic Controller (PLC).

1.7 Research Motivation

Control strategies applied to the column flotation process are presented in different journals. (Bergh & Yianatos, 1993)(Finch & Dobby, 1990) presented two simple control strategies for stabilizing the process. In one of those schemes, the froth layer height is controlled by manipulating the non-floated flow rate, and the wash water is manually controlled. The research study was motivated by challenges when working with Multiple Input and Multiple Output (MIMO) systems that are not controllable by conventional linear feedback controllers. Conventional feedback control design consists of various drawbacks, especially with the introduction of complex industrial processes. The introduction of nonlinear controller design, decentralization, and decoupling of a system overcome these drawbacks.

1.8 Contributions of the Research and Deliverables

The contribution of this thesis's deliverables is based on advancing the most conventional controller called Proportional-Integral-Derivative (PID), which has been widely used in a variety of processes. PID has been regarded as a powerful strategy for regulatory control, but if the process is interrupted and optimal operating conditions change continuously, PID performance will suffer. This issue arises from the fact that the PID does not obviously use constraints, making it difficult to adapt to changes.
Another drawback of PID controllers is their high sensitivity to interactions between process variables. In processes with very complex dynamics, such as column flotation, PIDs are not sufficient to keep the plant in optimal conditions without improvement. Hence, addressing these problems by complementing the PIDs with advanced control techniques such as decentralization and decoupling design methods. This study is implemented using a Programmable Logic Controller (PLC), this implementation of the designed technique can also be applied in industry.

1.9 Chapters Breakdown

1. Introduction
2. Literature review and development of the flotation column models.
3. Control based Theory

4. Matlab/Simulink software development and simulation of the open-loop system.
5. Control design based on the decentralization, Matlab/Simulink software development, and simulation of the closed-loop system intended for tracking the set-point and disturbance rejection.
6. Control design based on dynamic decoupling, Matlab/Simulink software development, and simulation of the closed-loop system for the desired set-point tracking and disturbance rejection. Complete a comparative analysis of the simulated results achieved in points 5 and 6.
7. Real-time implementation of the closed-loop with different control conditions, using TwinCAT 3 software and PLC (to prove the effectiveness of TwinCAT 3 model transformation).
8. Conclusion

1.10 Conclusion

There are several strategies for specific control of the bias and froth layer height, and improper combinations of control and operational variables reduce control system performance and reduce the system's stability margins. It is important to use analytical tools to measure the interactions and select the best combination of control and manipulated variables. It has been noted that the predictable values in the air holdup vary from experiment to experiment, more investigation needs to be done to determine different factors affecting air holdup in the cleaning zone. The proposed system model was evaluated for stability, set-point tracking, and accuracy.

CHAPTER TWO:
LITERATURE REVIEW

2.1 Introduction

In mineral processing systems many researchers have been interested in the use of flotation columns throughout the last two decades. For the metallurgical sector, flotation columns are a significant topic of research. The control objective of the flotation column is to ensure that the metallurgical performance, expressed in terms of the content and recovery of valuable minerals in the concentrate, is consistent and agrees with the process operation (Persechini et al., 2004). It is confirmed historically that column flotation is a commonly used separation method in the mineral industry such as the separation of coal, zinc, copper, lead, iron, molybdenum, antimony, and many more metals (Zahiri et al., 2021; Bürger et al., 2020). Column flotation was first founded in the 1960s for its high productivity, high improvement rate, low-cost operation, and many advantages. This process has now become the focus of study and application for many researchers (Li et al., 2019).

Generally, an alteration in a particular manipulated variable disturbs more than one controlled variable, because of the process's internal interactions. A control technique that aims to regulate many variables at once must consider the interactions between the controlled and manipulated variables. Hence, this area of research is always interesting for many control engineers, as conventional controllers cannot take into account the internal interconnections between the variables. The ideal combination of regulated and modified variables is a deciding factor in the success of this type of process control. The complex interactions that exist between the controlled and manipulated variables in a column flotation process require research into the development and implementation of a unique real-time optimization control strategy that accounts for the Multiple-Input, Multiple-Output (MIMO) nature of the system (Liuyuan et al., 2011).

In mineral concentrators, flotation columns have turned out to be a standard piece of the scheme, particularly for cleaning operations. The literature review based on the layout and automatic control of flotation columns is presented and discussed in this chapter. It also looks at how new academic advancements in these fields can improve current industry practices. Later, the development and controller design of a flotation column system are given special attention.

2.2 Literature review

This research study was motivated by the linear and nonlinear characteristics to be controlled in a dynamic system. Process automation has a significant role in the process industry because it increases the productivity of processes under operation. Controlling is a strategy used to stabilize a system. Nonlinear dynamics and strong interactions between variables are some of the main problems associated with stabilising controlled flotation column systems. These characteristics reduce the effectiveness of conventional Proportional-Integral (PI) or Proportional-Integral-Derivative (PID) control without a manager (any advanced method as an addition) to coordinate the control loops. With the aim of controller design, it is important to obtain accurate measurements of the process's natural performance, (Vieira et al., 2007). Therefore, understanding the basic system's operation is the key to successful control of any process. The following keywords were mostly used for information collection for the current study: different linear and nonlinear dynamical systems, flotation, columns, different control, and design methods.

2.2.1 Process Control theory

The studies in column flotation have shown an extraordinary potential use of liner experiential models. But those model approaches can have limitations such as conditions identified in the calibration data (operating points, ore properties, etc), and some may require regular recalibration. (Ogunnaike & Ray, 1994), recommends the importance of being familiar with the important features of control system implementation, that is, how is the actual movement from the controller to the process and back, as well as how the required controller's computations are performed. It is essential to identify the overall process control system with the main concern of monitoring the system's outputs. Constructive decisions need to be made regarding how best to manipulate the inputs and apply these decisions to the process for successful operation. (Veselý & Thuan, 2011), noted that complex or large-scale systems are a novel approach to scientists that study how interactions between parts give rise to the collective behaviours of the system, and how it co-operates and forms a relationship with its environments. This study is important to be understood well for any successful process control design.

Several variables significantly affect the performance of column flotation (Sastri, 1998). The classical column flotation design is known to have two main zones: the collecting zone and the froth zone (Bergh & León R, 2005). The flotation technique separates fine solid particles based on their surface's physical and chemical properties. Column

flotation is industrially known as a continuous solid-to-solid separation process performed in a vessel where a three-phase system is present: solid particles, air bubbles, and water (Persechini et al., 2004; Vieira et al., 2004). The process is normally started in the presence of the feed inlet (liquid present), by an injection of air continuously in the pulp, which then forms some air bubbles. A general classification of column flotation design is made of two principal zones: the collection zone and the froth/ cleaning zone as shown in Figure 2.1. The pulp feed enters near the top of the collection zone. Hence, particles are contacted counter-currently with air bubbles generated near the bottom of the column.

The wash water is applied to the top of the column, to clean any unwanted minerals from the Front. The greater the degree of freedom of operating variables, the greater the variability in metallurgical performance, which leaves more room for improved control (Bergh & Yianatos, 1993). Figure 2.1 is an illustration of the flotation column process.

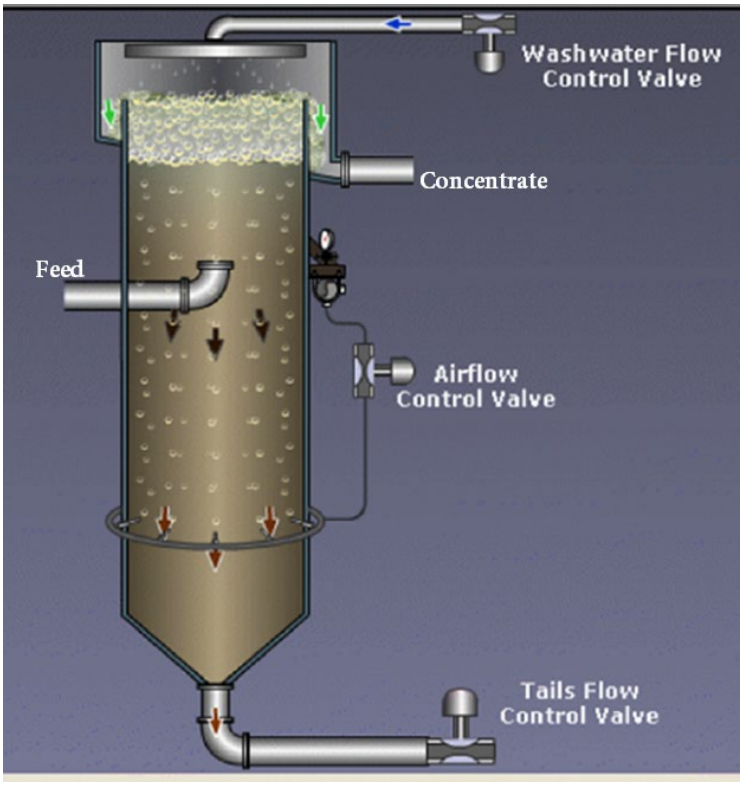

Figure 2.1: Schematic representation of a notation column (Maldonado et al., 2010)

There have been a number of efforts presented by researchers for controlling different multivariable processes such as column flotation. Nevertheless, it may be accepted that there are still drawbacks when it comes to controlling modern plants. The drawbacks are caused by the fact that these modern plants have different problems.

Therefore, advanced nonlinear control algorithms are preferable. This thesis focuses on the design of controllers used to control the column flotation process. Therefore, the literature review is in the following manner.

2.2.2 Model-based control methods and flotation system

In this section, the review of the existing literature based on different control design strategies covered over the years for the column flotation process is presented. Table 2.1 represents the reviewed publications of model-based control, and Figure 2.2 demonstrates the bar graph of the reviewed number of papers in conjunction with the year.

Table 2.1: The number of publications that have been reviewed on Model-Based Controllers and the flotation process versus the years

Reference	Year of Publication	Number of publications
Gilbert., 1969	1969	1
Ityokumbul 1992	1992	1
(Bergh L.G and Yianatos J.B, 1993)	1993	1
(Moolman *et al*., 1996) ;(Santos et al., 1996); (Zimmerman & Jeanmeure, 1996); (Bergh, Yianatos, & Cartes, 1996)	1996	4
(Itoh *et al*., 1998); (Sastri, 1998)	1998	2
(Del Villar et al. 1999)	1999	1
(Persechini *et al*.,2000)	2000	1
Carvalho M.T and Durao F	2002	1
(Singh et al., 2003); (Bergh and Yianatos, 2003).	2003	2
(Persechini.,2004); (Vieira *et al*., 2004)	2004	2
(Bergh and Leon, 2005); (Vieira, *et., al*., 2005); (Yianatos *et al*.,2005);	2005	4
Zhang et al., 2007); (Lundh *et al,* 2007); (Vieira S.M, *et al* 2007)	2007	3
(Bouchard et al., 2009); (Mohanty S, 2009); (Maldonado *et al*., 2009)	2009	3
(Nunez Felipe et al.,2010); (Nakhaei F, 2010); (Maldonado M et al., 2010); (Aldrich *et al*., 2010)	2010	4
(Shean B.J and Cilliers J.J, 2011); (Veselý et al., 2011); (Liuyuan et all, 2011)	2011	3
(Calisaya et al., 2012); (Behin and Bahrami 2012); (Xu et., al 2012); (Yang & Fan, 2012)	2012	4
(Bahadori *et al.,* 2013); (Sobhy and Tao); (Wang *et al*., 2013)	2013	3
(Tang *et al*. 2014); (Jahedsaravani, *et al*., 2014); (Antonyová and Antony, 2014)	2014	3
(Jovanović and Miljanović. 2015); (Mittal R and Bhandari M); (Guang He *et al.,* 2015)	2015	3
(Riquelme *et al.,*2016); (Capaci et.al 2016); (Bauer *et al.,* 2016); (Blanco et al., 2016)	2016	4
(Horn *et al., 2017*); (Fragoso *et al*., 2017); (Xue *et al*., 2017)	2017	3
Abankwa et al, 2018); (Yahui et al., 2018; Castro *et al*., 2018);(Nadda and Swarup 2018)	2018	4

Reference	Year of Publication	Number of publications
(Li et al., 2019); (Grigorova, 2019); (Li et al., 2019); (Jamsa-Jounela, 2019)	2019	4
(Bürger et al., 2020); (Azhin et al., 2020)	2020	3
(Ng et al., 2021); Quintanilla et al., 2021); (Zahiri et al., 2021); (Bilal et al., 2021)	2021	4

The following bar graph demonstrates the number of publications in conjunction with the years.

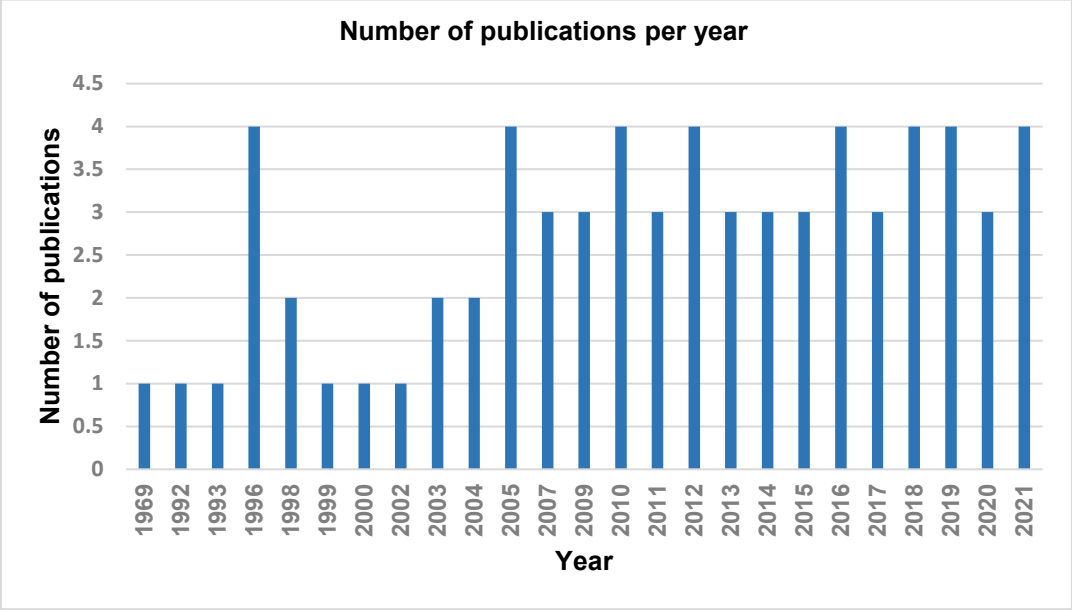

Figure 2.2: Number of publications in conjunction with years

The literature has made a clear understanding of the primary objectives based on the flotation process, which are the concentrate grade and column recovery that significantly measures the quality of the process productivity. To maintain high accuracy and availability, online approximation of these indices usually involves a large amount of work in the calibration and maintenance of on-stream analysers (Bergh & Yianatos, 1993). As a result, secondary objectives such as hydrogen ion concentration (pH: hydrogen potential) at the feed, air flow rate, froth depth, and wash water flow rate are commonly controlled (Bergh & Yianatos, 1993). It is noted that Distributed Control Systems (DCS) or local controllers are commonly for implementation purposes.

Variation of the controller's set points under DCS is a preferable control strategy to achieve good process performance when primary objectives are measured. This is usually applied in the form of experimental systems. Cascade control of gas hold-up (using gas flow rate control) and bias (using wash water flow rate control) become intermediate objectives if the secondary objectives were controlled but the primary objectives were not monitored. Color, form, size, and speed of the froth can all be

considered advanced objectives, depending on how the secondary objectives are regulated and the feed's properties. The problem in both circumstances is determining how to link performance targets to concentrate grade and process recovery.

Flotation is also used in a water treatment process to clarify wastewater. This process of wastewater treatment makes use of dissolved air flotation, where air bubbles are injected near the bottom of the basin containing the treated water. The bubbles become linked to particulate matter and flock particles as they rise through the water. Particles will rise to the surface due to the floating force of the combined particle and air bubbles (Bahadori et al., 2013). At that time, the wash water is used to perform the final cleaning of useless particles that might still be attached to the usable mineral before the move to the next stage (scaling).

According to (Shean & Cilliers, 2011), flotation remains relatively inefficient and is still not fully understood, but, the introduction of this process goes as far back as the 1900s. There has been a significant amount of research and development in this field. Shean & Cilliers, 2011, presents different flotation control strategies such as model-based optimising flotation controllers that can be used on the grade recovery curve to find the best operating point. The recovery and grade set points are subsequently presented to lower control systems or plant operators. Optimisation of the currently used flotation process control methods can produce large economic gains, but it remains unusual to find reports of advanced fully automated long-life operational, and optimised flotation control systems. The identification of the important factors to be controlled is essential for a complete column flotation response. The process identification model is then totally based on experimental data. It's important to remember that information not identified in the specified data will not simply show in the model by itself. It is the same as expecting a spectacular appearance of an unnamed functionalization in the final theoretical process model (Ogunnaike & Ray, 1994).

However, the useful process information content of the output data is very much dependent on the nature of the input function applied. Therefore, it is equally important to choose an input function capable of providing output that is good or useful in processing information. It is an added advantage if such information is also easily extracted. The typical input functions employed in process identification are Step, Impulse, Pulse (rectangular or arbitrary), White noise, Sinewaves, and Pseudo random binary sequences. When it comes to the effects of system dynamic performance it is important to have an accurate measurement for the control variables. (Bergh & Yianatos, 1993) identified that with the methods used in industry to estimate gas

holdup, froth depth, and bias, key measurement errors are produced. A proper understanding of the processes inside the column must first be established, and then more functional relationships among the variables can be accomplished. The principle of the flotation process has been discussed in the following section.

2.2.3 Existing literature for the flotation system modelling

In a column flotation, it is mostly known that an aside inlet into the flotation column is used to provide the feed inflow. The air comes in through a distributor at the bottom of the column, and the wash water comes in from the top. The wash-water washes away light hydrophilic particles that can be transported to the froth zone and removed as tailings. The hydrophilic particles flow down to the bottom of the column and are removed as tailings, whereas the hydrophobic particles become attached to the air bubbles and rise to the froth zone (Mohanty, 2009). As indicated in Figure 2.3, useful particles of concentrated elements are removed from a side opening only at top of the column.

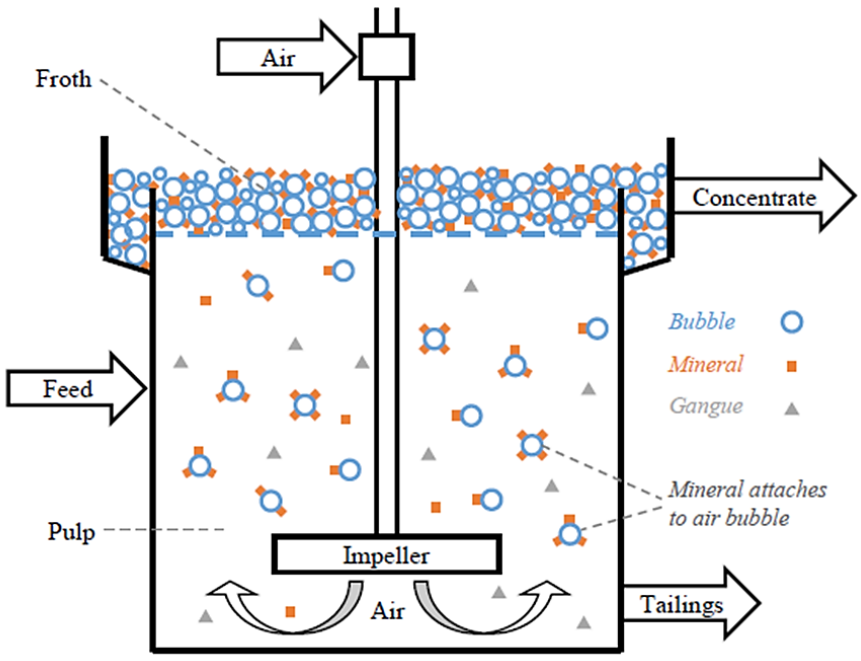

Figure 2.3: Schematic diagram of a Flotation Column (Weimeng, 2014)

The hydrophobic minerals that are connected to the bubbles are included in the concentrate, as well as a component of the hydrophilic gangue that is transported upward and entrained in water channels between bubbles, eventually being trapped in the froth (Vieira et al., 2007). To improve recovery it is necessary to increase the number of minerals reporting to the concentrate and to reduce gangue recovery one needs to reduce the number of minerals reporting to the concentrate (Weimeng, 2014).

The bubble-particles attachment in the pulp phase is facilitated by the collectors that are used to gather hydrophobic particles. Underdosing collector often causes loss of recovery; overdosing collector can generate overloaded bubbles, which could also reduce flotation recovery and decrease product grade (Ng et al., 2021).

2.2.4 Modeling of a Flotation system

The column flotation modeling is a process that differentiates the collection and froth zones to analyse the overall recovery of the whole system, (Yianatos et al., 2005). Flotation is a solid-to-solid separation process based on physical and chemical properties. Air is continuously injected into the pulp through a sparger at the bottom of the column, giving rise to the formation of a group of air bubbles of mineral particle surfaces. Three process variables are said to have been experimented with, which are height in the collection zone, air holdup, and biased water flow rate. These variables are key variables to the metallurgical column performance and they are directly related to grade and recovery, (Carvalho & Durão, 2002).

However, controller design is mostly based or focused on monitoring collection zone height, the bias water flow rate, and regulation control of these variables, such as air holdup in the collection zone, froth layer height (h), and bias (Q_B) are tightly controlled when an external disturbance of the feed flow (Q_F) occurs. (Carvalho & Durão, 2002), presented well-acceptable servo control results obtained from a two-system control. Carvalho & Durão, 2002 demonstrated that more work can be done to adapt the controller design to the three-phase system (air, water, and mineral particles). This is also one of the driving motivations to pursue this study.

Froth flotation is a common method to remove a certain type of mineral from minerals while depressing the number of undesired minerals in the extracted concentrate. It is also stated that for polymetallic ore different flotation circuits and a grinding circuit can be combined to form a concentrator used for extracting several mineral types from the same ore. The process of extracting from ore is done by adding certain chemical substances to selectively clarify the desired mineral hydrophobic. Generally, a flotation process consists of several flotation cells together with cyclones, crushers, and mixing tanks. In a flotation cell, air bubbles are used to lift the mineral. The resulting froth layer is then skimmed to produce the concentrate (Horn et al., 2017).

The simplest control of the flotation system is the automatic regulation of froth depth with tailing flow-rate, and the physical regulation of wash water and gas flow rates

(Bergh & Yianatos, 1993). The literature shows good developments regarding the modeling of the process for control and optimization purposes.

However, these models usually lack an intense variables interaction study and, practically they only analyse the steady-state operation without considering the dynamic behaviour of the system said (Castro et al., 2018). The availability of mathematical models is an important requirement for the application of optimization and automated setup of the flotation process. Yahui et al., 2018 propose a modeling method that provides the foundation for an application of discrete model designs, which is well-known in the theory of finite-dimensional systems. This revealed that Model Predictive Controller (MPC) and Moving Horizon Estimator (MHE) need to be addressed for the column flotation system.

Controlling the froth depth with the wash water flow rate and the relative bias with the tailing flow rate is another popular method. The use of the tailing flow rate to regulate the bias helps to speed up the process reaction to feed-flow rate changes. In fact, both approaches have produced comparable outcomes, demonstrating what the two controllers gain have lost due to their lack of synchronization. A third control loop is occasionally added to the system. Three individually tuned control loops with substantial interactions between them usually require the detuning of more than one of them to restore overall performance. Furthermore, nonlinearities in the process may cause a well-tuned control loop to behave unsatisfactorily for a specific plant operational condition, or possibly make the system unstable for other operating areas,

This process is far too complicated to be managed effectively using only distributed control and traditional algorithms like PID. It is commonly known that a significant number of control approaches and algorithms that have proven successful in other processes will not be able to satisfactorily resolve all of the column flotation control challenges (Bergh & Yianatos, 1993). It is necessary to calculate, whether traditional PID or advanced model-based control, may be able to optimize the process in a limited operating range. (Shean & Cilliers, 2011), explains the different levels of the control system ladder for flotation processes, and advanced optimisation control. Difficulties based on the implementation of process automation and optimisation are highlighted as a major problem for the flotation columns system. However, they hoped that after some time through continuous simplification and continuous development of new robust technologies, it may be possible to succeed in the advanced automation and optimisation of flotation control. Such an outcome would certainly be financially worthwhile.

(Persechini et al., 2004) presented a design control strategy that evaluated air-water operation and ore (mineral or rock) operation in a pilot-scale column using a multi-loop PI control technique. Based on the froth layer height, the estimated value showed correct dynamic behaviour, but did not correspond to the expected result, as described by (Persechini et al., 2000). Only control of the bias water flow rate showed satisfactory results and returned to the steady state whenever the set point is changed. (Carvalho & Durão, 2002), presents a flotation column control system that is composed of a personal computer, where the fuzzy control algorithm is executed, a Programmable Logic Controller (PLC), where the PID low-level control of flow rates is achieved, by instrumentation in the field and by the controlled process. The study here is based on the two-phase system which is the air and water. Estimation of height and air holdup are archived using two pressure sensor measurements. The bias water flow rate is estimated from underflow and feed flow rates. The Association or involvement of control of the mineral particles with a flotation column is said to be done in the future.

In the analysis of the flotation column, (Calisaya et al., 2012) considered two hydrodynamic variables. They consider the fraction of wash water beneath the interface and gas hold-up in the collection zone. These variables were controlled by manipulating the wash-water flow rate and the gas flow rate respectively. Future research could focus on determining the relationship between froth depth, gas hold-up, and the wash water fraction below the interface. The research suggests that the metallurgical and economic performance of the flotation unit should be investigated. The overall goal of the current study is to improve the full-scale flotation column in real-time.

2.2.5 Identification of the key variables

The theoretical modeling and steps based on process identification have been discussed by (Ogunnaike & Ray, 1994). The importance of assessing how the experience model fits the facts is emphasized during process identification. Model validation is usually done by comparing prediction performance to additional process data and assessing the system's accuracy. This can be carried out either in the time domain or in the frequency domain.

The literature generally focuses on the review of linear and nonlinear control systems, with an interest in a column flotation process. (Vieira et al., 2004), presented a column flotation process that involves the separation of several components, such as collectors, regulators, activators, and pH modifiers. (Bouchard et al., 2009), pointed out the importance of dynamic models for process control analysis, and recommend

additional work to be done in multivariate statistics for online monitoring and dynamic modeling which is presently an active field of research, but new technology needs to be used in the implementation of this process. The identification of the critical variables needs to be achieved together with their accuracy in measurement, and their ability to be dynamically altered in a coordinated manner, these are all critical components in flotation column operation and optimization. However, the lack of process understanding prevents further growth in several ways despite significant efforts made in recent years (Bergh & Yianatos, 1993).

2.3 Controller design of the flotation of the process

Improvement of the controllability on flotation columns is subjected to the proper understanding of the control approach, gaining of process information, data processing, and control application. Stable operation of flotation columns is said to be achieved if the concentrate grade and column recovery are accomplished. Process control plays a vital role in enhancing many process operations, but not enough reports of industrial applications that focus on flotation columns. The froth depth is commonly managed using PID controllers at the regulatory level, according to (Bergh & Yianatos, 1993). It is also noted that fluctuation in flotation feed quality carries a great challenge when it comes to the control of the number of collectors.

(Sastri, 1998), suggest that stabilizing the operationally and optimum performance of column flotation, is required to use control instrumentations. Among the several sorts of stabilizing controls, the most basic is to manipulate the tailings rate to manage the interface level. Wash water addition is manual in most of these systems, and there is no bias control. To limit the impacts of gas and bias rates, a thick froth is usually maintained. Although some manual intervention is still required, it is acknowledged that significant progress in the dynamic modeling of a column flotation process was made since the first attempts in the late 1980s (Sastri, 1998), (Santos & Cruz, 1996). More information and Fuzzy predictive control application to a column flotation process were described by (Vieira et al., 2007). The flotation column system is challenging to manage due to its nonlinearity. As a result, the predictive controller was used in real-time on a column flotation pilot plant. Since a basic linear model could not achieve the required control action. It takes some time for the controlled variables to reach the reference, as the process under study is very slow.

2.3.1 Linear and Nonlinear Proportional-Integral (PI) and Proportional-Integral-Derivative (PID)

According to (Maldonado et al., 2009), control of bias and froth depth can be completed by making use of use of input variables such as feed rate, air rate, wash water rate, tails rate, and concentrate rate. They focused on two PI controllers which were designed to control the two-phase system. A frequency-response tuning approach was used to tune both PI controllers. Loops are locally controlled and experimentally implemented to regulate all flow rates. The modeling and design methods utilized in this research have effectively demonstrated to be an operative tool for developing a column flotation process control strategy. Relative Gain Array (RGA) approach is used to evaluate the amount of interaction between controlled and manipulated variables. The range of values evaluated for the process variables demonstrated a minimal degree of interaction between control loops.

The airflow rate, wash water flow rate, and froth depth are normally measured online, and tailings, air, and wash water flow rates are manipulated. Flotation Control known as stabilizing strategy is included in some circuits, it consists of pH control and chemical reagent dosage control. The non-existence of precise measurements, high interaction among variables, and non-linear dynamics are the main problems related to stabilizing control. With no supervisor to coordinate the control loops, the efficiency of traditional PID control is reduced by these characteristics, said (Bergh & Yianatos, 2003). Therefore, if a conventional PI or PID controller is used for a flotation control, it must be used with an additional controller or any simplification method that can deal with high interaction within this process to accomplish better control of the column flotation. It is important to be well-informed about the existing number of interactions between the control loops, a useful technique for the development of the decoupling multi-loop control system. Each loop must be individually designed using the permitted PI controllers. Measured results are utilized to test and validate this process. The controlled dynamic behavior of the flotation column has met most of the requirements for a closed-loop system designed for water-air and ore operations. As a result, the application of water-air operation for modeling the flotation process, as well as the controller design has brought about good results when it comes to ore operation (Maldonado et al., 2009).

When the set-point is lower than the original interface level, the reaction is faster, but when the set-point is higher than the original interface level, the response is slower, this comparison was conducted by (Mohanty, 2009) through a three-phase system performance. As a result of the reviewed observations, the controllers based on

Artificial Neural Networks (ANN) are advisable for implementation instead of traditional PI or PID controllers. However, ANN-based controllers are only useful or usable within the range for which they were trained. This concludes that while creating data for system identification, precautions must be exercised to ensure that the whole operational range of the column is covered. On the other side, the literature has proven the usefulness and the success of PID controllers in the control of some industrial processes. As long as PI and PID are supplemented by advanced methods such as decoupling, decentralization, Model Predictive Controller (MPC), and many more.

(Maldonado et al., 2009), presents a combined PI and multivariable predictive control strategy for the implementation of a water, and gas pilot flotation column. A PI controller is used to control the froth depth, and a predictive controller is defined as the reduction of tracking errors of the gas hold-up while maintaining numerous operational restrictions between their upper and lower bounds. According to Maldonado et al., 2009, a high set point of the gas hold-up is designed to optimize the bubble surface area for particle collection while keeping the bias rate above the minimum value required for froth cleaning. Finally, the proposed solution could be useful in real-time optimization standard approaches by avoiding the assumption of steady-state conditions and using secondary variables to improve flotation column operation. For the sake of simplicity in this study, these authors have assumed the effect of the wash-water flow rate on gas hold-up to be zero.

Most industrial processes are naturally large-scale systems that require the use of a control strategy based on a system approach. (Veselý & Thuan, 2011) developed four localized PI controllers for large-scale DC systems that ensure the closed-loop uncertain system's strong stability is achieved. This paper presented decentralized approach for linear large-scale dynamic systems. This system model is given by means of a time-invariant matrix of 16 order-type structures with 4 inputs and 4 outputs variables. The aim of the design procedure presented by (Veselý & Thuan, 2011) is to design 4 PI controllers that promise to have robustness properties in terms of the performance for this closed-loop system. The order of the PI design procedure has decreased to the order of the particular subsystem, which is the main advantage of the proposed approach.

A modified adjoin transfer matrix-based decouple was designed by (Guang et al., 2015), for a Module Suspension Control System in magnetic levitation (Maglev) train. (Guang et al., 2015) states that the optimization concerning the performance index and robustness index is accomplished to determine the controller parameters. Then, depending on the intended close loop system performance, a compensated controller

is acquired. The model reduction method is used to generate a simpler controller with a PID structure due to the complexity of the obtained resultant controller. It should be noted that a PID controller with a pure differential term will result in an unlimited high-frequency gain. This is unwanted; hence a second-order low-pass filter is used in the PID controller to substitute the standard technique of using pure differential terms. Therefore, it is possible to deliver suitable decoupling and set-point tracking performance using an obtainable decoupling design strategy that is associated with the experimental results by means of the traditional Single-Input-Single-Output (SISO) controllers. Thus, this method is good, especially for industrial implementation.

2.3.2 Model Predictive Control

Model-based Predictive Controllers, known as MPCs, are the additional noticeable methods of regulating process systems with high nonlinearities. In this approach, a controller is designed based on the future prediction of the available system behavior by using a process model. Because hydrodynamic factors are strongly related to the flotation unit's metallurgical and economic performance, using an intelligent control strategy is critical for optimizing its operation (Calisaya et al., 2012). They developed, implemented, and evaluated MPC to control strategic hydrodynamic variables of a three-phase (air-water-ore) pilot flotation column in an industrial environment. Based on the findings there is a need to find the relationships between froth depth, gas holdup, and wash water fraction underneath the interface and the metallurgical and economic performance of the unit. Another important part missing here is the real-time optimization of full-scale column flotation. They also used a control strategy developed using the MatLab MPC toolbox for the control of the pilot column flotation process.

According to (Vieira et al., 2007), predictive control is a generic methodology for tackling time-domain control issues with one common feature: control based on the prediction of future system behavior using a process model. Model-based Predictive Controllers (MPC) use an existing model to predict the process outputs at future discrete moments over a prediction horizon. The use of MPC for complex processes such as froth flotation is a powerful control strategy. MPC can manage multivariable processes with nonlinearities, non-minimum phase behavior, or large time delays because of the explicit usage of a process model and the optimization technique (Vieira et al., 2007); (Maldonado et al., 2009); and (Riquelme et al., 2016). This control approach optimizes the process by using models that can predict its outputs, minimising a cost function that depends on process variables and process constraints (Quintanilla et al., 2021). Because of its many appealing properties, such as handling

multivariable systems with time delays, Model Predictive Control (MPC) has been widely used in the process industries.

Through this method, a sequence of future control actions can be computed using model minimization of the certain objective function (Vieira et al., 2007). The sequence of future control signals is determined by improving a cost function that represents the control objective while keeping control signal amplitude and slew rate limits into account, (Maldonado et al., 2009) deals with the study based on hydrodynamic characteristics of flotation columns, and the use of a two-phase system to demonstrate the advantages of using predictive control for flotation column process optimization. The control algorithm used was based on a simple PI controller, for control of froth depth, since this does not represent a major problem within the column. A MIMO model predictive control scheme is engaged to deal with the two secondary variables (gas hold-up and bias rate), because, of its proven ability for dealing with existing time delays and constraints. The method has performed well, however for future research it would be good to add another variable to be controlled within the flotation system, to understand design limitations and drawbacks.

(Tang et al., 2014) presents some investigation based on the track of the desired performance of networked flotation processes using Robust Model Predictive Control (RMPC). The developed results are then applied to a networked flotation process that is made up of three layers: direct control layer, set-point control layer, and optimization layer. The exponential MPC is designed for the set-point layer, where uncertainties, saturations, and successive packet dropouts with time-varying probabilities are considered.

(Nadda & Swarup, 2018), propose a control strategy that adopted decoupled control design. The robust controller used has incorporated a Nominal control where the inputs for each subsystem are designed based on a feedback control approach. Robust Compensator where the inputs are designed to limit the effects of equivalent disturbances to improve the effectiveness of this control strategy. The technique based on the Pole-placement method to achieve the desired tracking performance and robust compensator is used to handle the influence of coupling, nonlinear dynamics, external disturbance, and parametric uncertainties. The strategy used has made the close loop poles to be comparable to the pole spread of another existing control strategy in the literature (such as classical centralized control and existing decentralized and decoupled control), but this is achieved with the least control effort compared to other design methods. According to (Nadda & Swarup, 2018), further performance

improvements may be obtained through some tuning of parameters in an optimization technique.

2.3.3 Controller design based on Fuzzy logic

Fuzzy logical modeling is a commonly used modeling tool for dynamic and nonlinear processes. In a laboratory setup of a flotation column, (Vieira et al., 2007) introduced fuzzy multivariable modeling with model predictive control. The hybrid type of controller using fuzzy logic implication when operating conditions are considered to be normal is proposed by (Carvalho & Durão, 2002). The mathematical conversion step is becoming more and more inspiring owing to the availability of excellent software tools like Fuzzy Logic Toolbox for MATLAB and to the possibility of directly using the resulting definition of the fuzzy logic system in the control application. But, the starting values of the parameters involved in the translation step usually need to be adjusted for the controller to achieve acceptable or improved performance. (Zoitl & Lewis, 2014), state that “the most significant trend has been to incorporate machine-learning techniques into the fuzzy control design process with generally good results”, (Carvalho & Durão, 2002). The combination of expert logic and fuzzy logic, in addition to the distributed traditional control of hybrid systems, has proven to be a viable solution for dealing with dimensional problems. Therefore, there are multiple rules and parameters that do not significantly reduce the performance of the entire process, (Núñez et al., 2010).

(Bergh et al., 1998) presents a flotation columns process simulator accomplished by adding or including a decentralized traditional PID control simulator on the process.
This simulator contains three basic control loops. Cascade froth depth with tailing flow control, gas flow control, and wash water flow control. Standard tuning processes were used to get the control settings. In this paper, a dynamic simulator in combination with a static simulator was used to predict concentrate grades and make sure that the process yields the desired state. Expert and fuzzy supervisor are the two simulators developed by (Bergh et al., 1998). This simulator uses rules related to concentrate quality and process recovery through instrumental variables to generate set-point values or standards for the three control loops: froth depth, airflow, and wash water flow. Every supervisor works with the same data, which is presented in a number of formats.

2.3.4 Neural network-based controller design

According to (Nakhaei et al., 2010), an Artificial Neural Network (ANN) is a technique for experimental modeling that simulates the behavior of biological neural structures.

The ability to represent a problem using data (data-driven) rather than defining it methodically is the main advantage of ANN (Horn et al., 2017). ANNs are extremely effective at representing complex and non-linear systems said (Nakhaei et al., 2010; Horn et al., 2017). In column flotation plants, the suggested NN model accurately evaluates the effects of operational variables. (Nakhaei et al., 2010) suggest that this method and its results may be utilized as a skilled scheme in column flotation plants to improve system parameters and analyze their interactions for the projected Cu grade without having to do additional laboratory tests.

Another method that produced good results is a Model Predictive Controller (MPC) designed based on the ANN model as presented by (Mohanty, 2009), which is used to control the interface level of a flotation column by manipulating the tailings flow rate. The model predicts the future interface level using two past values and one present value of the tailings valve opening as well as the interface level as inputs. This model is used to create or design a Model Predictive Controller that regulates the interface level.

2.3.5 Multivariable Control and Internal Model Control (IMC)

The literature presents, a large number of process variables that are collected regularly by Distributed Control Systems at a high frequency (DCS). According to (Bergh & León R, 2005), very connected process input variables, low signal or noise ratios, and missing data are some of the key issues encountered in modeling the process for identification and monitoring purposes. Principal Component Analysis (PCA) and Partial Least Squares (PLS) techniques can mathematically projection of high-dimensional processes and quality data to reduced-dimensional. It is also noted that the generation of linear models from summary data sets is a key feature of PCA and PLS. A substantial percentage of the measurement error will be recognized as the number of PCAs in the model grows. Due to the obvious reasons having a bigger dimensionality, results in complex graphical analysis, hence these authors (Bergh & León R, 2005) also discussed the drawbacks of increasing the number of PCA in a model. According to (Vieira et al., 2005), the performance indexes are computed using testing data which is different from the so-called training data used to build the models. Software used for validation is not indicated, however, the method and the presented results are appreciated. (Abankwa et al., 2018) determine the center of flotation of a vessel in waves. The results show that multiple acceleration measurements can be used to correctly determine the center or position of flotation of a vessel in waves. The location of a vessel’s center of flotation during operation at sea plays an important role

in the vessel’s longitudinal stability. The ability to accurately estimate the location center of flotation improves safety monitoring as it indicates how changes in the distribution of weight affect the vessel.

A data-driven adaptive optimal feedback control approach using Adaptive Dynamic Programming (ADP) is presented by (Li et al., 2019) without knowing the flotation process dynamics. This method is proposed to overcome the natural complexity of the flotation process, which seems to persist as a great challenge for optimal controller design. Simplicity is highlighted as a major advantage of the method proposed here because it has proven to be independent of the exact knowledge of flotation dynamics with good disturbance rejection and fast set-point tracking. The simulation demonstrated that the flotation process can be effectively controlled by the policy iteration method (PI) based ADP algorithm. For this thesis or current study, a similar method is adopted, but with full knowledge of the flotation process.

Since the system under study is a multivariable process, it is not easy to just identify proper connections without testing, the Relative Gain Array (RGA) assists in the classifications of proper loop connections (Ogunnaike & Ray, 1994; Bristol, 1966). For multivariable controller design, the Relative Gain Array approach provides two forms of important information. The first is a measurement of the process interactions, and the second is a set of recommendations for the optimum pairing to minimize the interactions' significance. The procedure and the discussion of the loop pairing based on Interaction analysis as discussed by (Ogunnaike & Ray, 1994) have been used in this thesis. When it comes to controlling interconnected systems, three major challenges arise. One is the practical limitation of the number of variables and configuration of feedback loops, which supports decentralized control structures. The presence of hesitations in both, the subsystems and the interconnections add additional concern. A third concern is the control systems' reliability in the event of component failures. There are high chances of encountering failures in real engineering systems and they could cause instabilities in the system's operation (Pujol et al., 2007).

The analysis has proven that Internal Model Control (IMC) tuning procedures are less sensitive to errors made when determining process dead time ~~through step tests~~. The recommendation of the Internal Model Control (IMC) is triggered by the fact that the controller design might offer good set-point tracking but with poor disturbance response, which is particularly important for processes with a small-time delay. However, in many process control applications, disturbance rejection is more critical than set point tracking for unstable processes. This method allows one to obtain the

needed response, by considering different behaviors for different values of the tuning filter. Nevertheless, the use of IMC can cause a long settling time for load disturbances that delay significant processes, which is something undesirable in the control industry.

2.3.6 Differential geometric concepts: Control approaches

According to (Núñez et al., 2010), they are numerous control schemes have been applied for the stabilization of the column flotation process, including decentralization control, fuzzy approaches, and model predictive control which attempt to control froth depth, air holdup, and water bias. To improve flotation process instrumentation (Mohanty, 2009) and (Núñez et al., 2010), provide many orientation efforts, intending to provide better measurements for control resolutions. (Núñez et al., 2010), validated a classified hybrid fuzzy scheme that is implemented on top of the plant Distributed Control System (DCS). This paper also recommended a future to include systematic controller tuning to achieve an improved time response performance. In detail, the tuning procedure is said to consider membership functions, concentrate grade, least recovery, and manipulated variables acceptable domain.

When there is no previous information about the system or it is only partially known, fuzzy modeling using measures of the process variables is a method to be considered for usage because it permits an approximation of nonlinear systems. According to the experts, fuzzy modeling typically involves three steps: structure identification, parameter estimates, and model validation (Vieira et al., 2004). The genetic algorithm described in this paper is based on the real-coded genetic algorithm to optimize fuzzy models, as proposed. The use of this model is advisable to be used for future system control in a model predictive control framework.

Another important strategic method is nonlinear Partial Differential Equations (PDEs) and steady-state profiles, which are utilized in the linearization of nonlinear systems. The Cayley-Tustin time discretization transformation is applied to the linear hyperbolic PDEs system and maps the continuous infinite-dimensional system to a discrete infinite-dimensional system (Yahui et al., 2018). Relating to the simulation results of the linearized model and the discretized model, it can be seen that the anticipated method by (Yahui et al., 2018), of discretization, can well preserve the characteristics of the original infinite-dimensional system. This paper advises that the future should address the Model Predictive Controller (MPC) and moving horizon estimator (MHE) design for the column flotation processes because the nonlinear hyperbolic PDEs system is constructed for interface and froth regions.

2.3.7 Implementation of the Column Flotation Process

This subsection is based on reviewing implemented column flotation process. (Lundh et al., 2017), said the significant difference in the recovery for the zinc, in column five, is at least one percentage unit higher when MPC is used compared with the existing manual control strategy. They presented how model predictive control can be applied to a froth flotation circuit. The importance of its operation is discussed, and for implementation, the sensors and actuators are used to influence the process. Then, the elements forming control and estimation strategy using two approaches and how they can be implemented on Expert Optimizer is explained. A test period with the MPC based on grey-box modeling is also presented.

(Mohanty, 2009) presented real-time operations using monitoring control and data acquisition (Elipse SCADA). A schematic diagram of the experimental equipment is shown in Figure 2.4. This laboratory scale is just a common example proposed by (Mohanty, 2009), it has a pilot column with a diameter of 100 mm, a height of 2.5 m, two pumps, an air diffuser, two electromagnetic flowmeters, and two variable range metals. It consists of two flowmeter tubes, two electric butterfly valves, and a differential pressure transmitter. According to (Mohanty, 2009), the inflow is measured by an electromagnetic flowmeter and controlled manually. A centrifugal slurry pump delivers the feed to the column. A variable area metal tube flow meter measures the wash water flow rate, which is manually controlled by an electrically operated butterfly valve. The wash water was delivered or supplied using a peristaltic pump. A variable area metal tube flow meter measures the airflow rate, which is manually controlled.

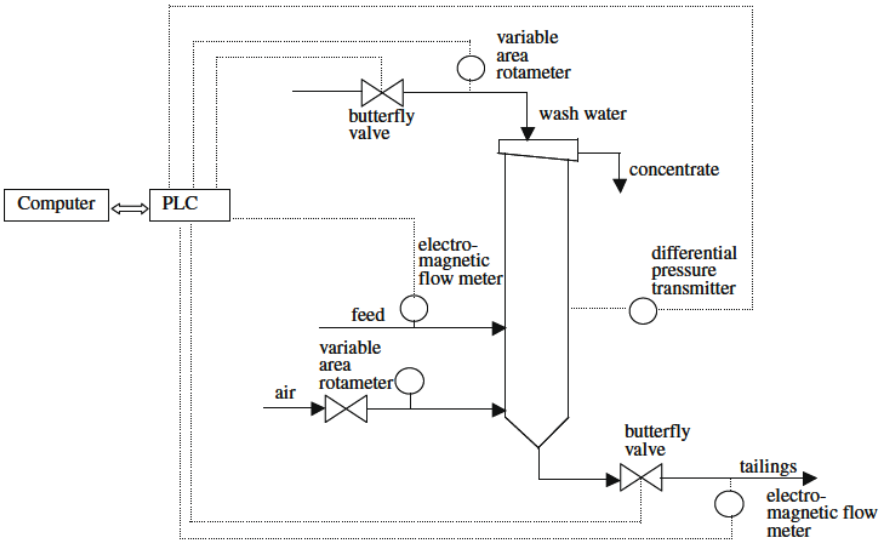

Figure 2.4: Schematic diagram of the experimental setup (Mohanty, 2009)

An electromagnetic flow meter detects the tailings flow rate, which is then controlled by an electrically powered control valve (see Figure 2.4). All the equipment is connected to a programmable logic controller (PLC), which is connected to a PC through a conventional RS485 Modbus network connection for monitoring and operation. For real-time operation, the author used commercially available Eclipse SCADA software that runs in a Windows environment. The software is RS485 Modbus compliant and is used to show all measured variables in real-time as well as control the flotation column from the PC.

(Maldonado et al., 2009) describe another experimental setup in which a prototype flotation column with 15 stainless-steel conductance electrodes is used to quantify froth depth and gas hold-up. To evaluate the conductivity profile at the top of the column across the interface, nine of these electrodes are used, each measuring 5.1 cm in diameter and 1.5 cm in height, there are flash mounted on the column wall at 10 cm intervals. The outstanding 6 electrodes are all ring type, with an outer diameter of 2 cm and a height of 1 cm, they are coupled to the flow cell connected to the wash water in pairs of 5 cm intervals. The column feed tube and the branch on the side of the gas hold-up sensor have been prepared and used, for example, to measure the conductivity of the corresponding current. A peristaltic pump is used to add wash water to the top of the column and a turbine flow meter is used to measure its flow rate. To regulate the supply, residue, wash water, and gas flow rates to their respective settings, some local control loops like PID are used. Data acquisition is performed by Supervisory Control And Data Acquisition SCADA software running on the Windows XP operating system.

(Nakhaei et al., 2010) have used an electromagnetic flowmeter to measure the wash water flow rate, which was then controlled by a pneumatic valve. A large-scale flowmeter measures airflow rate and a pneumatic valve control it. A variable-speed peristaltic pump controls the pulp feeding, and a variable-speed peristaltic pump controlled by a frequency inverter controls the non-floated flow rate. The air hold-up in the recovery zone and the froth layer height are determined using the pressure data from two pressure gauges mounted in the upper half of the column. The instruments are connected to a data-collecting system that converts the output variables from analog to digital and the modified variables from digital to analog.

(Liuyuan et al., 2011), implemented a liquid level control system in which a pressure sensor is used to detect the current height of the Pulp Level, replicating it on the oscilloscope variations by comparing with the presented level using an Adaptive fuzzy PID controller for examination and calculation of the PWM wave frequency of the drive

actuators (peristaltic pump), and regulating the peristaltic pump through different PWM frequency. Lastly, the detailed Level information will finally be returned straightaway to the industrial PC, which means once a Level sensor exported current signals (4 – 20 mA), it will be analysed by a microcomputer through AD conversion. In this scenario relays and alarms are connected with the microcomputer, so that when an emergency arises, the system would close and automatically ring an alarm.

The utilization of simplified models in the Real-Time Optimization (RTO) layer has the advantage of greatly reducing the time it takes to solve problems in chemical plants. Furthermore, a basic model is simple to understand as well as maintain and update if necessary. However, as stated by (Rodrguez-Blanco et al., 2016), RTO is not always able to achieve optimal process operation for a variety of reasons, including the presence of significant uncertainty in the plant models and variation between control architecture layers that work at different time scales and use various models. The Modifier-Adaptation (MA) methodology requires the addition of new constraints to the optimization problem, which takes into consideration the process's grade of activation to provide adequate information in the measurements and gradient accuracy. During the improvement of chemical plant operations, the solution time is greatly reduced, allowing RTO to be used in real processes.

2.4 Comparative analysis and discussion on the developments in the existing literature

Based on the comparison of the different reviews made, the fuzzy modeling controller design seems to be the best in the application of the column flotation control process. It is also noted that ANN-based MPC controllers showed better performance in control actions when compared with conventional PI controllers (Mohanty, 2009). Nevertheless, the simplicity of the PID structure encourages industrially engineering applications and it is proven as the most effective technology for the applications of multivariable systems. Hence, this thesis adopted the decentralized and decoupling controller design with the PI-transformed type of controller. The selection of the control strategy adopted for this research is motivated by the objective of industrial application contributions. It also noted that, although multivariable PID structures are good controllers, they still need supporting modems or advanced methods to successfully work in some uncertain systems.

Based on the reviews conducted above, Table 2.2 summarizes some of the reviewed papers based on the control model methods for the column flotation process, it emphasizes the purpose of the design, along with the results, shortcomings, and recommendations.

Table 2.2: **Review papers on the flotation system and the design of the controllers**

Reference Paper	Aim of paper	Controlled variables	Methods for control design or identification	Software development, simulation, and implementation	Achievements and drawbacks
(Bergh & Yianatos, *1993*) *"Control alternatives for flotation columns"*	To study what impact wash water, and gas flow rates, as well as the position of the tailing valve, have on froth depth, gas holdup, and bias.	The controlled variables are froth depth, bias, and gas holdup.	PID and other traditional algorithms, such as distributed control, were used. This was based on the manual manipulation of wash water and gas flow rates, as well as the automatic regulation of froth depth with tailing flow rate.	Peristaltic Masterflex pumps were used to regulate the feed and wash water flow rates. Rotameters were used to measure gas and tailing flow rates, and valves were used to control them.	Besides its low cost and simplicity, this arrangement has the advantage of not interfering with other objectives. However, manual regulation requires human involvement during process operation, which is a main disadvantage of the scheme applied here.
Sastri, 1998 *"Column Flotation Theory and Practice"*	To provide relevant information about flotation, including the specific advantages of column flotation over mechanical flotation cells.	Counter-current flow of slurry and air bubbles	The important findings from RRL, Bhubaneswar, have been highlighted, with the parameter estimation method.	Only the development of column flotation for the concentration of low-grade ores was examined.	This is a good initiative that was taken by the Regional Research Laboratory (RRL) in the early 1960s to develop a leading column flotation technique for Indian ores. But, the manual addition of wash water still needs to be improved by automation.
Bergh *et al*., 1998. "Fuzzy supervisory control of flotation columns"	This paper aims to use a dynamic simulator of the process to develop and test the developed controllers.	Control of foam depth, airflow, and wash water flow by treatment rules related to concentrate quality and process recovery.	Metallurgical static simulator, Supervisor simulator	Dynamic simulator; Supervisor simulator, Metallurgical static simulator. Distributed conventional PID control simulator	Obtaining the control parameters needs to be improved. Parameters were obtained using standard tuning procedures.
Del Villar et al. 1999. *"Automatic control of a laboratory flotation column"*	To deal with the operation of industrial flotation columns that calls for the control of variables, the interface function, and the unfairness rate, with the aid of using manipulation of a few suitable operating variables.	Two-phase system: control bias and froth depth.	Using the distributed PI control strategy, to control bias and froth depth. Frequency response tuning techniques are used to tune both PI controllers.	To adjust all flow rates, local control loops are used. Variable-speed Masterflex peristaltic pumps are used for liquid pumping.	Generally said that input variables can be manipulated through control of air rate, tails rate, wash water rate, concentrate rate, and feed rate. Even though the tests were completed on a two-phase system, the whole procedure used can now be extended to a three-phase system. It is not clear what simulation software was used for testing the operation.

Reference Paper	Aim of paper	Controlled variables	Methods for control design or identification	Software development, simulation, and implementation	Achievements and drawbacks
Persechini et al. (2000) *"Dynamic Model of a Flotation Column"*	To apply dynamic modeling of the multivariable flotation column.	The controlled variables are the froth layer height, bias, and air holdup in the recovery zone.	The Pilot-scale of the air-water system is under control using manipulated variables such as wash water, air, and non-floated fraction flow rates.	The experimental data was collected from a pilot-scale column and evaluated against simulation results. Simulation is obtained, not clear which Software tools are used.	Gathered experimental data will be used for further analysis. It continues to be important to take into account a few essential aspects, in particular, the initial reaction of the froth layer peak behaviour. In this paper the modifications of the airflow charge are inverse to the steady-state gain, characterising a non-minimal section system.
Carvalho and Durao (2002). *"Control of a flotation column using fuzzy logic inference"*	This paper aims to control the flotation column using Fuzzy logic interpretation.	The controlled variables are the flow rates of the air and water valves.	PID is used for Flow rate local control. Fuzzy controller for Fuzzy processing.	MATLAB Fuzzy Logic Toolbox. The application of real-time optimisation methods such as a modified Nelder and Mead algorithm or genetic algorithms may remove the weakest aspects of the fuzzy control design process through online parameter tuning, at least of a parameter subset.	Height and air holdup are estimated using two pressure sensors, and the bias water flow rate is estimated from underflow and feed flow rates. The methods used seem to work, only if good starting values of the fuzzy system parameters can be provided, so guaranteeing the success of the tuning phase. But, the method did not involve the mineral particles, it is still necessary to include control of them in the flotation system.
Singh et al., (2003). *Flotation stabilization and optimization*	FloatStar manipulation is advanced to calculate superior degree set-points or aeration quotes that target to optimize the residence times, mass pulls, and circulating masses inside a flotation circuit.	Level and grade of the element.	For a simpler circuit, compare traditional PID and FloatStar control. In this paper, FloatStar's effective stability has made it easy to research the subject of flotation circuit improvement.	Simulated results show that basic proportional-integral controllers do not produce satisfactory results. Therefore, the need for advanced or modem techniques aimed at improving the performance of the well-known PID control is advisable.	It is possible to get good performance from a flotation plant, but maintaining that performance has proven problematic. The recovery costs of a flotation process could be about 90% and regularly lower, making flotation one of the least environmentally friendly methods. As a result, significant research and development have gone into the stability and improvement of flotation circuits over the previous few decades.
(Bergh and Yianatos, 2003). "Flotation column automation: state of the art"	To review the current trends and state-of-the-art in flotation column automation and control.	Concentrate grades.	To measure airflow, orifice plates and dp/cells, mass flow meters, and vortex-type devices are often used. For measuring supply, water, and tailing flow rates, magnetic flow meters are nearly standard.	The main drawback identified was the maintenance and readjustment program required to maintain the quality of the estimate over the long term. At this time, no industrial application using this method	Fuzzy logic and Artificial Neural Networks (ANN) have been shown to be effective methods for incorporating into these systems. Even though froth image analysis has been highly active, no automatic control applications are predicted until the generated parameters can be connected with

Reference Paper	Aim of paper	Controlled variables	Methods for control design or identification	Software development, simulation, and implementation	Achievements and drawbacks
			Ultrasonic flow meter devices are also capable of handling pulps, although their implementation is slow.	has been successfully reported.	concentrate grade and recovery, as well as the other manipulated variables.
Vieira et al., 2004. "C*ombination of Fuzzy Identification Algorithms Applied to a Column Flotation Process*".	To optimize fuzzy models based on the real-coded genetic algorithm.	The inputs applied to the system are: airflow rate, wash water, rejected flow rate, and feed flow rate. The system is Froth flotation.	Fuzzy modeling identification technique is used. Generic algorithm for fuzzy model optimization.	Optimal Parameter Estimation: evolutionary computation techniques. Fuzzy modeling approach is used to validate the results presented here. No indication of the software name used.	The proposed method used worked very well. The future proposed is to use this method in a model predictive control framework. Not clear what method is used for acquiring the real data used.
Persechini et al. (2004). *"Control strategy for a column flotation process"*	Ensure that the specified metallurgical is produced for the flotation process, as measured by the grade and recovery of the valuable mineral in the concentrate.	Three controlled variables: the froth layer height, the air holdup, and the bias	Designed PI controllers.	Simulation results available (not clear which Software tools and no runtime results shown).	The proposed control techniques are validated by testing the designed controllers in a pilot-scale plant. A real-time operational system was stated, but not practically done.
Bergh and León., 2005. *"Simulation of Monitoring and Diagnosis of Flotation Columns Operation Using Projection Techniques*"	To demonstrate the principles and applications of data analysis methods, particularly the use of PCA models in plant monitoring, including how to use the processed data to correct an operating problem once it has been identified.	Monitored variables are: gas, wash water flow rate, and froth depth.	Principal Component Analysis (PCA) and other multivariate mathematical projection methods.	Microsoft Excel platform is used to simulate the column flotation monitoring	The advantage is that this monitoring tool is web-based, thus it can be used as part of a larger supervisory control scheme. However, one limitation is that this method can only be used to analyze steady-state data. Therefore, additional methods will still be needed for the control and manipulation of input variables.
Vieira, *et., al*., 2005. *"Fuzzy modeling strategies applied to a column flotation process"*	To automatically identify a MIMO model obtained from experimental data, using a fuzzy modeling strategy.	In the collection zone, the controlled variables are Froth layer height, the air holdup and the bias flow rate	fuzzy modeling strategy, and fuzzy modeling identification technique.	Different experimental data are used to validate the final model. The data was collected in a pilot-scale laboratory flotation column with a height of 3.2 meters and a diameter of 80 millimeters.	Fuzzy modeling strategy is the best option so far. Usually, the feed flow rate is kept constant, however, in the real world, this is not always possible and can produce oscillations.

Reference Paper	Aim of paper	Controlled variables	Methods for control design or identification	Software development, simulation, and implementation	Achievements and drawbacks
Vieira S.M, *et al* (2007). *"Real-Time Fuzzy Predictive Control of a Column Flotation Process"*	To regulate the flotation of a column using fuzzy predictive control.	States: Flow rates for feed, wash water, air, and rejected stream. Manipulated variable: air and rejected flow rates. Outputs: Froth layer height and air holdup.	To regulate a laboratory setup of a flotation column, fuzzy multivariable modeling with fuzzy model predictive control is used.	Collection Zone height is inferred through the soft sensor. PLC for instrument connection, PC, but no software mentioned being used.	This is a very good paper the findings show that the methods used resulted in the effective quality of all the controlled variables. However, it is noticed that the controlled variables take some time to reach the reference, but the nature of this process is a generally slow process also.
Lundh *et al,*2007. "Model Predictive Control for Flotation Plants"	Developing and testing a model predictive control-based technique on a zinc flotation circuit.	Controlling produced concentrate and the tailing.	Model Predictive Control-based approach.	The recommended tool for implementing advanced process control is ABB's cpmPlus Expert Optimizer, especially for model predictive control in mineral processing and other industry.	On a zinc flotation (position: froth flotation), a predictive control-based technique has been created and tested. The use of MPC is stated to be at least one percentage unit greater than the existing manual control strategy.
Maldonado *et al.,* (2009) "Potential use of model predictive control for optimizing the column flotation process"	Implement a two-phase pilot flotation column using a PI and a multivariable predictive control strategy.	Two-phase (water–gas): The froth depth and gas hold-up.	Control algorithm: GlobPC The control of froth depth does not represent a major problem, therefore, a simple PI controller decided to be used as is the case in the industry. A MIMO model predictive control scheme is retained to deal with the two secondary variables, gas hold-up, and bias rate.	A pilot flotation column running with a two-segment machine is enough to illustrate the benefits of the usage of predictive management for this procedure optimization.	Because of its demonstrated ability to deal with existing time delays and constraints, model predictive control is used. For the sake of simplicity, the effect of wash-water flow rate on gas hold-up is assumed to be zero in this study. Not clear in the model whereof is the tracking errors of the bias rate were done
Mohanty, 2009. "*Artificial neural network-based system identification and model predictive control of a flotation column*"	The purpose of this paper is to discuss the design of a model predictive controller based on a neural network for managing the interface level in a flotation column.	Liquid–gas and liquid gas-solid systems are two types of two-phase systems.	In order to capture additional information about the system identification multilayer signals are advantageous. For system identification, tailored pseudo-random excitation signals are used in a number of applications.	A standard RS485 Modbus network connection to a PC for monitoring and operation is used to connect all instruments. Software for supervisory control and data acquisition is used as well.	ANN controller designed based on MPC control has proven to work much better than conventional PID controllers. But then again, experimental the airflow rate was controlled manually and measured by a variable area metal tube flow meter. Because air hold-up and bias are important controlled parameters of a flotation column, future work is proposed to include the design of an

Reference Paper	Aim of paper	Controlled variables	Methods for control design or identification	Software development, simulation, and implementation	Achievements and drawbacks
					ANN-based controller for a multiple-input-multiple-output (MIMO) system.
Núñez et al., 2010 *"Hierarchical hybrid fuzzy strategy for column flotation control"*	Aim to present a hybrid fuzzy technique for controlling metallurgical performance in column flotation.	Concentrate grade: Recovery: This hybrid scheme has three different operation scenarios, defined by a recovery concentrate grade domain panel.	A hierarchical hybrid fuzzy controller is designed.	X-ray analyzers are responsible used for real-time measurements of feed, concentrate, and tailings grades. A hierarchical hybrid fuzzy scheme is implemented on top of the plant distributed control system (DCS).	The authors propose upcoming research to combine new operational scenarios, with their respective control strategies, that can yield a higher recovery-concentrate grade or the inclusion of new process variables in the panel.
Nakhaei *et al.,* 2010. "*Prediction of Copper Grade at Flotation Column Concentrate using Artificial Neural Network*"	The research aims to use NN's ability to predict Cu grade under various operational scenarios.	The controlled variable is a percentage of Cu grade. The inputs to the network are wash water, non-floated flow rates, and froth height.	Non-linear statistical identification technique. Artificial Neural Network (ANN)	All of the instruments are interconnected to a data acquisition system, which handles the analog-to-digital conversion of the output variables as well as the digital-to-analog conversion of the controlled variables.	The Feed-Forward ANNs (FFANNs) method was utilized in this study to estimate the extracted copper grade in the flotation column using real-world data.
Shean and Cilliers, 2011. *"A review of froth flotation control"*	To explains the different levels of the control system ladder for flotation processes.	Significant progress is based on the control of pulp levels, airflow rates, and reagent dosing.	Level control, advanced control, and optimisation.	Without name specifications, it is said to have used commercial advanced or optimising flotation control software.	Good methods are reviewed and recommended, but they lack real-time industrial implementation trust or resources up to now. Not clear what software was used, and no implementation was made.
Veselý et al., 2011 "*Robust decentralized controller design for large scale systems*"	To control linear large-scale dynamic systems using a decentralized approach.	A linear model of four cooperating DC motors.	The decentralized Robust PI controller is designed using the V-K iteration method.	The Simulation of the DC motors was conducted without specification about which software was used.	The order of the PI-designed procedure has decreased to the order of the particular subsystem, which is the main advantage of the proposed controller design approach.

Reference Paper	Aim of paper	Controlled variables	Methods for control design or identification	Software development, simulation, and implementation	Achievements and drawbacks
Liuyuan *et al,* 2011 "*The Study of Detecting and Controlling System of Mineral Pulp Level*"	To establish the detecting and control system of the Mineral Pulp Level.	Liquid Level Control or Water Tank Level control.	Fuzzy control and PID control. Simulations are done in MATLAB software. Real-time monitoring is achieved through LabView.	The technology used for implementation: Microcomputer/PLC. Labview Virtual Instrument, Labview hang Computer technology, and Signal processing.	The use of online inspection technology used on the flotation process and automation is the main highlight of this paper. The system is highly automated and easy to operate with man-machine information flow, which corresponds with the modern trend of production automation and intelligence.
Calisaya et al., 2012 *"Multivariable Predictive Control of a Pilot Flotation Column"*	Controlling the hydraulic performance of a pilot flotation column in an industrial environment using a three-phase system.	The controlled variables are the fraction of wash water beneath the interface and the gas hold-up in the collection zone.	PI controller is used with control parameters developed using the MatLab MPC toolbox.	Control of air hold-up and wash-water through a constrained model predictive control (MPC) strategy is implemented in MatLab.	The iterative reduction error minimization method supplied by MatLab System Identification Toolbox was used to identify the process transfer functions. The only outstanding part is to determine how to froth depth, gas holdup, and wash water fraction beneath the interface relate to the unit's metallurgical and economic performance.
Tang *et al.* 2014. "*Robust Model Predictive Control Under Saturations and Packet Dropouts with Application to Networked Flotation Processes*"	Using Robust Model Predictive Control (RMPC) and subsequent packets, investigate the track-based target performance of networked flotation operations.	Control of three different layers.	Robust Model Predictive Control (RMPC) method.	Although not specified, the economic objective index's simulated tracking performance with and without RMPC appears to be simulated in MatLab.	The simulations presented do support the effectiveness of the proposed method. However, it is noted that it is still necessary to reduce the conservativeness and consider more practical occurrences to reflect more realistic factors, maybe using parameter-dependent techniques.
Guang He *et al.,* 2015 "*Decoupling Control Design for the Module Suspension Control System in Maglev Train*"	A module suspension system is proposed to solve the coupling issues of the two levitation units of the module in the magnetic levitation train.	Two variables are under control (TITO system).	A simplified PID structural controller is designed using the model reduction method. A decoupling feedback control system is used.	Practically CMS04 low-speed maglev train is used	Based on the strong stability of the decoupled module suspension control system, an engineering-oriented decoupling control approach was applied and tested effectively on an actual full-scale maglev train.
Blanco et al., 2016. "*Modifier-Adaptation methodology for RTO applied to Distillation*	The use of the MA approach to the optimal management of distillation columns as a depropanizer column is presented in this study.	Two variables are being controlled Steam Flow and Reflux Flow	Nested Modifier-Adaptation and Dual Modifier-Adaptation.	Real-Time Optimization technique.	The time taken to arrive at the solution is greatly decreased. The benefits of utilizing simplified steady-state models in the RTO layer are demonstrated in this paper. According to the results,

Reference Paper	Aim of paper	Controlled variables	Methods for control design or identification	Software development, simulation, and implementation	Achievements and drawbacks
Columns using a simplified steady-state model"					feasibility is not guaranteed during the intermediate iterations.
Riquelme *et al.,*2016. "*Predictive control of the bubble size distribution in a two-phase pilot flotation column*"	The purpose of this is to control the BSD such that it reaches the desired distribution set-point.	Air and water	An image analysis approach and a dynamic non-linear model for BSD are used to assess BSD in real-time.	A modified version of the McGill bubble viewer was used to create the bubble visualizations.	A bubble viewer connects the sampling tube to the bubble viewer. Bubbles are exposed in the viewing chamber, photographed using a computer-controlled device camera, and then returned to the column. It is necessary to conduct a series of tests to assess the impact of BSD on concentrate grade and recovery during flotation.
Horn et al., 2017. "*Performance of Convolutional Neural Networks for Feature Extraction in Froth Flotation Sensing*"	Control of platinum flotation froth images at four distinct platinum grades.	Platinum-grades quality control	The paper uses data-driven sensors to achieve its objective.	Imaging is used for the comparison of the quality of CNN features and traditional texture feature extraction techniques.	Linear and nonlinear soft sensor models were trained using extracted feature sets. According to the collected data, there was insufficient information to distinguish between the types of features discovered by CNN, This requires further analysis.
Yahui et al., 2018. "*Three-Phases Dynamic Modelling of Column Flotation Process*"	Is to develop a three-phase discrete dynamic model of column flotation with a focus on interface and froth regions.	Control and monitor the Froth and Interface regions.	Nonlinear Partial Differential Equations (PDEs) are used as a transportation method within the flotation system. Furthermore, this paper uses the Cayley-Tustin time discretization method.	Only simulated for comparison.	When comparing the simulation results of the linearized and discretized models, it is clear that the suggested discretization method is compatible with the original infinite-dimensional system's properties.
Nadda and Swarup., 2018 *"Decoupled control design for robust performance of quadrotor"*	The purpose of this study is to provide a reliable controller for each quadrotor component to accomplish the specified reference trajectory.	Control quadrotor.	Nominal control and a Robust controller designed with a compensator.	A control strategy for a quadrotor UAV is simulated in MATLAB	Robust compensator parameters are selected and tuned by trial and error according to the responses of the quadrotor.
Li et al., 2019 "*Optimal Reagents Control for Flotation Processes: An Adaptive Dynamic Programming Approach (ADP)"*	Introduce a data-driven adaptive optimal feedback control technique using adaptive dynamic programming.	Optimal Control of the concentrate grade and tailing grade.	Data-driven adaptive optimal feedback control using Adaptive Dynamic Programming	Numerical simulation is applied.	The simulation illustrates that by using online production data, the ADP controller can overcome the disturbance.

Reference Paper	Aim of paper	Controlled variables	Methods for control design or identification	Software development, simulation, and implementation	Achievements and drawbacks
Azhin et al., 2020 "*Modelling and boundary optimal control design of hybrid column flotation*"	The interconnection of a CSTR is used to model a three-phase continuous hybrid flotation column that aims to combine the benefits of mechanical cells with flotation columns.	Two Plug-Flow Reactors (PFR) representing pulp and froth zones	Optimal model-based controller design.	The performance of the controller has been demonstrated through a numerical simulation of the physical plant and relevant operating conditions.	Returning to a steady state following a disturbance in the initial condition, the LQR-based optimum controller exceeded the PI-based controller. At this point only simulated, no implementation is presented.
(Quintanilla et al., 2021) "*Modelling for froth flotation control: A review*"	A critical literature review on modeling for froth flotation control is presented.	Control of Froth flotation, however, the Froth height is considered constant	The dynamic models are used to implement the control strategies such as image analysis, Artificial Neural Networks (ANN), Fuzzy Logic (FL), and Model Predictive Control (MPC)	Only reviews based on modeling and control strategy. No simulations were applied.	This review has classified and analysed models used for flotation MPC strategies, providing a framework for future studies. The drawback of the PID controller is addressed by complementing it with advanced control techniques.
Ng et al., 2021. "*Improvement of coal flotation by exposure of the froth to acoustic sound*"	To address the challenge of improving coal flotation performance and the subsequent froth breakdown simultaneously.				
(Bilal et al., 2021) "*Effects of coarse chalcopyrite on flotation behavior of fine chalcopyrite*"	To use the Carrier-flotation approach to improve recovery by attaching small particles to bigger carrier particles.	Control of volumetric flows of the feed input and Underflow outlet.	Conventional flotation, Sample preparation, and Carrier-flotation methods were used in the Control of dissolved air flotation (DAF) and column froth flotation (CFF) in industrial wastewater treatment	Microtrac is used to analysis the size of the Particle. Dynamic simulations are obtained with a recently developed numerical method. Responses to control actions are demonstrated with scenarios	Calculations have theoretically proven that hydrophobic interaction played a more dominant role in the attachment of fine chalcopyrite particles on the carriers. No practical implementation was presented.

2.4.1 Summary of the literature reviewed

The challenges of the controlled system arise from the fact that it is a MIMO system. In MIMO systems, the coupling between different inputs and outputs makes controller design very difficult. In general, every input has an impact on the system's outputs. Signals might interact in unexpected ways as a result of this coupling. Designing additional controllers to compensate for the process and control loop interactions is one of the solutions. Decoupling control is an approach that can be implemented in a variety of ways (static, dynamic, diagonal, block-diagonal, triangular, or inverted). The alternative option is to construct a MIMO system with decentralized control. The sequential loop tuning approach, the detuning method, the independent loop tuning method, and the Relay auto-tuning method have all been examined. Each strategy has advantages and disadvantages.

Although many controller design methods were reviewed for different processes, ANN, MPC, and fuzzy logic control are the most promising and successful controllers used in the column flotation process. However, when it comes to industrial applications, most industries still use PID, because of its structure and is one of the first developed control strategies with a simple structure and well-known tuning rules, which makes it maintain dominance in practicing engineering applications for several decades (Guang et al., 2015). Though more advanced control algorithms have been developed, PID controllers are always preferred unless they do not give a satisfactory performance (Guang et al., 2015).

2.4.1 Discussions

Flotation is a mineral separation technique that uses variations in hydrophobicity to separate iron ore. The grade and recovery of the important mineral determine good column flotation performance. When dealing with this flotation process, the most important thing to remember is to investigate the relationship between controlled and manipulated variables to create a good controller for its operation. The current research focuses on the column flotation system's controller design.

The existing literature based on control strategies for set-point tracking, monitoring, system stabilization, and disturbance rejection problems for different processes is reviewed. The reviewed literature is constructed based on modern control concepts such as model predictive control, fuzzy logic, neural network-based controller design, geometric differential concepts, internal model control, and multivariable control concepts.

Different models and applications for different processes were used to confirm the usefulness of many control strategies. Table 2.2 is an illustration of different effective control strategies that were reviewed, and this continues as more researchers come up with innovative ideas. According to the reviewed literature, the Model Predictive Control brings more positive outcomes in managing uncertainty for the MIMO process with constraints. It is important to review many methods and gain more knowledge, and understanding of many control design methods available for successful control usage in MIMO systems. Although MPC is a mostly supported strategy, the analysis of the literature shows little evidence of successful MPC implementation on a flotation industrial scale (Quintanilla et al., 2021). As a result, more research is needed to improve modeling and controller design for flotation control applications.

2.5 Conclusion

Different control methods and their application for the multi-variable column flotation process are reviewed. A flotation system is presented, and the importance of its selection is highlighted. Historical and current methods used to design controllers for linear and nonlinear systems are reviewed. The motivation of this study is based on the requirements to design different innovative control algorithms for control of the column flotation process. Different control models that are involved in linear and nonlinear control design and the benefits associated with them are presented in Table 2.2. As discussed, traditional methods are also applied to achieve the research objective. Based on the interest in industrial engineering applications, multivariable PI/PID controllers are designed in this thesis.

The decentralized-decoupled control techniques with an emphasis on the column flotation models are adopted for control development purposes. The reason for the decoupling recognition technique, as opposed to only the decentralization method, is its ability to eliminate existing interactions within the system. It is also an efficient way of controlling a wide range of industrial systems. Controlling the multiphase process with inherent instability involves control approaches that are useful when it comes to eliminating interactions between control loops.

The implementation approach suggested in this thesis is to apply the Matlab/Simulink transformation principles to the TwinCAT 3.1 software environment and use them to implement closed-loop control of the flotation process. This is accomplished by introducing and applying new function blocks of the closed-loop system to the function library of the Programmable Logic Controller (PLC) system to achieve the visualized

objectives. This approach is described and implemented in Chapter 7. The next chapter (Chapter 3) emphasizes the operation of the column flotation process.

CHAPTER THREE:
THEORY-BASED OF FLOTATION PROCESS

3.1 Introduction

The column flotation method, which was chosen as a case study in this research, is discussed in this chapter. The characteristics and dynamic performance of the column flotation process are analysed to assist in increasing a solid understanding of the system's behaviour for various changes that might occur under operation conditions. Generally, the interface level is controlled by using the tailings flow rate or the wash water flow rate. When comparing the two manipulations which are tailing flowrate and wash water it can be concluded that the wash water has a slow reaction at the interface. The selection of the appropriate pairing of controlled and manipulated variables is recognised as a determining element for grade prediction and process control performance due to process interactions (Nakhaei et al., 2010). Different industrial use of the flotation system is covered in section 3.2, the column flotation process, mathematical development of the required input flow rates, and other relevant variables are prepared in section 3.3. Section 3.4 is the summarized conclusion of the MIMO system under study.

3.2 History of Flotation systems

In traditional mechanical cells, the separation of precious minerals from gangue is far from optimal. In the early 1960s, a technique called column flotation was developed, Sastri 1998. In the beginning, naturally occurring chemicals such as fatty acids and oils were used as flotation elements in large quantities to increase the hydrophobicity of the valuable minerals, (Sobhy & Tao, 2013). Since then, the process has been adapted and applied to a wide variety of materials to be separated, and additional collector agents, including surfactants and synthetic compounds, have been adopted for various applications, such as mining, wastewater treatments, paper recycling, and many more, (Sastri, 1998). The bubble size and air hold-up, as well as the flow rates, are the key elements determining recovery and grade in the collection zone (Sastri, 1998). As presented flotation process is used in different industrial environments. The following subsection focuses on the overview of the mining flotation process.

3.2.1 Mining

The method of separating minerals from gangue using the difference in hydrophobicity is known as froth flotation. Ionic liquids and cleaning fluids are used to increase the hydrophobicity differences between valuable minerals and unwanted gangue (Vieira et

al., 2005). It is possible to economically process complex ores mainly due to selective mineral separation (Sastri, 1998). Before any further improvement, the flotation method is used to separate a wide range of sulfides, carbonates, and oxides (Jainsa-Joiuiela, 2019). It is a complicated multivariable process that is subjected to a number of disturbances including variations that might occur at the feed and equipment degradation. According to the investigation made based on Mineral Processing, the important mineral processing unit is a column flotation (Vieira et al., 2005). The significance of the froth zone in flotation has been underlined by (Vera et al., 2002), who have also described how to measure froth performance in terms of the froth zone recovery factor. The suggestions on the presented model include the consideration of scope for modification and further research that can be based on different angles of the flotation system, such as determining an expression based on measurable system parameters, evaluating the temporal dependency of the froth stability parameter, and so on.

Platinum purification from mining is a multistep process with a large number of interconnections. (Horn et al., 2017) presents, multiple flotation tanks that are cascaded into each other with chemical dosages and conventional recycle loops to guarantee maximum recovery of platinum in the process. Comparing the quality of CNN features and traditional texture features, (Horn et al., 2017), presented a flotation process intending to minimise the intensive of platinum in concentrators while maximising platinum grade in the final concentrate before the meltdown. Lower final concentration results in a more energy-concentrated meltdown. The last solid waste reduction stage is flotation cells, hence their performance is the key to achieving the process’s objectives. According to the results gathered no sufficient information was provided to distinguish between the types of features detected by the CNN, therefore, further investigation is required in this regard.

Alternative control of flotation columns was applied by (Bergh & Yianatos, 1993). This paper reviewed experimental control based on logical rules, that can be very successful in avoiding driving the process outside some general operating regions, such as fuzzy control, neural systems, and expert systems, but these methods are usually not effective in managing the dynamic development of the control variables. In this paper, the column is manually adjusted to steady-state operation, and a predefined step change in one of the independent variables is introduced. While the dependent variables' transient reaction has been recorded. The automatic control of froth depth with tailing flow rate, as well as the manual control of wash water and gas flow rates, are the most basic controls used in this process.

3.2.2 Wastewater treatments

The progressive use of the flotation process is also found in waste-water treatment industrial plants, where it removes grease, oil, and suspended solids from wastewater (Ross et al., 2000). One of the water treatment methods is Dissolved Air Flotation (DAF), which removes suspended wastes from wastewater or other liquids (Wang et al., 2004). Figure 3.1 is a representation of the elements that create a completed Dissolved Air Flotation (DAF) system. Three methods are commonly used for the separation of the suspended oil and fats from water and wastewater, they are filtration, gravity separation, and air flotation. The most useful and widely used practice is Air flotation because this method is adaptable (Behin & Bahrami, 2012). Petrochemical, chemical plants, oil refineries, natural gas processing plants, and similar industrial facilities are using DAF components to remove oil from wastewater management.

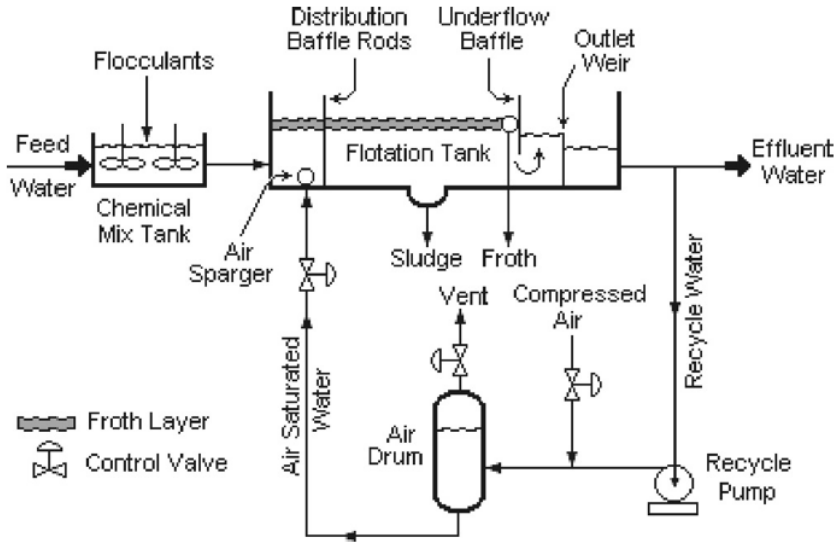

Figure 3.1: **Schematic of dissolved air flotation system (DAF), (Bahadori et al., 2013)**

The air applied or released forms small bubbles which follow the suspended matter and floats to the water's surface, where it can be removed by a scanning device. Particles with a greater concentration than the liquid can be made to float, and those that rise to the surface are removed as residuals for further processing, according to (Bahadori et al., 2013). Any remaining particle material is filtered out of the purified liquid (Edzwald, 2010). Similar, to other gravity separation techniques, raw water is liquefied and dispersed in water before entering the DAF basin. The water is injected into the basin's contact zone near the floor. The contact zone is separated from the clarifying zone by a baffle wall, which prevents short-circuiting said (Edzwald, 2010). DAF has been utilized in drinking water treatment for decades as a sediment-free alternative to

sedimentation. For these types of supplies, it is more effective than sedimentation at eliminating turbidity and particulates.

3.2.3 Paper recycling

One of the methods for recovering recycled paper is froth flotation. This process is known as de-inking or floating in the paper industry. The purpose is to eliminate the hydrophobic pollutants out of recycled paper and get rid of them. Printing ink and stickies are the most common pollutants. A typically, two-stage system with three, four, or five flotation cells in series has been used by (Wang et al., 2013).

Itoh *et al.*, 1998 developed a tactile sensor capable of sensing paper quality, which makes use of the increase in quartz-crystal tuning fork impedance at resonant vibration while the base of its quartz-crystal tuning fork for wristwatch application is in contact with the paper. On the other hand, the sensing mechanism of the quartz crystal tuning-fork tactile sensor is used to sensor the mixing ratio of pulp to the recycled paper ingredient. It functions as a paper-quality sensor capable of sensing.

3.3 Column Flotation Process

Column flotation is a generally used separation technique in mineral production. The process of column flotation is defined by a complex dynamical model which includes air, water, and solid three-phase flows (Yahui et al., 2018). Froth flotation is usually a technique used to extract certain types of minerals from ore while depressing the number of undesired minerals in the removed concentrate. This process is done by adding certain chemical mixtures to selectively render the desired mineral hydrophobic. In a flotation cell, air bubbles then lift the mineral, and the resultant froth layer is then skimmed to produce the concentrate. Generally, a flotation process is made up of several flotation cells together with cyclones, mills, and mixing tanks. Intended for poly-metallic ore different flotation circuits and a grinding circuit can be combined to form a concentrator used for removing several mineral types from the same ore, (Lundh, et all*., 2015*), (Vhora & Patel, 2016).

(Vieira et al., 2007) agrees that flotation is a technique for separating small solid particles depending on their surface's physical and chemical properties. Through industrial, this can be described as a continuous solid-to-solid separation process implemented in a container, where a three-phase scheme presents: solid mineral particles, air bubbles, and water. As seen in Figure 3.2, the air is continuously pumped into the pulp, resulting in the development of air bubbles. Through the formation of

steady bubbles, particles can be moved to the container's surface when a proper frother in a sufficient concentration is applied.

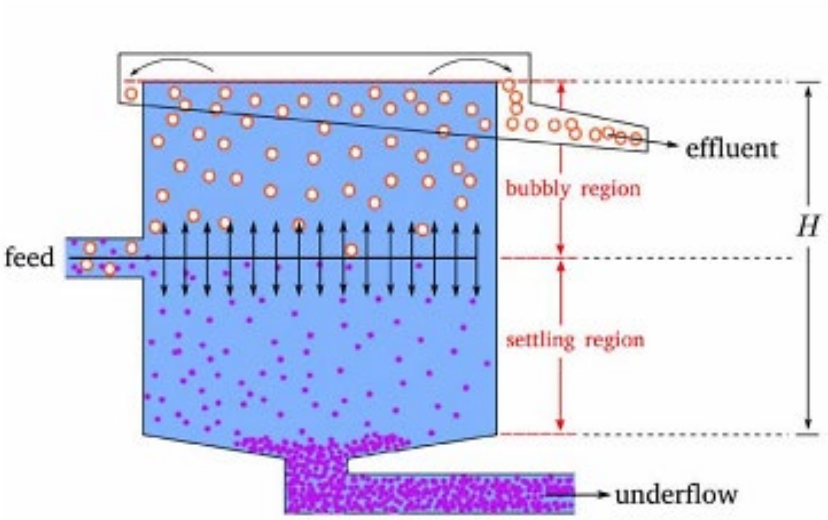

Figure 3.2: **Diagrams of a flotation cell showing the material flows (Vieira et al., 2007); (Weimeng, 2014)**

After the collision, the valued particles adhere to the air bubbles, these particles will then move up to the top of the container, then they will be recovered as the floated product. Unusable particles move downwards and settle down at the bottom leaving the column as an underflow (Carvalho & Durão, 2002). In a flotation process, the substances are controlled with reliability and robustness assurances, this acts as an important role in reducing substances consumption and improving the system's stability during the flotation processes. Column flotation control carries a great challenge for optimal controller design due to the natural complexity of the flotation process, said (Li et al., 2019). According to Bilal et al., 2021, the recovery of the column flotation is determined by model control, and collision possibility, and also the size of the particles plays an important role in the recovery process. They presented a model in which the chance of a particle attaching to an air bubble is 1 and the chance of a particle detaching from an air bubble is 0. For hydrophobic particles, these assumptions are correctly said, (Bilal et al., 2021).

The substances in the concentrate include not only the hydrophobic minerals that are gathered by being attached to the bubbles but also part of the hydrophilic gangue that is carried upward and pressurized in water channels between bubbles eventually becoming stuck in the froth (Weimeng, 2014). As a result, near the top of the overflowing bubbles within the column, a shower of clean water is necessary to be applied to wash the floated product, this help in producing better hydrophilic particles that were surrounded by the bubbles of hydrophobic particle collections (Vieira et al.,

2007) and (Bouchard et al., 2009). Increasing the volume of minerals reporting to the concentrate can improve the recovery and reducing the amount of gangue can improve the grade.

3.3.1 Description of Column Flotation System

A general characteristic of column flotation unit has three input streams: feed mineral inlet pulp, air injection, and addition of wash water. This process also consists of two output streams: the concentrate and tailings. During normal operating conditions, the column content is divided into separate regions according to the amount of air content: the collection zone in the lower part, and the cleaning zone in the upper part of the column (Bergh & León R, 2005). The separation between valuable minerals and gangue is performed by, usually adding chemical substances such as frothers, collectors, activators or depressants, and pH modifiers. This is done at an earlier stage or follows the common practice of adding at the column itself. Because of its hydrophobic qualities being natural or artificial, the created froth carries the mineral particles that are valuable and overflows them into the column concentrate wash, while the useless particles (gangue) are retrieved as tailings at the bottom. As shown in Figure 3.3, the additional wash water improves concentrate quality by removing entrained unwanted particles from the froth (Bergh & Yianatos, 1993).

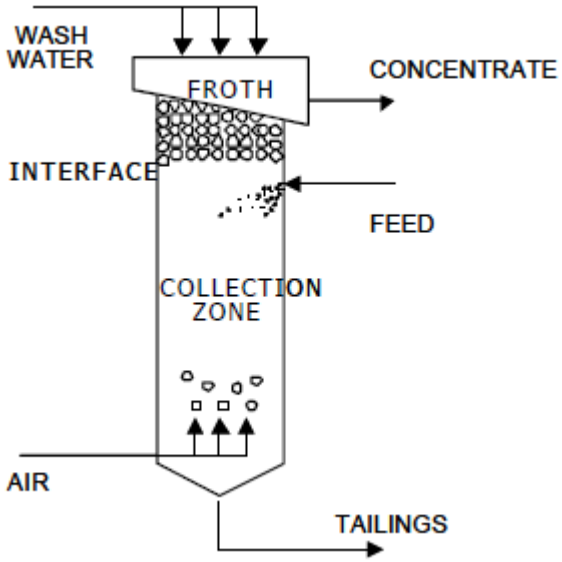

Figure 3.3: Representation of Flotation Column (Bouchard et al., 2009)

The pulp feed comes at the top of the collection zone, as shown in Figure 3.3. According to the manufacturer, the pulp feeding is regulated by a peristaltic pump with variable speed capability and a frequency inverter (Persechini et al., 2000). As

mentioned before valuable elements will then collide and follow the bubbles, and move upwards to the pulp froth interface, (Calisaya et al., 2012).

The froth zone is a movable bubble bed, approximately 1m in froth depth, which is contacted with wash water added near the overflow level. The wash water addition is measured using an electromagnetic flowmeter, together with the integral opening assembly, this flow rate is controlled by a pneumatic valve (Calisaya et al., 2012). The rate of airflow is measured by a mass flow meter, after the measured signal has been received, a pneumatic valve is used to control the airflow rate.

3.3.2 Mathematical models of the Flotation System

Since one of the specific control objectives in the column flotation process is to keep the froth layer height (h); the air holdup in the collection zone (ε_{gcz}) and the bias (Q_B) at desired values, by manipulating the wash water (Q_W), the air (Q_g), and non-floated fraction flow rates (Q_T), the flotation column is often modeled as a multivariable interacting process. The main control variables that mostly affect the performance of the flotation process are froth layer height, the air holdup in the collection zone, and bias. In terms of controlling the flotation process the flow rates of wash water (Q_W); flow rates of air (Q_g); and non-floated (Q_T); can be selected as manipulated variables for keeping the controlled variables: froth layer height, air, and bias at the desired values, (Persechini et al., 2004). This is done to make sure that the flotation process can constantly have stable operation conditions.

They are many reviewed models that can be used for a flotation process study, the important thing is to identify the system model for each study and the area of focus. (Nakhaei et al., 2010), presented a column flotation with the Neural Network (NN) model for accurate estimation of the effects of operational variables within column flotation plants. (Nakhaei et al., 2010), claims that the method used and its related results can be used as a skilled system in column flotation plants, to optimize the process parameters and to evaluate their interactions, for the expected Cu grade without having to conduct the new experiments in the laboratory.

The state of the system needs to be identified before control actions or approaches are taken. Generally, once the state of the system has been determined an appropriate control action must take place. Similar to most processes, column flotation behaviour is dependent on the usual operating conditions. For example, the tail's flow rate influence on froth depth is dependent on the airflow rate value (Bouchard et al., 2009).

For the flotation column system controlled and manipulated variables always need to be considered. In general, the most important variables that need to be considered/ observed are as follows: column Froth Layer Height (h), Air holdup, Feed pulp flow rate, and Wash water flow rate.

Controlled and Manipulated Variables

This section aims at clarifying the importance of managing the characteristic of the column flotation process. As mentioned before the column flotation process has variables that need to be controlled which are: Froth layer height *h* (Pulp-froth interface), Air holdup in the collection zone, and Bias. and the process flow rate variables that need to be manipulated are the Wash-water flow rate added at the top of the column, non-floated fraction, and Air flow rate. Experimental flotation columns are mostly composed of transparent acrylic with specific internal diameter, height, and related instruments. (Persechini et al., 2000) propose an instrumental flotation column as shown in Figure 3.4.

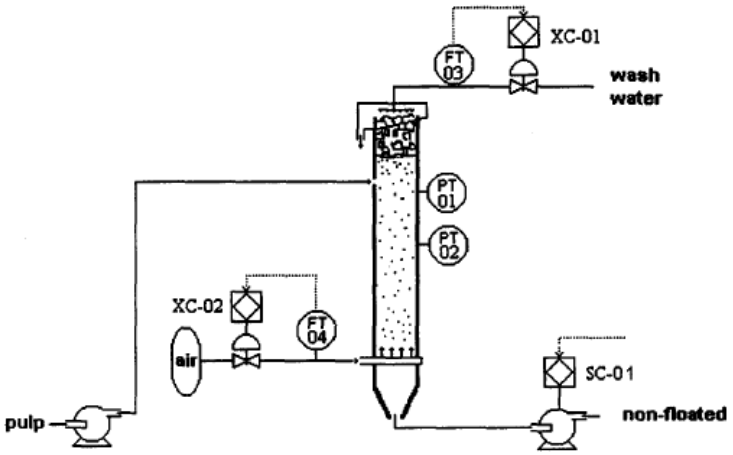

Figure 3.4: **Representation of Flotation Column (Persechini et al., 2000)**

According to Figure 3.4 shown above, the measurement of the wash water flow rate is undertaken by means of an electromagnetic flowmeter labeled as FT-03, with an integral opening assembly. A pneumatic valve labeled XC-01 controls the flow rate of the wash water. A mass flowmeter indicated as FT-04 is used to measure the airflow rate. The airflow rate is manually controlled using a flowmeter to set its desired value. The non-floated flow rate is also controlled by a variable speed peristaltic pump indicated as SC-01 in Figure 3.4 driven by a frequency inverter, said (Persechini et al., 2000). As Equations (Eq. 3.1 - 3.4) indicated, the values of the air holdup in the recovery zone and the froth layer height are calculated using the pressure elements indicated as PT-01 and PT-02, (Persechini et al., 2000).

To be able to model and design a controller for the flotation column process, it is important to understand all operational zones of the column flotation shown in Figure 3.4. Based on instrumentation and level flotation control as reviewed by (Shean & Cilliers, 2011), it is essential to gather useful information about the input disturbances, and process operating parameters. The required final product quality is measured before performing optimisation and system control. Good process understanding, with the quality of measured information, mainly defines the competence of an implemented control system.

However, instrumentation for measuring important parameters like ore composition, flowrates, less ore-specific properties, and essential properties like surface chemistry, bubble size distribution, bubble lifting, and so on remains difficult to measure and conclude (Bergh & Yianatos, 2011). To reject the effects of input disturbances, this paper suggests Advanced Flotation Control (AFC). According to De Villar et al., 1999, two PI controllers were constructed to control the two-phase system, and the frequency-response tuning method was used to tune both PI controllers.

Froth zone: (Froth layer height h or Pulp-froth interface)

The flotation process includes froth flotation, which is a significant variable. It was first utilized in the early twentieth century and is one of the most useful separation methods in mineral processing, according to experts (Vieira et al., 2007). The froth zone is a floating bubble layer with a froth depth of nearly 1 m that is contacted with wash water counter-currently. The distance between the top of the column and the point of the pulp-froth interface is measured in froth depth. It establishes the distance between the cleaning and collection zones. As a result of its integrating dynamic behaviour, it must be closely monitored and controlled for stable column operation. (Maldonado et al., 2010).

The Froth layer height is given by the following equation

$$h = \frac{P_1 H_2 - P_2 H_1}{(P_1 - P_2) + \rho_{fz} g (H_2 - H_1)} \quad (3.1)$$

Where H_1 = 230 cm*, and* H_2 = 350 cm which are pressure meter distances from the top of the column, P_1 and P_2 are the pressure measured values, ρ_{fz} the average value of the froth layer density. According to (Persechini et al., 2004) average value of the froth layer density (ρ_{fz}) is not measured but estimated as a function of the froth layer height (froth layer density was estimated by (Persechini et al., 2004) to be: ρ_{fz}=ρ_w = 1g/cm^3).

It has been noted that the height needs to be calculated to know the pulp levels in the cleaning zone.

To calculate the froth layer height, it is important to understand the average value of the froth layer density. As the value of froth layer density is not measured, it can be established indirect (inferred) from the relation of (Persechini et al., 2000):

$$\rho_{fz} = \frac{\int_0^h \rho(z)dz}{h} \quad (3.2)$$

Where $\rho(z)$ is a density variation function along the axial direction z, characterised by the longitudinal axis with the starting point at the top of the column. Since there is no presented equation for$\rho(z)$, it is necessary to use an experiment to find a function that can represent the average density (ρ_{fz}), in face of the variations of the front layer height, air, and water flow rate. The experimental flotation column in reality is made up of a see-through acrylic tube that allows one to see and record the actual interface position. As a result, the operator can measure the froth layer height at the same time as collecting data. Through experiments, it is possible to determine or measure the values of the froth layer height at the same time along with the pressure gauges. Then if the front layer density is not estimated; it can be calculated from equation 3.2 (if froth layer height is known), by manipulating to get equation 3.3 as shown below.

$$\rho_{fz} = \frac{P_1(H_2-h)-P_2(H_1-h)}{gh(H_2-H_1)} \quad (3.3)$$

According to the findings, the average froth layer density can be approximated as a function of layer height $(\rho_{fz} = F(h))$.

Air holdup in the collection zone

The gas volume proportion within the collection zone is represented by air holdup. The air is frequently used as a flotation mixture, and specialists have been interested in applying the air hold-up to monitor the gas spreading distribution throughout the column (Bouchard et al., 2009). According to (Persechini et al., 2004), the air holdup in the collection zone is calculated as shown in Equation (3.4)

$$\varepsilon_{gcz} = 1 - \frac{\Delta P}{\rho_{sl} g \Delta H} \quad (3.4)$$

Where: ΔP is the pressure difference between P_1 and P_2, ΔH the distance between the two pressure meters, and lastly pulp density (ρ_{sl}). (Persechini et al., 2004) claims that the value of ρ_{sl} can be considered constant for water-air systems and approximately given by $P_w = 1g/cm^3$ in the whole recovery zone.

(Calisaya et al., 2012) assumed no solid conductivity and considered measuring air hold-up sufficiently close to the interface.

Bias (Non-floated).

The bias is represented by the following equation (3.5)

$$Q_B = \frac{A(H_t - h)\dot{\rho}_{cz} - Ah\dot{\rho}_{cz}}{\rho_w} + Q_T - Q_F \quad (3.5)$$

Where: A is the column section, H_t is the total height of the column, and P_{cz} is the average density within the recovery zone which can be calculated by Equation (3.6)

$$\rho_{cz} = (1 - \varepsilon_{gcz})\rho_{sl} \quad (3.6)$$

As known ε_{gcz} is the average air holdup for the collection zone, which can be assumed to be the air holdup calculated in equation 3.4.

Table 3.1 below aims to show the interaction between the controlled and manipulated variables as discussed by (Persechini et al., 2004), (Vieira et al., 2007), (Calisaya et al., 2012), and many more as discussed in the literature review. They are three controlled variables that strictly affect the grade and the recovery in the flotation column.

Table 3.1: Flotation Process variables (Vieira et al, 2007)

States	Manipulated	Controlled Variable set-point	Disturbances
Height (*H*). Feed pulp flow rate. Air holdup. Wash water flow rate.	Flowrate for a Wash-water valve, Non-floated fraction, and Air flowrate	Froth layer height *h* (Pulp-froth interface). Air ($\varepsilon_{gc}{}^{sp}$) holdup in the collection zone. Bias.	Feed pulp flow rate. Wash water flow rate. Feed pulp density ρ_{fz}. Reject pulp density ρ_{fz}.

In the Flotation modeling process, it is important to know the input flowrates: Q_W (wash water); Q_g (air), and Q_T (non-floated fraction) that influence the air holdup behaviour.

3.3.3 Flotation Column Plant description: Case study II

According to (Bergh & Yianatos, 2003), the main objectives in flotation column systems are concentrate grade and column recovery. They (Concentrate grade and recovery) indicate process productivity and product quality indices. Importantly we discuss the flotation models for this process control. This section discusses the controlled variables of the flotation column.

As indicated previously, the flotation column process is characterised by specific variables, namely froth height, bias rate, gas hold-up, and bubble size. The diagram representation of the flotation column is shown in Figure 3.5 below.

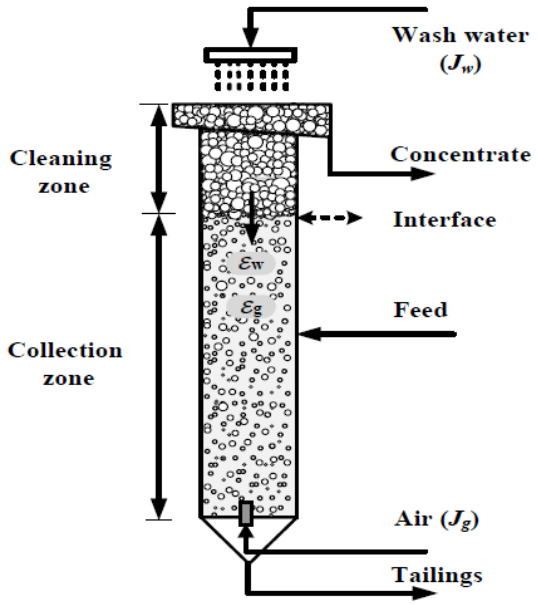

Figure 3.5: Representation of Flotation Column (Calisaya et al., 2012)

The important variables that are with the column flotation shown above (Figure 3.5), are defined, and briefly analysed as per the following paragraphs:

Froth Depth: this variable corresponds to the distance between the top of the column and the position of the pulp froth interface. It determines the relative height of the collection and the cleaning zones. This variable behaves as an integrator, it must be carefully monitored and controlled for a stable operation, (Bouchard et al., 2009).

Wash Water: this is the addition of a fine spray of water to the top of the flotation column, on the surface of the overflowing concentrate stream. This is done to stabilize the froth and make the final removal of useless bubble particles from the concentrate launder easier. The achievement of wash-water takes place if an appropriate water mass balance is existing in the lower part of the column, (Calisaya et al., 2012).

Gas Hold-up: is the volumetric segment of gas measured within the collection or air zone. Where the volume might refer to the whole zone (overall gas hold-up) or part of it, (local gas hold-up). The final relation for measuring the gas hold-up is as shown in Equation (3.7).

$$\varepsilon_g = 100\left(\frac{k_{sl}-k_{sgl}}{k_{sl}-0.5k_{sgl}}\right) \qquad (3.7)$$

Where k_{sl} is a pulp conductivity only (solid and liquid) and k_{sgl} is the pulp-gas mixture conductivity. Siphon and open cells as respectively shown in Figure 3.6 are used to measure the conductivities of this pulp.

Bias Rate is the net downward water stream of wash water from the cleaning zone to the collection zone.

Bubble size: A Bubble Size Distribution (DSB) is formed by bubbles of various sizes, as seen in Figure (3.6). The collection of mineral elements by bubbles is greatly dependent on the amount of froths surface available as they pass through the column. Therefore, the bubble surface and bubble ascending speed are important in the successful operation of the flotation system.

(Calisaya et al., 2012), propose the schematic diagram represented in Figure (3.6), showing the three input streams.

1. Pulp Feed.
2. Air Injection.
3. Wash-water addition.

The schematic diagram also shows the two output streams.

1. Concentrate.
2. Tailing.

Within normal operations of the floatation column, the column content shows two distinct regions in terms of the amount of air content.

1. The collection zone is in the lower part of the column, with less than 30 % air content.
2. The Cleaning zone is in the upper part of the column, with more than 70 % air content.

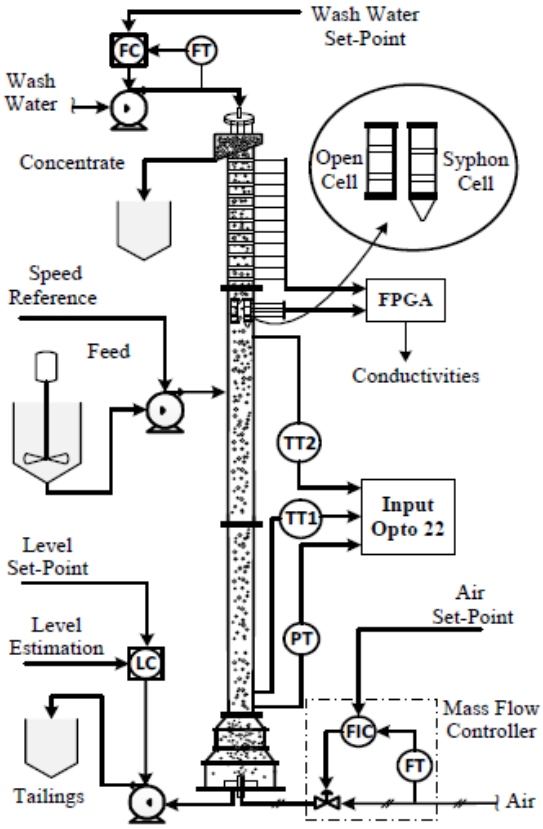

Figure 3.6: **Diagram representation of the pilot flotation column (Calisaya et al., 2012)**

The pilot flotation column developed by (Calisaya et al., 2012) has a height of 7.32 meters and a diameter of 151 millimeters, including feed and tailing ports, a froth overflow launder, a pierced ring for adding wash water over the froth, and an absorbent sparger at the bottom for air injection. All the transfer functions used for the simulation of this plant are presented in the publication of (Calisaya et al., 2012).

(Calisaya et al., 2012) presented a fully automated column, with local control loops to regulate all flow rates (tailings, wash-water, and air) and froth depth, as shown in Figure 3.6. A Controller for controlling hydrodynamic variables ($\mathcal{E}_w$ and $\mathcal{E}_g$) and the necessary sensors for measuring all relevant variables. A profile-based sensor is one of the conductivity sensors used to measure froth depth. This is determined by an algorithm that uses a bigger slope approach, and the conductivities are measured by a Field-Programmable Gate Array (FPGA). The variables considered are the gas hold-up and the percentage of wash water below the interface. Further attention is developed with the focus on discovering the connection between foam depth, gas holdup, wash water fraction underneath, and cleansing moisture content material and the metallurgical and financial overall performance of the plant.

The final objective focus on the real-time implementation of a full-scale column. The following Table 3.2 is based on the comparison of the different column flotation processes:

Table 3.2: Application of different column flotation processes

Paper	Model/ mass balance	Technology used	No of variables	Remarks
Calisaya *et al*., 2012 *"Multivariable Predictive Control of a Pilot Flotation Column"*	MPC toolbox: Hydrodynamic variables are controlled through a constrained model predictive control (MPC) strategy.	MatLab System Identification Toolbox. (Prediction error minimization method is used to identify process transfer functions).	In the collection zone, the measured variable is the gas hold-up and the wash-water fraction is measured underneath the interface.	Find relationships between, gas holdup, froth height, and wash water fraction underneath the interface.
Shean and Cilliers., 2011. *"A review of froth flotation control*"	Review of four essential levels of process control	The name of the software used is stated.	Basic, advanced, and optimization flotation control are all topics covered in this paper.	Reports of fully automated advanced and optimizing flotation control systems successfully functioning for extended periods are still rare to find despite significant advancements in base-level controls.
Vieira S.M, *et al., 2007*. *"Real-Time Fuzzy Predictive Control of a Column Flotation Process"*	*Fuzzy modelling and* MPC	PLC for instrument connection, PC, with no software name declared.	Froth layer height and air holdup control	It is noticed that the controlled variables took some time to reach the reference, but the nature of this process is generally slow process.
Persechini *et al., 2004*. Control strategy for a column flotation process.	Modeling and PI control strategy for a column flotation	Simulation results are available, but not clear which software tools are used, and no runtime results are shown.	Froth layer height, Air hold up, and the bias.	A real-time operational system was stated, but not practically done.
Vera *et al.,* 2002. *"The modeling of froth zone recovery in batch and continuously operated laboratory flotation cells"*	To integrate methods for modeling froth zone performance in batch and constant operation in laboratory flotation cells.	Data required from the industrial cells are measurable through, the prediction of the froth zone performance of large industrial cells in plant operation.	Concentrate volumetric flow rate, pulp density, froth quantity, gas rate, and bubble size distribution	Pulp and Froth phases are considered. How does the bias flow-rate influence the other parts of the system that must be investigated?
Carvalho and Durao (2002). "*Control of a flotation column using fuzzy logic inference".*	Two pressure sensor measurements.	MATLAB Fuzzy Logic Toolbox	Air and water flow rate control.	Height and air holdup are estimated using two pressure sensor measurements. The bias water flow rate is estimated from underflow and feed flow rates
De Villar *et al.,* 1999 *"Automatic control of a laboratory flotation column"*	Regulation of all flow rates.	Variable-speed Masterflex peristaltic pumps are used for liquid pumping. The data acquisition was performed by SCADA software. The exchange of data between the computer and the instruments is done through an Analog Devices card.	Two variables are controlled, but this can be extended.	It is not clear what simulation software was used for testing the operation. However, the tests were completed on a two-phase system, and the whole procedure used can now be extended to a three-phase system.
Itoh *et al*., 1998 A Paper-Quality Monitor	A Quartz crystal tuning-fork tactile sensor is used as a sensing mechanism.	The tuning forks in tactile sensors were used to increase the impedance of	The paper-type sensor was used as a measuring device	It may be concluded from the findings that this sensor may be used as a paper-quality sensor capable of sensing the mixing ratio

Paper	Model/ mass balance	Technology used	No of variables	Remarks
Using a Quartz-Crystal Tuning-Fork Tactile Sensor.		quartz crystals in resonance vibrations to detect the quality of the paper.	(HP-4195A Impedance analyser).	of pulp to recycle paper in industrial processing.
Bergh et al., 1998. *"Fuzzy supervisory control of flotation columns"*	Conventional PID distributed control simulator, Dynamic simulator, Supervisor simulator, and Metallurgical static simulator.	Four coupled simulators are used for the flow of information.	Control of froth depth, air flow rate, and wash water flow rate.	As influenced by process rules associated with concentrated grade and process recovery, the amount flow rate can be determined by operating variables.
Sastri *et al.,* (1998). *"Flotation column theory and practice"*	The current flow of slurry and air bubbles	Regional Research Laboratory (RRL) in Bhubaneswar	Two variables being controlled	In the early stages, column operation and design are primarily empirical. However, as the number of commercial facilities increased, methodical research has been conducted. The manual addition of wash water still needs to be improved to automation in this paper.
Bergh & Yianatos, *1993*. *"Control alternatives for flotation columns*"	Conventional PID and present model-based control cannot optimise the process in a narrow region of operation.	Rotameters are used for measuring gas and tailing flow rates. Valves are used for controlling the flow.	Froth depth, bias, and gas holdup are the controlled variables.	Control based on logical rules is shown to be ineffective in regulating the dynamic evolution of control variables with experimental flotation. In addition, the use of manual regulation requires human involvement during process operation, which is a main disadvantage of the applied scheme.

3.3.4 Summary of the reviewed

In conclusion, column flotation and measurements of a column system have been discussed and the significance of the major variables within this process are discussed and tabled in Table 3.2. Due to research interest, the emphasis is given mostly to the column flotation system model.

3.4 Conclusion

The flotation system has proven to be a complicated MIMO system, it is in the froth phase that the essential processes of particle transport to the concentrate launder and drainage to remove gangue entrainment occur. Many of the novel flotation technologies developed since the 1980s are aimed at improving methods of contacting air bubbles and treated mineral particles in the pulp phase, the froth phase has been recognised as a region that contributes significantly to the final flotation performance.

To solve the problem of column flotation MIMO system, a better understanding of the interaction among processes is required, and obtaining adaptable controllers is essential because this system is unpredictable. The next chapter is based on the flotation process of mathematical modeling. It is important to select and model the open behaviour of the column flotation system for the understanding of the system behavior.

CHAPTER FOUR:
DEVELOPMENT AND SIMULATION OF MULTIVARIABLE MODELS OF THE FLOTATION COLUMN PROCESSES

4.1 Introduction

The mathematical modeling of the column flotation system is discussed in this chapter. To develop a deep understanding of the system's behavior, the column flotation system model and dynamic features are evaluated. The system's dynamic behaviour based on numerous changes in the input circumstances is evaluated. The analysis of the open-loop system under study is performed based on the Matlab/Simulink simulation environment. Analysing the operation of this process it is noted that good paring needs to be achieved between the manipulated and the controlled signal. There are three considered important control signals such as wash water valve; the air valve; and the signal sent to the peristaltic pump for the non-floated fraction valve. These valves are used to manipulate the input flow rates.

Column flotation systems consist of more than one control loop, interrelating with each other, and these systems are called Multi-Input Multi-Output (MIMO) systems or multivariable systems. The idea of controlling this multivariable system is to manipulate various input variables at the same time to achieve the desired performance of several output variables. Controlling these processes is difficult since nonlinear processes lack many of the attributes of linear systems, and thus no systematic method can be utilized due to the various types of nonlinearities. Mathematical development and simulation of multivariable models of the flotation column processes are performed in this chapter. The results from the analyses are validated using Matlab/Simulink.

The chapter's organisation is as follows: Section 4.2, presents the problem formulation of column flotation systems, and the derivation of the controlled variables within this system is described. In section 4.3, a simulation of an open-loop column flotation process for different case studies based on scenario 1 (Low, average, and high level of the manipulated variables) is presented. In section 4.4, a simulation of the open-loop flotation column behaviour for different case studies of scenario 2 in which one variable is changed at a time is performed and the results are presented. The addition of the model to 3x3 (consider more variables within the column), maximises the interaction, the simulations of the 3x3 are presented in section 4.5 for both scenarios. Discussions are presented in section 4.6, and section 4.7 presents the conclusion.

4.2 Development of the Multivariable Flotation Process Model

The main point of consideration in this section is the dynamic model of the flotation process whose diagram is shown in Figure 4.1. As stated by (Persechini et al., 2004); controlling Multiple-Input, Multiple-Output (MIMO) processes is a difficult challenge to address since controlled and manipulated variables might interact. It is commonly known that within collection and cleaning zones, a change in one manipulated variable has an impact on other controlled variables. The best combination of controlled and manipulated variables is a key factor in the process control's effectiveness.

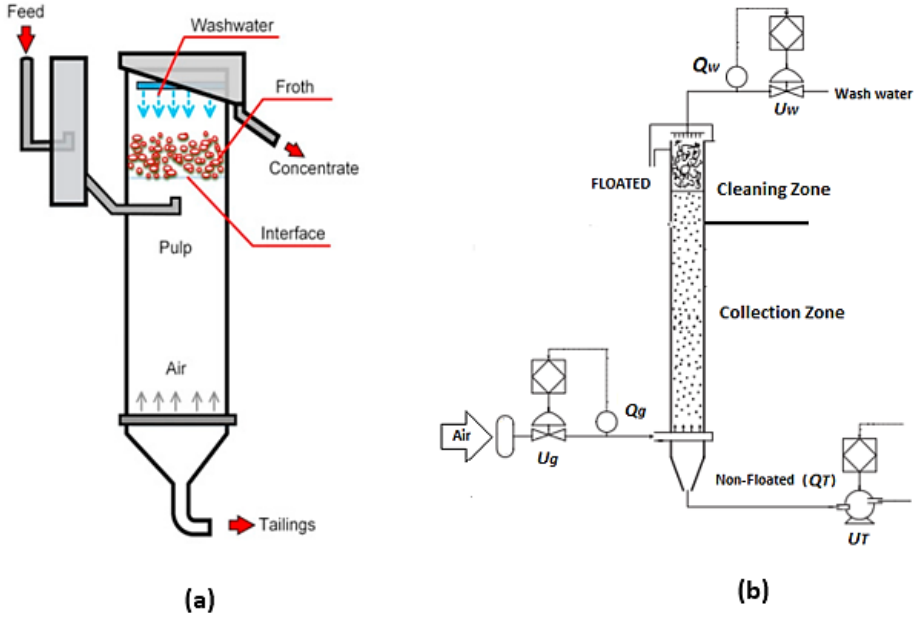

Figure 4.1: Schematic diagrams of the pilot flotation column and associated instrumentation (Tshemese-Mvandaba et al., 2021)

Figure 4.1 shown above represents the flotation column process that provides an emphasis to two zones: collection and cleaning zones. The general representation of the flotation column is shown in Figure 4.1 (a), and Figure 4.1 (b) is a modified flotation column using the variable adopted and used as flow rates in this thesis/ research. The process variables used in the diagram are described in Table 4.1:

Table 4.1: Process Variables

Measured Flowrate	Control valve or Pump valve
Q_w is the wash water flow rate measured using an electromagnetic flowmeter.	U_w is a pneumatic valve used to control the amount of Q_w.
Qg is the airflow rate measured by a mass flow meter.	U_g is a pneumatic valve used to control the amount of Q_g.
Q_T is the non-floated flow rate.	U_T is the speed of the peristaltic pump, it is used to control the non-floated fraction.

For control design, a dynamic model that represents the dominant features of the flotation process operation is presented by Equation (4.1). This is a mathematical model of the column flotation process as derived by (Persechini et al., 2000)

$$\begin{bmatrix} \boldsymbol{h(s)} \\ \boldsymbol{\varepsilon_g(s)} \\ \boldsymbol{Q_B(s)} \end{bmatrix} = \begin{bmatrix} \boldsymbol{G_{11}(s)} & \boldsymbol{G_{12}(s)} & \boldsymbol{G_{13}(s)} \\ \boldsymbol{G_{21}(s)} & \boldsymbol{G_{22}(s)} & \boldsymbol{G_{23}(s)} \\ \boldsymbol{s(K_1G_{11} + K_2G_{21})} & \boldsymbol{s(K_1G_{12} + K_2G_{22})} & \boldsymbol{1 + s(K_1G_{13} + K_2G_{23})} \end{bmatrix} \begin{bmatrix} \boldsymbol{Q_W(s)} \\ \boldsymbol{Q_g(s)} \\ \boldsymbol{Q_T(s) - Q_F(s)} \end{bmatrix} \quad (4.1)$$

Where: G_{11}, G_{12}, G_{13}, G_{21}, G_{21}, G_{23} are the transfer functions detailed by Persechini *et al*., (2000) and K_1, K_2 are the constants. In Equation (4.1) it is noted that the controlled variables are: h the froth layer height, ε_g the air holdup, Q_B the bias (fraction). The manipulated variables are Q_W the wash water inflow rate, Q_g the air input flow rate, and Q_T the non-floated fraction, which is manipulated through the respective valves. The feed inflow rates (Q_F) is assumed to be constant under this study to minimise the complexity of the control system.

The separate transfer functions are given as follows: (Persechini et al., 2000)

$$\mathbf{G_{11}} = \frac{-(\mathbf{1.029\times10^{-3}s+2.3\times10^{-5}})}{(\mathbf{s+4.02\times10^{-4}})(\mathbf{s+1.92\times10^{-2}})} \quad (4.2)$$

$$\mathbf{G_{12}} = \frac{\mathbf{-1.59\times10^{-4}s+4.33\times10^{-7}}}{(\mathbf{s+4.02\times10^{-4}})(\mathbf{s+7.981\times10^{-3}})} \quad (4.3)$$

$$\mathbf{G_{13}} = \frac{(\mathbf{1.029\times10^{-3}s+2.3\times10^{-5}})}{(\mathbf{s+4.02\times10^{-4}})(\mathbf{s+1.92\times10^{-2}})} \quad (4.4)$$

Equations (4.2 to 4.4) present the three transfer functions related to the froth layer height as will be discussed further in section 4.2.2. The rest of the value transfer functions within the flotation column are as follows.

$$\boldsymbol{G_{21}} = \frac{\mathbf{7.6\times10^{-5}}}{(\boldsymbol{s}+\mathbf{1.92\times10^{-2}})}, \quad (4.5)$$

$$\mathbf{G_{22}} = \frac{\mathbf{7.78\times10^{-5}}}{(\mathbf{s+7.81\times10^{-3}})}, \text{ and} \quad (4.6)$$

$$\mathbf{G_{23}} = \frac{\mathbf{-7.6\times10^{-5}}}{(\mathbf{s+1.92\times10^{-2}})} \quad (4.7)$$

The three transfer functions presented by Equations (4.5, 4.6, and 4.7) relate to the air holdup in the recovery zone. This is shown further in section 4.2.3.

The overall flotation column system as presented in Equation (4.1), shows the significant interaction between the controlled and manipulated variables. It can be seen that, in the matrix transfer function, the bias system is affected by the transfer functions of both the froth layer height (h) and the air holdup (ε_g) systems. With the focus on simplifying the complex flotation system in Equation (4.1) and the steady-state gains

G(t) as *t* turns to infinite the matrix transfer function from Equation 4.1 is simplified to the following Equation (4.8).

$$\begin{bmatrix} h(s) \\ \varepsilon_g(s) \\ Q_B(s) \end{bmatrix} = \begin{bmatrix} G_{11}(s) & G_{12}(s) & G_{13}(s) \\ G_{21}(s) & G_{22}(s) & G_{23}(s) \\ 0 & 0 & 1 \end{bmatrix} \begin{bmatrix} Q_W(s) \\ Q_g(s) \\ Q_T(s) - Q_F(s) \end{bmatrix} \quad (4.8)$$

According to the model provided by (Persechini et al., 2000), its validation must reach the following arrangements or conditions:

- constant feed flow rate and is equal to 20 cm^3/s.
- floated and non-floated fraction flow rate to be greater than zero.
- The height of the froth layer is between the lower and upper limits (the lower limit is 20 cm, which corresponds to the level at which the wash water is injected; the higher limit is 140 cm, which corresponds to the minimum value for which the pressure gauge is calibrated).
- This column uses a bubbly flow operation system.

To achieve these criteria, the input flow rate alternatives or variants must be regulated to particular limits.

4.2.1 Design of the input flow rates values

The input flow rates for the column flotation systems are generally designed following the model validation conditions as specified by (Persechini et al., 2000). It presents constrained conditions that are used to evaluate the validation of the process's natural/ open-loop response. These constraints are imposed on the flow rates of the non-floated fraction (Q_T), wash water (Q_W), and feed (Q_F) as listed in Table 4.2. The constraint conditions may be different based on the mineral material that is treated by the flotation process at that particular time.

Table 4.2: **Valid operational model conditions**

Constraint Conditions	Constant
$Q_W + Q_F - Q_T > 0$	$K_1 = -4.8 \times 10^4$
$Q_W + Q_F - Q_T < 0.25\ Q_g$	$K_2 = -3.8 \times 10^5$

It is noted that the manipulated variables used to control the froth layer height (h), air holdup (ε_g) and bias (Q_B), are influenced by the variable speed of the pumps. The signals are sent individually to the peristaltic pump for the non-floated fraction (U_T), the wash water valve (U_W), and the air valve (U_g), to manipulate the flow rates and then the inflow rate influences the process to the desired state. In this context, measuring the

controllable variables (which are ε_g in the collection zone, the h in the cleaning zone, and the bias (Q_B) in the non-floated region) is critical for the column flotation process. It's also critical to accurately monitor and understand how interactions between the regulated and manipulated (Q's) variables affect the overall system's dynamic performance (Bergh & Yianatos, 2003).

It is necessary to develop and understand the relationship between the flow rates (Q_T; Q_W and Q_g) and the corresponding pump signals U_T; U_W and U_g, as shown in Table 4.3 adopted from (Persechini et al., 2004), where the mathematical relationship between the flow rates and pump speed valves is given. From Table 4.3, it is possible to calculate or measure and analyse the system interactions. The constants K_1 and K_2 are determined by (Persechini et al., 2000). Within the bias model, these two constants directly affect the bias within the column. The bias is well-defined as the net sinking water flow rate through the froth layer (bias water flow rate is the net flow of wash water passing through the froth zone).

Table 4.3: **Relationship between input flow rates and their control signals (valves)**

Paper	Characteristic or parameter			
	non-floated fraction flow	**wash water**	**air flow-rate**	**bias**
Perserchini (2004)	$Q_T = 0.4U_T$	$Q_W = 0.38U_W + 3.43$	$Qg = 0.15Ug - 2.75$	$Q_B = Q_T - Q_F$ $Q_B = 0.4U_T - Q_F$
Perserchini (2000)	$Q_T = 28.9U_T$	$Q_W = 0.38U_W + 3.43$	$Qg = 0.15Ug - 2.75$	$Q_B = 28.9U_T - Q_F$

(Persechini et al., 2004), stated that several experiments were performed to find the transfer function or relationship between the input flow rates and the control signals. Based on the analysis of the corresponding data it was found that the steady-state transfer functions as shown in Table 4.3 best describe the relationship between each pair. Generation of the input flow rate signals is done following the conditions as set in Table 4.3, which are simulated here using Matlab/Simulink software. The generated input signals are presented in Figure 4.2, up to Figure 4.4 for the air-flow rate, wash-water flow rate, and non-floated fraction flow rate respectively. The outputs of the Matlab/Simulink models present the calculated input signals.

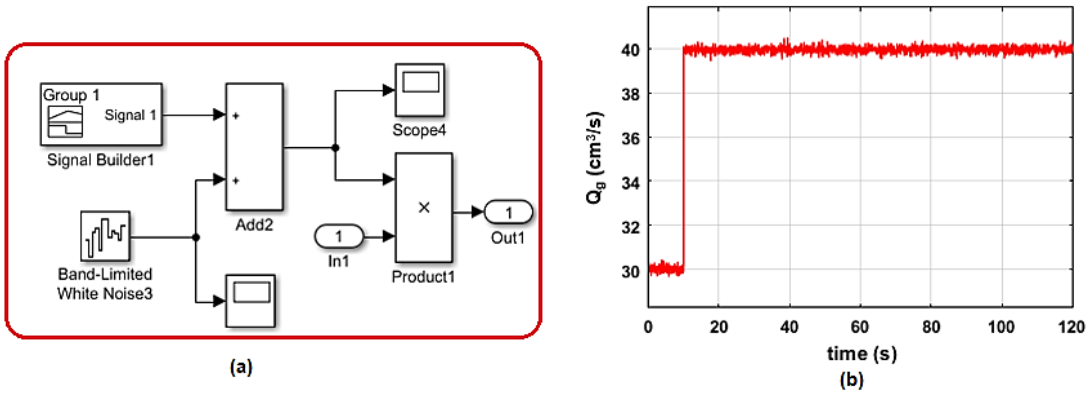

Figure 4.2: Model of the airflow and the resulting Air flowrate (Q_g) signal

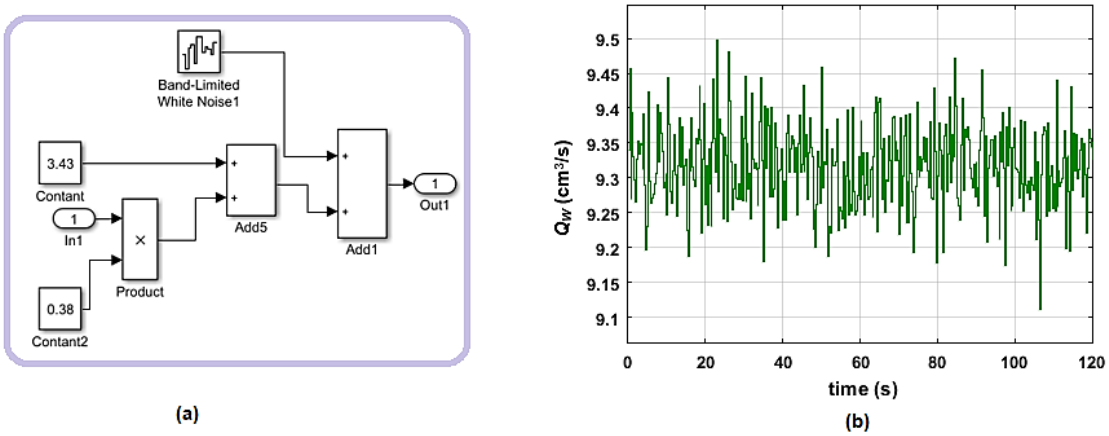

Figure 4.3: Wash water input flow rate (Q_W)

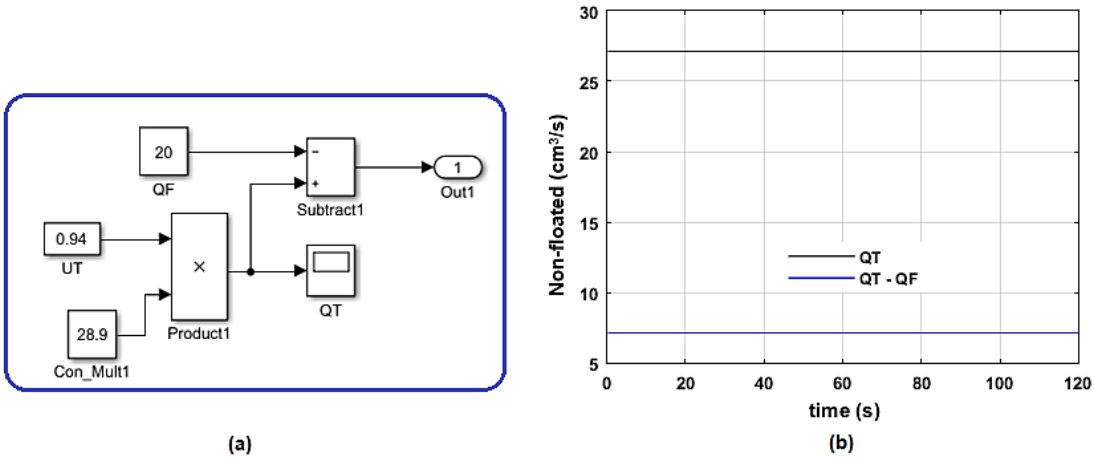

Figure 4.4: Non-floated fraction input flow rate (Q_T)

The generated input signals are used in this case study as reference conditions. The signal sent to the air valve (U_g) is used by the air holdup (ε_g) in the collection zone; a signal sent to the wash water valve (U_w) is used in deciding how much water is needed for the froth layer (h) in the cleaning zone. The following subsections present the simulation and explanation of the dynamic behaviour of the output variables in each zone within the column flotation model based on the process variables described in Table 4.1.

4.2.2 The froth layer height zone

The Laplace representation focusing on the three controlled variables, from the general pilot plant model as shown in Equation (4.1) is worked out focusing on the $h$plant model part. Concentrating on the h, the following equation is derived from the matrix Equation (4.1).

$$h(s) = G_{11}Q_w(s) + G_{12}Q_g(s) + G_{13}\big(Q_T(s) - Q_F(s)\big) \tag{4.9}$$

The transfer functions related to froth layer height as shown in Equations 4.2, 4.3, and 4.4, are then substituted into Equation (4.9), this is done to simplify and stimulate the expression of the h. It can be noted that,$G_{13}(s) = -G_{11}(s)$, then the h is:

$$\mathrm{h(s)} = \frac{1.029 \times 10^{-3}\mathrm{s} + 2.3 \times 10^{-5}}{(\mathrm{s} + 4.02 \times 10^{-4})(\mathrm{s} + 1.92 \times 10^{-2})}\big(\mathrm{Q_T(s) - Q_w(s) - Q_F(s)}\big) + \\ + \left(\frac{-(1.59 \times 10^{-4}\mathrm{s} + 4.33 \times 10^{-7}}{(\mathrm{s} + 4.02 \times 10^{-4})(\mathrm{s} + 7.98^{-3})}\right)\mathrm{Q_g(s)} \tag{4.10}$$

After several steps and substitutions, the h model represented by Equation (4.10) above is formed and simulated in Simulink. The Simulink model shown in Figure 4.5 is developed to represent the h and to simulate its transition behaviour under the step control signals (U_w, U_g, and U_T). The results are displayed in Figure 4.6. The step control signals (valve speed) are selected based on the operational system model conditions as described in Table 4.2.

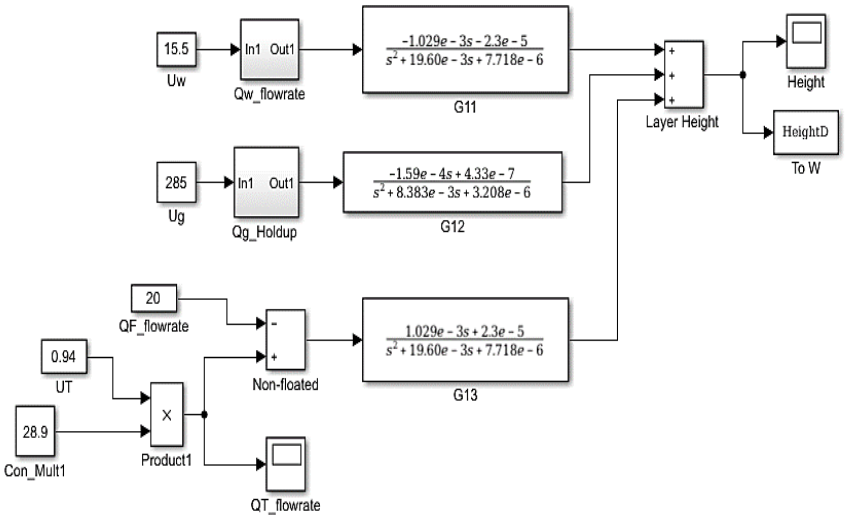

Figure 4.5: Simulink block diagram of the froth layer height (h) transfer function

The simulation results shown in Figure 4.6 represent the open-loop response of the column flotation process in the cleaning zone.

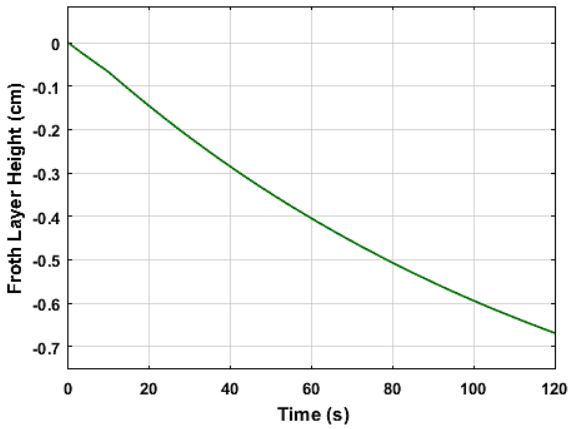

Figure 4.6: Dynamic behaviour of the h (froth layer height)

The characteristics of this process demonstrated that the time the system takes to rise is 92.0 seconds, the settling time is 116.18 seconds, the peak amplitude is 0.67 cm, and the peak time = 120s. The system response can change depending on the inflow rates that influence the behaviour of the system in the cleaning zone. Even though practically it cannot be accepted to have a negative response for the froth layer height (h), it is proven to be possible in an open-loop system due to the absence of the feedback signal. Hence, the controller design for the system under study is very important.

4.2.1 The air hold-up zone

This is the collection zone. The air hold-up (ε_g) system from the general column flotation model presented in Equation (4.1) is extracted and given by the air hold-up Equation (4.11). To model the process ε_g of the column collection zone behaviour, it is necessary to know the input flow rates (Q_T, Q_g, and Q_w) that influence the collection zone (ε_g) variables of the flotation system.

$$\varepsilon_{gcz}(s) = G_{21}Q_w(s) + G_{22}Q_g(s) + G_{23}\big(Q_T(s) - Q_F(s)\big) \tag{4.11}$$

Since G_{21} and G_{23} have the same transfer functions but are opposite in signs as shown by Equations (4.5 and 4.7), therefore, the air hold-up in the collection zone yields the following equation:

$$\varepsilon_{gcz}(s) = \frac{7.78 \times 10^{-5}}{s + 7.78 \times 10^{-3}} Q_g(s) + \frac{7.6 \times 10^{-5}}{s + 1.92 \times 10^{-2}} \big(Q_w(s) + Q_F(s) - Q_T(s)\big) \tag{4.12}$$

Equation (4.12) is expressed by substituting the transfer functions presented in Equation (4.5 - 4.7), into Equation (4.11). The Simulink block diagram of the ε_g model

is shown in Figure 4.7. The input flow rates developed in section 4.2.1 have been applied as inputs to the ε_g model. The input flow rates previously applied to the froth layer height (h) are applied again to observe the collection zone of the column flotation system. The results are shown in Figure 4.8.

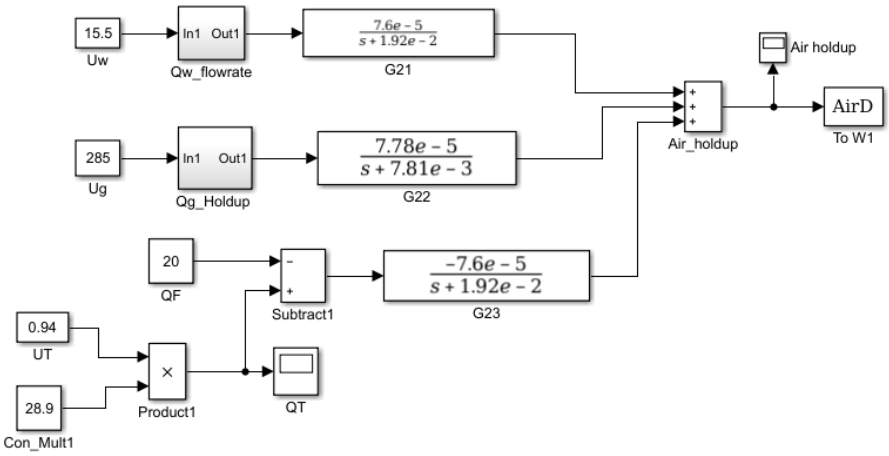

Figure 4.7: The Simulink model of the collection zone dynamic

According to Figure 4.8, the y-axis represents the amplitude of the resulting holdup and the x-axis presents the time the system took in seconds The simulation results show the behaviour of the air holdup process under the reference conditions adopted from (Persechini et al., 2000), as input flowrates values. The transition behaviour characteristics of this process show the system rise time as 91.6 seconds, the settling time as 116.15 seconds, the air hold-up peak value as 0.247%, and the peak time: as 120 seconds.

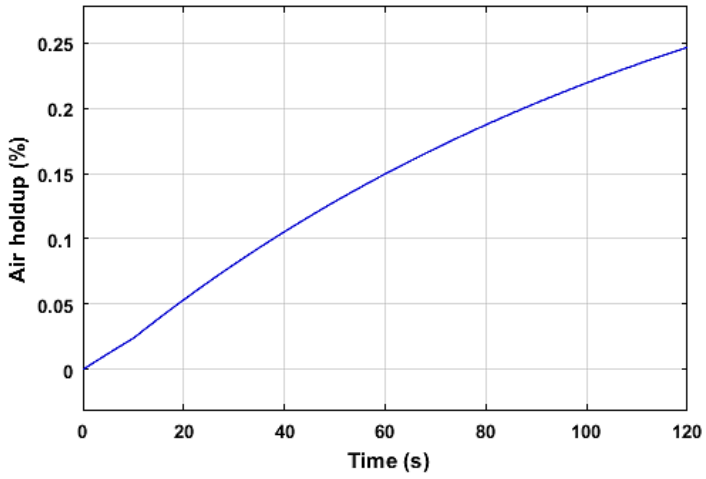

Figure 4.8: The air hold-up output dynamic behaviour

Evaluation of the flotation process reaction based on the collection zone is examined by applying more pressure into the air valve. Lastly, it can also be noted that from the feed flow through the collection zone, cleaning zone, and the non-floated, the whole

system must be considered to achieve good performance. The next part focuses on the system bias condition.

4.2.2 The Bias zone

The most important objective of the column flotation process is to keep the froth layer height, air holdup, and bias at the desired values by manipulating their input flow rates. The development of the bias (Q_B) from the general column flotation mathematical model shown in Equation (4.1), is as follows:

$$Q_B(s) = Q_T(s) - Q_F(s) \tag{4.13}$$

The final steady state of the value of the Q_B in this air-water system is affected by the non-floated fraction (Q_T) and the feed inflow rates (Q_F), which can be manipulated through their respective valves.

Equation (4.13) is programmed in Simulink to simulate the flow-rate behaviour of the non-floated zone as part of the column, by utilizing the transfer functions as presented before. The whole system under study shows the important interactions between the controlled and manipulated variables as shown in Equation (4.8). The Simulink diagram in Figure (4.9) represents the bias response.

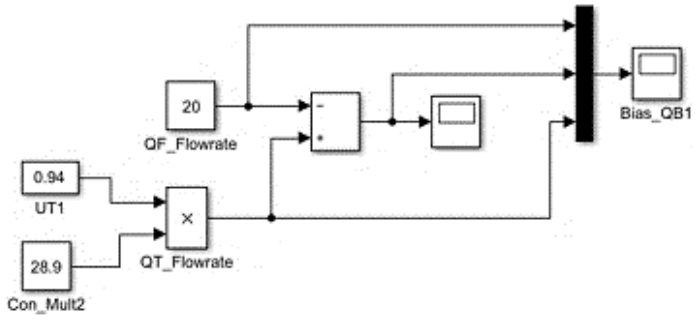

Figure 4.9: Bias Simulink block diagram

The open-loop transition behaviour of the Bias is shown in Figure (4.10).

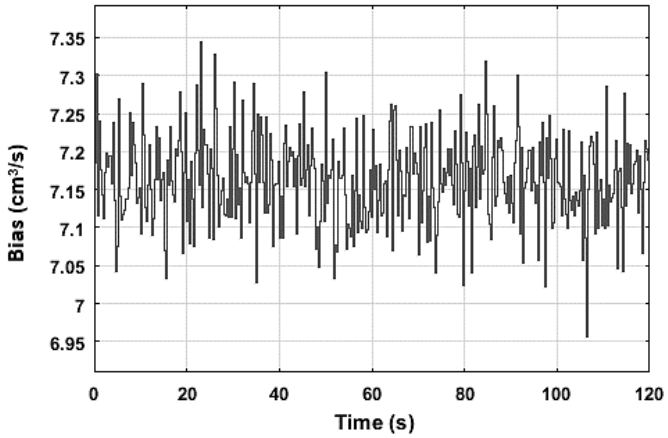

Figure 4.10: The Bias output dynamic behaviour with added noise at the output

In Figure 4.10, the y-axis represents the amplitude of the bias, and the x-axis presents the time in seconds. The characteristics of this open-loop bias response shown above have a rise time of 0.0181 seconds; a settling time is 119.95 seconds, a peak amplitude is 7.34 cm^3/s and a peak time of 22.8 seconds. The list of the characteristic behaviour of the open-loop column flotation system is shown in Table 4.4.

4.2.3 Open-loop characteristic behaviour

The open-loop simulation is completed for all three variables: froth layer height, air holdup, and bias. The important characteristics of the transition behaviour of the open-loop system are shown in Table 4.4 below.

Table 4.4: Transition behaviour characteristics of the open-loop system response

Parameters	Froth Height Value	Air holdup values	Bias (floated fraction)
Rise Time (tr)	92.0s	91.6	0.0181s
Settling Time (Ts)	116.18s	116.15s	119.95s
Peak (pv)	0.67 cm	0.247%	7.34 cm3/s
peak time (tp)	120s	120s	22.8s

The results obtained above (Figures 4.6, 4.8, and 4.10) are used as a foundation of this study for further investigation of the flotation process.

Performed case studies are presented in the following Table 4.5

Table 4.5: Case studies performed

Case Study name	Aim	The type of flowrate used	Action performed	Measured Values					
Case study Levels: Low	Investigation of the system's behaviour when all flow rates are adjusted to a lower level.	Wash water (Q_w) =4cm3/s and airflow (Q_g) are adjusted to 20 cm^3/s. To the yellow area Figure 4.12.	Use the right justification for figures, as in the next table. Remember to right-align the caption, also.	**Froth Height**			**Air Hold up**		
				93.88 s	117.16cm	0.72cm	89.89	116.1s	0.13%
Medium	Investigation of the system's behaviour when flowrates are adjusted to middle levels	Adjust all flow rates to the green range of Figure 4.12.	Adjustment of all input flow rates to the middle level of flow values.	**All the data is found in Table 4.7**					
Hight	Investigation of the system's behaviour when flowrates are adjusted to middle levels	Adjust all flow rates to the pink range of Figure 4.12.	Set all input flow rates to the highest possible values: the pink range of Figure 4.12.	**Froth Height**			**Air Hold up**		
				95.22	117.12	2.88cm	92.37	115.91	0.54%
Case study numbers: Reference	To establish the reference state of the system	Wash water =9.32 and air holdup step signal from 30-40 cm3/s	Define variable values of the valves and receive the initial input flow rates	94.926	117.20	1.62	91.516	115.9323	0.27
Case study 1 Evaluate the performance of the flotation when air is minimum	To analyze the transition behaviour of the flotation process when the airflow rate is decreased.	Decreasing the air holdup from a step signal of 30-40 cm3/s to a step signal of 5 cm3/s to 15 cm^3/s. Wash water (Q_W) = 9.32 cm^3/s.	The airflow rate is reduced to a maximum of 15 cm^3/s, and the wash water flow rate (Q_W) is kept at the reference condition.	In Table 4.9					
Case study 2 Performance of the flotation when air is increased.	Investigation of the system's behaviour when the airflow rate is increased.	Wash water (Q_W) = 9.32 cm^3/s. Increasing airflow rate (Q_g) to 80 cm^3/s.	To increase the airflow rate to 80 cm^3/s, the wash water flow rate (Q_W) is kept at the reference conditions.						
Case study 3 Evaluate the performance of the flotation when wash water is minimum.	Investigation of the system's behaviour when the wash water flow rate is decreased	The airflow rate (Q_g) is back to the reference condition (30-40 cm^3/s). The wash water flow rate is decreased from 9.32 cm^3/s to 8 cm^3/s,	Decreasing wash water from 9.32 cm^3/s to 8 cm^3/s. The Air holdup step signal is taken back to the reference condition (30-40 cm^3/s).						

Case Study name	Aim	The type of flowrate used	Action performed	Measured Values
Case study 4 Evaluate the performance of the flotation when wash water is minimum.	To investigate the transition behaviour of the flotation process when the wash water flow rate is increased	The wash water flow rate is increased.	The wash water flow rate is increased to 16 cm^3/s, the airflow rate is kept at the reference condition.	
All the case studies presented above based on two scenarios are repeated for the 3x3 model: 1. Study levels: Low-high 2. Case study number: 1-6				Simulation results for 3x3 study levels are presented in Table 4.11 Simulation results for 3x3 case study numbers are presented in Table 4.13

The next section of the chapter evaluates how the system responds to flow rates (non-floated rate, wash water rate, and airflow rate), that are being changed continuously. These adjustments are made systematically, from low rate, middle, and high (minimum, moderate, or halfway and maximum) rates of the flows for this flotation column system.

4.2.4 Development of the algorithm for the flotation process operation under different level variations of the input flow rate

Since the open-loop flotation system is under investigation, a study is introduced, to understand the system's sensitivity to inflow alterations applied simultaneously into the system. The flotation process is a dynamic system, and its behaviour depends on all flow rates. Evaluation of all flow rates is performed according to their possible ranges of minimum and maximum values for which the process can operate. Figure 4.11 is the flowchart of the technique followed to find different levels (low, middle, and high) of the input flow rates.

These levels were established through tries and errors under the conditions of the system's operational constraints as tabled in Table 4.2. Figure 4.11 is the flowchart representation to show the different levels of rates obtained. The parameter values are found through trial and error to force the flow rate into the required level of the column flotation tank. As an example, the level considered in the flowchart shown below is in the half-tank condition of the column flotation system investigated in this thesis.

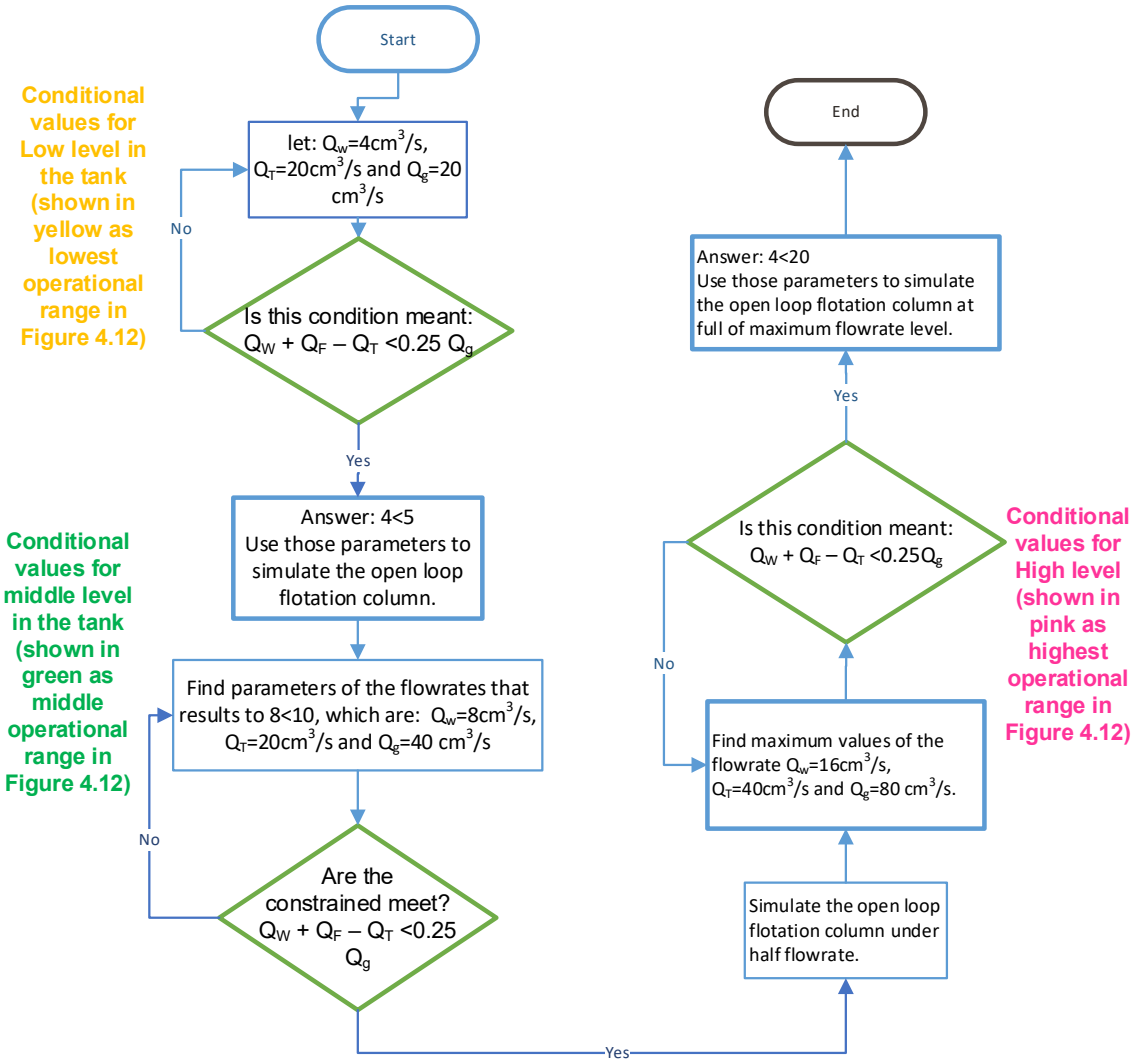

Figure 4.11: Flowchart representation of the inflow range of operation

The same procedure as demonstrated in Figure 4.11, is followed to establish all the operational ranges. The resulting operational limits are presented in the following Figure 4.12. The area shaded in yellow (Q_T =20 cm^3/s, Q_W =4 cm^3/s and Q_g =20 cm^3/s) are the minimum values of the inflow rates, the average operation range is represented in green were Q_T = 20 cm^3/s, Q_W = 8 cm^3/s and Q_g=40 cm^3/s), and the maximum flow rate area is shaded in pink (Q_T = 40 cm^3/s, Q_W = 16 cm^3/s and Q_g =80 cm^3/s), which are non-floated fraction flow, wash water and airflow respectively.

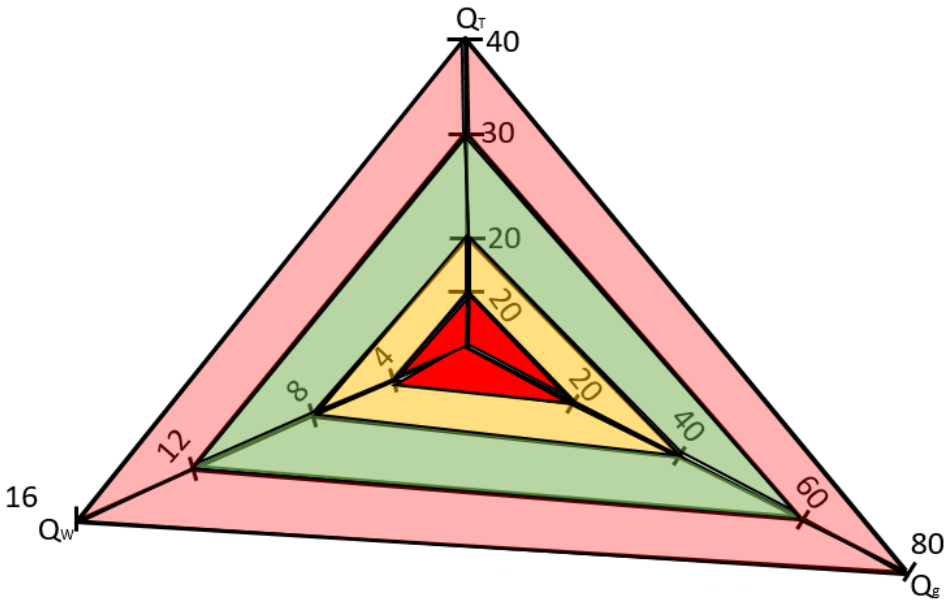

Figure 4.12: Operational ranges of the input flow rates

Each variable such as froth layer height, air holdup, and bias were independently tested respectively. The following section covers the modeling and simulation of the 2x2 column flotation model based on different levels.

4.3 Modeling and simulation of the 2x2 Flotation Column System

This section focuses on the development and simulation of the column flotation model. After the development, simplified Equations 4.16 and 4.18 are constructed in Matlab/Simulink to form a 2x2 column flotation model as shown in Figure 4.13. The values of the inflow rate are changed systematically to investigate the performance of the 2x2 column flotation process under different values of the input flow rates. The Two-Input Two-Output (TITO) model consists of the model given by Equation (4.14).

$$\begin{bmatrix} \mathbf{h(s)} \\ \boldsymbol{\varepsilon}_{\mathbf{g}}\mathbf{(s)} \end{bmatrix} = \begin{bmatrix} \mathbf{G_{11}(s)} & \mathbf{G_{12}(s)} \\ \mathbf{G_{21}(s)} & \mathbf{G_{22}(s)} \end{bmatrix} \begin{bmatrix} \mathbf{Q_W(s)} \\ \mathbf{Q_g(s)} \end{bmatrix} \tag{4.14}$$

The Laplace representation of the froth layer height resulted in the following:

$$\boldsymbol{h(s)} = \mathbf{G_{11}(s)Q_w(s)} + \mathbf{G_{12}(s)Q_g(s)} \tag{4.15}$$

Then using the transfer functions related to froth layer height as shown in Equations (4.2) and (4.3), Equation (4.15), is represented by Equation (4.16).

$$\mathbf{h(s)} = \frac{-1.029\times10^{-3}s-2.3\times10^{-5}}{s^2+19.602\times10^{-3}s+7.7184\times10^{-6}}\mathbf{Q_w(s)} + \frac{-1.59\times10^{-4}s+4.33\times10^{-7})}{s^2+8.383\times10^{-3}s+3.208\times10^{-6}}\mathbf{Q_g(s)} \tag{4.16}$$

The Laplace representation of the airflow rate is given by Equation (4.17)

$$\boldsymbol{\varepsilon}_{\mathbf{g}}(\mathbf{s}) = \mathbf{G_{21}(s)Q_w(s)} + \mathbf{G_{22}(s)Q_g(s)} \quad (4.17)$$

As Equations (4.5 and 4.6) presented early in this chapter are related to the air holdup model in the recovery zone of the flotation system, they are used here to represent Equation (4.17).

Substitute Equations 4.5 and 4.6 into Equation (4.17), resulting in Equation (4.18);

$$\boldsymbol{\varepsilon_g(s)} = \frac{7.6\times10^{-5}}{s+1.92\times10^{-2}}\mathbf{Q_w(s)} + \frac{7.78\times10^{-5}}{s+1.92\times10^{-3}}\mathbf{Q_g(s)} \quad (4.18)$$

Equations (4.16 and 4.18) are built-in Matlab/ Simulink to represent the 2x2 multivariable column flotation system model as shown in Figure 4.13.

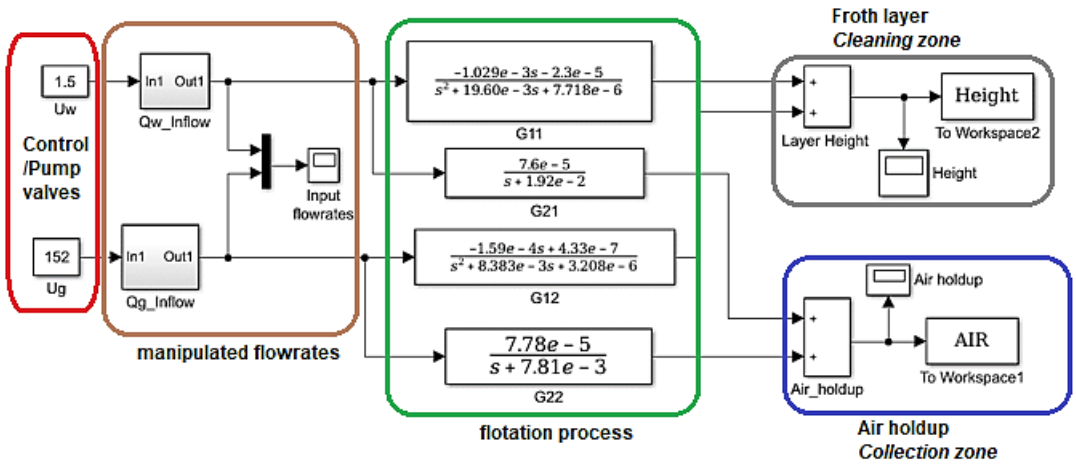

Figure 4.13: Flotation process 2x2 Simulation model

Figure 4.13 is a Simulink model that presents the 2x2 multivariable open-loop system, with different inflow levels. The acceptable minimum and maximum input flow rates of the column flotation process have been established in section 4.2 and these are accepted to be compulsory for the process to function properly. Now different levels are evaluated by changing the input flowrate systematically to investigate the performance of the flotation process under different levels within the column. The aim of the following Table 4.6 is to present the various cases to be used in the evaluation of the system behaviour under different inflow rates and valve pressures.

Table 4.6: **Case studies for investigation of the transition behaviour of the flotation process 2x2 model when all inflow rates are reduced or increased at the same time**

Cases Study	Aim	Action performed	Estimation and Measured Variables		Regions: Collection and Cleaning
			Pump Valve and manipulated variables		Regions: Collection and Cleaning
			Pump valve	Input flow	Zones
Case study 1: Low values of all inflow rates.	Investigation of the system's behaviour when all input flow rates are decreased at the same time	Reduction of all input flow rates to their minimum values that can be used.	U_w =1.5	Q_w =4	Froth Height
			U_g=152	Q_g =20	Air Hold up
Case study 2: Middle values of all inflow rates	Investigation of the system's behaviour when all input flow rates are set to their middle values at the same time	Set all flow rates to be at the middle level or half of their maximum values	U_W =12	Q_W=8	Froth Height
			U_g =285	Q_g =40	Air Hold up
Case study 3: High value of all inflow rates.	Investigation of the system's behaviour when all input flow rates are increased to their maximum values at the same time	Set all input flow rates to the highest possible values	Uw=33	Qw=16	Froth Height
			U_g=552	Q_g=80	Air Hold up

4.3.1 Simulation results for the behaviour of the 2x2 flotation system model

Investigations that were performed for the 2x2 system model are presented in this section following the conditions tabled above.

The following simulation results as shown in Figure 4.14 - Figure 4.16 are the transition behaviour of the 2x2 multivariable flotation system model for the case studies given in Table 4.6.

Figure 4.14 represents results under the low conditional values of the inflow rates. Figure 14(a) is the froth layer height resulting from the current adjustment of inflows, with a peak value of 0.7209 cm at a peak time of 120 seconds, rise-time = 93.8836, and settling time of 117.1619 seconds. Figure 24(b) shows the air holdup with a peak of 0.1323% as presented in the y-axis of Figure 4.14 (b), and this holdup response settles at 116.098 seconds.

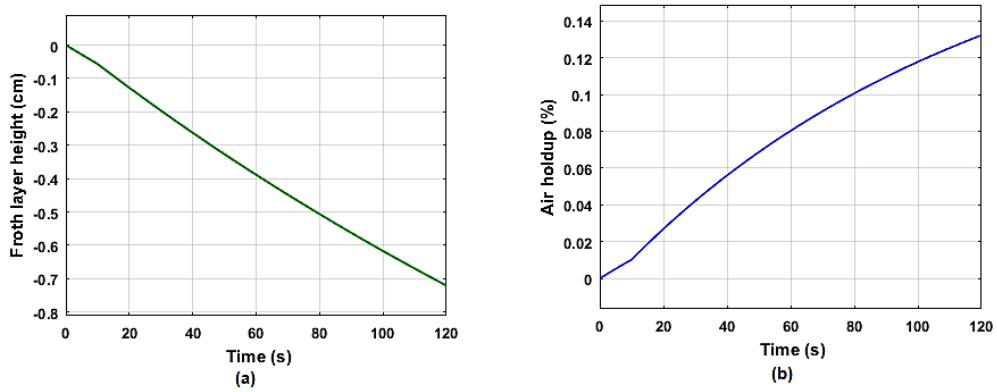

Figure 4.14: Effect of low flow rates on the transition behaviour of the flotation process: (a) The froth layer height behaviour (b) Air holdup behaviour

The next investigation is for the middle levels of the inflow rates. All flow rates are adjusted to have middle values and the results are shown in Figure (4.15). The characteristics of behaviour are tabled in Table 4.7.

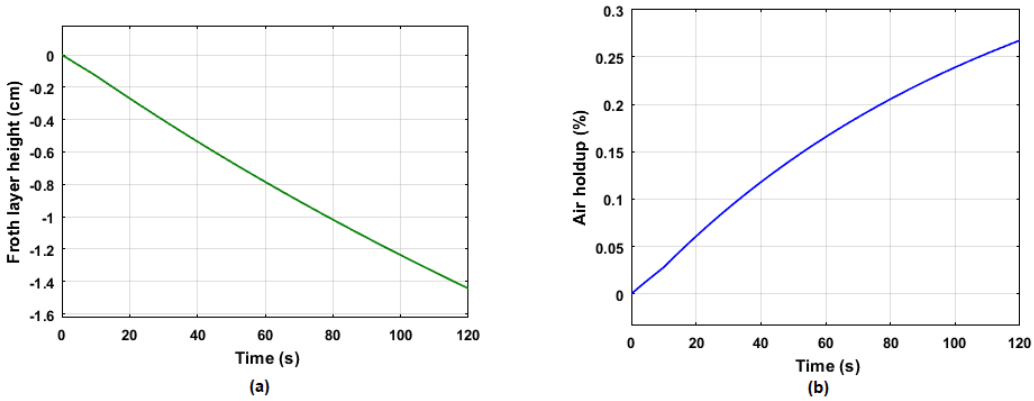

Figure 4.15: Effect of middle flow rates on the transition behaviour of the flotation process: (a) The froth layer height behaviour (b) Air holdup behaviour

The inflow rate for the wash water and airflow rate valves ($\boldsymbol{Qw}$ and $\boldsymbol{Qg}$) is increased from the middle-level position to the highest one. The simulated results are given in Figure (4.16). The amount of airflow rate applied is increased to 80 cm^3/s, and the amount of wash water is also adjusted to 16 cm^3/s for the high-level results shown below in Figure 4.16. The rising time of 95.22 seconds is recorded for the froth layer heig*ht* $\boldsymbol{(h)}$ with a settling time=117.12 seconds and a peak of 2.8886 cm as shown in Figure 4.16(a). The air holdup ($\boldsymbol{\varepsilon_g}$) is shown in Figure 4.16(b) with the rise-time= 92.3732s and settling time =115.9063 seconds with a peak of 0.5385 %.

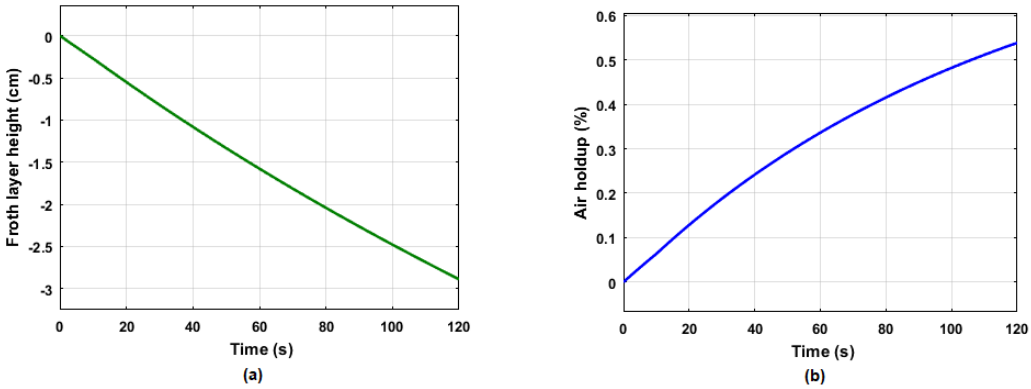

Figure 4.16: Effect of high flow rates on the transition behaviour of the flotation process: (a) The froth layer height behaviour (b) Air holdup behaviour

The following Table 4.7 shows the transition behaviour specifications of the 2x2 system model.

Table 4.7: Analysis of the transition behaviour of the 2x2 column flotation model

Case	Zones	Rise time (s)	Settling time (s)	Peak	Peak time (*s*)	Main characteristics
Case study 1: Low values of all inflow rates	Height	93.8836	117.1619	0.7209 cm	120	The system's response time is long compared to the reference condition due to the reduction applied to the input flow rates. The non-floated did not show any changes due to the reduction of the flow rates. Air holdup significantly increases due to the reduction of the inflow rates, the cause of this behaviour needs to be investigated. The system peak is reduced due to the reduction of the input flow rates.
	Air Holdup	89.8915	116.0980	0.1323 %	120	
Case study 2: Middle values of all inflow rates	Height	94.7707	117.1351	1.4430 cm	120	The hold-up response time is becoming shorter as the system level of the input flow rate increases. But the froth height in the cleaning zone increases as the pressure level increases.
	Air Holdup	91.5274	115.9710	0.2674%	120	
Case study 3: High value of all inflow rates.	Height	95.2217	117.1205	2.8886 cm	120	Rise time in the collection zone is increased, due to an increase in the flow rate applied. Only air holdup significantly reduces due to increased inflow rates. The system peak became higher for the collection and cleaning zones, due to the increase in all inflow rates
	Air Hold up	92.3732	115.9063	0.5385%	120	

4.3.2 Simulation of the 2x2 multivariable column system model

The developed open-loop flotation system based on the Two-Input Two-output (TITO) model shown in Figure 4.13, is simulated with the in-flowrates presented in Table 4.8. The emphasis is on evaluating the column flotation system's reaction to the inflow rate changes. In this case, the focus is on one flow rate variable changed at a time. Table 4.8 introduces the case studies performed.

Table 4.8: **Classification of the cases performed in a 2x2 column flotation process model**

Cases Study	Aim	Action performed	Measured Variables		
			Control and manipulated variables		Regions: Collection and Cleaning
			Pump valve	**Input flow**	**Zones**
Reference Case study	To establish the reference state of the system.	Define variable values of the valves and receive the initial input flow rates	U_W =15.5	Q_W=9.32	Froth Height
			U_g =285	Q_g =40	Air Hold up
1	Investigation of the transition behaviour of the flotation process when the airflow rate is decreased.	The airflow rate is changed from 40 cm3/s to 15 cm3/s, and the wash water flow rate (Q_W) is kept at the reference condition	U_W =15.5	Q_W=9.32	Froth Height
			U_g =118	Q_g =15	Air Hold up
2.	Investigation of the transition behaviour of the flotation process when the airflow rate is increased.	The Airflow rate is adjusted to 80 cm3/s, wash water flow rate (Q_W) is kept at the reference conditions	U_w=15.5	Q_w=9.32	Froth Height
			Ug=552	Q_g=80	Air Hold up
3	Investigation of the transition behaviour of the flotation process when the wash water flow rate is decreased.	The wash water flow rate is decreased from 9.32 cm3/s to 8 cm3/s, and the airflow rate (Qg) is kept at the reference condition	U_W = 12	Qw = 8	Froth Height
			U_g = 285	Qg = 40	Air Hold up
4	Investigation of the transition behaviour of the flotation process when the wash water flow rate is increased.	The wash water flow rate is increased to 16 cm3/s, the airflow rate is kept at the reference condition	U_W=33	Qw=16	Froth Height
			U_g=285	Qg = 40	Air Hold up

All the cases introduced in Table 4. 8 above, are simulated, and the following results are obtained, see Figure 4.17 – Figure 4.21. In a reference case study, the airflow rate is changed from 30 cm^3/s to 40 cm^3/s at 10 seconds and the wash water flow rate (Q_w) signal is at 9.32 cm^3/s. These two in flowrates are applied input to Figure 4.13 and resulted in Figure 4.17 shown below.

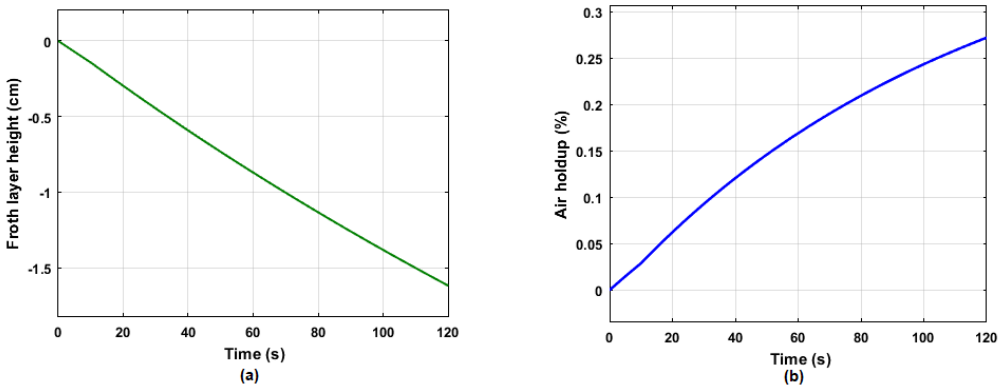

Figure 4.17: **Simulation results under reference conditions: (a) Froth layer height and (b) Air hold up**

Figure 4.17(a) shows an open-loop response of the froth layer height based on reference condition as presented in Table 4.8. This action resulted in a froth layer height with a rise-time of 94.926 seconds, settling at 117.2012 seconds. and the peak of 1.62 cm. This decrease may be explained by a lack of feedback signal for a cleaning zone and the volume of the amount of air holdup collected in the collection zone as presented in Figure 4.17(b) with a peak of 0.27% at the time of 120 seconds.

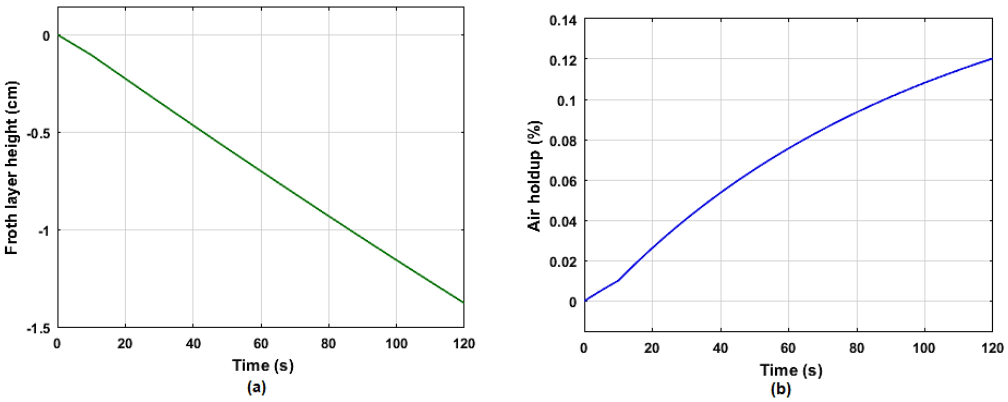

Figure 4.18: **Case study 1: Simulation results of (a) Froth layer height and (b) Air hold up**

The amount of airflow rate is reduced to 15 cm^3/s, and due to that small movement of liquid from the collection zone to the cleaning zone, the same effect may be verified in the test results represented in Figure 4.18 for case study 1. In this case, the rising time of 94.74 seconds is recorded for the froth layer height with a settling time=117.4855 and a pick of 1.3775 as shown in Figure 4.18(a). In Figure 4.18(b) above, the air holdup rise-time= 88.9727s and settling time =115.7223 seconds with a peak of 0.1203%. The column did not reach the accepted steady state due to the lack of liquid levels and the feedback signal.

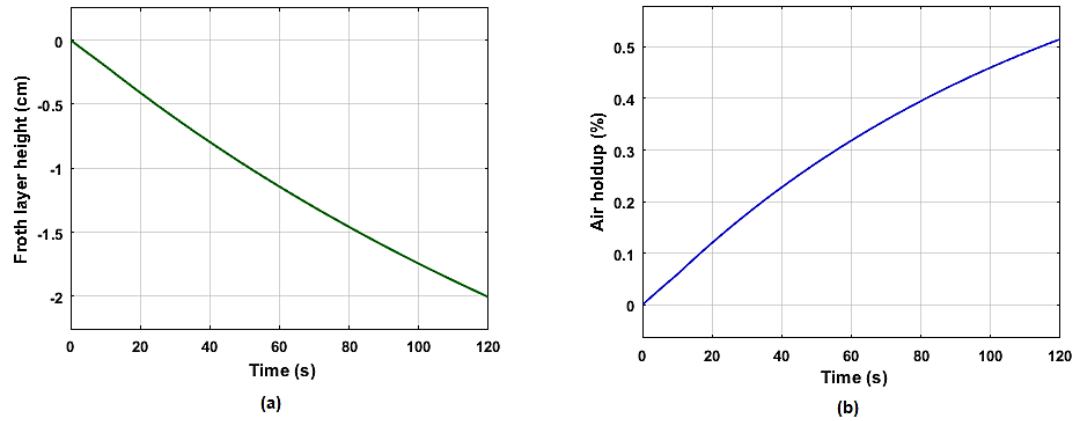

Figure 4.19: Case study 2: Simulation results of (a) Froth layer height and (b) Air hold up

The amount of airflow rate is increased to 80 cm^3/s, while the amount of wash water remained the same for the test results represented in Figure 4.19 for case study 2. In this case, the rising time of 94.55 seconds is recorded for the froth layer height with a settling time=116.809 seconds and a peak of 2.006 cm as shown in Figure 4.19(a). In Figure 4.19(b) above, the air holdup rise-time= 92.505 s and settling time =116.054 seconds with a peak of 0.5148 %.

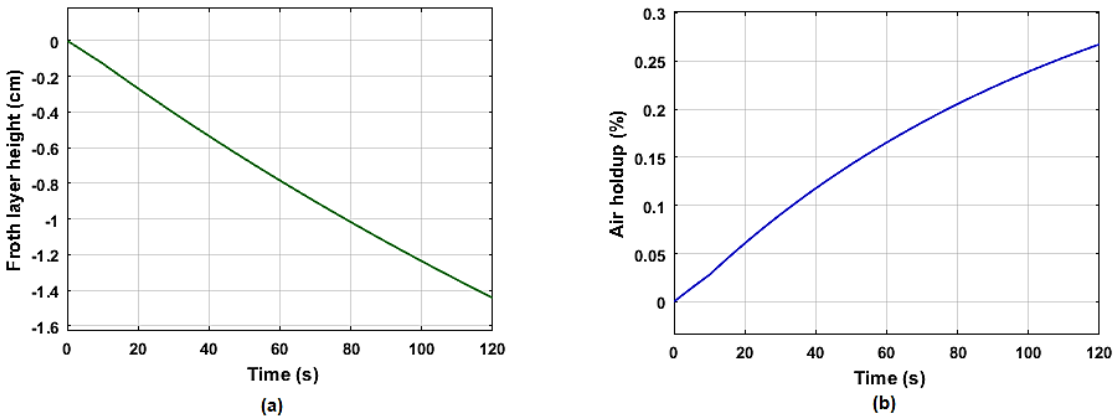

Figure 4.20: Case study 3: Simulation results of (a) Froth layer height and (b) Air hold up

In case study 3, the airflow rate is returned to a step change of from 30 cm^3/s to 40 cm^3/s at 10 seconds and the wash water flow rate ($\boldsymbol{Qw}$) is decreased to signal at 8 cm^3/s. The test results of this case are represented in Figure 4.20(a) for a froth layer height ($\boldsymbol{h}$) and Figure 4.20(b) presented the air holdup ($\boldsymbol{\varepsilon_g}$) response in the collection zone. It is noted that the reduction in wash water flowrate, caused the rise-time of the $\boldsymbol{h}$ to be slow, time = 94.7707 seconds, and the settling-time increased to 117.1351 seconds with the peak dropping to 1.443 cm, as shown in Figure 4.20(a) with the peak time of 120 seconds. On the other hand, as the wash water flow rate drops, causes a reduction of $\boldsymbol{\varepsilon_g}$ in the collection zone. See, all the characteristic test results as presented in Table 4.9.

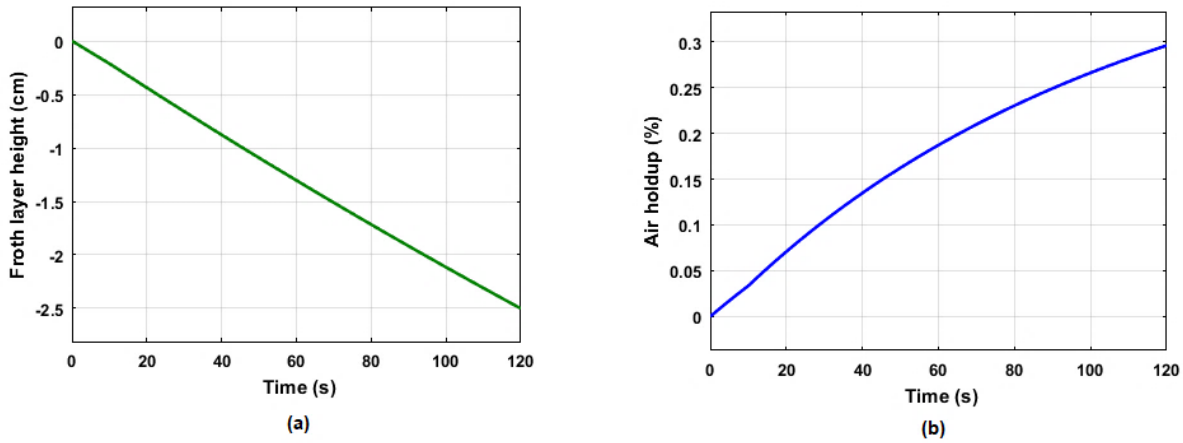

Figure 4.21: **Case study 4: Simulation result of (a) Froth layer height (b) Air hold up**

In all the specific cases as tested at this point (section 4.2), the column did not reach steady-state due to the lack of the liquid level, amount of air applied, and lack of the controller. Therefore, the focus of this thesis is to design the controllers that are aiming at improving or correcting the system behaviour to be at the acceptable or validated operation as was presented in section 4.2.

Table 4.9: **Performance of a 2x2 column flotation process model under the case studies 1 to 4**

Case Study	Zones	Rise time (s)	Settling time (s)	Peak	Peak time (s)	Main characteristics		
						Settling time	Rise time	Peak
ref	Froth Height	94.9264	117.2012	1.62	120	The results taken here are used as a reference or a baseline for all the following case studies performed.		
	Air Holdup	91.5162	115.9323	0.27	120			
1	Froth Height	94.74	117.4855	1.3775	120	The system's settling time became slightly longer as the air pressure is reduced.	The system's rise time in the cleaning zone has increased as the air pressure is decreased.	The peak became shorter for the air Holdup varied from 0.2721 to 0.1203%, and decreased for the height: 1.6195-1.3775 cm. This is expected when the pressure valve releases less amount of air.
	Air Holdup	88.9727	115.7223	0.1203	120			
2	Froth Height	94.55	116.809	2.006	120	The system in the collection zone reduced its settling time due to the increased volume of the airflow rate.	The Froth layer height is slightly shorter now and the holdup response time is slower, as the gas flow rate increases	An increase in air flow rate has caused an increase in the froth layer height. From 1.3775 *cm to* 2.0063 *cm* for height, and air peak increased from 0.1203*% to* 0.5148*%.*
	Air Holdup	92.5053	116.054	0.5148	120			
3	Froth Height	94.7707	117.1351	1.4430	120	An increase in the froth layer height and holdup slightly decreases or took a little less time, as per the decrease in wash water inflow rate.	The system rise time in the collection (holdup) reduces due to the decrease in the wash water inflow rate.	The maximum peak of the layer height slightly decreases due to the reduction applied to the inflow rate of the wash water, while the hold-up increases due to the same changes.
	Air Holdup	91.5274	115.9710	0.2674	120			
4	Froth Height	95.2781	117.3765	2.5018	120	Air holdup in the collection zone has shown a slow decrease due to An increase in (wash water) Qw flow rate. It can be noted that the froth layer height is marginally increased.	The holdup is less due to the increase in wash water, and the froth slightly increased.	The system peak increased due to the increase in the applied wash water flow rate.
	Air Holdup	91.3911	115.7482	0.2958	120			

4.3.3 Summary based on the 2x2 multivariable system models transition behaviour

The simulation has been carried out using the modeling equations as given earlier, and it was based on research on the dynamic behavior of the flotation process. By mathematically solving the differential-algebraic equations and transfer functions, the state variables' transient response was discovered. As of the simulated time responses of the h and the ε_g as shown in Figures 4.17 to 4.21, it is noted that in both outputs, there is a need for controllers to be designed, because of a steady-state error or negative response such as in froth layer height (h). Controlling the process is essential because if the process is interrupted from its steady-state point, it will not be able to recover without feedback signal control. The TITO system without feedback control has proven to be unstable. The transition behaviour characteristics of all cases are presented in Table 4.9.

Since many variables need to be monitored or controlled in a flotation system, the following section 4.4, is based on the modeling and simulation of the 3x3 system. The 3x3 flotation model is developed in Simulink by considering the bias variable or non-floated region of the column as presented in Equation (4.1). This variable plays a major role in the non-floated friction section of the column.

4.4 Simulation of the 3x3 matrix transfer function of the flotation system under different levels of the input flow rates

A simplified Equation of the 3x3 column flotation model as presented in Equation (4.8) is constructed in Matlab/Simulink. Figure 4.22 is a Simulink model that presents the flotation column 3x3 multivariable open-loop system, with different inflow levels. Following evaluated and acceptable minimum and maximum input flow rates as presented in section 4.2 for the proper functionality conditions of this process. The values of the inflow rate are changed systematically to investigate the performance of the 3x3 flotation process under different values of the input flow rates.

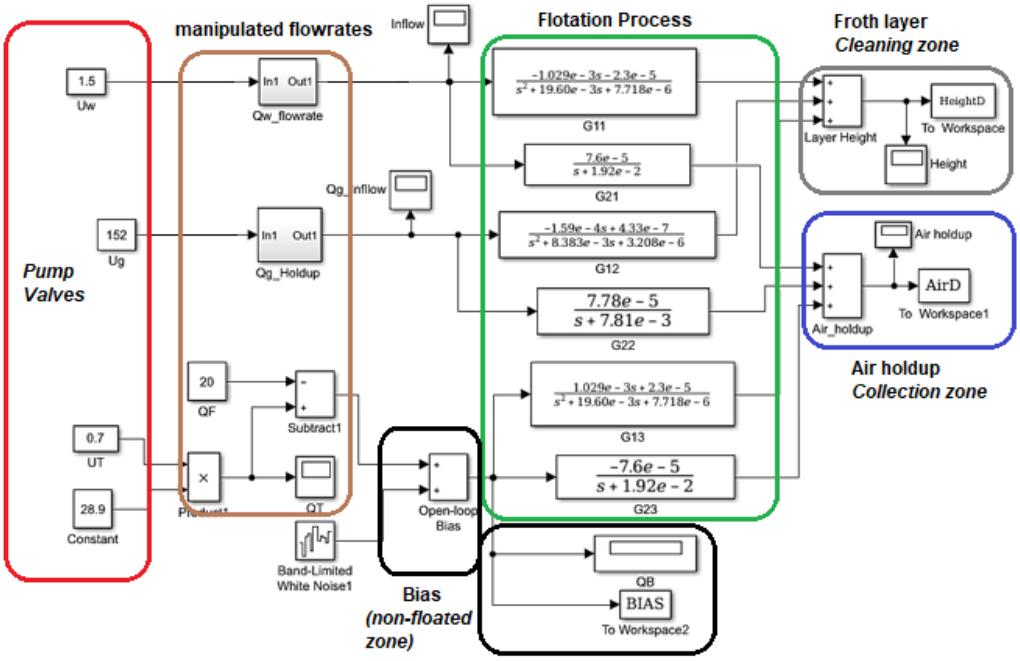

Figure 4.22: Simulink block diagram of the flotation open-loop process

The same evaluation performed for the 2x2 model is now performed again for the 3x3 system model shown above. The aim of the following Table 4.10 is to present the various cases to be used further in the evaluation of the 3x3 flotation column system behaviour under different inflow rates and valve pressures.

Table 4.10: Cases for investigation of the 3x3 model of the Flotation process

Cases Study	Aim	Action performed	Estimates of the Valve values and Measured input flows		Regions: Collection and Cleaning
			Manipulated variables		
			Pump valve	Input flow	Zones
Case study 1: Low values of all inflow rates.	Investigation of the system's operation when all input flow rates are decreased at the same time	Reduction of all input flow rates to the minimum values of the system inflows that can be used.	U_W =1.5	Q_W =4	Froth Height
			U_g=152	Q_g =20	Air Hold up
			U_T=0.7	Q_T =20	Bias
Case study 2: Middle values of all inflow rates	Investigation of the system's operation when all input flow rates are set to their middle values	Set all flow rates to be at the average level.	U_W =12	Q_W=8	Froth Height
			U_g =285	Q_g =40	Air Hold up
			U_T =0.7	Q_T =20	Bias
Case study 3: High value of all inflow rates.	Investigation of the system's operation when all input flow rates are increased at the same time to their maximum values	Set all input flow rates to their maximum values.	Uw=33	Qw=16	Froth Height
			U_g=552	Q_g=80	Air Hold up
			U_T=1.4	Q_T=40	Bias

4.4.1 Summary of the flotation system behaviour under different values of the inflow rates

The characteristics of the observed transition behaviours of the flotation system model under these levels are presented in Table 4.11. Analysis of the transition behaviours is done by taking the middle position of the valves discussed above as a reference. The following results prove that as the wash water flow rate, airflow rate, and non-floated flow rates are increased individually at the same time, the settling time of the froth layer height responses is slightly reduced. The rise time of the froth layer height and the air hold-up is also reduced slightly by the same changes. See the characteristics as presented in Table 4.11. Through the simulations, it can be noted that changing more than one inflow value at the same time, can lead to undetectable or malfunctioned process operation, or this can cause unrealistic results in the flotation process.

The flotation process is very complex, and due to that, it is very difficult to construct a simple model that captures the behaviour of the whole system and presents it at once. That is why the results are shown in different figures for the different zones of the system. Table 4.11 presents the system's holdup response due to a reduction in air injection through the air valve.

Table 4.11: Characteristics of the transition behaviour of the flotation process model under various levels of the input flow rates

Case	Zones	Rise time (s)	Settling time (s)	Peak	Peak time (*s*)	Main characteristics
Case study 1: Low values of all inflow rates	Height	93.8836	117.1619	0.7209 cm	120	The system's response time is longer, the Air Holdup significantly increases and the system peak is reduced due to the reduction applied to the input flow rates. The bias or non-floated did not show any changes due to this reduction. The flotation column cannot function properly under low inflow rates
	Air Holdup	89.8915	116.0980	0.1323 %	120	
	Bias	0.0181	119.9479	0.4085	22.80	
Case study 2: Middle values of all inflow rates	Height	94.7707	117.1351	1.4430 cm	120	The rise time in the collection zone is becoming shorter as the system level of the input flow rate increases. No significant change within the froth layer height (cleaning zone).
	Air Holdup	91.5274	115.9710	0.2674%	120	
	Bias	0.0181	119.9479	0.4085	22.8000	
Case study 3: High value of all inflow rates.	Height	95.2217	117.1205	2.8886 cm	120	The system response time in the cleaning zone is less due to the increase in the flow rate. The Air Holdup significantly reduces. The system peak becomes higher for the holdup (collection zone) and bias (non-floated).
	Air Hold up	92.3732	115.9063	0.5385%	120	
	Bias	0.0181	119.9479	20.6385	22.80	

The next section 4.5 is an open-loop simulation, with inflow rates changed one at a time.

4.4.2 Transition behaviour and analysis of the system's response under different levels of the inflow rates

Different tests were performed, using the process model given in Figure 4.22 and the plant constraints as shown in Table 4.2. The open-loop model of the flotation process (air-water system) is simulated in Simulink. In this process, the inflow rates are adjusted in such a way that the system is manipulated from low, average, and high-level inflow rates. The system responses to these changes are presented below. The following simulation results (Figure 4.23) are obtained for the system using the lower-level input flow rate values. The representation of the adjusted inflow rate is shown in Figure 23 (a). The froth layer height resulting from the current adjustment of inflows is shown in Figure 23 (b) with a ramp behaviour that took 93.78 seconds (s) to rise and settles at 117.136 seconds at a peak of 0.69 cm. Figure 23(c) shows the air holdup rising from 0%-0.1315% as presented in the y-axis, and this holdup response settles at 116.112 seconds as presented in the x-axis. Figure 23(d) is a bias response that reaches a peak of 0.4085 cm^3/s at 22.80 seconds and settles at 119.9479 seconds.

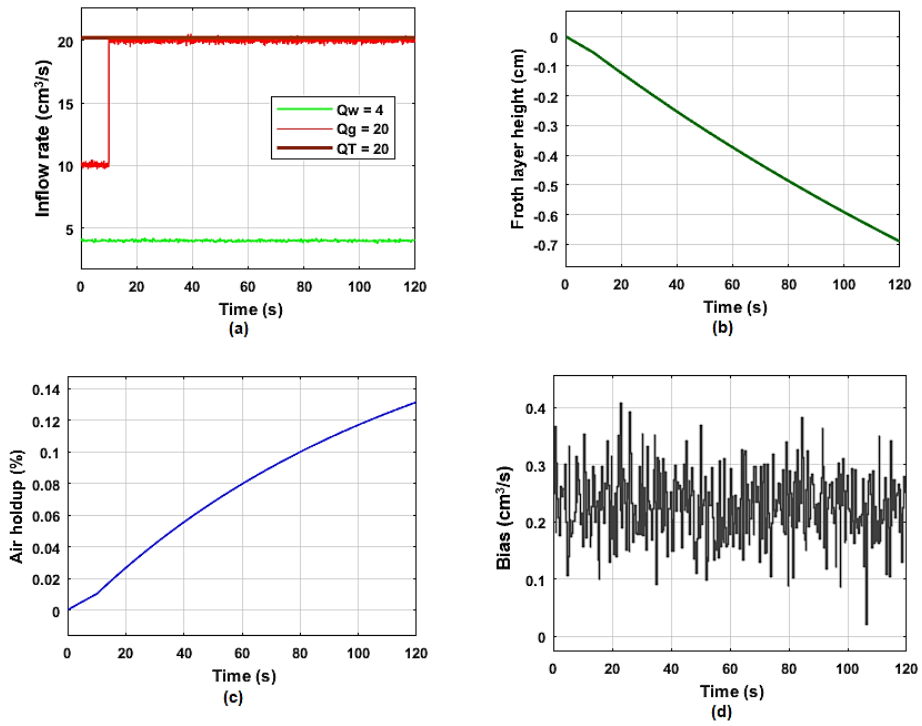

Figure 4.23: Effect of the low flow rates on the flotation process (a) Input flow rates (b) The Froth Layer Height behaviour (c) Air Holdup behaviour (d) The Bias behaviour

The following simulation results of the transition behaviour of the 3x3 model, as shown in Figure 4.24, are obtained under the middle conditional values of the inflow rates. This means all the inflow rates are adjusted accordingly as shown in Figure 24(a) for the system flow rate to be in the middle. Figure 24(b) is the froth layer height resulting from the current adjustment of inflows, the peak has increased to 1.4125 cm at 120 seconds of peak time, and the rise and settling time are traced to be at 94.7363 seconds and 117.1217 seconds respectively. Figure 24(c) shows the air holdup rising from 0%-0.2666% as presented in the y-axis of figure 4.24 (c), and this holdup response settles at 115.9781 seconds. Figure 24(d) is a biased response that has remained the same as it was in the low-level case study.

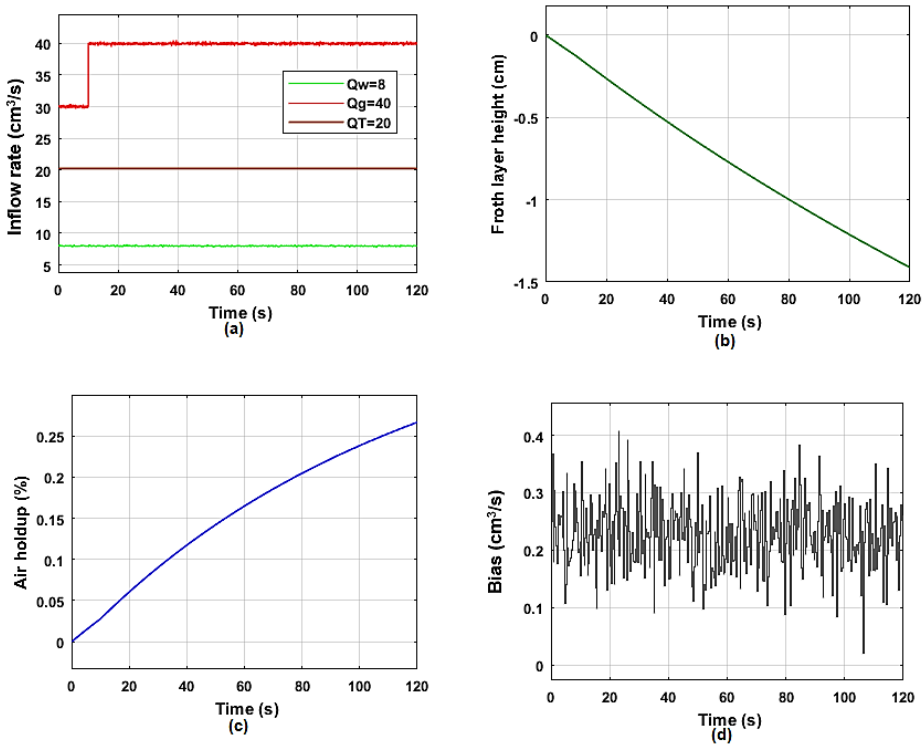

Figure 4.24: **Effect of the medium flow rates on the flotation process (a) Input flow rates (b) The Froth Layer Height behaviour (c) Air Holdup behaviour (d) The Bias behaviour**

The following Figure 4.25 shows the results from the system behaviour under high values of the valves for the air, non-floated fraction, and wash water flow rates. The inflow rates are all adjusted accordingly as shown in Figure 25(a) for the system to be at a high level. Increasing the flow rates gives an optimistic response to the froth layer height as shown in Figure 25(b) with a shorter rise-time of 24.6587 seconds, and a peak of 0.2522 cm at 72.90 seconds of peak time.

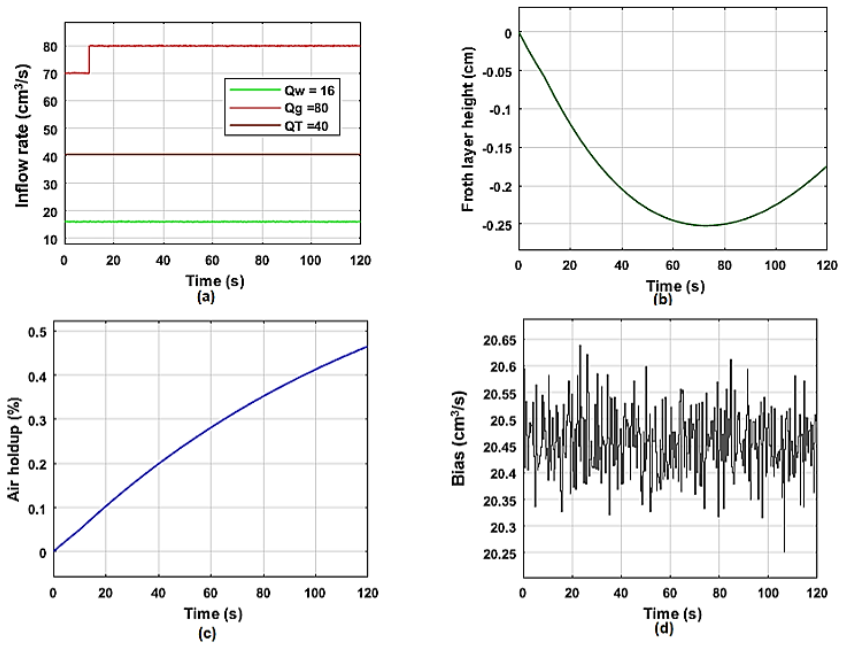

Figure 4.25: Effect of the high flow rates on the flotation process (a) Input flow rates (b) The froth layer height behaviour (c) Air holdup behaviour (d) The bias behaviour

4.5 Investigation of the influence of the changes only of one input flow rate to the transition behaviour of the flotation process 3x3 model

The emphasis is on evaluating the effect of the changes in one of the input flow rates over the behaviour of the flotation system 3x3 model. In this case, the focus is on one flow rate change at a time. The investigation is done through a simulation of the model of the flotation process given in Figure 4.26.

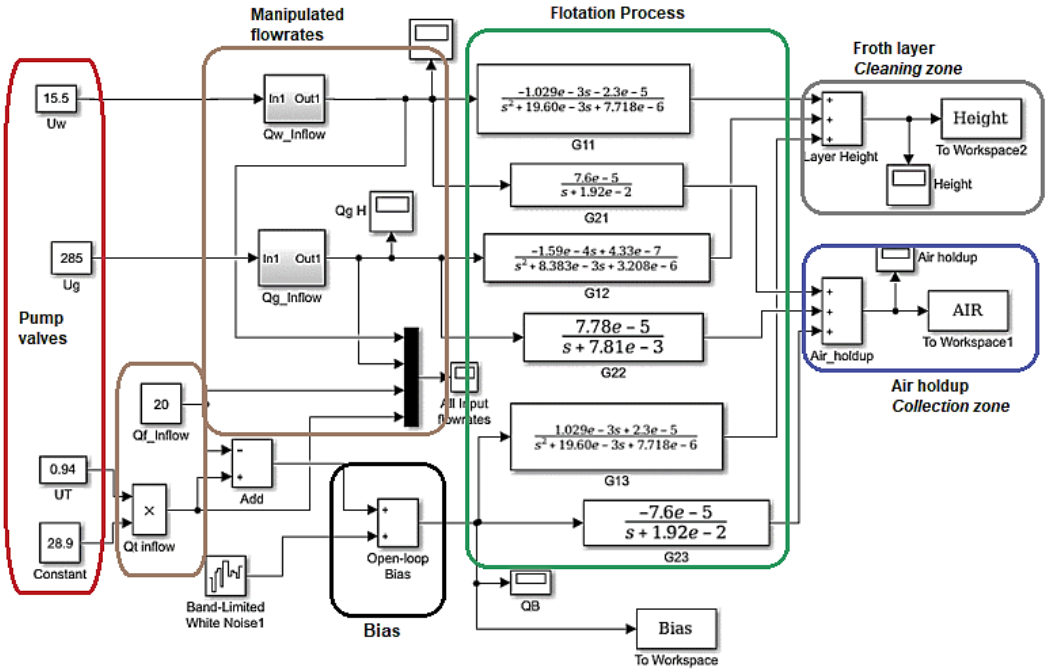

Figure 4.26: Column flotation system model

For comparison of the results from the investigated case studies, first, a reference case study is introduced. Table 4.12 describes the considered case studies showing the values of the valves and the inflow rates.

Table 4.12: Classification of the cases performed for the 3x3 multivariable model of the column flotation system

Cases Study	Aim	Action performed	Measured Variables		
			Pump valve and manipulated variables		Regions: Collection and Cleaning
			Pump valve	Input flow	Zones
Reference Case study	To establish the reference state of the system for comparison.	Define the values of the valves and receive the initial input flow rates	U_W =15.5	Q_W=9.32	Froth Height
			U_g =285	Q_g =40	Air Hold up
			U_T =0.94	Q_T =27.17	Bias
1	Investigation of the performance of open-loop flotation process behaviour when the airflow rate Qg has been decreased.	The airflow rate is changed from 40 cm^3/s to 15 cm^3/s, and the wash water flow rate (Q_W) and the non-floated flow rate are kept at the reference condition.	U_W =15.5	Q_W=9.32	Froth Height
			U_g =118	Q_g =15	Air Hold up
			U_T =0.94	Q_T =27.17	Bias
2.	Investigation of the transition behaviour of the flotation process when the airflow rate Qg has been increased.	The airflow rate is adjusted to 80 cm3/s, wash water flow rate (Q_W) and the non-floated (Q_T) are kept at the reference condition.	U_w=15.5	Q_w=9.32	Froth Height
			Ug=552	Q_g=80	Air Hold up
			U_T=0.94	Q_T=27.17	Bias
3	Investigation of the transition behaviour of the flotation process when the non-floated fraction flow rate Q_T has been decreased.	Non-floated flow rate (Q_T) is decreased from 27.17 to 20 cm^3/s, wash water flow rate (Q_W) and the airflow rate (Q_g) are kept to the reference condition.	U_w=15.5	Q_w=9.32	Froth Height
			U_g = 285	Q_g = 40	Air Hold up
			U_T=0.7	Q_T =20	Bias
4	Investigation of the performance of open-loop flotation process behaviour when the non-floated fraction flow rate Q_T has been increased.	Increase the non-floated flow rate (Q_T) to 40 cm^3/s, wash water flow rate (Q_W) and the airflow rate (Q_g) are kept to the reference conditions.	U_w = 15.5	Q_W = 9.32	Froth Height
			U_g=285	Q_g = 40	Air Hold up
			U_T = 1.4	Q_T = 40	Bias
5	Investigation of the open-loop transition behaviour of the flotation process when the wash water flow rate Qw has been decreased.	The wash water flow rate is decreased from 9.32 cm^3/s to 8 cm^3/s, and the airflow rate (Q_T) and the non-floated (Q_T) are kept at the reference condition.	U_W = 12	Q_w = 8	Froth Height
			U_g = 285	Q_g = 40	Air Hold up
			U_T= 0.94	Q_T = 27.17	Bias
6	Investigation of the transition behaviour of the open-loop flotation process when the wash water flow rate Qw has been increased.	The wash water flow rate is increased by 16 cm^3/s, and the airflow rate and the non-floated are kept at the reference condition.	U_W=33	Q_w=16	Froth Height
			U_g=285	Q_g = 40	Air Hold up
			U_T=0.94	Q_T=27.17	Bias

The following results shown below demonstrate the behaviour of the column flotation process 3x3 model under the condition selected as a reference one. The reference condition is selected using the inflow results as presented by (Persechini et al., 2000). Figure 4.27 is a representation of the froth height, air hold up, and the Bias zones behaviours respectively shown in Figure 27 (b, c, and d) under the reference conditions.

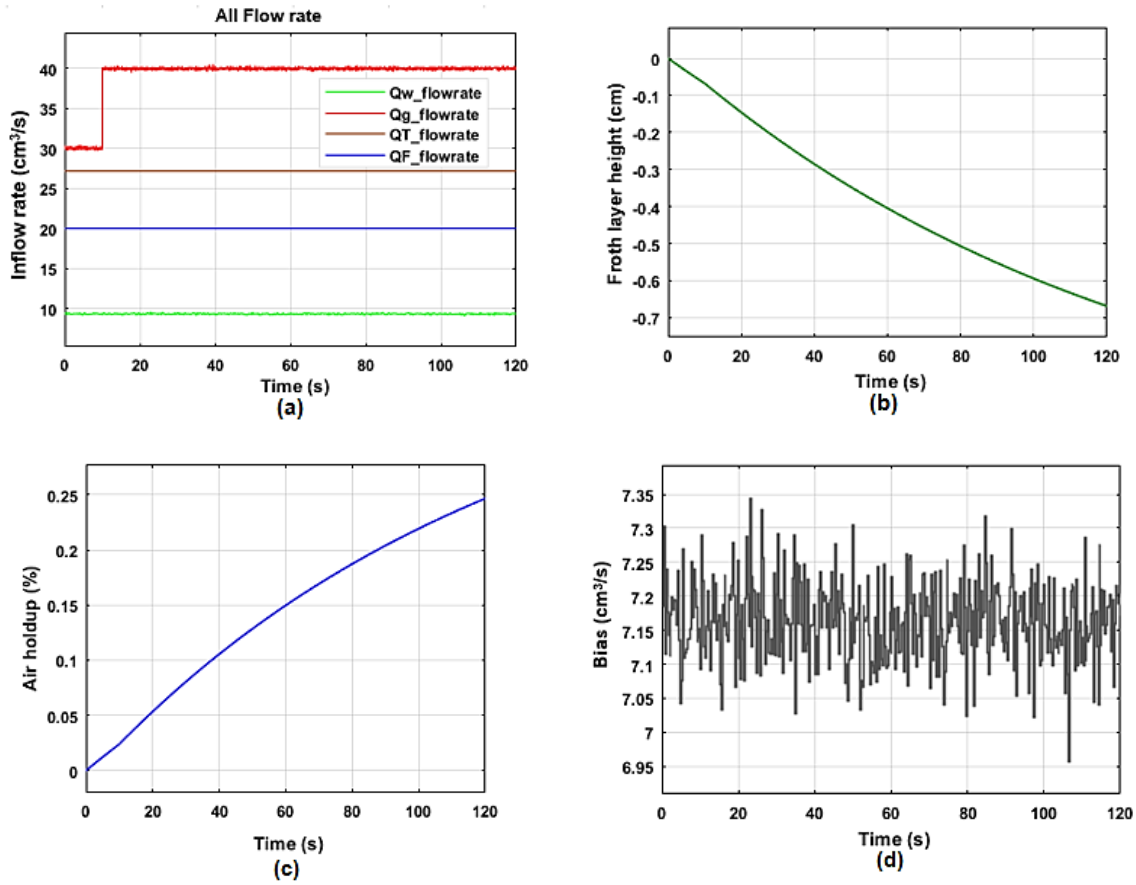

Figure 4.27: **Flow rate effect of the reference case study condition on the flotation process (a) Input flow rates (b) The Froth Layer Height behaviour (c) Air Holdup behaviour (d) The Bias behaviour**

The introduction of separate changes in the flow rates is necessary to assess how the system responds if some changes are made to the input flow rates or for any reason the whole process is forced by the random input flow rate changes. The following section (4.4.1) focuses on adjusting one variable at a time and the open-loop process responses using Matlab/Simulink simulation are documented and observed.

4.5.1 Investigation of the flotation system 3x3 model transition response

The results in Figure 4.28 represent the open-loop system behaviour for Case study 1. The wash water and the non-floated inflow rates are retained at the reference condition, while the input flow rate of the air zone is decreased to 15 cm^3/s as shown in Figure

4.22 (step signal from 5 cm^3/s - 15 cm^3/s). This is done to investigate the effect of the airflow rate on the column flotation process behaviour.

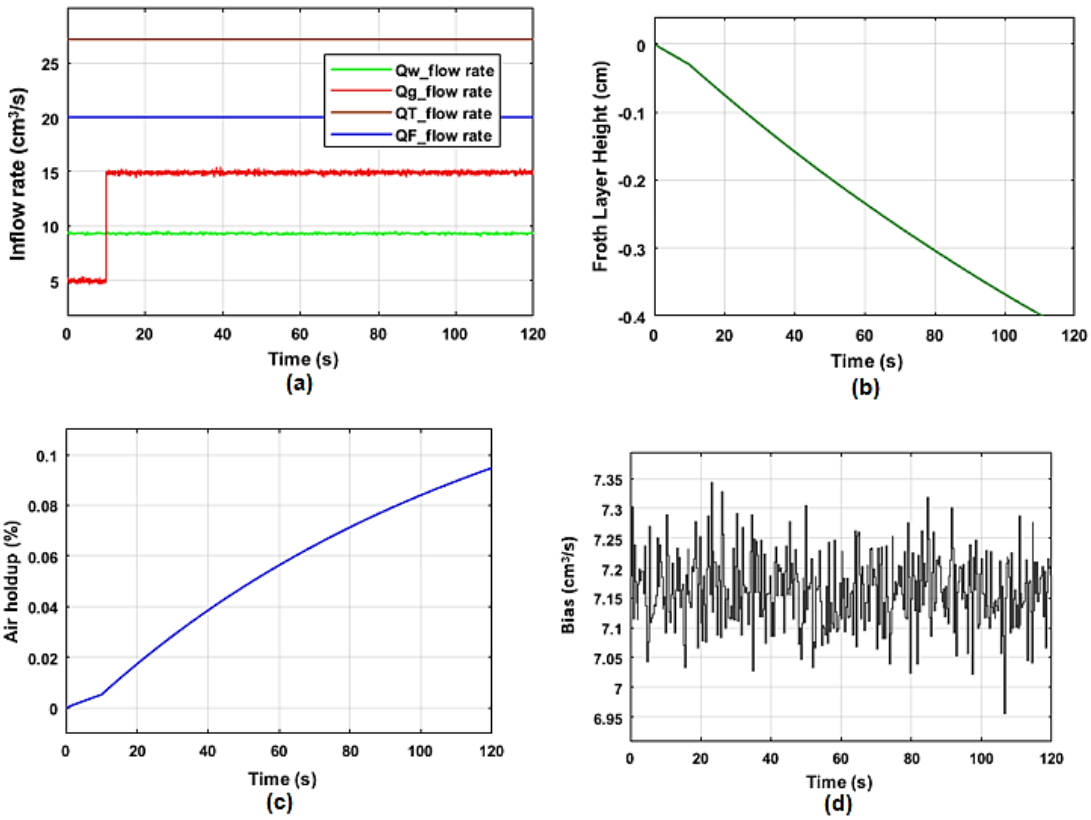

Figure 4.28: **Flow rate effect of Case study 1 on the flotation process (a) Input flow rates (b) The Froth Layer Height behaviour (c) Air Holdup behaviour (d) The Bias behaviour**

The indication of the value of the Bias, through steady-state value in a flotation (water-air) system, is given by $Q_B = Q_T - Q_F$ Therefore, assuming a constant value for the feed flow rate (Q_F) and considering the steady-state Bias pair as shown in Table 4.2, (also highlighted in Equation 4.13), the simulated bias resulted to Figure 4.25. The model in Equation 4.13 has a transition behaviour as shown in Figure (4.26) which is satisfactory compared with the results shown by (Persechini et al., 2000). As the input flow is reduced through the air valve from 40 to 15 cm^3/s, the settling and rise times are much longer for the non-floated and holdup zones, where the height zone settling time is slightly reduced and the rise time is increased slightly.

In Case study 2 the inflow rate of the air zone has been increased to 80 cm^3/s, keeping the wash water and height zone at the reference condition. The plant model constraints given in Table 4.2 are tested to prove that the changes made are still within the allowable range of operation. The results in Figure 4.29 shows changes in the behaviour of the column processes due to the increased air inflow rate into the collection zone as presented as a red signal in Figure 4.29 (a). The transition

characteristics of the considered 3 processes are presented in Table 4.13, under Case study 2, and also shown below in Figure 4.29 (b, c, and d).

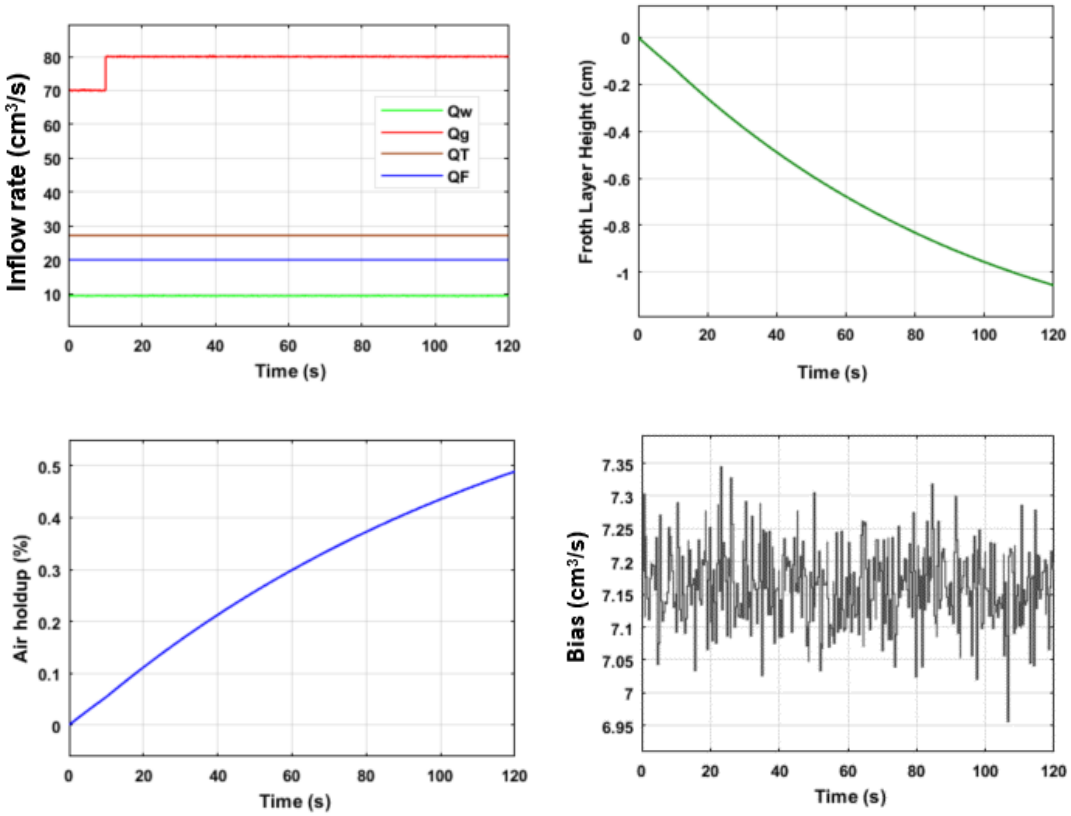

Figure 4.29: **Case study 2: Effect of the flow rate on the flotation process (a) Input flow rates (b) Froth Layer Height behaviour (c) Air Holdup behaviour (d) Bias behaviour**

In Figure 4.29 (b) the froth layer height system response is much faster in rising time and settling time as more air is applied through the air valve, the characteristics are presented in Table 4.13. The bias in Figure 4.29 (d) shows no significant changes in the settling, and rising time and the system peak time is still at 22.8 seconds. The cleaning zone of the system in this condition has proven to give a better performance when the air inflow rate is much faster.

The airflow rate in the collection zone is taken back to a reference condition, and now the non-floated fraction flow rate is reduced. The performance of the system under Case study 3 is shown in the following Figure 4.30, the transition behaviour characteristics of the system under this condition are fully shown in Table 4.13.

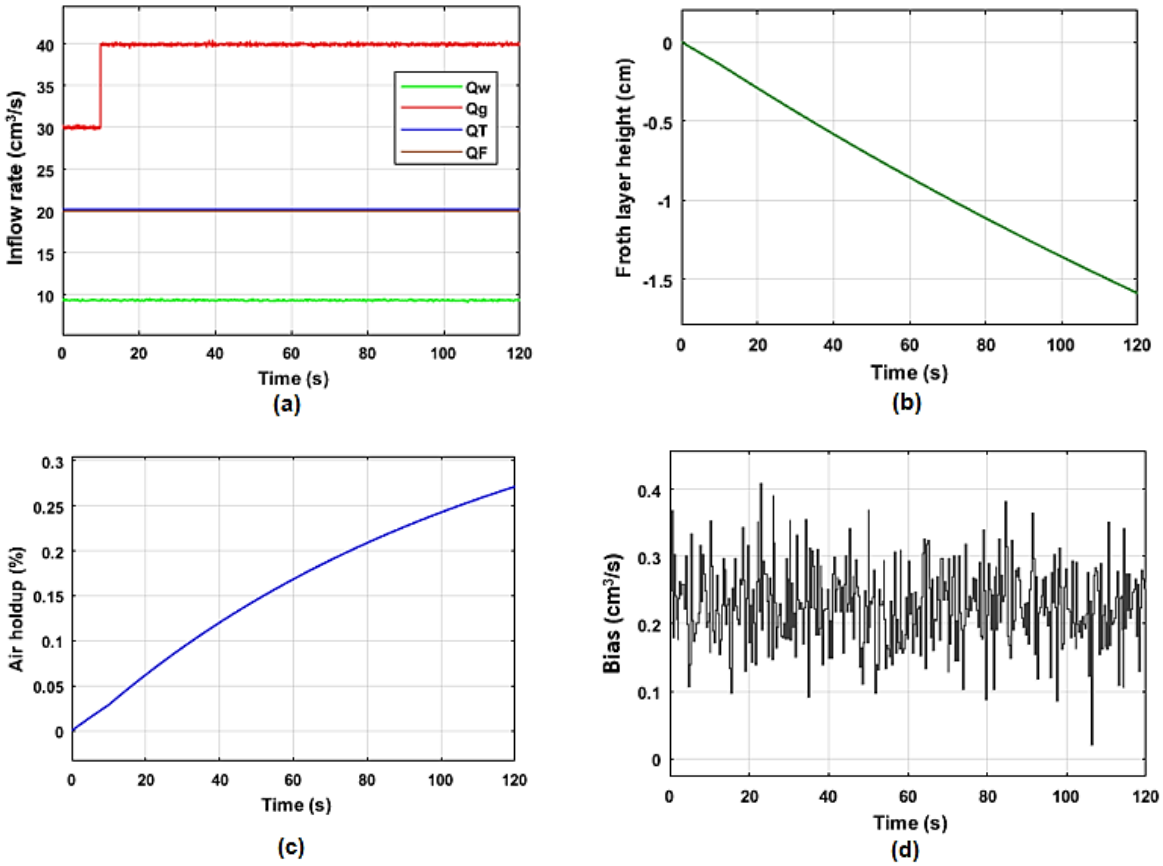

Figure 4.30: **Case study 3: Effect of the flow rate on the flotation process (a) Input flow rates (b) Froth Layer Height behaviour (c) Air Holdup behaviour (d) Bias behaviour**

The flow rate of the non-floated (Q_T) is increased under Case study 4 as presented in Table 4.12. The effects of the input flow rates shown in Figure 4.31 (a) on a column flotation system are demonstrated in Figure 4.31 (b) shows a respectable response of the froth layer height in terms of the positive direction, but the peak of 1.095 is still no acceptable for validation of the process as presented in section 4.2. Nevertheless, this case study has proven the importance of applying a high level of airflow rates and high non-floated fraction as shown in Figure 4.31 (d) within the column flotation system. The transition behaviour characteristics are recorded in Table 4.13.

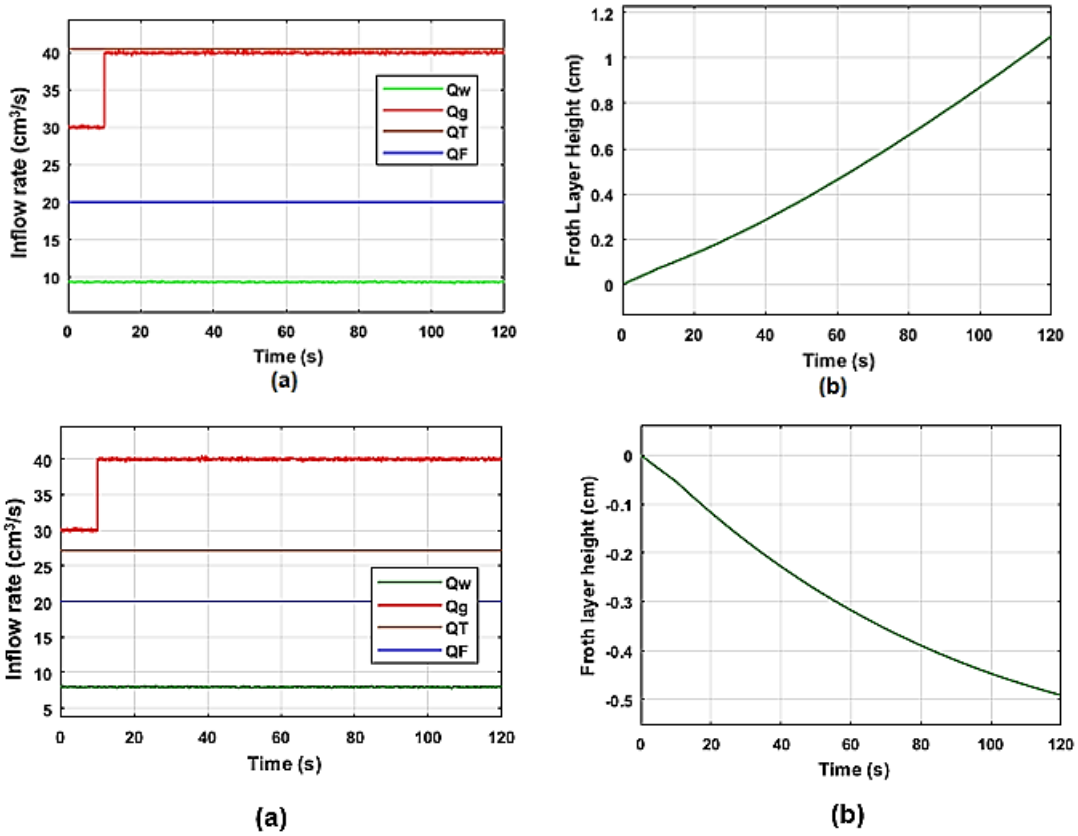

Figure 4.31: **Case study 4: Effect of the flow rate on the flotation process (a) Input flow rates (b) Froth Layer Height behaviour (c) Air Holdup behaviour (d) Bias behaviour**

To understand how the system responds due to the froth layer growth or decay, the inflow rate has been decreased and increased. See Case studies 5 and 6 in Table 4.12. The following results in Figure 4.32 (b) demonstrated the system response in the cleaning zone to changes applied in a wash water input flow rate Figures 4.32 (a).

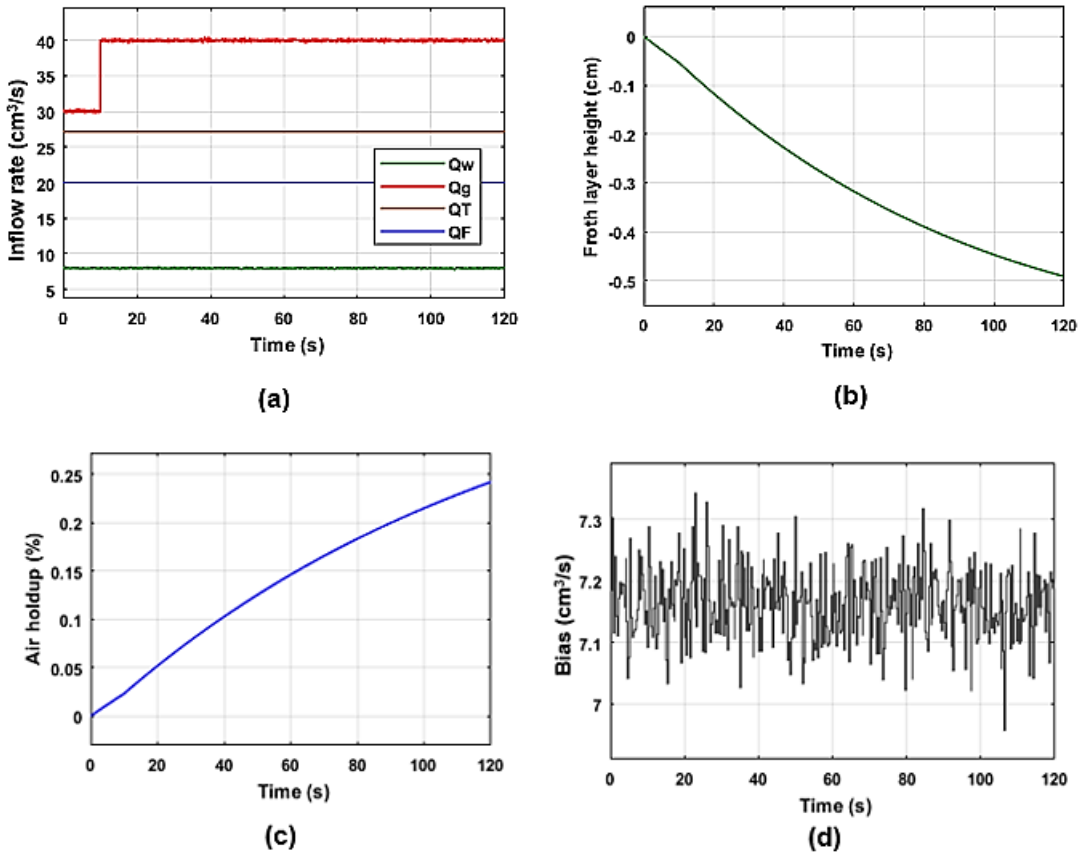

Figure 4.32: **Case study 5: Effect of the flow rate on the flotation process (a) Input flow rates (b) Froth Layer Height behaviour (c) Air Holdup behaviour (d) Bias behaviour**

Figure 4.32 (c) and Figure 4.32 (d) shown above demonstrate how the 3x3 process model responds in the collection and bias zones if the wash water input flow rate is reduced as shown in Figure 4.32(a). The following results in Figure 4.33 (a,b, and c) are the demonstration of how the model responds to an increase in the wash water flow rate shown in Figure 4.33(a). Table 4.13 shows detailed transition behaviour characteristics of all column processes.

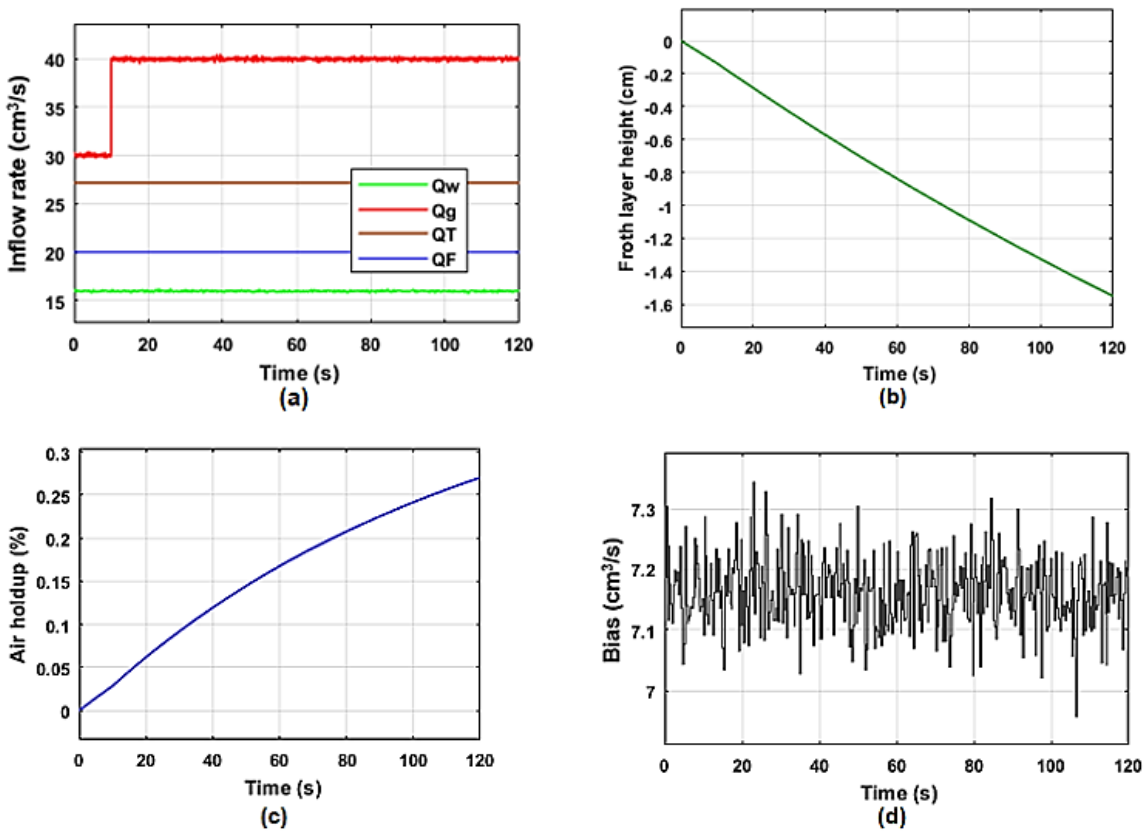

Figure 4.33: **Case study 6: Effect of the flow rate on the flotation process (a) Input flow rates (b) Froth Layer Height behaviour (c) Air Holdup behaviour (d) Bias behaviour**

From Figure 4.28 up to Figure 4.33, different cases are considered to analyse how the 3x3 model of the column flotation process will respond to the increasing and decreasing of the inflows rate. Some irregular or unexpected results are results from the simulation that indicated the need for controller design, so to drive the system to a more realistic or accepted behaviour. All the case studies were performed to understand how bad the system is without a controller and to acquire open natural data for the system controller design.

The results from the simulation are compared with those reviewed for the flotation plants.

The case studies performed show that the most effective method for controlling the column flotation process is through carefully pairing:

- the height of the froth layer and the signal transmitted to the wash water valve, to decide on the amount of water to be released.
- the collection zone air holdup and the transmitted signal to the air valve to control the amount of air released; and, finally,
- the bias for the non-floated and the signal supplied to the peristaltic pump.

Table 4.13 discusses and analyses the system responses due to the different case studies.

Table 4.13: Analyses of the column flotation 3x3 model transition behaviour

Case Study	Zones	Rise time (s)	Settling time (s)	Peak	Peak time (s)	Main characteristics		
						Settling time	Rise time	Peak
ref	Froth Height	92.0	116.19	0.6687	120	The simulation results from the reference inflow rates of the 3x3 system model are compared with the baseline or 2x2 system model reference as introduced early. The most dominant or important features of the system have shown much improvement or responded much better than the 2x2 system model. This shows the possibility of better performance if all the important variables are considered or taken into account.		
	Air Holdup	91.55	116.15	0.247	120			
	Bias	0.0181	119.948	7.3445	22.80			
1	Froth Height	92.5722	117.0311	0.4267	120	The rise time of the layer height is longer in case 1, due to a reduction in input air flow rate.	The settling time of the system has slightly increased due to the reduction applied in the air pressure flow.	The peak height has decreased as the rate of the airflow is reduced and the hold-up peak became shorter
	Air Holdup	88.771	116.250	0.0948	120			
	Bias	0.0181	119.95	7.3445	22.80			
2	Froth Height	90.6434	115.3394	1.0555	120	The rise time of the froth layer height slightly improve/ became shorter, the hold-up responded more rapidly, and the bias remains the same.	The system in the collection zone reduced its settling time due to the increased volume of the airflow rate.	The peak response of the hold-up is now much higher, due to the increase in the airflow rate, and that also resulted in to increase in the froth layer height.
	Air Holdup	92.6197	116.1170	0.4893	120			
	Bias	0.0181	119.9479	7.3445	22.80			
3	Froth Height	94.9013	117.1910	1.5889	120	As the flow of the non-floated (bias) is reduced within the system, the rise time of the collection and cleaning zone increases.	A reduction in the non-floated flow rate resulted in a slight increase in the layer height.	Decreased essentially for holdup and bias. The Froth layer height slightly increased.
	Air Holdup	91.5202	115.9392	0.2713	120			
	Bias	0.0181	119.9479	0.4085	22.80			
4	Froth Height	94.1845	118.0978	1.0952	120	The rise time of the system slightly decreases due to an increase in the non-floated flow rate.	Increase in settling time for froth layer height and collection zone (holdup). The bias remains the same.	Increase for bias, but the froth layer height and collection zone (holdup) slightly decrease.
	Air Holdup	91.4078	116.6045	0.1992	120			
	Bias	0.0181	119.9479	20.6385	22.80			
5	Froth Height	89.0108	115.1277	0.4922	120	The system in the cleaning zone took less rise time due to a reduction in the wash water inflow rate.	a decrease in the froth layer due to a decrease in the wash water inflow rate. A little decrease in the collection zone is noted.	Layer height and the bias-measured values of the flotation system decreased, due to the reduction applied to the input flow rate of the wash water.
	Air Holdup	91.5751	116.1913	0.2419	120			
	Bias	0.0181	119.9479	7.3445	22.80			
6	Froth Height	94.8704	117.1777	1.5510	120	Holdup rise time slightly reduces and the layer	Bias remain the same, as the wash	Froth layer height and holdup increase due to

Case Study	Zones	Rise time (s)	Settling time (s)	Peak	Peak time (s)	Main characteristics		
						Settling time	Rise time	Peak
	Air Holdup	91.5232	115.9474	0.2703	120	height increases due to an increase in the wash water. The bias remains the same.	water increase, but height increases due to the increase in wash water inflow rate, while holdup is slightly reduced.	the increase in the applied wash water flow rate. The bias remains the same.
	Bias	0.0181	119.9479	7.3445	22.80			

4.5.2 Summary based on the behaviour of the measured variables

Various system behaviours are observed, as different tests were conducted, and this section presents a summary of the observations made and recorded in Table 4.13. Initially, in case study 1; the airflow rate has been decreased, which resulted in a decrease in the collection zone (holdup) volume and caused a reduction of the floated (cleaning zone) flow rate as a result the froth layer height decreased (Settling and rise time became longer). Due to an increase in airflow rate applied (Case study 2), the settling time of the froth layer height in the cleaning zone slightly increases and the rise time decreases, the bias has shown no significant change. The literature (Persechine et al., (2004) and 2012), states that a reduction in the non-floated flow rate should result in a higher holdup in a collection zone. A reduction in the non-floated flow rate is applied under Case study 3, which increases the rise time of the froth layer height, see Figure 4.30(a). An increase in the non-floated flow rate has also caused an increase in the holdup (collection zone).

The settling time of the Froth layer height has increased slightly due to an increase in the non-floated fraction flow rate as presented in Case study 4. An increase in bias is due to an increase in the non-floated fraction flow rate (Case 4). Since the bias is directly affected by the non-floated flow rate, it should be reduced due to the reduction in non-floated inflow. A decrease in bias and layer height due to a decrease in the wash water flow rate causes the air holdup of valuable minerals to be increased due to the reduction of the wash water flow rate (Case study 5). A decrease in wash water also reduces the possibility of extracting cleaner froth. The collection zone holds more valuable minerals due to the increase in wash water (Case study 6).

4.6 Comparison of the 2x2 and 3x3 multivariable system models transition behaviours

According to the simulation results conducted for the open-loop 3x3 and 2x2 multivariable models of the flotation system, it is noted that the reaction of the 2x2 model can sometimes, but not always perform better than this of the 3x3 model, more remarkable for the hold-up in the collection zone. Through the simulation results, it is noted that the 2x2 multivariable flotation system model has responded much better than the more complicated 3x3 system model, but that is significantly experienced in the collection zone. Analysing natural behaviour contributed towards the determination of whether a system is stable or not, and how stable it is as well as the speed of its response. Hence, the column flotation system model and dynamic characteristics were analysed to achieve a good understanding of the system’s transient behaviour when a step reference input is applied. The system's dynamic behavior is assessed based on

multiple changes in the input circumstances, as presented in section 4.3 and section 4.4. The following Table 4.14 shows the comparison between the two models. It highlights the advantages of using one over the other model for the design of controllers. The comparison analysis focuses on the common case studies with these two system models, which means reference stage, case studies 1, 2, 5, and 6 from Table 4.9 and Table 4.13 as discussed before.

Table 4.14 below highlights the advantages and disadvantages of the 2x2 and 3x3 models. Throughout the results from the simulations of the transition behaviours of these models, it is noted that as the wash water flow rate increases above the limits presented in Figure 4.12 some unwanted minerals can be screened or wrongly selected due to the result in higher froth layer concentration. Therefore, this is not advisable to be done experimentally.

Considering real-life scenarios column flotation system processes performed different functions at once with one aim of cleaning the minerals, Therefore, although this is comparable with the literature, better modeling is performed in this Chapter by contracting the whole model at once rather than the individual variable with a separate model.

Table 4.14: Comparison of the performance of the 3x3 and 2x2 multivariable models of the column flotation process

Case Study	Zones	3x3 model		2x2 model		Comparison	
		Rise time (s)	Settling time (s)	Rise time (s)	Settling time (s)	Advantages	Disadvantages
Reference (Q_w=9.32, Q_g=40 & Q_T =27.17)	Froth Height	92.0	116.19	94.9264	117.2012	The 3x3 has faster settling than the 2x2 model in the cleaning zone. The 2x2 has a better rise and faster settling time than the 3x3 model in the collection zone.	The 3x3 is a little bit slower in rising time and settling time than the 2x2 model in the collection zone (hold-up).
	Air Holdup	91.55	116.15	91.5162	115.9323		
	Bias	0.0181	119.945	N/A	N/A		
1 (Q_w=9.32, Qg=20 & QT =27.17)1	Froth Height	92.57	117.0311	94.7389	117.4855	In this kind of system, the operation of the pressure gauge is very important, therefore, the 3x3 has proven to be enhanced in terms of the rise time more than the 2x2 model in the collection zone (holdup) and cleaning zone (layer height).	The decrease in air inflow rate results in a slower system operation. Therefore, this is not good for the cleaning zone of the system.
	Air Holdup	88.77	116.250	94.5529	115.7223		
	Bias	0.0181	119.95				
2 (Qw=9.32, Qg=80 & QT =27.17	Froth Height	90.6434	115.3394	94.5529	116.8085	In this condition, the 2x2 has proven to be much better than the 3x3, in terms of settling time and rise time in the collection zone.	Addition of the Bias to form a 3x3 model causes a reduction of settling time in the cleaning zone (froth layer height).
	Air Holdup	92.6197	116.1170	92.5053	116.054		
	Bias	0.0181	119.9479				
3 (Qw=8, Qg=40 & QT =27.17)	Froth Height	94.9013	117.19	94.7707	117.1351	The Froth layer height and the hold-up of the 2x2 model are faster than the 3x3 model at this point, due to a lower inflow rate of the wash water.	The decrease in wash water threatens the possibility of a cleaner froth layer.
	Air Holdup	91.5202	115.94	91.5274	115.9710		
	Bias	0.0181	119.9479				
4 (Qw=16, Qg=40 & QT =27.17)	Froth Height	94.1845	118.0978	95.2781	117.3765	The 2x2 has a good and faster rise time and settling time than the 3x3 system model in the collection zone.	The collection zone holds more valuable minerals due to the increase in the wash water.
	Air Holdup	91.4078	116.6045	91.3911	115.7482		
	Bias	0.0181	119.9479				

The data received from Chapter 4 is used for further control design. The negative response of the froth layer height is practically not accepted; it is proven to be possible in an open-loop system due to the absence of the control signal. Therefore, the control to be designed must be capable of producing an acceptable positive response to all regions within the system under study.

4.7 Conclusion

Modeling of the Column Flotation process by 2x2 and 3x3 multivariable models and simulation studies are presented in this chapter. The optimal situation with the research hypotheses is used to formulate the 3x3 mathematical model of Column Flotation, in which the considered inputs are the water flow, airflow, feed flow, and non-floated fraction flow rates, and the monitored outputs are the froth layer height in the cleaning zone, air holdup from the collection zone, and non-floated bias. The transition behaviour responses of these models are shown in different graphs and all performance characteristics are presented in Tables 4.4 & 4.7 and Tables 4.8 & 4.10 for the different case studies. The case studies and the transition response of the 2x2 system in section 4.3, are demonstrated in Tables 4.10, and 4.12. Then the comparison of both multivariable flotation models understudy is tabulated in Table 4.14.

The development and evaluation of open-loop behavior for the variables of a pilot flotation column operating in an industrial environment were detailed in this chapter. The air hold-up, layer height, and bias (non-floated fraction) are all factors to consider. The maximum value of wash water (Q_w), the minimum froth layer height, and the lowest gas holdup are the most essential limitations, according to several evaluations. The layer height keeps the froth from splitting, the wash water keeps the froth pure and clean, and air holdup keeps the froth going. All the limitations in Table 4.2 ensure that the system operates within the predetermined and possible operational ranges. Even though practically it cannot be accepted to have a negative response for the froth layer height, it is proven to be possible in an open-loop system due to the absence of the feedback signal. Hence, the controller design for the system under study is very important, as indicated in sections 4.2, and section 4.3. The MATLAB command “step info” is used to find the values of settling time and peak values. This command computes the step-response characteristics for a dynamic system model. The design of the controller is needed to achieve the necessary or appropriate results of this system, this is proven through simulation evaluations. As it can be noted that the system in this chapter did not reach the acceptable amplitude response or the column did not reach steady-state due to various reasons such as liquid levels, and gas flow rates.

The next chapter presents a method of designing decentralized controllers for this coupling multivariable system /process model. The open-loop characteristic behaviour as presented in Table 4.4 is used as a reference for the controller design of the closed-loop system in furthering the investigation under study. The following Chapter aims at improving the flotation system behaviour, through the reduction of the interactions and controller design. It will concentrate on the design parameters of the decentralized control and the development of a closed-loop Matlab/Simulink software model. The following Chapter covers the simulation of the closed-loop flotation system for set-point tracking control and disturbance rejection this is simulated using Matlab/Simulink software.

CHAPTER FIVE:
DESIGN OF THE DECENTRALIZED CONTROLLER FOR A MULTIVARIABLE SYSTEM

5.1 Introduction

This chapter focuses on decentralized controller design for the flotation system model discussed in chapter 4. With the use of a thoughtful selection of single-loop pairings, the decentralized controller is created. Through Relative Gain Array (RGA), control decentralization is used to minimize the effects of process interfaces. A set-point tracking technique based on internal model controllers (IMCs) is adopted in the design. Presented in this chapter is the initial concept of the proposed decentralized controller, as well as the details of the implementation procedure for the system under study. This concept is explained in detail in this chapter. Using Matlab/Simulink to simulate the closed-loop system and validate the performance of the proposed control strategy, the performance of the closed-loop system is verified.

The chapter has the following structure: Section 5.2 of this chapter discusses the decentralized control approach and the motivation behind it. Section 5.3 describes how the RGA is derived and its interpretation. Section 5.4 discusses the Internal Model Controller and adopted linear Proportional-Integral-Derivative (PID) control design. Section 5.5 presents a feedback PID controller based on IMC and a simulation of the 2x2 flotation system model. The simulation of the 3x3 closed-loop flotation system is presented in section 5.6. Section 5.7 presented system evaluation based on the different disturbances. Analyses of the simulation results are presented in section 5.8, and finally, this chapter's conclusion is given in section 5.9.

5.2 Multi-Input Multi-Output and Decentralization control approach

Multi-Input Multi-Output (MIMO) or multivariable systems is a new approach to science that studies how relationships between parts give rise to the collective performances of a system that interacts and form a relationship with its environments. The system under study (flotation column) is one of the multivariable processes with an objective of metallurgical performance control to ensure compliance with the process operation as shown by the grade and recovery of valuable minerals in the concentrate. (Yahui et al., 2018). Many advancements in controller design methods have been made with a focus on improving control of the multivariable processes. However, the flexibility that comes with the decentralized technique in terms of operation significantly contributes to the industrial usage of this method. The interconnections that exist between the control and manipulated loops are the major challenge in decentralizing the system model for

MIMO systems. The popularity of decentralized control is due to its simplicity and option availabilities of loop independent operation (Hernandez-Alcantara et al., 2017). The following sub-section is based on the discussion of the decentralized method.

5.2.1 Decentralization method

In comparison with centralized control, decentralized control avoids a single point of failure, which in turn increases robustness performance in many systems. decentralization strategy is an appropriate approach for multivariable system control and is suitable for control system breakdown into a single input single output (SISO) control loop. In decentralization, the design of a controller is usually based on two steps which are as follows; single-loop pairings that are thoughtfully chosen, as well as individual pairing control tunning loops. The Relative Gain Array (RGA) approach is used to pair input and output variables to design decentralized controllers (Bristol, 1966; Ogunnaike & Ray, 1994). The process interactions measurement and optimal pairing recommendations provide helpful information in minimizing the effects of the interactions for the multivariable controller design technique. On the other hand, it is important to note that the steady-state gains information is required for this method. When a controller is constructed for each output variable on a specific input variable, the purpose of using RGA is to evaluate the influence of interactions within the system's operation. RGA is a tool that measures the interaction between the controlled and manipulated variables (Thulasi Dharan et al., 2017). It specifies how the controlled and manipulated variables should be paired to produce optimal control loops.

5.2.2 Selection of Loops Interaction variables and Simplification

Certain processes control and measure several variables. Those systems are called multi-input multi-output (MIMO) systems. Controlling such systems using a collection of simple controllers is extremely difficult, because of the interaction between the signals, (Astrom & Hagglund, 1995). A block diagram of such a system is shown in Figure 5.1 below. The use of two single-loop controllers is a simple method of controlling such a system, each controller deals with one loop. To achieve this, one must first decide how the controllers should be connected, which means $h(s)$ in Figure 5.1 should be controlled by U_1. As said before this is called the pairing problem. This problem can be simple if there is little interaction between the loops, which can be identified from the reactions of all outputs to all inputs. Therefore, loop simplification is very important in complex systems. In Figure 5.1 the first blocks are comparators, used to compare the setpoints signal and the feedback signal. The output of each comparator is any error signal applied to the controllers (second block).

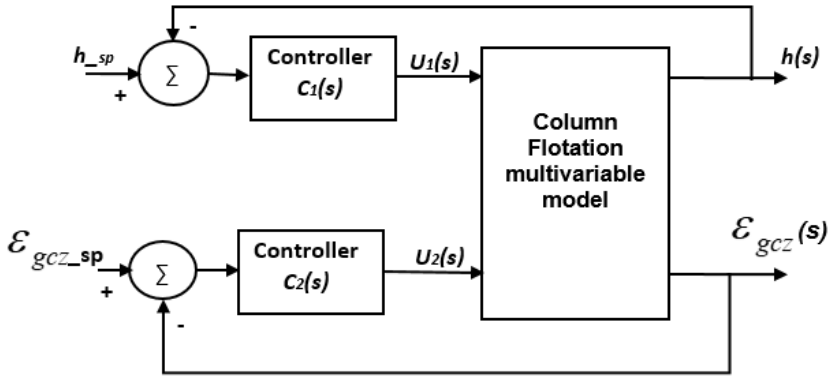

Figure 5.1: Block diagram for the decentralized control of the MIMO system

The last block represents the column flotation process controlled by the control signals $U_1(s)$ and $U_2(s)$. The output of the flotation process (last block) is the front layer height and air holdup respectively shown in Figure 5.1. If there is an uncertain connection between the loops, the single-loop technique will perform well. The loops can then be fine-tuned independently. However, when there is a coupling between the loops, as shown in Figure 5.2, there may be difficulties. The last block represents the column flotation multivariable model in Figure 5.1 and is replaced or comprehensively opened to show different transfer functions that are present within the model, as shown in Figure 5.2.

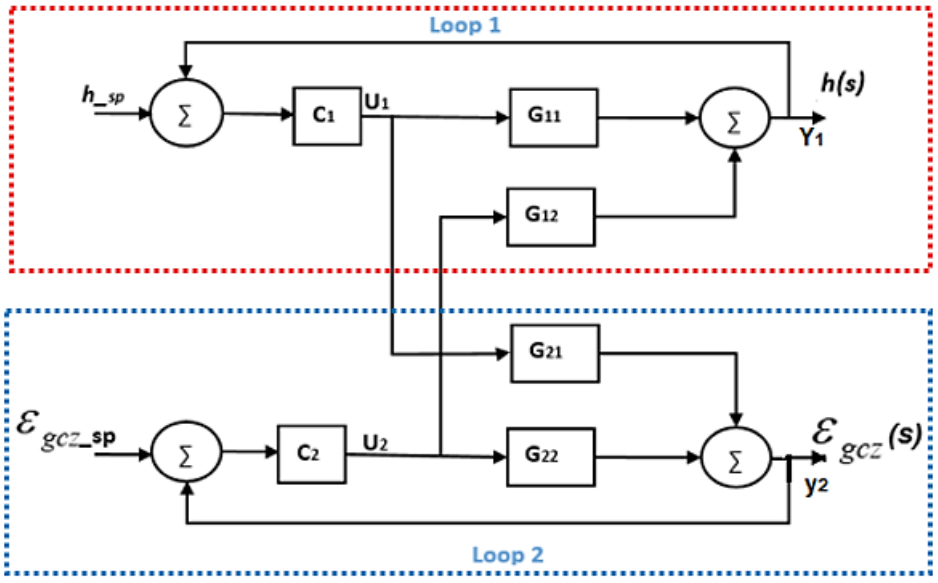

Figure 5.2: Loop interactions for a 2x2 multivariable system

Since the system under study is a multivariable process, is not easy to just identify proper connections without testing, the Relative Gain Array (RGA) assists in the classifications of proper loop connections (Ogunnaike & Ray, 1994; Bristol, 1966).

5.3 The Relative Gain Array (RGA)

Relative Gain Array (RGA) approach is used to determine suitable input-output pairing while developing decentralized diagonal controllers. According to the authors (Chen & Seborg, 2002), RGA was introduced (Bristol, 1966), as a measure of process interactions in multi-input, multi-output control problems. Due to its simplicity and utility, the RGA analysis has been widely used to identify promising decentralized multi-loop control systems based on limited information, and steady-state gains. It is important to note that each element in the RGA matrix for a *nxn* system represents the ratio of the open-loop gain for a specific loop in the situation where all other loops are open, to the closed-loop gain for that loop when all other loops are closed (Bristol, 1966). Equation 5.1, which is presented below, mathematically describes each member in the matrix:

$$\boldsymbol{\lambda_{ij}} = \frac{\boldsymbol{open-loop\ gain\ between\ y_i\ and\ u_j}}{\boldsymbol{closed-\ pen-loop\ gain\ between\ y_i\ and\ u_j}}; \boldsymbol{i} = \overline{\mathbf{1,N}}\ \boldsymbol{and}\ \boldsymbol{j} = \overline{\mathbf{1,N}}$$

$$\lambda_{ij} = \frac{(\partial y_i/\partial u_j)_u}{(\partial y_i/\partial u_j)_y} \tag{5.2}$$

The number of loops in the procedure is denoted by *n*. For all control variables, the subscript *u* denotes constant values excluding u_j (i.e., all loops open). The subscript *y* specifies that all outputs excluding y_i are kept constant by the control loops (i.e., all loops are closed). Dimensionless magnitude is denoted by λ_{ij}. From Equation (5.1), we define λ_{ij} the relative gain between output variable y_i and input variable u_j as the ratio of two steady-state gains (Ogunnaike & Ray, 1994). The relative gain is intended for all the input/output arrangements of a multivariable system, and the results are presented in an array of the form shown below:

$$\wedge = \begin{bmatrix} \lambda_{11} & \lambda_{12} \ldots . \lambda_{1n} \\ \lambda_{21} & \lambda_{22} \ldots . \lambda_{2n} \\ \ldots & \ldots \quad \ldots \\ \lambda_{n1} & \lambda_{n2} \ldots . \lambda_{nn} \end{bmatrix} \tag{5.2}$$

Entries ∧ satisfying the following two properties:

$\sum_{i=1}^{N} \lambda_{i_j} = 1 for j = 1,2, \ldots\ldots\ldots N$ Summation in a column

$\sum_{j=1}^{N} \lambda_{i_j} = 1 for j = 1,2, \ldots\ldots\ldots N$ Summation in a row

The 2x2 matrix transfer function of the flotation process under consideration is presented in the following subsection. Now, it is important to find the steady-state gain matrix of the system, the RGA matrix, and the matching of the loops.

5.3.1 Relative Gain Array and Interaction Measures

For multivariable controller design, the Relative Gain Array approach provides two forms of important information. The first is a measurement of the process interactions, and the second is a set of recommendations for the optimum pairing to minimize the interactions' consequences. The procedure and the discussion of the loop pairing based on Interaction Analysis as discussed by the authors (Ogunnaike & Ray, 1994) have been used in this chapter. Following the interaction analysis and RGA technique as explained before, now consider the mathematical model presented in Equation 5.3 which is the steady-state process gain matrix and work out the required RGA matrix.

$$G_p(s) = \begin{bmatrix} G_{11}(s) & G_{12}(s) \\ G_{21}(s) & G_{22}(s) \end{bmatrix} \tag{5.3}$$

Where the transfer functions of $G_{11}(s)$, $G_{12}(s)$, $G_{21}(s)$, and $G_{22}(s)$ are given in Chapter 4 as Equation (4.2, 4.3) and Equation (4.5, 4.6) respectively. The RGA is concerned with steady-state conditions, which therefore only need the steady-state form of the model under study as shown in Equation 5.4. Now let ***K*** be the matrix of steady-state gains of the transfer function matrix *G(s)* as *s* turns to zero:

$$G_p(0) = \begin{bmatrix} G_{11}(0) & G_{12}(0) \\ G_{21}(0) & G_{22}(0) \end{bmatrix} = \begin{bmatrix} \mathrm{K}_{11} & \mathrm{K}_{12} \\ \mathrm{K}_{21} & \mathrm{K}_{22} \end{bmatrix} = \begin{bmatrix} -2.980 & 0.135 \\ 0.004 & 0.0097 \end{bmatrix} \tag{5.4}$$

The calculation of RGA's from first principles and the Matrix method for calculating RGA's is presented by (Ogunnaike & Ray, 1994), therefore the procedure of RGA uses a 2x2 system is given by Equation 5.5. The RGA of the steady-state gain matrix *G*(0), is defined by (Ogunnaike & Ray, 1994) and (Chen & Seborg, 2002).

$$\Lambda = \begin{bmatrix} \lambda_{11} & \lambda_{12} \\ \lambda_{21} & \lambda_{22} \end{bmatrix} = K \cdot (K^{-1})^T \tag{5.5}$$

Where: $(K^{-1})^T$is the transpose of (K^{-1}). In the above equation 5.5, it is important to note that the operator "·" indicates the multiplication of an element-by-element of the equivalent elements. The corresponding relative gains can be calculated as follows:

$$\Lambda = \begin{bmatrix} \lambda_{11} & \lambda_{12} \\ \lambda_{21} & \lambda_{22} \end{bmatrix} = \begin{bmatrix} \lambda_{11} & 1-\lambda_{11} \\ 1-\lambda_{11} & \lambda_{11} \end{bmatrix} \tag{5.6}$$

from the definition of the inverse of a matrix, the following step is followed to find the RGA gain:

$$K^{-1} = \frac{1}{|K|}\begin{bmatrix} K_{22} & K_{12} \\ K_{21} & K_{11} \end{bmatrix} \quad (5.7)$$

Where $|K|$, the determinant of K is given by:

$$|K| = K_{11}K_{22} - K_{12}K_{21} \quad (5.8)$$

and taking the transpose of the matrix given in Equation 5.7, the following is obtained:

$$(K^{-1})^T = \frac{1}{|K|}\begin{bmatrix} K_{22} & -K_{21} \\ -K_{12} & K_{11} \end{bmatrix} \quad (5.9)$$

Now carry out a term-by-term multiplication of the elements of the matrices in Equations 5.5 and 5.9, the following is obtained:

$$\lambda_{11} = \lambda_{22} = \frac{1}{1-\frac{K_{12}K_{21}}{K_{11}K_{22}}} = \frac{1}{\frac{K_{11}K_{22}-K_{12}K_{21}}{K_{11}K_{22}}} = \frac{K_{11}K_{22}}{K_{11}K_{22}-K_{12}K_{21}} \quad (5.10)$$

While the $\lambda_{12} = \lambda_{21} = 1 - \lambda_{11}$

With regards to the steady-state gains presented in Equation 5.4, the RGA matrix is obtained as shown in equation 5.11, the evaluated RGA has yielded the following:

$$\wedge(K) = \begin{bmatrix} \frac{K_{11}K_{22}}{K_{11}K_{22}-K_{12}K_{21}} & \frac{-K_{21}K_{12}}{K_{11}K_{22}-K_{12}K_{21}} \\ \frac{-K_{21}K_{12}}{K_{11}K_{22}-K_{12}K_{21}} & \frac{K_{11}K_{22}}{K_{11}K_{22}-K_{12}K_{21}} \end{bmatrix} = \begin{bmatrix} 0.9817 & 0.0183 \\ 0.0183 & 0.9817 \end{bmatrix} \quad (5.11)$$

5.3.2 Interpreting the RGA Elements

To interpret the resulting RGA matrix shown in Equation 5.11, following the recommendations as presented by (Ogunnaike & Ray, 1994). It is recommended that for this 2x2 system the output variables *h* be paired with U_1 and the output ε_{gcz} with input U_2, for the decentralized control. The recommended pairing's steady-state input-output relationship should thus be:

$$\begin{bmatrix} h(0) \\ \varepsilon_{gcz}(0) \end{bmatrix} = \begin{bmatrix} G_{11}(0) & G_{12}(0) \\ G_{21}(0) & G_{22}(0) \end{bmatrix} = \begin{bmatrix} -2.980 & 0.135 \\ 0.004 & 0.0097 \end{bmatrix} = \begin{bmatrix} U_1(0) \\ U_2(0) \end{bmatrix} \quad (5.12)$$

The pairing rule known as RGA does not take into account the stability of the resulting control structure. For that reason, the resultant control operational stability must be checked. This is done according to the rule of the Niederlinski index (Jain & Babu, 2016). The Niederlinski guide is derived from the steady-state gain matrix and is commonly characterized as in Equation 5.13 (MUGA, 2015) :

$$NI = \frac{|G(0)|}{\prod_{i=1}^{n} g_{ii}(0)} < 0 \quad (5.13)$$

The Niederlinski Index is calculated by first finding the determinant of the modified steady-state gain matrix and the product of its diagonal elements as follows:

$$|\mathrm{G}(0)| = \det\left(\begin{bmatrix} -2.980 & 0.135 \\ 0.004 & 0.0097 \end{bmatrix}\right) = -0.028906 - 0.00054 = -0.029446$$

$$\mathrm{NI} = \frac{-0.029446}{-0.028906} = 1.0187$$

The decentralized multivariable control under study may be naturally stable because NI>0 for the recommended coupling. This, as well, is based on the RGA matrix as presented in Equation 5.11. As a result, for controller pairing, the controlled and manipulated variables should be paired so that the associated relative gains are positive and as close to one as possible (Bristol, 1966). To ensure closed-loop stability, loops should not be built with negative relative gains.

5.4 Internal Model Controller-based Proportional-Integral-Derivative (PID) feedback control design

When it comes to controlling interconnected systems, three major challenges arise. One is the practical limitation of the number and configuration of feedback loops, which supports decentralized control structures. The presence of hesitations in both, the subsystems and the interconnections add additional concern. A third concern is the control systems' consistency in the event of component failures. There are high chances of encountering failures in real engineering systems and they could cause instabilities in the system's operation (Pujol et al., 2007). This is particularly important in interconnected systems, where failures can patent themselves in the form of a total outage or incomplete degradation in each subsystem or actuator channel. The following Figure 5.3 represents the internal model control structure.

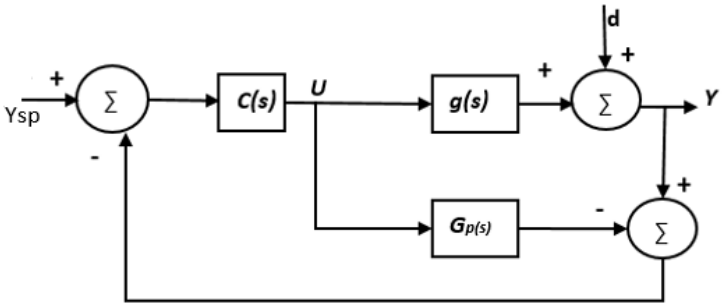

Figure 5.3: **The Internal Model Control (IMC) structure.**

Figure 5.3 presents the relationships between the conventional feedback controller, *g(s),* and the internal model controller, c(s). Equation 5.14 is useful in the controller design discussion and can be easily followed:

$$g_C(s) = \frac{C(s)}{1 - G_P(s)C(s)} \qquad (5.14)$$

The equivalent conventional control structure to the internal model controller is shown in Figure 5.4. After the successful design of the controller, Figure 5.4 is implemented in Simulink in a form of a multivariable system.

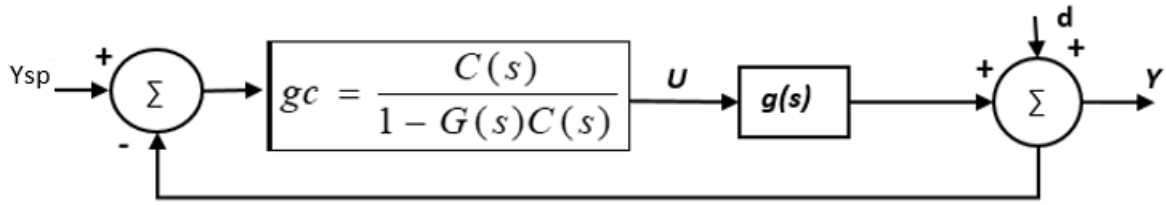

Figure 5.4: Equivalent Conventional Control Structure

5.4.1 Design and Implementation of Internal Model Controllers

It has been highlighted that for the implementation of the Internal Model Control (IMC) scheme, there are practical issues that need to be taken into consideration, as described by the author (Ogunnaike & Ray, 1994).

As a result, the IMC design procedure must be modified following the three steps presented below:

1. Process model factorization: The process model is separated into two parts as presented in Equation 5.15:

   $$\bar{g} = \bar{g}_+ \cdot \bar{g}_- \quad (5.15)$$

   $\bar{g}_+$ has all the non-invertible aspects (time delays, right-half plane zeros) with a steady-state gain of 1, $\bar{g}_-$is the remaining invertible part.

2. Controller Specification and Filter Design: The controller is specified as follows:

   $$C(s) = \frac{1}{\bar{g}_-} \cdot f(s) \quad (5.16)$$

   Where $f(s)$ is a filter usually of the form

   $$f(s) = \frac{1}{(\lambda s + 1)^n} \quad (5.17)$$

   with parameter Lambda (λ) and *n* has chosen to ensure proper control (that means the numerator order is less than, or almost equal to the denominator order).

3. Equivalent Conventional Controller form: If necessary, the IMC controller, ***c(s)***, may be converted to the conventional form, $g_c(s)$, for implementation. This is accomplished by using Equation 5.18.

   $$g_C(s) = \frac{C(s)}{1 - G(s)C(s)} \quad (5.18)$$

The details of the IMC design procedure have been prepared and now will be followed to design the control parameters of the froth layer height, air holdup, and later for the bias. The bias is only included when the system is extended to the 3x3 system.

5.4.2 Internal Model Control-based PID feedback control design for the Froth Layer Height control loop

The procedure for Internal Model Control (IMC) design and the practical issues discussed will be used in this section to design the control parameters for the froth layer height. To design a controller for the froth part of the system whose transfer function is given in Equation 5.19 factorization is essential.

$$G_{11}(s) = \frac{-1.029\times10^{-3}s-2.3\times10^{-5}}{s^2+19.60\times10^{-3}s+7.718\times10^{-6}} = \frac{-3(44.4s+1)}{129.6\times10^{3}s^2+2.5\times10^{3}s+1} \quad (5.19)$$

Factorization of the process model is done using the proposed IMC design procedure through the following steps:

By separating the process into parts, its model is factored into invertible and non-invertible divisions following the factorization steps presented in section 5.4.1, therefore,

$G_{11}(s) = G_{11+}(s) \cdot G_{11-}(s)$

$G_{11+}(s)$ contains all the non-invertible aspects (time delays, right-half plane zeros) with a steady-state gain. $G_{11-}(s)$ as the remaining invertible part.

From equation (5.21),$\mathrm{G}_{11+}(s) = 44.4s + 1$, and

$$G_{11-}(s) = \frac{-3}{129.6\times10^{3}s^2+2.5\times10^{3}s+1} \quad (5.20)$$

Therefore, from the IMC controller design specifications and filter design, the closed-loop response is generally given by the following equation.

$$C(s) = \frac{1}{\tilde{G}_P} f(s) \quad (5.21)$$

Where: $f(s)$ is a filter usually of the form of $f(s) = \frac{1}{(\lambda s+1)^n}$, Lambda ($\lambda$) is a flexible variable filter factor and *n* is a factor that can be used to ensure proper control. Now use the IMC method and specifically describe the closed-loop response of the layer height control design with a filter-included element as described by (Ogunnaike & Ray, 1994).

$$C_{11}(s) = G_{11-}(s)^{-1} f(s) \quad (5.22)$$

Calculate the PID parameters for the layer height loop using the IMC technique

$$C_{11}(s) = \frac{130\times10^3 s^2+2.5\times10^3 s+1}{-3} \times \frac{1}{(\lambda s+1)} = \frac{130\times10^3 s^2+2.5\times10^3 s+1}{-3(\lambda s+1)} \quad (5.23)$$

Substitute Equation 5.23 into Equation 5.18 this results in the following Equation 5.24

$$g_{C_{11}}(s) = \frac{\frac{130\times10^3 s^2+2.5\times10^3 s+1}{-3(\lambda s+1)}}{1-\left(\frac{-3(44.4s+1)}{130\times10^3 s^2+2.5\times10^3 s+1}\times\frac{130\times10^3 s^2+2.5\times10^3 s+1}{-3(\lambda s+1)}\right)} = \frac{130\times10^3 s^2+2.5\times10^3 s+1}{-3\lambda s-3+133s+3}$$

$$\therefore g_{C_{11}}(s) = \frac{130\times10^3 s^2+2.5\times10^3 s+1}{130\lambda s} = \frac{130\times10^3 s^2}{130\lambda s} + \frac{2.5\times10^3 s}{130\lambda s} + \frac{1}{130\lambda s} \quad (5.24)$$

Re-arrange and complete the factorisation of this controller

$$\therefore g_{C_{11}}(s) = \frac{2.5\times10^3}{130\lambda}\left(1 + \frac{1}{2.5\times10^3 s} + 52s\right) \quad (5.25)$$

Now the structure of Equation 5.25 is of an ideal PID structure, therefore, from the generally PID control structure.

$$G_C(s) = K_P\left(1 + \tau_I\frac{1}{s} + \tau_D s\right) \quad (5.26)$$

Therefore, for froth layer height the Proportional-Integral-Derivative (PID) control parameters lead to the following:

$$K_P = \frac{2.5\times10^3}{130\lambda},\ \ \tau_I = \frac{1}{2.5\times10^3};\ \ \tau_D = 52$$

To ensure proper control and through severally test Lambda (λ) is chosen to be -0.27. Therefore, the control parameters resulted to: $K_P = -71; \tau_I = 0.0004$; and $\tau_D = 52$

5.4.3 IMC-based PI or PID feedback control design for the Air holdup control loop

Following the procedure for IMC controller design and practical issues that need to be considered as presented by the author (Ogunnaike & Ray, 1994), the controller for the air hold-up is designed as follows.

Design a controller for the air holdup system whose transfer function is given by Equation 5.29:

$$G_{22}(s) = \frac{7.78\times10^{-5}}{s+7.981\times10^{-3}} = \frac{9.75\times10^{-3}}{125.3s+1} \quad (5.29)$$

Using IMC strategy and converting it to a conventional feedback form. Since the transfer function of the $G_{21}(s)$ is invertible, we obtain

$$G_{22-}(s)^{-1} = \frac{125.3s+1}{9.75\times10^{-3}} \quad (5.30)$$

Therefore, from the IMC specifications and filter design Equation 5.31 is produced:

$$C_{22}(s) = \frac{1}{G_{22-}(s)} f(s) = \frac{125.3s+1}{9.75\times10^{-3}} \times \frac{1}{(\lambda s+1)^n} = \frac{125.3s+1}{9.75\times10^{-3}(\lambda s+1)} \quad (5.31)$$

As said previously $f(s)$ is a tuning filter with an adjustable factor Lambda (λ) similar to the closed-loop time, and *n* is the order of the filter. Now design the controller for the air holdup closed-loop response using an IMC-based PID feedback structure. Recall the general Equation 5.20 and solve Equation 5.32.

$$g_{C_{22}}(s) = \frac{C_{22}(s)}{1-G_{22}(s)C_{22}(s)} = \frac{\frac{125.3s+1}{9.75\times10^{-3}(\lambda s+1)}}{1-\left(\frac{9.75\times10^{-3}}{125.3s+1}\times\frac{125.3s+1}{9.75\times10^{-3}(\lambda s+1)}\right)} \quad (5.32)$$

Results after factorisation of Equation 5.32 are shown below:

$$g_{C_{22}}(s) = \frac{\frac{125.3s+1}{9.75\times10^{-3}(\lambda s+1)}}{1-\left(\frac{9.75\times10^{-3}}{125.3s+1}\times\frac{125.3s+1}{9.75\times10^{-3}(\lambda s+1)}\right)} = \frac{\frac{125.3s+1}{9.75\times10^{-3}(\lambda s+1)}}{\frac{9.75\times10^{-3}(\lambda s+1)-9.75\times10^{-3}}{9.75\times10^{-3}(\lambda s+1)}} = \frac{125.3s}{9.523\times10^{-3}\lambda s} + \frac{1}{9.523\times10^{-3}\lambda s}$$

$$\therefore g_{C_{22}}(s) = \frac{125.3s}{9.523\times10^{-3}\lambda}\left(1+\frac{1}{125.3s}\right)$$

Therefore, the PID controller for the air holdup loop has resulted in a PI controller presented in Equation 5.33,

$$G_C(s) = K_P\left(1+\tau_I\frac{1}{s}\right) = g_{C_{22}}(s) = \frac{125.3}{9.75\times10^{-3}\lambda}\left(1+\frac{1}{125.3s}\right) \quad (5.33)$$

because of the order of the system, the resulting PI control parameters are:

$$K_{P2} = \frac{125.3}{9.75\times10^{-3}\lambda}, \tau_{I2} = \frac{1}{125.3} \quad (5.34)$$

To ensure proper control Lambda (λ) is chosen to be 1.6. Therefore, the control parameters resulted in:$K_P = 8032$, $\tau_I = 0.008$. The Internal Model Control design–based on the PID feedback control design has been concluded in this section 5.4 and Table 5.1 presents the resulting control parameters.

Table 5.1: **PID feedback control parameters designed based on IMC**

Parameters	Layer Height	Air holdup
Proportional	-71	8032
Integral	0.0004	0.008
Derivative	52	0
Tuned filter factor Lambda & n	-0.27	1.6

Since all needed control parameters have been successfully obtained, the next section is based on the simulation of the Two Inputs and Two Outputs (TITO) system.

5.5 Simulation results of the Two-Inputs and Two-Output closed-loop system

This section is based on the simulation of the decentralized flotation model. The designed control parameters presented in Table 5.1 above are used to simulate the 2x2 flotation model as presented in the following subsection. Figure 5.5 represents the proposed closed-loop Simulink model of the decentralize column flotation system.

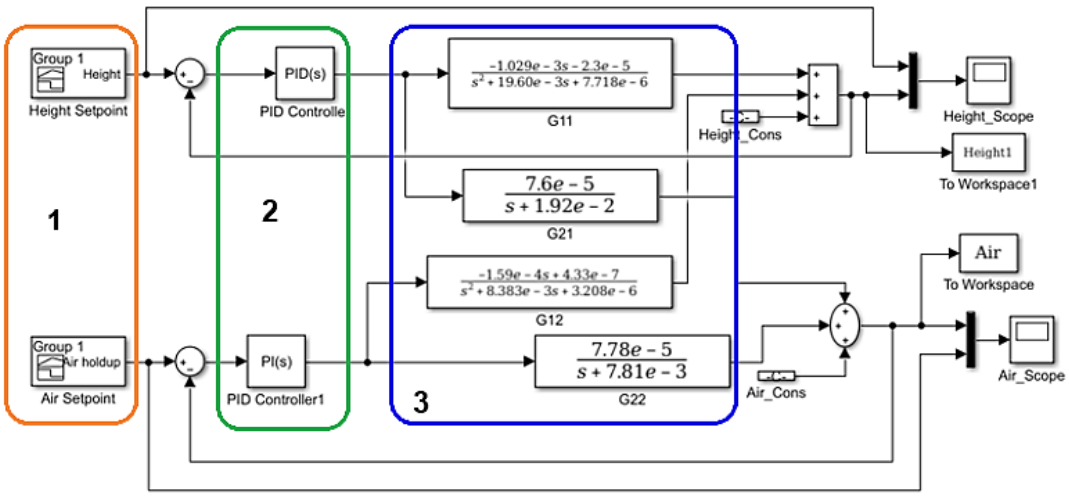

Figure 5.5: Decentralized Simulink model of the closed-loop TITO system

Investigations of the behaviour of the closed-loop system are performed to check the system's capability for set-point tracking. The set-point is set and adjusted using a Simulink block called signal builder, the two set-points for h and ε_g are labelled with orange colour (Point 1) in Figure 5.5. The control area shown by a green colour (Point 2) receives the error signal, which is produced by the difference between the set point and the system's output feedback signal. The control action aims at correcting the offset to make sure each system loop follows any set point or value. Table 5.2 introduces the study cases for various set-points changes that are used for the investigation of the proposed closed-loop 2x2 multivariable system's performance. The set-points of h=*60cm* and ε_g =*18%* as tabled below are used as the base/reference of the first case study for these investigations.

Table 5.2: Different set-points of the decoupled closed-loop system

Case Study	Set-points		Decoupled Plant with PI controller	
			Froth Layer Height	Air holdup
1	h	40-60(*cm*)	Establish a set point of the Froth layer height, (step from 40-60cm).	Establish a set point of the Air holdup (step from 10-18%).
	ε_g	10-18(%)		
2	h	40-60(*cm*)	The Froth layer height is kept at the same set point, to only investigate if by any chance the set-point change for Air holdup will influence that of the Froth layer height.	The set-point of Air holdup is increased or changed to a high value, to observe the closed-loop behaviour of the system.
	ε_g	12-20-15(%)		

3	h	50-70-60(cm)	The set-point of the Froth layer height is changed to observe the closed-loop behaviour of the layer height.	The set-point of the Air holdup is returned to its initial value to only investigate the influence of the changes made in the froth height.
	ε_g	10-18(%)		
4	h	80-60-80(cm)	Both set-points of the Air holdup and Froth layer height are changed, to observe the system's operational behaviour.	This is done to observe the closed-loop behaviour of the Froth layer height and the Air holdup in abnormal conditions
	ε_g	4-5-4 (%)		

5.5.1 Performance indexes of the transition processes of the 2x2 decentralized system

The following Figures (5.6 to 5.11) demonstrate the transition behaviour of the decentralized IMC-based PID feedback control designed for a closed-loop flotation system and evaluation conducted using different cases introduced in Table 5.2.

Case study 1: Start the process

In case 1, the amount of air is applied at the bottom of the column, and the air holdup (ε_g) in the collection zone is set to start from 10% - 18 %.

Figure 5.6 (a) shows the result of the froth layer height (h) and Figure 5.6 (b) displays the results of the air holdup (ε_g). The froth layer height (h) is set at 40 cm for 10 seconds (see set-point in red) and after 10 seconds a step change is applied from 40 cm to 60 cm. As can be noted that the blue response is the froth layer which is tracking the applied set-point change.

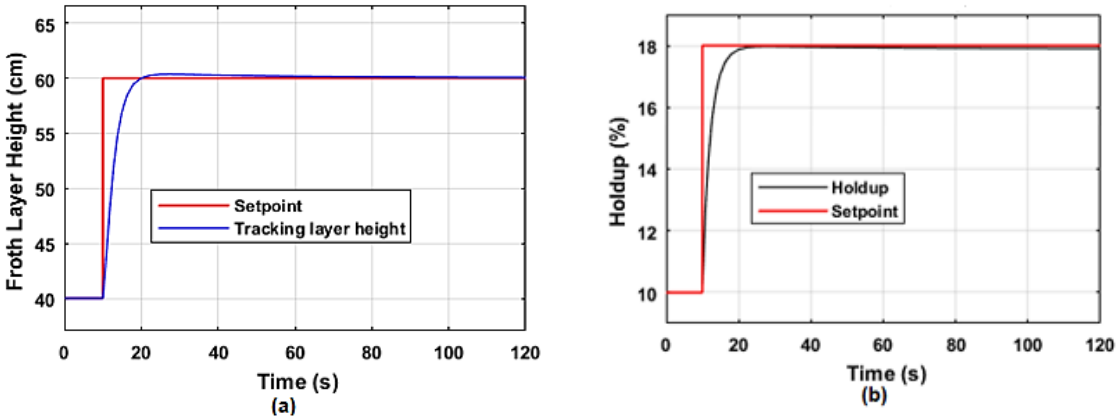

Figure 5.6: **Case study 1: Closed-loop response of the Froth Layer Height and Air Holdup processes**

On the other hand, Figure 5.6 (b) presents the response of the holdup (ε_g) within the air zone of the column flotation system, note that the black line, which is the holdup, effectively tracked the set-point that is changed from 10% to 18%. More cases with different step set-point changes were applied randomly to observe how well the designed controller can track those changes.

In the following case, variations or setpoint changes are applied in the air holdup loop.

Case study 2: Setpoint change applied on the Air holdup loop

Case 2 presents the set-point changes applied on the holdup loop while no change is applied on the froth layer loop. In Figure 5.7 the set-point of the holdup is changed from the step signal in Case 1 with a peak of 18% as shown in Figure 5.6(b) to the pulse signal with a peak of 20% in Figure 5.7(b) shown below.

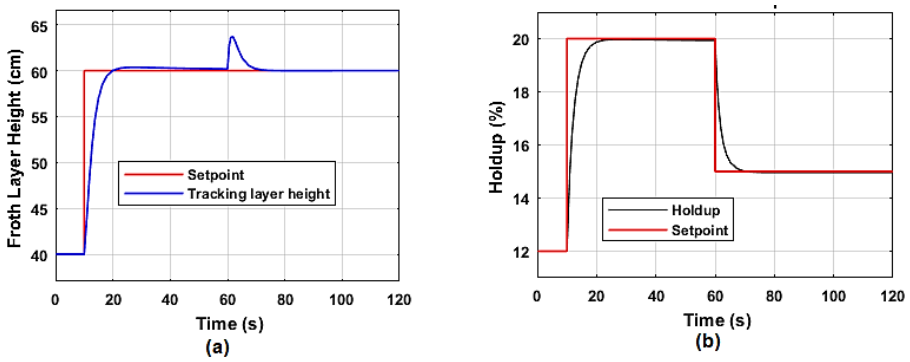

Figure 5.7: **Case study 2: Closed-loop response of the Froth Layer Height and Air Holdup processes**

As these changes were applied, the set-point of the froth layer height is kept at the step signal of 60 cm as shown in Figure 5.6 (a) and Figure 5.7 (a), under case 1 and case 2 respectively. When the holdup set-point is dropped or changed from 20% to 15% after 60 seconds, the change created an overshoot on the froth layer height loop, because of the rapid drop of the amount of air hold-up from the collection zone. This experiment demonstrated the necessity of improving Case study 2.

Improved Case study 2: Progressive variation of setpoint changes

This Case aims to show the importance of the progressive variety of small changes in a flotation system. Figure 5.8 shows how the overshoot from the froth layer height (Figure 5.7 (a)) is reduced by careful adjustment of the air holdup. As it can be noted from Figure 5.8 (a and b) increasing the amount of air holdup did not negatively affect the other loop, which is froth height, only decreasing the amount of air applied would badly influence the cleaning zone (froth height) of the flotation system. Therefore, the importance of not having a large decrease in the air is noted.

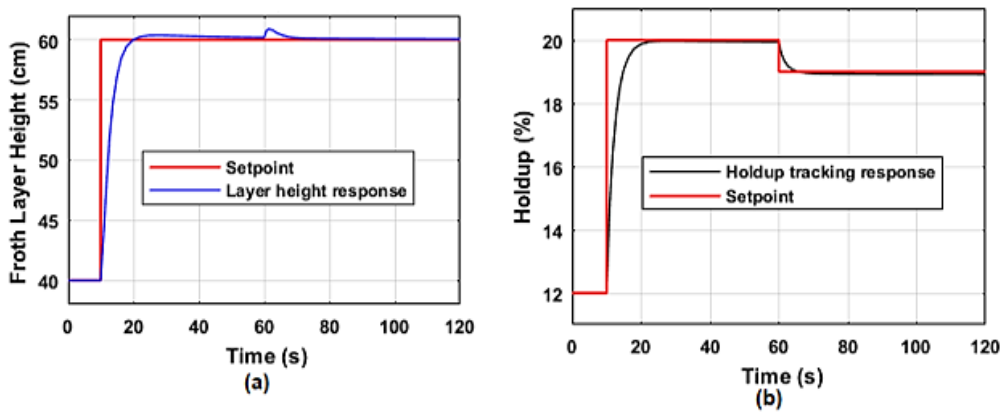

Figure 5.8: **Improved Case study 2: Closed-loop response of the Froth Layer Height and Air Holdup processes**

Any inattentive move when decreasing the amount of air holdup may have destructions on the other loop or within the cleaning zone.

Case study 3: Air holdup remains the same and Froth layer height is changed

In Case 3, the set-points for the layer height control varied from 50 cm to 70 cm, then from 70 cm to 60 cm and Figure 5.9(c) shows variation from 50 cm to 70 cm, then from 70 cm to 67 cm while the set-point for the holdup is kept from 10 % to 18%. The results of all these evaluations or changes applied in Case study 3 are shown in Figure 5.9.

In figure 5.8 and Figure 5.9, the setpoint is the change from the step of 60 cm for a froth layer height to pulse signal with a peak of 70 cm (from 70 cm - 60 cm) and air holdup 20% peak of the pulse back to step with 18% peak in Figure 5.9. The setpoint changes on the froth layer height loop created an overshoot on the air hold from the collection zone. This experiment indicated the need to improve the state of the system, which resulted in Figure 5.9 (c) and Figure 5.9 (d).
The little overshoot of the air holdup as observed in Figure 5.9(b) has been eliminated as seen in Figure 5.9(d), by adjusting the regulator of the wash water in the cleaning zone (froth layer height from 70 cm - 67 cm) Figure 5.9c. Therefore, the importance of progressive variations in setpoint alteration is again noticeable.

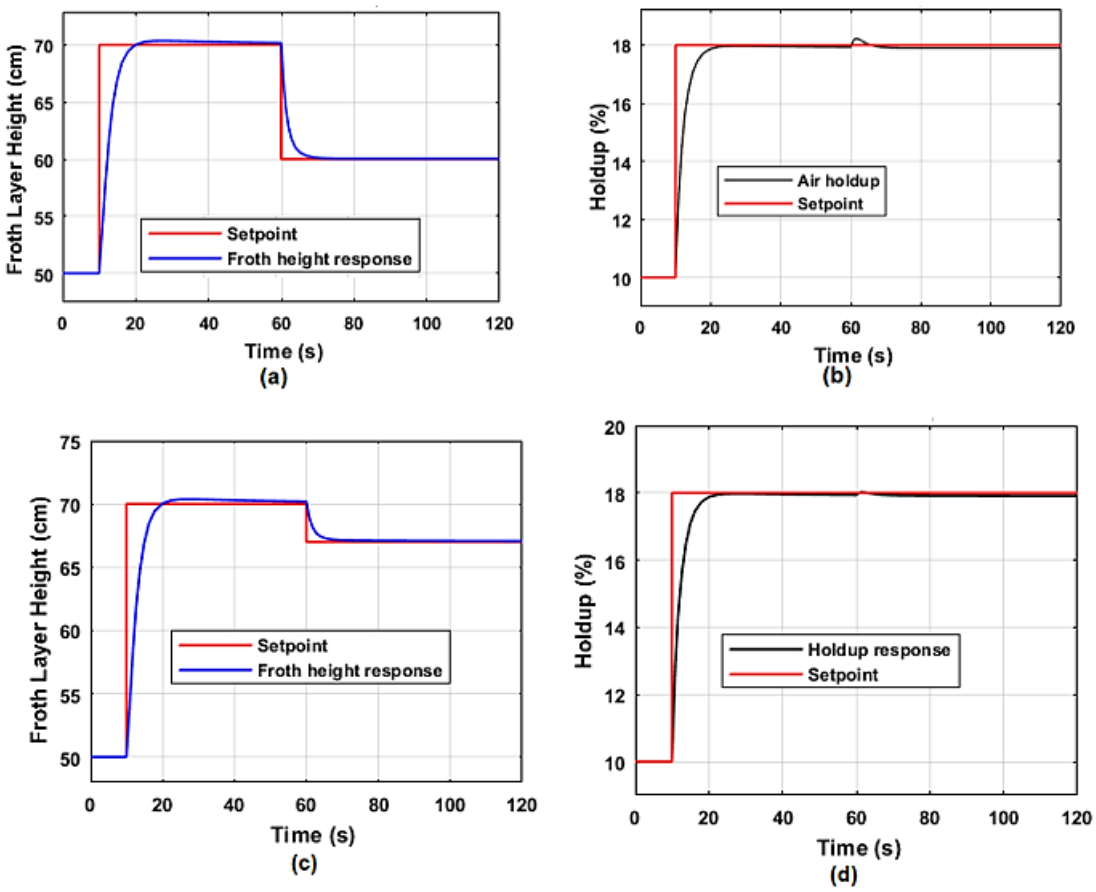

Figure 5.9: Case study 3: Closed-loop response of the Layer Height and Holdup

Case study 4: Same time Regulation of Froth layer height and Air holdup

In case study 4, the set-point changes are applied in both loops collection and cleaning zones (Froth layer height loop and Holdup loop) at the same time. Figure 5.10 presents these changes, as can be noted in case study 4, the set points were changed after 10 seconds and again at 60 seconds. The results show a decent set-point tracking is still accomplished with a slight overshoot on the air hold-up as shown in Figure 5.10 (b). The set-points for the froth layer height are varied from 80 cm to 60 cm, then from 60 cm to 80 cm as shown in Figure 5.10 (a), while the set-point for the holdup is varied from 4% to 5%, then from 5% to 4% shown in Figure 5.10 (b).

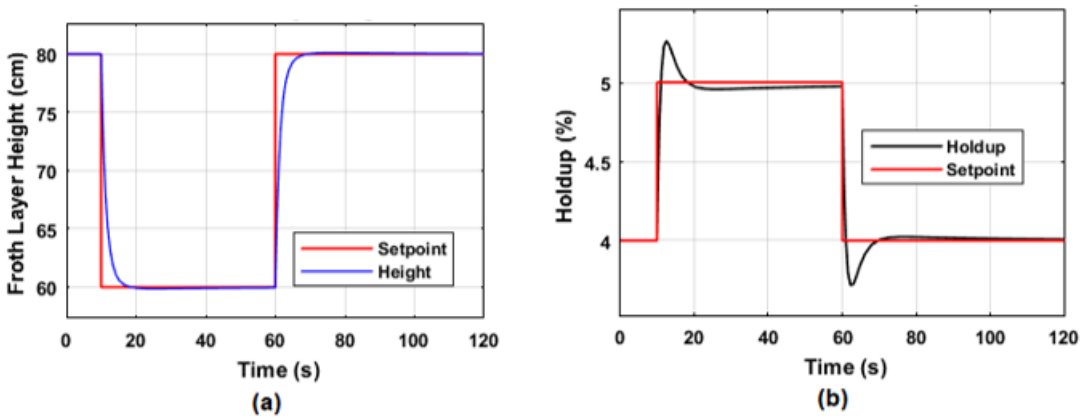

Figure 5.10: Case study 4: Closed-loop response of the Froth Layer Height and Air Holdup processes

Improved Case study 4: Progressive variation of setpoint changes

To eliminate the overshoot in Figure 5.10 (b) shown above, the set-point of the froth layer height is varied from 80 cm to 74 cm at 10 seconds, then from 74 cm to 80 cm at 60 seconds as shown in Figure 5.11 (a). While the set-point for the holdup is kept from 4% to 5%, then from 5 %to 4% as in Figure 5.11 (b). The performances shown in Figure 5.10 and Figure 5.11 for the tracking of set-points and characteristics response are tabled in Table 5.3.

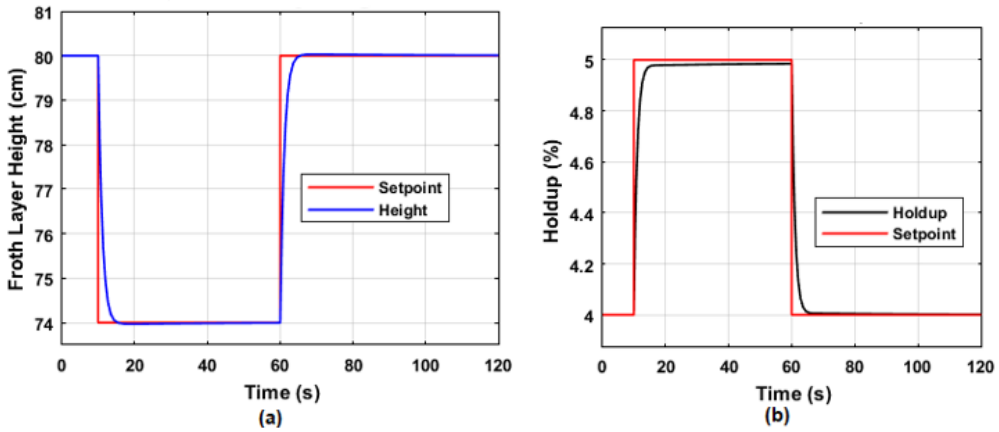

Figure 5.11: Case study 4: Closed-loop response of the Froth Layer Height and Air Holdup processes

The transition behaviour characteristics of the froth height and air holdup flotation processes under case study 1 to case study 4 are measured and recorded in Table 5.3. All the Figures from 5.6 to 5.11 are used to analyse the influence of the set-point changes of the closed-loop decentralized control processes behaviour.

Table 5.3: Transition processes performance indexes

Cases Study	Set-points		Transition behaviour characteristics of the decentralized Froth Layer Height and the Air Holdup				
			Rise time [sec]	Settling time [sec]	Peak time [cm] and [%]	Overshoot [cm] and [%]	Steady-state error [cm] and [%]
1	***h***	40-60(***cm***)	5.48	18.73	27.166	0.36	0
	ε_{gcz}	10-18(***%***)	4.86	18.32	27.166	0.03	0
2	***h***	40-60(*cm*)	5.43	68.32	61.92	3.68	0
	ε_{gcz}	12-20-15(%)	0.77	68.53	27.166	0.03	0
3	***h***	50-70-60(cm)	1.80;	67.5	27.166	0.36	0
	ε_{gcz}	10-18(%)	4.84	64.5	61.996	0.21	0
4	***h***	80-60-80(*cm*)	0.49	66.0	75.01	0.1	0
	ε_{gcz}	4-5-4 (%)	0.0044	68.56	12.51	0.26	0

5.5.2 Results analysis of the IMC-based PID feedback control design for the 2x2 decentralized system

Analysis for the setpoint tracking has been carried out as presented in Figure 5.6 to Figure 5.11. The investigation results indicate that both the trajectories behaviour of the froth layer height and air holdup do follow the set-point variations. The investigation conducted in section 5.5.1 has proven to be successful in terms of set-point tracking and good settling time. Table 5.3 provides the various performance indices for the froth layer height and air holdup transition responses as the set-points variation is applied.

5.6 Controller design of the 3x3 decentralized system

The model of the system is now increased to a 3x3 input-output system, the same process that was followed for the 2x2 system is used again for the 3x3 model.

5.6.1 Relative Gain Array and Interaction Measures

Now following the interaction analysis and RGA technique as explained already, the resulting mathematical modeling is accomplished as follows:

$$G_p(s) = \begin{bmatrix} G_{11}(s) & G_{12}(s) & G_{13}(s) \\ G_{21}(s) & G_{22}(s) & G_{23}(s) \\ G_{31}(s) & G_{32}(s) & G_{33}(s) \end{bmatrix} \quad (5.35)$$

All the transfer functions of Equation 5.35 are presented in Chapter 4, Equations 4.2 to 4.7. The steady-state conditions of Equation 5.35 resulted in the steady-state process gain matrix in Equation 5.36. Letting K be the matrix of steady-state gains of the transfer function matrix G(s) as *s* turns to zero:

$$G_p(0) = \begin{bmatrix} G_{11}(0) & G_{12}(0) & G_{13}(0) \\ G_{21}(0) & G_{22}(0) & G_{23}(0) \\ G_{31}(0) & G_{32}(0) & G_{33}(0) \end{bmatrix} = \begin{bmatrix} -2.980 & 0.135 & 2.98 \\ 0.004 & 0.0097 & 0.004 \\ 0 & 0 & 1 \end{bmatrix} \quad (5.36)$$

The RGA of the steady-state gain matrix presented in Equation 5.36 is defined by the authors (Ogunnaike & Ray, 1994; Chen & Seborg, 2002).

$$\wedge = \begin{bmatrix} \lambda_{11} & \lambda_{12} & \lambda_{13} \\ \lambda_{21} & \lambda_{22} & \lambda_{23} \\ \lambda_{31} & \lambda_{32} & \lambda_{33} \end{bmatrix} = G \cdot G^{-1})^T \quad (5.37)$$

Where: $(G^{-1})^T$is the transpose of (G^{-1}). In the above Equation 5.37, important to note that the operator "·" indicates the multiplication of an element by element with its corresponding elements. The corresponding relative gains can be calculated as presented in Equation 5.38.

$$\wedge = \begin{bmatrix} \lambda_{11} & \lambda_{12} & \lambda_{13} \\ \lambda_{21} & \lambda_{22} & \lambda_{23} \\ \lambda_{31} & \lambda_{32} & \lambda_{33} \end{bmatrix} = \begin{bmatrix} \lambda_{11} & 1-\lambda_{11} & 1-\lambda_{11} \\ 1-\lambda_{11} & \lambda_{11} & 1-\lambda_{11} \\ 1-\lambda_{11} & 1-\lambda_{11} & \lambda_{11} \end{bmatrix} \quad (5.38)$$

from the definition of the inverse of a matrix, as followed for a 2x2 matrix in section 5.3, carry out term-by-term multiplication of the elements of the matrices in Equation 5.37. With regards to the steady-state gains in Equation 5.36, the RGA matrix is obtained as follows:

$$\Delta(\mathrm{K}) = \begin{bmatrix} \frac{\mathrm{K}_{11}\mathrm{K}_{22}}{\mathrm{K}_{11}\mathrm{K}_{22}-\mathrm{K}_{12}\mathrm{K}_{21}} & \frac{-\mathrm{K}_{21}\mathrm{K}_{12}}{\mathrm{K}_{12}\mathrm{K}_{21}-\mathrm{K}_{11}\mathrm{K}_{22}} & \frac{-\mathrm{K}_{13}\mathrm{K}_{31}}{\mathrm{K}_{13}\mathrm{K}_{31}-\mathrm{K}_{12}\mathrm{K}_{21}} \\ \frac{-\mathrm{K}_{21}\mathrm{K}_{12}}{\mathrm{K}_{12}\mathrm{K}_{21}-\mathrm{K}_{11}\mathrm{K}_{22}} & \frac{\mathrm{K}_{11}\mathrm{K}_{22}}{\mathrm{K}_{11}\mathrm{K}_{22}-\mathrm{K}_{12}\mathrm{K}_{21}} & \frac{-\mathrm{K}_{23}\mathrm{K}_{32}}{\mathrm{K}_{23}\mathrm{K}_{32}-\mathrm{K}_{11}\mathrm{K}_{22}} \\ \frac{-\mathrm{K}_{13}\mathrm{K}_{31}}{\mathrm{K}_{13}\mathrm{K}_{31}-\mathrm{K}_{12}\mathrm{K}_{21}} & \frac{-\mathrm{K}_{23}\mathrm{K}_{32}}{\mathrm{K}_{23}\mathrm{K}_{32}-\mathrm{K}_{11}\mathrm{K}_{22}} & \frac{\mathrm{K}_{22}\mathrm{K}_{33}}{\mathrm{K}_{22}\mathrm{K}_{33}-\mathrm{K}_{23}\mathrm{K}_{32}} \end{bmatrix} \quad (5.39)$$

The results evaluation of RGA yields the following:

$$\Delta(K) = \begin{bmatrix} 0.98 & 0.018 & 0 \\ 0.018 & 0.98 & 0 \\ 0 & 0 & 1 \end{bmatrix} \quad (5.40)$$

Interpreting the RGA Elements

(Ogunnaike & Ray, 1994), discussed the procedure for loop pairing based on interaction analysis. To interpret the resulting RGA matrix shown in Equation 5.39, following the recommendations as presented by the authors (Ogunnaike & Ray, 1994) for the decentralized control. The recommended pairing's steady-state input-output relationship should thus be:

$$\begin{bmatrix} h(0) \\ \varepsilon_{gcz}(0) \\ B_{bias}(0) \end{bmatrix} = \begin{bmatrix} G_{11}(0) & G_{12}(0) & G_{13}(0) \\ G_{21}(0) & G_{22}(0) & G_{23}(0) \\ G_{31}(0) & G_{32}(0 & G_{33}(0) \end{bmatrix} = \begin{bmatrix} -2.980 & 0.135 & 2.98 \\ 0.004 & 0.0097 & 0.004 \\ 0 & 0 & 1 \end{bmatrix} = \begin{bmatrix} U_1(0) \\ U_2(0) \\ U_3(0) \end{bmatrix} \quad (5.41)$$

Recommended initially for control loop pairing is to pair the controlled and manipulated variables so that the relative gains are positive and as close to one as possible (Bristol, 1966). As a result, for the recommended pairing's steady-state input-output relationship and upon analysis of Equation 5.40, is concluded that this column flotation process is controlled as follows:

- the froth layer height is controlled by manipulating U_1 (U_W: wash-water flowrate control signal).
- the air holdup in the collection zone is controlled by manipulating U_2 (U_g: air flowrate control signal).
- the bias is controlled by manipulating U_3 (U_T: non-floated flowrate control signal).

The following section is based on designing the PID controller through the Internal Model Control (IMC).

5.6.2 IMC-based PID feedback control design for the Bias control loop

Design a controller for the bias system whose transfer function is given by $G_{33}(s) = 1$, then the controller design of loop 3 is as follows.

Factorization of the process model using the proposed IMC design procedure is in the following steps: as presented and used in sections 5.3 and 5.4. Remember Figure 5.4 and the calculation of the PID parameters for the first two loops using the IMC technique, then follow the same process for the design parameters of the 3rd loop (the bias).

$$C(s) = C_{33}(s) = \frac{1}{G_{33}(s)} f(s) = 1 \times \frac{1}{(\lambda s+1)} = \frac{1}{(\lambda s+1)} \quad (5.42)$$

Substitute the above equation (Eq. 5.42) into equation (5.18) this results in the following:

$$g_{C_{33}}(s) = \frac{C_{33}(s)}{1-G_{33}(s)C_{33}(s)} = \frac{\frac{1}{(\lambda s+1)}}{1-\left(1\times\frac{1}{(\lambda s+1)}\right)} = \frac{\frac{1}{(\lambda s+1)}}{\frac{(\lambda s+1)-1}{(\lambda s+1)}} = \frac{1}{(\lambda s+1)-1} = \frac{1}{\lambda s} \quad (5.43)$$

Therefore, the ideal PID structural equation (5.43) leads to the following:

$$G_C(s) = K_P\left(1 + \tau_I \frac{1}{s}\right) = g_{C_{33}}(s) = \frac{1}{\lambda}\left(0 + \frac{1}{s}\right) \quad (5.44)$$

To ensure proper control and through severally test Lambda (λ) is chosen to be 1.85. Therefore, the control parameters for the bias loop resulted in: $K_P = 0$, $\tau_I = 0.54$.

Table 5.4 introduces the study cases for various set-points changes that are used for the investigation of the proposed closed-loop 3x3 multivariable system's performance.

Table 5.4: **Case studies for the set-point variation to perform analysis of the different set-point effects in a 3x3 multivariable Column Flotation process**

Cases Study	Set-points		Decentralized 3x3 Column flotation system with PI controller		
			Froth Layer Height	Air holdup	Steady-state error [cm] and [%]
1	*h*	40-60 (*cm*)	Set points for the froth layer height, air holdup, and bias are introduced.	Introduce the set points and observe the closed-loop behaviour of the MIMO system under study.	Establish the set point of the bias (step from 7.4-8-7.4(cm^3/s).
	ε_{gcz}	10-18 (%)			
	Bias	7.4-8-7.4 (cm^3/s)			
2	*h*	40-60 (*cm*)	The set point for height is kept and changes are made on the set point for the air holdup to observe the closed-loop behaviour of the whole system.	While the Froth layer height set-point is kept, changes were made on the air holdup to observe the closed-loop behaviour of the whole system	Previously bias set-point remains the same, while changes are applied to the air holdup.
	ε_{gcz}	12-20-15(%)			
	Bias	7.4-8-7.4 (cm^3/s)			
3	*h*	50-70-60 (cm)	To observe the capability of the set-point tracking, the set-point for the froth layer height is changed.	Air holdup remains the same as in case 1, while the froth layer height is changed. This is prepared to detect how much the interconnections within the system are strong.	The bias is kept constant while the height in the cleaning zone is changed, to observe the closed-loop behaviour of the system.
	ε_{gcz}	10-18 (%)			
	Bias	7.4-8 (cm^3/s)			
4	*h*	40-60 cm	The set-point of the froth layer height is returned as in case 1, while the bias is changed to observe the system behaviour.	The air holdup & froth layer is taken back to the set point as in case 1, while the bias is changed to observe the closed-loop behaviour of the air holdup.	The froth layer height is returned to the initial condition, the air holdup remains as in case 3 and the bias is changed to a step signal with a peak of 8.5 (cm^3/s). The aim is to observe the closed-loop behaviour of the system.
	ε_{gcz}	10-18 *%*			
	Bias	8-8.5 (cm^3/s)			
5	*h*	80-60-80 (*cm*)	All set points are pushed outside limits, and they change as time goes on.	How is the system behaviour when the air holdup and wash water are increased over the limits as declared in Chapter 4	All set-point is pushed into outside limits that are declared in Chapter 4, to observe how the system performs under hush conditions.
	ε_{gcz}	4-5-4 (%)			
	Bias	7-6.5-7(cm^3/s)			

5.6.3 Simulation of the closed-loop 3x3 MIMO system

Table 5.4 presents the study cases followed to evaluate the reaction of the system model shown in Figure 5.12, under different set-point changes as defined. The aim at this point is based on the evaluation of the performance of the 3x3 system and how these loops influence each other.

This section focuses on the simulation of the closed-loop MIMO flotation system with set-point changes as defined in Table 5.4 for the 3x3 flotation system. In the same way, as performed for the 2x2 closed-loop system, the simulation for the 3x3 multivariable closed-loop system is performed.

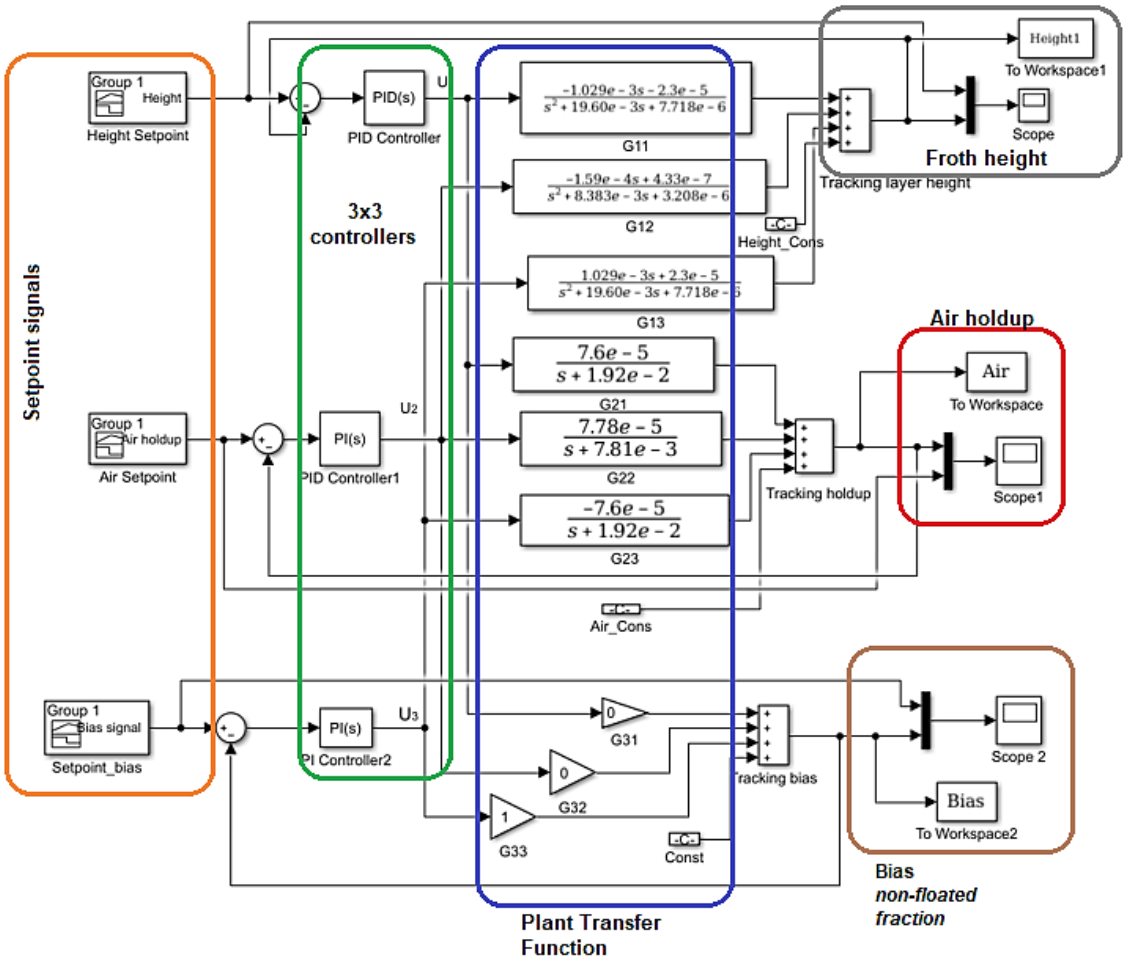

Figure 5.12: Decentralized MIMO control implemented in Simulink.

The 3x3 scheme proposed in this thesis has been modeled in Simulink as shown in Figure 5.12 above. The section labelled in orange colour in Figure 5.12, represents the setpoint signals of the whole scheme. The set-point adjustments are performed using the three signal builders for h, ε_g, and bias (Q_B) as labelled with orange colour in Figure 5.12. The area with controllers as indicated by the green colour receives the error signal, which is produced by the difference between the set point and the system's

output feedback signal. The control action aims at correcting the offset to make sure each system loop follows any set point or value.
The investigations of the closed-loop system are performed to check the system's capability for set-point tracking.

Table 5.4 introduces the study cases for various set-points changes that are used for the investigation of the proposed closed-loop 3x3 multivariable system's performance. The set-points of $h=60cm$, $\varepsilon_g = 18\%$, and the bias = 7.4 cm^3/s are used as the reference of the first case study for these investigations. The following Figures (5.13 – 5.18) present the transition behaviour of the decentralized IMC-based PID feedback control designed for a closed-loop flotation system.

Case study 1: Starting evaluation of the 3x3 process

In this Case study, the set-point of the froth layer height is set to start at 40 cm and increase to 60 cm at 10 seconds, the holdup is set to start at 10% and increase to 18%, and the bias starts at 7.4 to 8 and changed back to 7.4 cm^3/s at 60 seconds. As predictable the decentralized system gave good results for this case, the controlled loops Froth layer, Air hold and Bias respectively followed the specified set points.

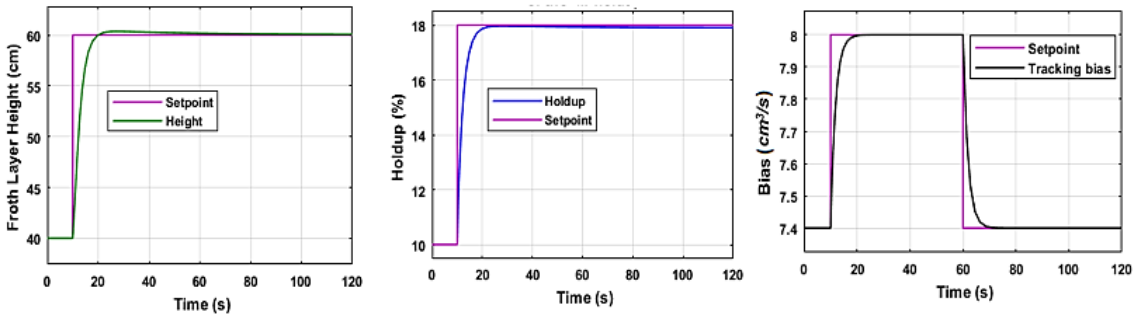

Figure 5.13: Case study 1: Decentralized closed-loop response of the Froth Layer Height, Holdup, and Bias

Case study 2: Set-point change applied on the Air holdup loop

Due to the findings obtained from the 2x2 system, this case only applied the progressive variation or small changes in a 3x3 flotation system presented in Figure 5.12. As seen in Figure 5.14 (b), the set-point changes are applied in the collection zone, and the amount of the applied air holdup change is reduced at 60 seconds. Through evaluation and results analyses it was noted that a large amount of air reduction resulted in an overshoot on the froth layer loop. This concluded with the task of evaluating the improved version of case 2 from the 2x2 model, but now in a 3x3 model.

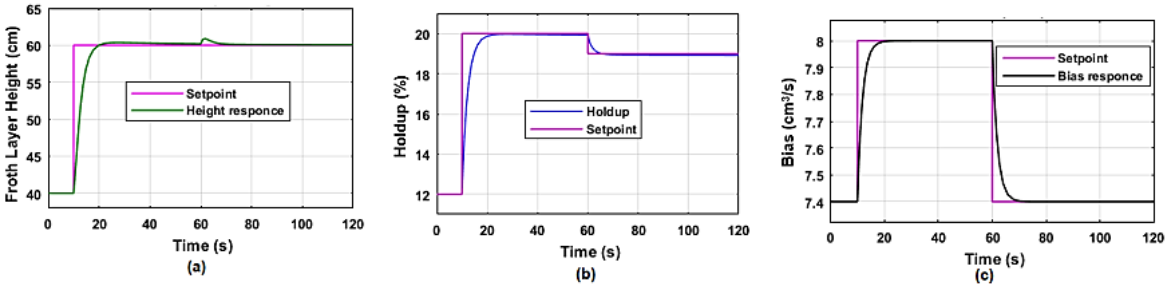

Figure 5.14: Case study 2: Decentralized closed-loop response of the Froth Layer Height, Holdup, and Bias

The evaluation is made to observe the closed-loop behaviour of the whole system and the tracking capabilities of the three loops when one loop is under forced changes. In the next case, Air hold up, and the Bias remains the same as in case 1, while the froth layer height is changed. This is prepared to distinguish the capability of the designed controller to overcome the interconnections within the system.

Case study 3: Set-point change applied on the Froth layer loop

The investigation has been done to prove that the limits of the set-point changes must also be considered for the 3x3 system as it was proven and recorded for the 2x2 system. In Case study 3, the set-point changes were applied to the froth layer zone (from 50 cm – 70 cm and to 67 cm), to observe the closed-loop behavior of the whole system. The results from the changes shown in Figure 5.15 (a) are presented in Figure 5.15. It can be observed that Figure 5.15 (b) and Figure 5.15 (c) achieve their respective set-point while there is a small degree in the froth layer height at 60 sec shown in Figure 6.15 (a).

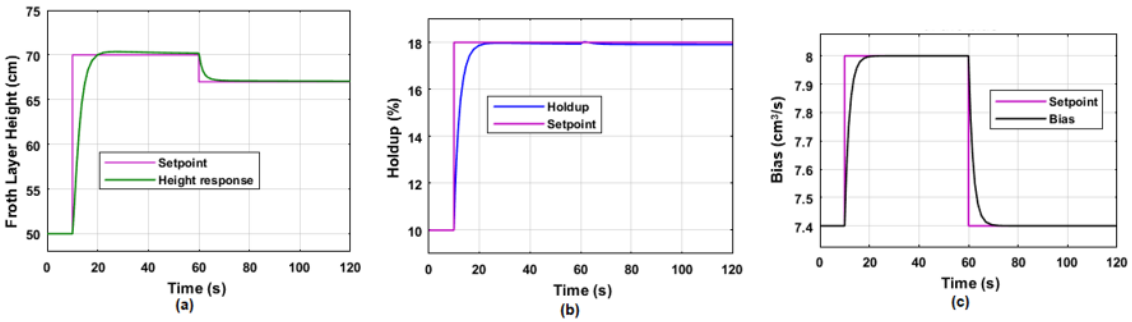

Figure 5.15: Case study 3: Decentralized closed-loop response of the Froth Layer Height, Holdup, and Bias

Case study 4: Set-point change applied to the Bias

Case study 4, offered in Figure 5.16 displays the results based on the set-point changes applied to the non-floated fraction. It can be noted that only the bias changed or followed the new set-point value with no undesirable effect on the froth height and

holdup loops. Therefore, as anticipated the changes made to the system did not affect the other loops.

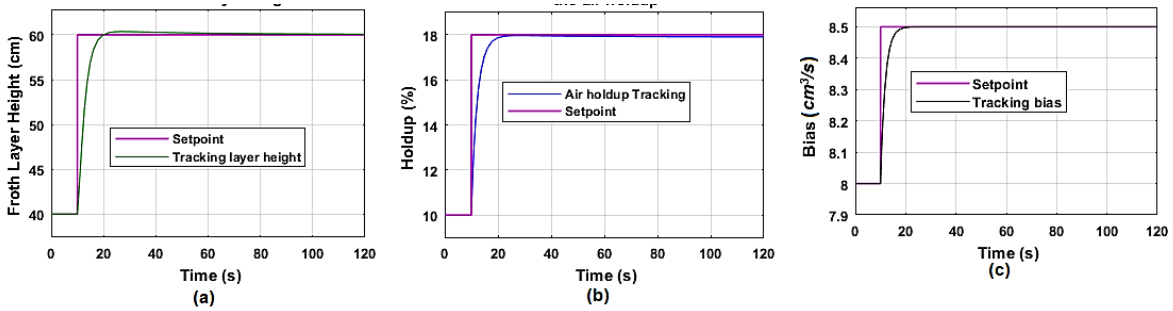

Figure 5.16: Case study 4: Decentralized closed-loop response of the Froth Layer Height, Holdup, and Bias processes

For a decentralized system, this is only possible when the set-points are all steps and if any of them have a pulse set-point signal, then the number of changes applied must not just be random but must be limited. This is a major problem or a shortfall of having a decentralized controller only. Figure 5.17 (b) is a practical display of the problem of random changes, or large set-point reduction as applied in Figure 5.17 (a).

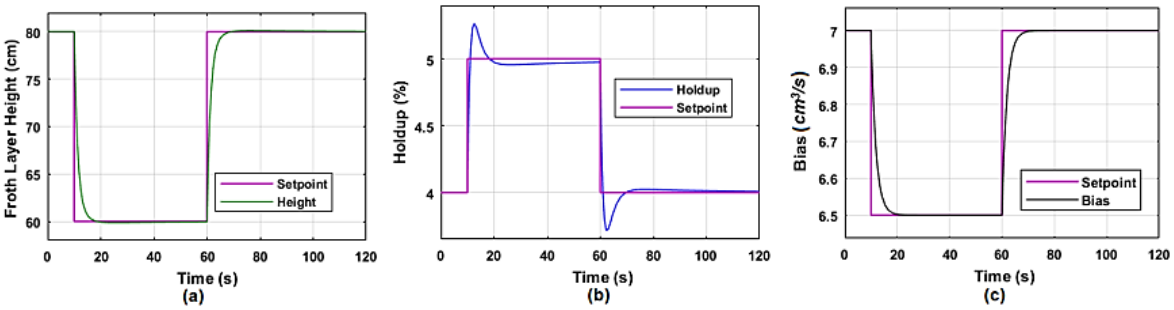

Figure 5.17: Case study 5: Decentralized closed-loop response of the Froth Layer Height, Holdup, and Bias

Improved Case study 5: Progressive variation of setpoint changes

To eliminate the overshoot in Figure 5.17 (b) shown above, the set-points for the froth height are varied from 80 cm to 74 cm, then from 74 cm to 80 cm (a), while the set-point for the holdup is kept from 4% to 5%, then from 5 %to 4% (b). Now, the results of Figure 5.17 are successfully improved as shown in Figure 5.18 (b).

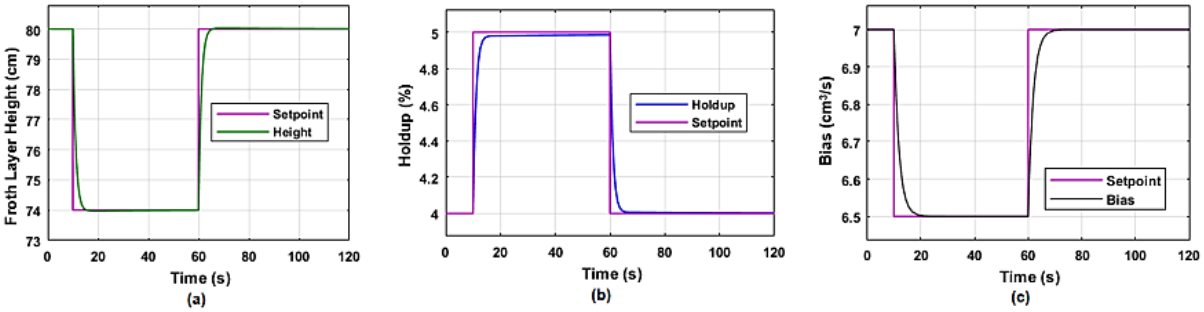

Figure 5.18: Case study 5: Decentralized closed-loop response of the Froth Layer Height, Holdup, and Bias

The investigation has been done to prove that the limits of the set-point changes must be considered also for the 3x3 system as it was proven and recorded before (any big change within the air zone of the flotation system can have a bad influence like system be unstable or overshoot on the cleaning zone, which is the froth height response). Figures 5.14 to Figure 5.16, demonstrate the results of the 3x3 model with the range of the set-points used for the 2x2 system with no overshoot.

Table 5.5 shows the characteristic of the transition behaviour of the 3x3 multivariable closed-loop system. It can be noted that all the set points are tracked successfully for froth layer height, air holdup, and bias.

5.6.4 Performance indexes of the transition processes of the 3x3 decentralized system

The features of the transition behaviour for the decentralized closed-loop system under the considered case studies are measured and presented in Table 5.5.

Table 5.5: Transition processes performance indexes

Cases Study	Set-points		Decentralised Froth layer height under the designed PI controller			Decentralised Air hold-up under the designed PI controller			Decentralised Bias under the tuned PI controller		
			Rise time (s)	Settling time (s)	Peak Time & Overshoot	Rise time (s)	Settling time (s)	Peak time % & Overshoot	Rise time (s)	Settling time (s)	Peak time % & Overshoot
1	*h*	40-60(*cm*)	5.43	18.74	26.99 & 0.36	4.91	18.35	26.99 & 0.03;	1.066e-14	67.55	60 & 0
	ε_{gcz}	10-18(%)									
	Bias	7.4-8-7.4 (cm^3/s)									
2	*h*	40-60(*cm*)	5.38;	68.32	61.92& 3.68	0.77	68.53	26.99 & 0.03	1.066e-14	67.3	60&0
	ε_{gcz}	12-20-15(%)									
	Bias	7.4-8 (cm^3/s)									
3	*h*	50-70-60(cm)	1.78	67.49	26.99 & 0.36	4.89	64.53	62 & 0.2	1.066e-14	67.46	60&0
	ε_{gcz}	10-18(%)									
	Bias	7.4-8(cm^3/s)									
4	*h*	40-60 cm	5.43	18.74	26.99 & 0.36	4.91	18.35	26.99 &0.03	4.12	17.35	74 & 0
	ε_{gcz}	10-18 %									
	Bias	8-8.5 (cm^3/s)									
5	*h*	80-60-80(*cm*)	0.49	66.03	75.01 & 0.11	0.0044	68.56	12.51 & 0.26	7.6	67.37	7&0
	ε_{gcz}	4-5-4 (%)									
	Bias	7-6.5-7(cm^3/s)									

The next section (Section 5.7) aims to prove the system's capabilities for disturbance rejection.

5.7 The performance of the system under disturbances applied at the outputs of the system

Using a random sequence with an association of time, the system is disturbed at the output by injecting a noise disturbance as illustrated in the Simulink block diagram of Figure 5.19. This is done to investigate the effects of the disturbance in the froth layer height and air holdup loops which are respectively Y_1, and Y_2 when only loop 1 is disturbed at a time.

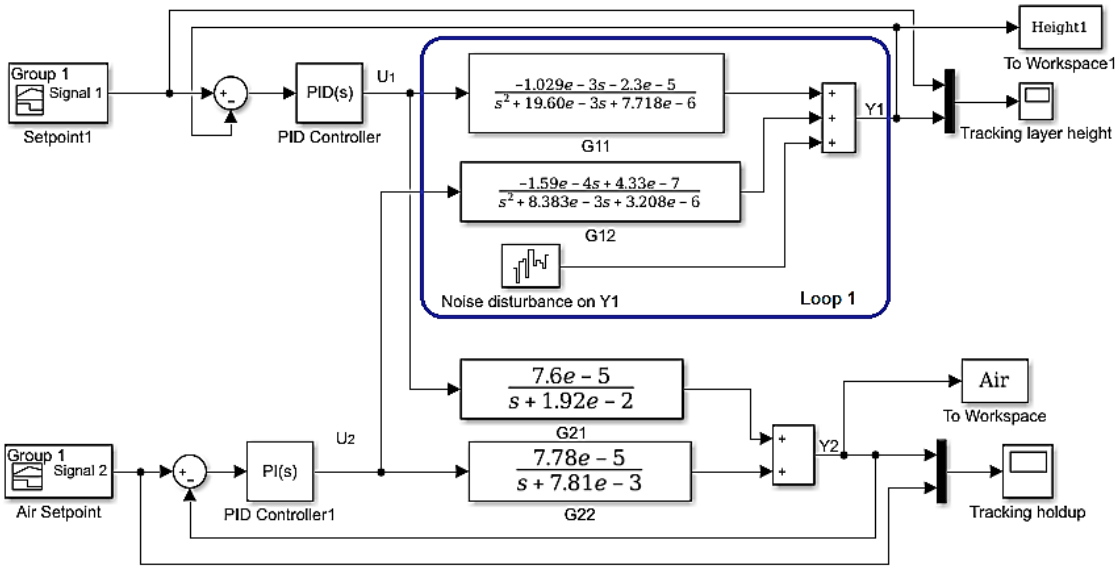

Figure 5.19: Decentralized controls subject to disturbances at the output of the MIMO system

For the first case, the disturbance with different noise magnitudes is applied in the cleaning zone (froth layer height). The following section presents the results of the system under the influence of the disturbance applied in the froth layer height.

5.7.1 Results of the system under the influence of disturbance applied on the Froth Layer Height (Loop 1)

The decentralized coupled system shown in Figure 5.19 is used to investigate the performance of the designed control parameters for different variables or random noise magnitudes added to the output signal of the froth layer height (Y_1). The results of these evaluations are shown in Figure 5.20 to Figure 5.24. The simulation results indicated that the disturbance effects did not affect set-point tracking, and loop 2 is also not affected by the disturbance applied in loop1 as presented by the results shown below.

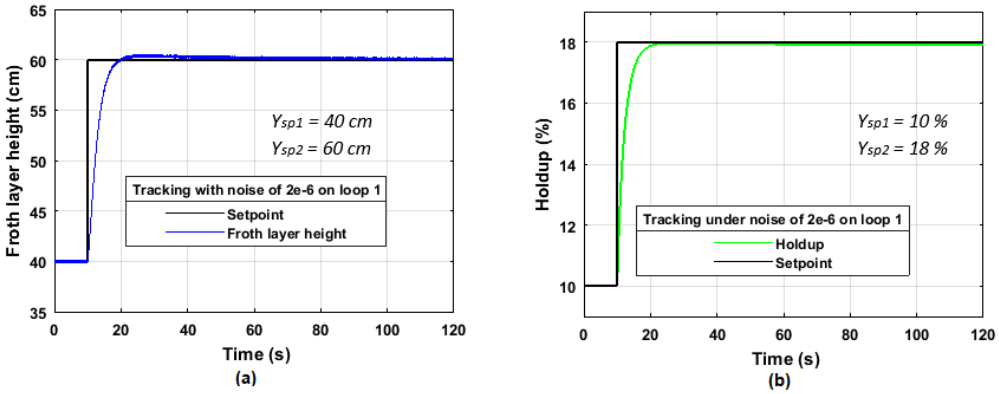

Figure 5.20: Closed-loop response of the Froth Layer Height and Holdup under disturbances of $2e^{-6}$ noise magnitude

For the results in Figure 5.21, the noise magnitude applied is increased from $2e^{-6}$ in Figure 5.20 to $1e^{-5}$ in Figure 5.21. Figure 5.21 (a) is the response of the froth layer height, notice that the noise presence is an indication of the applied disturbance. The result in Figure 5.21 (b) is the air holdup, as it can be noted there is no presence of noise, which means the disturbance in loop 1 (which is the cleaning zone) did not disturb loop 2 (which is the collection zone).

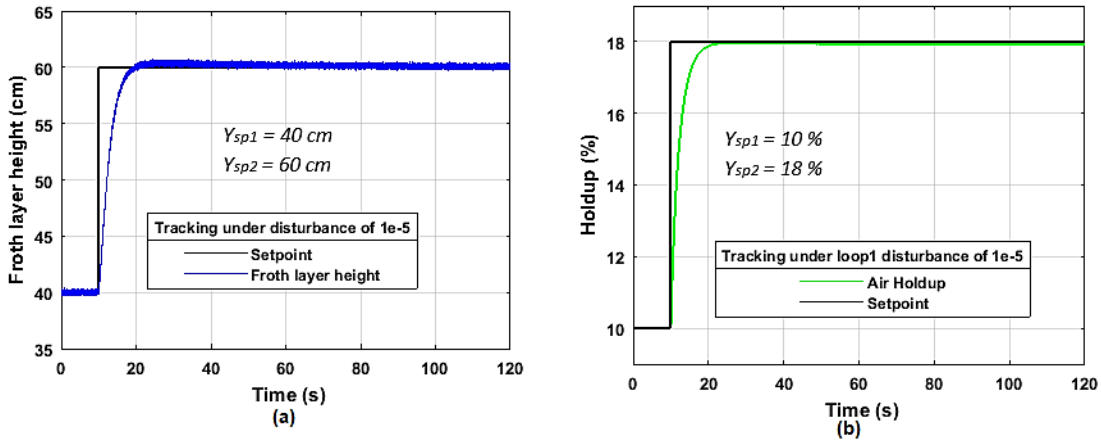

Figure 5.21: Closed-loop response of the Froth Layer Height and Holdup under disturbances of $1e^{-5}$ noise magnitude

The noise magnitude applied is increased to $9e^{-5}$ as indicated in Figure 2.22. As it can be noted that only Figure 5.22 (a) experienced more fluctuation as the noise magnitude increased.

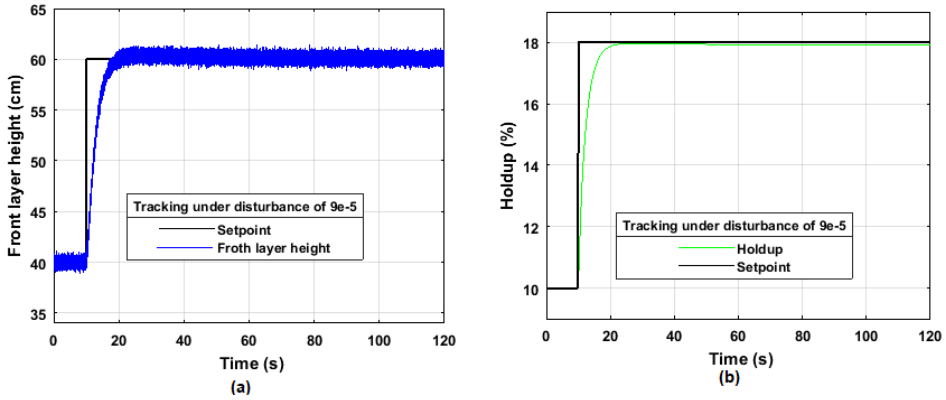

Figure 5.22: Closed-loop response of the Froth Layer Height and Holdup under disturbances of $9e^{-5}$ noise magnitude

A further increase to $5e^{-4}$ is applied in noise magnitude at the froth layer height loop as presented in Figure 5.23. Figure 5.23 (a) and Figure 5.24 (a) show the results of the changes made in noise magnitude, as it has been increased to $1e^{-3}$.

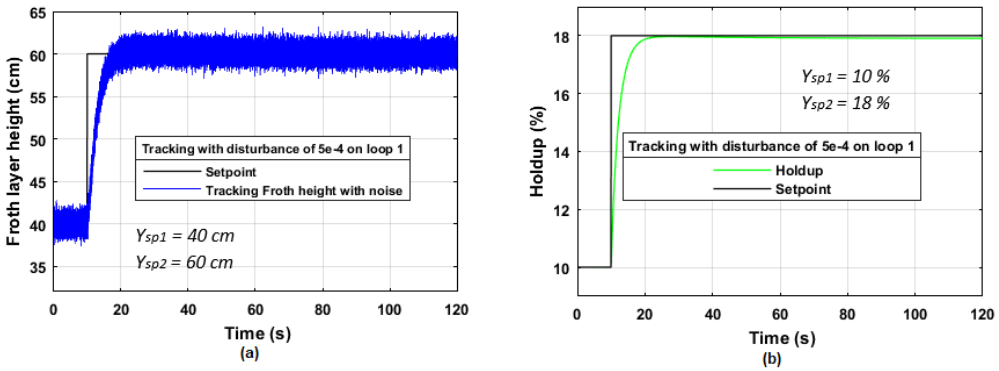

Figure 5.23: Closed-loop response of the Froth Layer Height and Air Holdup under disturbances $5e^{-4}$ noise magnitude

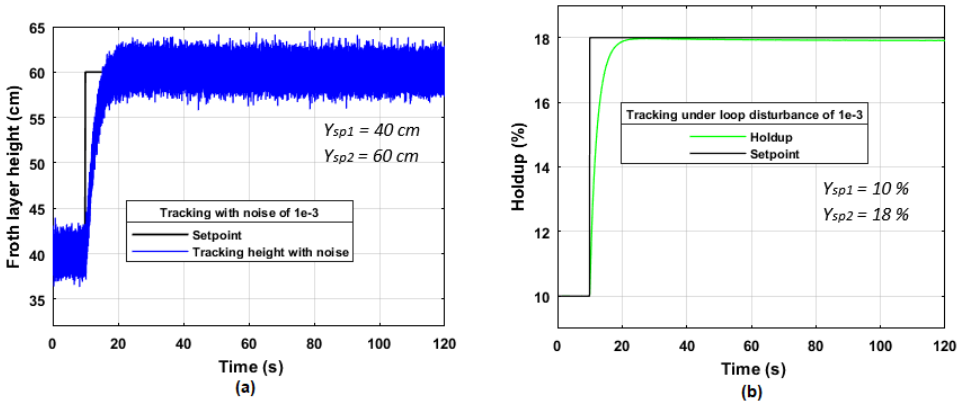

Figure 5.24: Closed-loop response of the Froth Layer Height and Air Holdup under disturbances $1e^{-3}$ noise magnitude

This investigation of increasing the magnitude of the added random noise continued to observe setpoint tracking under the influence of the disturbance and examine how these variations affected Loop 1 of Loop 2. All the results from Figure 5.20 to Figure 5.24 the air holdup (Loop 2), as it can be noted there is no presence of noise or any

sign of disturbance due to loop 1. This means the disturbance in loop 1 did not disturb loop 2 anywhere.

Similarly, the disturbances in the next section are applied to the interaction junctions of the air holdup zone (Loop 2).

5.7.2 Investigation on the disturbance influence applied on Loop 2 air holdup

In the second case, the disturbance is applied in the air holdup (Loop 2 or collection zone). This is done to investigate the effects of the disturbances applied to the air holdup zone with no disturbance in the froth zone, as shown in Figure 5.25.

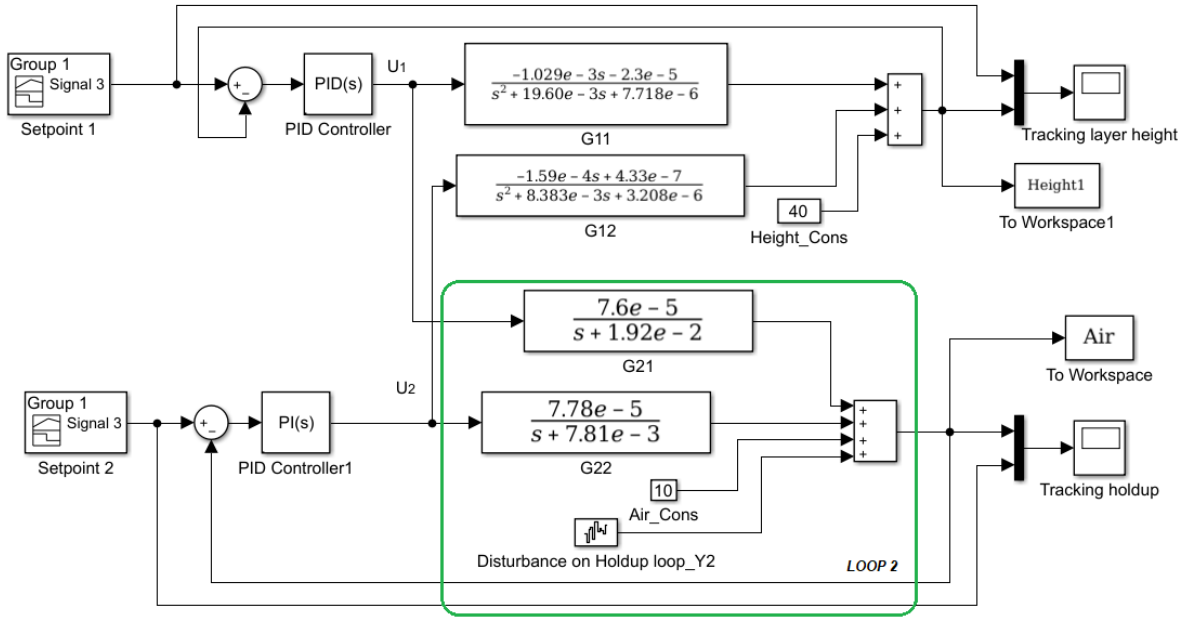

Figure 5.25: Decentralized coupling controls subject to disturbances at the output (Y_2)

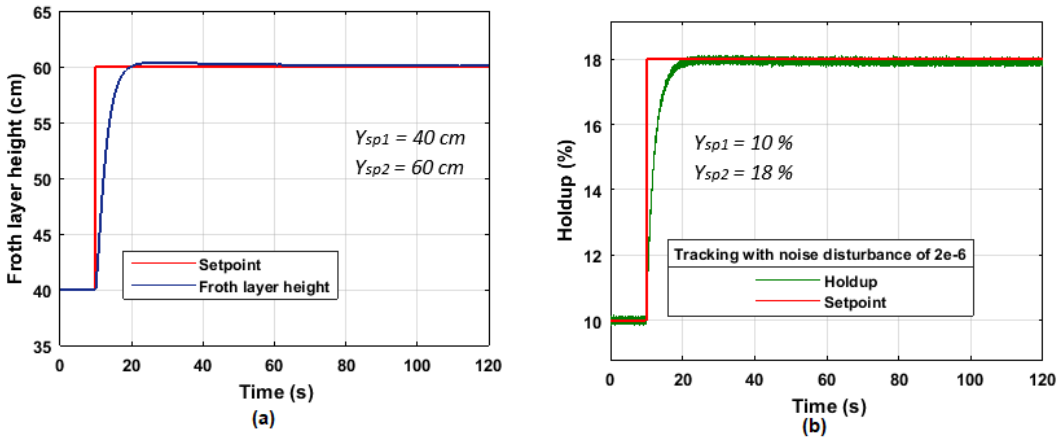

Figure 5.26: Closed-loop response of the Froth Layer Height and Holdup under disturbances of $2e^{-6}$ noise magnitude

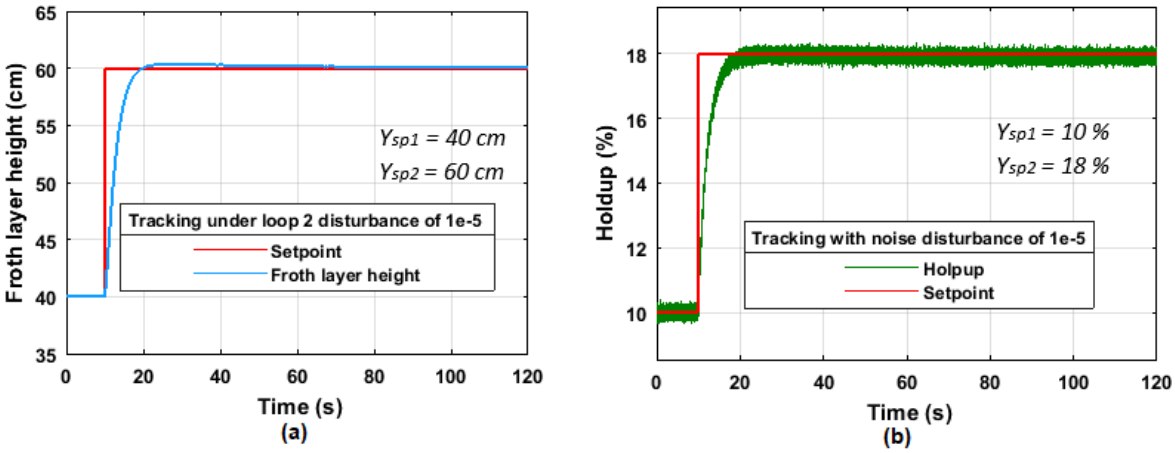

Figure 5.27: Closed-loop response of the Froth Layer Height and Holdup under disturbances of $1e^{-5}$ noise magnitude

For the results in Figure 5.27, the noise magnitude applied is increased as presented from Figure 5.26 to $1e^{-5}$ in Figure 5.27. Figure 5.27 (b) is the response of the holdup, notice that the noise presence is an indication of the applied disturbance. The result in Figure 5.27 (a) presents a froth layer height with some very small noise associated with the height response.

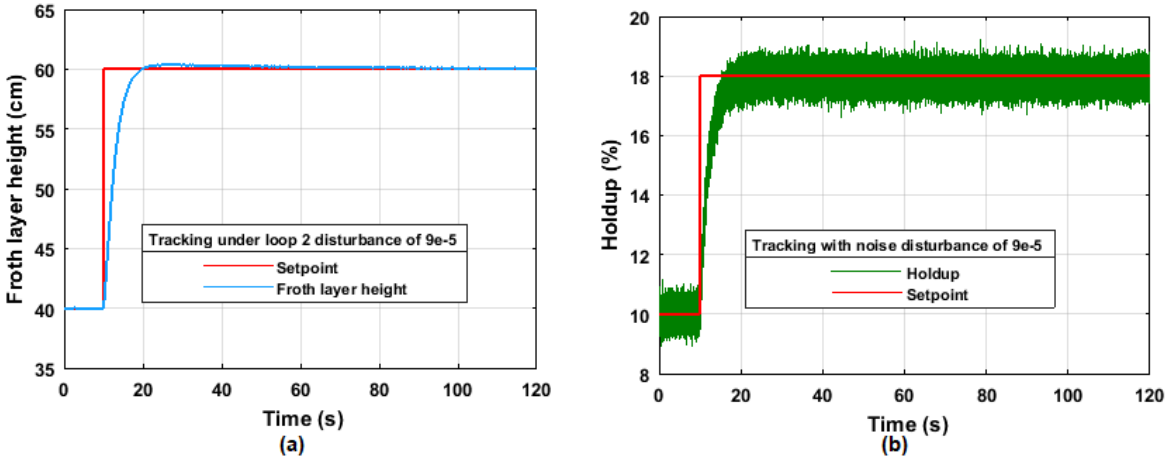

Figure 5.28: Closed-loop response of the Froth Layer Height and Holdup under disturbances of $9e^{-5}$ noise magnitude

The noise magnitude is increased as presented in Figure 5.27 to Figure 5.30. The result has proven that as the collection or holdup zone is disturbed, the cleaning zone (Loop 1) gets affected. See Figure 5.28 (a), which presents fluctuations from 0.36 cm - 0.4 cm.

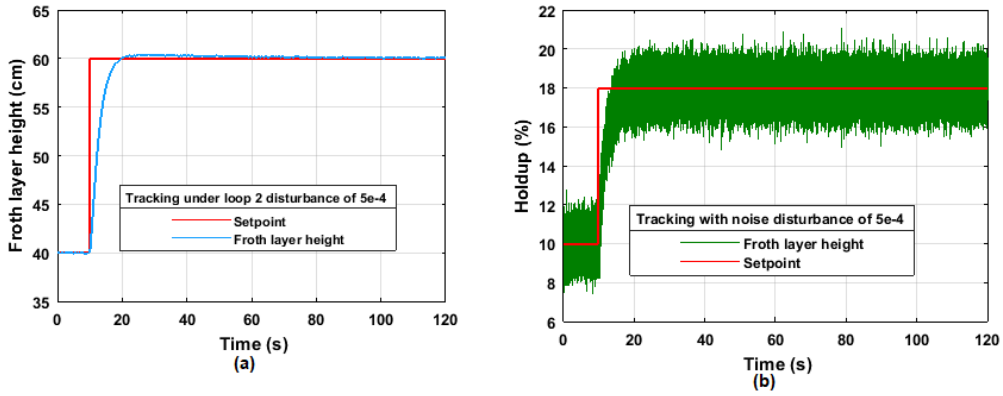

Figure 5.29: Closed-loop response of the Froth Layer Height and Holdup under disturbances of $5e^{-4}$ noise magnitude

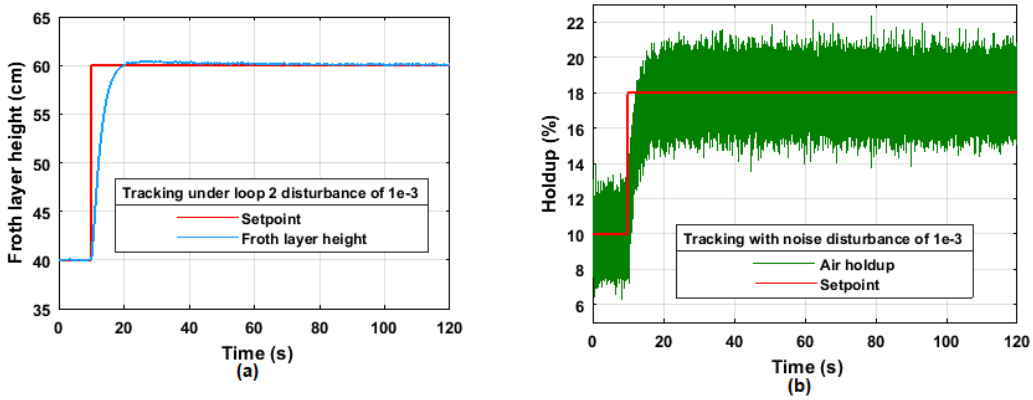

Figure 5.30: Closed-loop response of the Froth Layer Height and Holdup under disturbances of $1e^{-3}$ noise magnitude

Looking at all the results under the disturbance, from Figure 5.20 to Figure 5.24, and using Table 5.6 it can be noted that the presence of the disturbance in loop 1 did not disturb loop 2. Only 0.03 % of the overshoot was experienced by the holdup zone, under this condition. In the second scenario, as the disturbance is moved from loop 1 to loop 2, with the same noise magnitudes, the froth layer height obtains an overshoot of 0.36 cm

Table 5.6: Analysis of the disturbance effect over height, and air holdup

The position where the disturbance is applied	Noise magnitude	Decoupled Froth layer height under the designed PI controller					Decoupled Air hold-up under the designed PI controller				
		Rise time (s)	Settling time (s)	Overshoot	Peak time	Steady-state error	Rise time (s)	Settling time (s)	Overshoot	Peak time	Steady-state error
Loop 1	$2e^{-6}$	5.30	60.50	0.50	25.93	0	4.86	17.97	0.031	27.72	0
	$1e^{-5}$	5.11	60.69	0.69	24.49	0	4.87	17.97	0.031	27.72	0
	$9e^{-5}$	4.88	61.452	1.452	78.68	0	4.865	17.97	0.03	27.72	0
	$5e^{-4}$	13.56	63.253	3.25	78.68	0	4.87	17.97	0.03	27.72	0
	$1e^{-3}$	13.670	64.5482	4.55	78.68	0	4.87	17.971	0.029	27.72	0
Loop 2	$2e^{-6}$	5.37	60.36	0.36	27.69	0	4.55	18.12	0.12	33.997	0
	$1e^{-5}$	5.37	60.364	0.36	27.72	0	4.22	18.36	0.36	78.68	0
	$9e^{-5}$	5.38	60.373	0.373	27.72	0	13.4	19.25	1.25	78.68	0
	$5e^{-4}$	5.385	60.39	0.39	27.72	0	11.94	21.05	3.05	78.68	0
	$1e^{-3}$	5.394	60.401	0.401	27.72	0	11.27	22.34	4.34	78.68	0

The noise magnitude is increased from $2e^{-6}$ to $1e^{-3}$ respectively. As the magnitude of the disturbance applied in the system is increased, as seen in Figure 5.20 to Figure 5.30 the set-point tracking is still successful. Table 5.6 above presents the characteristics of the system transition behaviour under the applied disturbances.

5.8 Discussion of the simulation results

Decentralization of multivariable systems has proven to be one of the effective strategies to minimise or eliminate interactions and to introduce fully decentralized control of the system whenever need be. Relative Gain Array (RGA) approach is used to determine suitable input-output pairing while developing decentralized diagonal controllers. This technique improves the evaluation of the amount of interaction between controlled and manipulated variables. It specifies how the controlled and manipulated variables should be paired to produce optimal control loops, as presented in section 5.3. The benefits of using the relative gain array approach are explained in sections 5.2 and 5.3. Figures 5.20 to Figure 5.30 show that the disturbance and noise did not affect the system's ability to maintain the setpoint. Table 5.6 presents the various performance indices for the multivariable system response when the set points are varied, and unpredictable disturbance is applied. The investigation conducted shows that the closed-loop system under study follows exactly all the set-point variations. This proves the effectiveness of the designed decentralized controllers, regardless of the set-point variations or disturbances applied in a system. However, it is also noted that limitations on the set-point variations need to be considered to see figures with big overshoots like Figure 5.8 and Figure 5.11.

While comparing the results from Table 5.3 (case study 1) and Table 5.6, it can be noted that the system's responses, with and without disturbances have similar behaviour.

5.9 Conclusion

In conclusion, it is noted that the designed controllers for the 2x2 and 3x3 multivariable systems performed according to the specifications. All the results shown demonstrated successful performance in terms of set-point tracking (Table 5.3, 5.4, and 5.5) and disturbance rejection. Nevertheless, it is also noted that the coupled decentralized method could not handle the cases where the height or holdup control valves are not softly adjustable or closed/open. Any big change within the air holdup zone of the flotation system has a bad influence like system overshoot. The other loop which is the froth height response or cleaning zone also experiences instability when the airdrop

gap is big. System overshoot takes place once rapidly or implementation of big set-point variation, this gives us a good reason to find another technique to eliminate this problem. The flotation systems need to be controlled by controllers that can handle any range of changes.

Therefore, the next chapter discusses the decoupling method for the design of controllers to control the decoupled multivariable system. The open-loop characteristic behaviour as presented in Table 4.4 is used as a reference for the design of the closed-loop controller system. The following Chapter aims at improving the flotation system behaviour, through the reduction of the interactions using decoupling the system and using any method to design controllers that can handle any range of set-point variation.

CHAPTER SIX:
DECOUPLING CONTROLLER DESIGN FOR THE FLOTATION MULTIVARIABLE PROCESS

6.1 Introduction

This Chapter aims at improving the flotation system behaviour, through reduction of the process interactions and a convenient controller design. It describes the decoupling of the process models and the design of the controllers for the decoupled flotation system. This is done to achieve a completely closed-loop system where the change of the input in one loop does not affect or change the other loop. A decentralized system based on dynamic decoupled control is developed and simulated for set-point tracking and disturbance rejection using Matlab/Simulink software.

The organisation of this chapter is as follows: Section 6.2 deals with the development and decoupling of the 2x2 multivariable model of the column flotation process. Simulation of the 2x2 multivariable model is covered under section 6.3. Decoupling and simulation of the column flotation process 3x3 multivariable model are presented in section 6.4. Section 6.5 is based on the evaluation of the dynamic decoupling method under the influence of the disturbances. Section 6.6 is a comparison of the system behaviour under the decentralized decoupled method and decentralized coupled method. The conclusion is drawn and presented in section 6.7.

6.2 Development and decoupling of the 2x2 multivariable model of the flotation column process

Decoupling control, in general, refers to a diagonal decoupling of the process's input/output linkages such that they are independent. Decoupling strategies are primarily separated into two types: dynamic and static decoupling (Mikles & Fikar, 2002). The manipulated variables will influence the respective controlled outputs independently under any operational situations, according to dynamic decoupling. Static decoupling, on the other hand, is only concerned with the process of steady-state situations, therefore decoupling is only guaranteed for a specified set of input values. A diagram of the closed-loop control system with decoupling is shown in Figure 6.1, where D's represent decouplers, C's are the controllers and G's represent the transfer function of the plant. The plant (transfer function $G_p(s)$) involves the design of a transfer function matrix of the de-coupler $D(s)$, such that $G_p(s)xD(s)$ is a diagonal transfer function matrix $M(s)$.

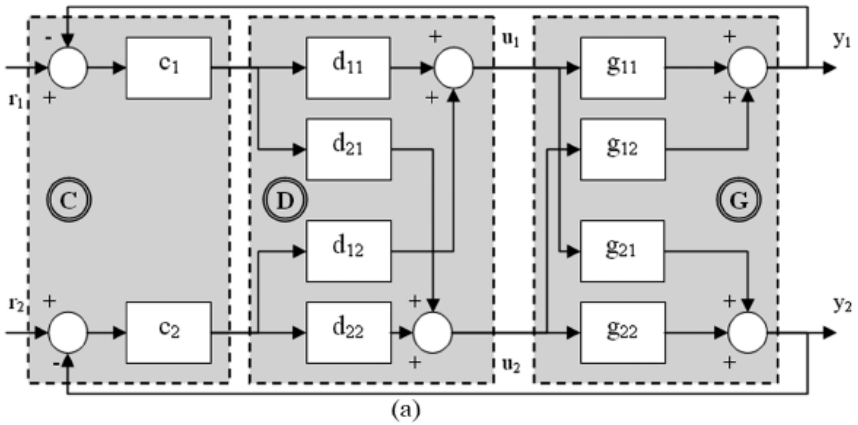

Figure 6.1: **The decoupled closed-loop control system**

The development follows the ***D(s)*** in a way that reduces process interactions. The modified process gain matrix ***G_P(s)*D(s)*** is seen by the controller ***C(s)*** as a set of two entirely separate loops. Therefore, the various loops' independent control is enabled by their designed controllers.

At this point, the technique for a systematic design of the dynamic decoupling strategy is presented for the column flotation Two-Input Two-Output (TITO) or Multiple-Input, Multiple-Output (MIMO) system under study. The simplified decoupling method is applied to the general flotation plant model, as presented in Chapter 4, Equation 4.1. This model can be rewritten or customized to form a TITO system as shown in Equation (6.1):

$$\begin{bmatrix} h(s) \\ \varepsilon_g(s) \end{bmatrix} = \begin{bmatrix} G_{11}(s) & G_{12}(s) \\ G_{21}(s) & G_{22}(s) \end{bmatrix} * \begin{bmatrix} Q_W(s) \\ Q_g(s) \end{bmatrix} \quad (6.1)$$

Where: h is the height of the froth layer measured in cm, and ε_g is the air holdup in the collection zone measured in %. Q_w and Q_g are the inflow rates of the wash water and the air, respectively. For the development of reliable closed-loop systems, there are three main types of decoupling strategies accessible, each with its own set of benefits and drawbacks (Vhora et al., 2017). The strategies are ideal decoupling, simplified decoupling, and inverted (adjoint-based decoupling). Based on the advantages mentioned by Gagnon *et al.,* 1988., and the nature of the process under study, a dynamic simplified decoupling method is selected to be used to design a decoupler of the flotation column model. Because of the simple elements, the simplified decoupling method is more common. On the other hand, controller tuning can be challenging at times, so an estimate of element transfer functions is frequently recommended in practice to help with controller tuning.

6.2.1 Decoupler of the 2x2 Model of the Flotation Column process

As mentioned above, there are two main strategies for the design of decoupling controllers which are: static decoupling and dynamic decoupling. Static decoupling refers to the compensation of the process interactions in a steady state. This form of decoupling does not compensate for the dynamic response interactions that arise during system transient conditions. On the other hand, dynamic decoupling is a strategy used for compensating the dynamic process interactions during both steady-state and transient conditions. Since the flotation system is an interconnected plant, the most desirable strategy to implement would be dynamic decoupling to ensure the process interactions are completely compensated for in the system (Ogunnaike & Ray, 1994).

Figure 6.2 represents a 2x2 column flotation model with a de-coupler at the input of the plant model, and a controller to be designed. After the decoupling has been accomplished, simulations of the closed-loop system with and without decouplers are carried out. The following block diagram represents a 2x2 column flotation system with a decoupler model connected at the input of the plant model.

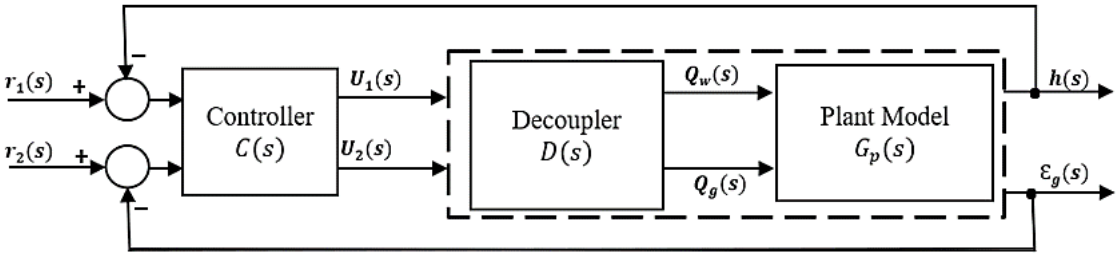

Figure 6.2: **The decoupled block diagram of a flotation control system**

It is known that decoupling may be done using several different techniques, including the rearrangement of the pairing of variables, minimizing interactions by detuning conflicting control loops, opening loops, and putting them in manual control, and using linear combinations of manipulated or controlled variables. However, connecting decouples directly to the process resulted in better performance when considering the process under study. This arrangement ensured that the alteration of the input in one loop does not affect or change the other loop, hence this scheme is selected. The location of the decouplers is selected such that a complete decoupling of the closed-loop system is achieved, as demonstrated in section 6.3.

Figure (6.3) below represents the decoupling of separate transfer functions at the input of a $2x2$ process transfer function.

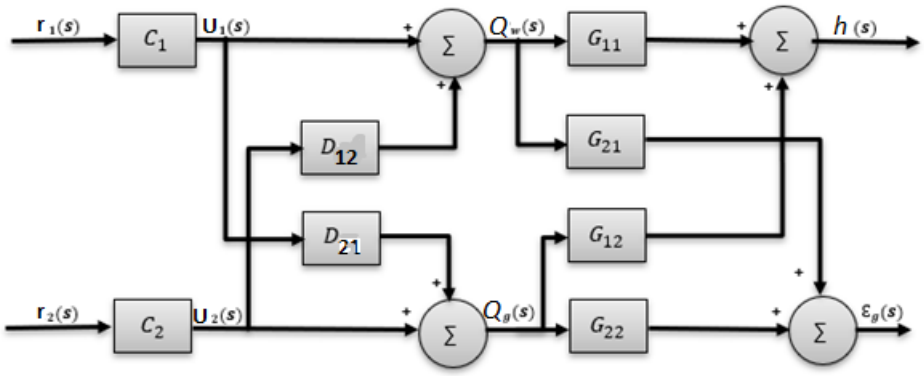

Figure 6.3: **Elements of the decoupled open-loop control system**

The original process transfer function matrix ($G_p(s)$) requires the creation of a transfer function matrix $D(s)$, such that $G_p(s) \bullet D(s)$ is a diagonal transfer function matrix $M(s)$ as shown below in Equation (6.2).

$$M(s) = G_P(s) \cdot D(s) \tag{6.2}$$

The matrix Equation (6.2) can be represented by its components, as follows:

$$\begin{bmatrix} M_{11}(s) & M_{12}(s) \\ M_{21}(s) & M_{22}(s) \end{bmatrix} = \begin{bmatrix} G_{11}(s) & G_{12}(s) \\ G_{21}(s) & G_{22}(s) \end{bmatrix} \cdot \begin{bmatrix} D_{11}(s) & D_{12}(s) \\ D_{21}(s) & D_{22}(s) \end{bmatrix} \tag{6.3}$$

The idea is to design the elements of the De-coupler in such a way that the interconnections between the process model outputs are eliminated which will allow the design of the process controllers to be fully decentralized. Setting the diagonal matrix for the representation of the decoupled process, the following is applied:

M_{12}=M_{21}=0 and D_{11}=D_{22}=1, therefore

$$\begin{bmatrix} M_{11}(s) & 0 \\ 0 & M_{22}(s) \end{bmatrix} = \begin{bmatrix} G_{11}(s) & G_{12} \\ G_{21}(s) & G_{22}(s) \end{bmatrix} \cdot \begin{bmatrix} 1 & D_{12}(s) \\ D_{21}(s) & 1 \end{bmatrix} \tag{6.4}$$

Multiplication of the matrixes in Equation (6.4) produces Equation (6.5);

$$\begin{bmatrix} M_{11}(s) & 0 \\ 0 & M_{22}(s) \end{bmatrix} = \begin{bmatrix} G_{11}(s) + G_{12}(s) * D_{21}(s) & G_{11}(s) * D_{12}(s) + G_{12}(s) \\ G_{21}(s) + G_{22}(s) * D_{21}(s) & G_{21}(s) * D_{12}(s) + G_{22}(s) \end{bmatrix} \tag{6.5}$$

Using Equation (6.5), solve the matrix *M(s)* for *M(s)* to be diagonal:

$$G_{11}(s) * D_{12}(s) + G_{12}(s) = 0$$
$$G_{21}(s) + G_{22}(s)D_{21}(s) = 0 \tag{6.6}$$

From Equation (6.6), the expressions for D_{12} and D_{21}, are obtained. The results are shown in Equation (6.7).

$$D_{12}(s) = -\frac{G_{12}(s)}{G_{11}(s)};\ D_{21}(s) = -\frac{G_{21}(s)}{G_{22}(s)} \tag{6.7}$$

By substituting the dynamic decouplers given by D_{21}(s) and D_{12}(s) from Equation (6.7) into Equation (6.5), the decoupled model of the process is obtained. The obtained decoupled model of the process is represented by Equation (6.8).

$$\begin{bmatrix} M_{11}(s) & 0 \\ 0 & M_{22}(s) \end{bmatrix} = \begin{bmatrix} G_{11}(s) - \frac{G_{21}(s)}{G_{22}(s)} G_{12}(s) & 0 \\ 0 & G_{22}(s) - \frac{G_{21}(s)G_{12}(s)}{G_{11}(s)} \end{bmatrix} \tag{6.8}$$

The next step is to substitute the general transfer function models of the flotation column as introduced in Chapter 4 from Equations (4.2) to (4.7). This is done to design a controller for each loop of the decoupled model given by Equation (6.8).

The decoupled column flotation model presented in Equation (6.8), confirms two independent control loops with highly minimized interactions. Nevertheless, the reduction of the order of each loop is necessary, because the diagonal transfer matrix *M(s)* can become complicated (Engineering, 1992).

To make the design and tuning of the controllers easier, the terms in Equation (6.8) could need to be approximated by a simpler lower-order transfer function.

6.2.1.1 Order reduction of the transfer functions of the two decoupled loops

Equation (6.8) shows that the height transfer function of the decoupled froth layer is as illustrated in Equation (6.9):

$$\mathrm{h(s)} = \mathrm{M_{11}(s)} = \mathrm{G_{11}} - \frac{\mathrm{G_{12}G_{21}}}{\mathrm{G_{22}}} \tag{6.9}$$

And the decoupled air holdup transfer function is given in Equation (6.10)

$$\varepsilon_{\mathrm{gcz}}(\mathrm{s}) = \mathrm{M_{22}(s)} = \mathrm{G_{22}} - \frac{\mathrm{G_{21}G_{12}}}{\mathrm{G_{11}}} \tag{6.10}$$

Now factorization and simplification of Equation (6.9) and Equation (6.10) are done to reduce the order of the decoupled transfer functions for the froth layer height and the air holdup. The following Equation (6.11) is obtained by substituting the transfer functions and simplifying the froth layer height Equation (6.9).

$$M_{11} = \frac{-6.797\mathrm{e}^{-08}\mathrm{s}^4 - 3.699\mathrm{e}^{-09}\mathrm{s}^3 - 6.146\mathrm{e}^{-11}\mathrm{s}^2 - 3.032\mathrm{e}^{-13}\mathrm{s} - 1.122\mathrm{e}^{-16}}{7.78\mathrm{e}^{-05}\mathrm{s}^5 + 3.671\mathrm{e}^{-06}\mathrm{s}^4 + 5.543\mathrm{e}^{-08}\mathrm{s}^3 + 2.717\mathrm{e}^{-10}\mathrm{s}^2 + 1.925\mathrm{e}^{-13}\mathrm{s} + 3.698\mathrm{e}^{-17})} \tag{6.11}$$

Continuous-time zero/pole/gain model or Arrays of the zero-pole-gain model of Equation (6.11) is shown in Equation (6.12):

$$\mathrm{M_{11}} = \frac{-0.00087368(\mathrm{s}+0.02686)(\mathrm{s}+0.0192)(\mathrm{s}+0.007964)(\mathrm{s}+0.000402)}{(\mathrm{s}+0.0192)(\mathrm{s}+0.0192)(\mathrm{s}+0.007981)(\mathrm{s}+0.000402)(\mathrm{s}+0.000402)} \tag{6.12}$$

The zeros in the numerator polynomials represented by $(s + 0.02582)(s + 0.0192)(s + 0.007991)(s + 0.000402)$ can be canceled with the poles of the denominator polynomial represented by $(s + 0.0192)(s + 0.0192)(s + 0.007981)(s + 0.000402)$, resulting in a simplified transfer function as shown in Equation (6.13).

$$M_{11}(s) = \frac{-873.68\times10^{-6}}{s+0.000402} \tag{6.13}$$

The same technique followed to simplify the froth layer height transfer function is used to simplify the holdup air zone transfer function given by Equation (6.10), which resulted in Equation (6.14).

$$\varepsilon_{gcz}(s) = \frac{6.6057\times10^{-5}(s+0.02686)(s+0.0192)(s+0.007964)(s+0.000402)}{(s+0.02235)(s+0.0192)(s+0.007981)(s+0.00781)(s+0.000402)} \tag{6.14}$$

Cancellation of the numerator and denominator polynomials of similar terms from the above Equation (6.14), resulted in the following Equation (6.15):

$$\varepsilon_{gcz}(s) = M_{22} = \frac{6.6057\times10^{-5}}{s+0.00781} \tag{6.15}$$

Now the combination of Equation (6.13) and Equation (6.15) into a matrix format results in ***M(s)*** as:

$$M(s) = \begin{bmatrix} M_{11} & 0 \\ 0 & M_{22} \end{bmatrix} = \begin{bmatrix} \frac{-873.68\times10^{-6}}{s+0.000402} & 0 \\ 0 & \frac{6.6057\times10^{-5}}{s+0.00781} \end{bmatrix} \tag{6.16}$$

The PI controllers' parameters for the process's individual loops are designed using the matrix ***M(s)***.

6.2.1.2 Summary of the decoupled 2x2 process model

Table 6.1 gives an overview of the derived transfer functions for the decoupled 2x2 model of the flotation process.

Table 6.1: **Obtained expressions of the decoupled process**

Decoupling Scheme	***D(s)***	***M(s)*** $M(s) = G_P(s) \bullet D(s)$
Ideal	$D(s) = \begin{bmatrix} D_{11}(s) & D_{12}(s) \\ D_{21}(s) & D_{22}(s) \end{bmatrix}$	$G_P(s) = \begin{bmatrix} G_{11}(s) & G_{12}(s) \\ G_{21}(s) & G_{22}(s) \end{bmatrix}$

Dynamic Decoupling	$D(s) = \begin{bmatrix} 1 & -\frac{G_{12}}{G_{11}} \\ -\frac{G_{21}}{G_{22}} & 1 \end{bmatrix}$	$M(s) = \begin{bmatrix} G_{11}(s) - \frac{G_{21}(s)G_{12}(s)}{G_{22}(s)} & 0 \\ 0 & G_{22}(s) - \frac{G_{21}(s)G_{12}(s)}{G_{11}(s)} \end{bmatrix}$ $M(s) = \begin{bmatrix} \frac{-873.68\times10^{-6}}{s+0.000402} & 0 \\ 0 & \frac{6.6057\times10^{-5}}{s+0.00781} \end{bmatrix}$

The next section describes the process of design of the decentralized PI controller for the decoupled model of the flotation process.

6.2.2 Design of a PI controller using a Pole Placement Method

This section describes the process of designing an independent PI controller for each apparent loop of the decoupled system using the Pole Placement technique. Pole placement is a feedback control system theory approach for placing a system's closed-loop poles in pre-determined places in the s-plane (Suh et al., 2001). After the system transfer function has been mathematically specified, the desired transfer function should be defined as well, and each coefficient of the same order in a closed-loop polynomial should be associated with or compared to its equivalent. The desired system response is achieved using this pole placement controller design method, and the controller gains are easily calculated analytically. In this situation, the accuracy of the closed-loop system transfer function is critical, and implementing this method for high-order systems is also costly, hence It is important to reduce system orders (Engineering, 1992). This method is used to determine the relationship between closed-loop pole position and various time-domain process requirements.

The aim is to design controllers to keep the system outputs as close to the target values as possible by reducing the errors between input and output or feedback to zero at a steady state using shorter response times. The control integral action is very helpful in eliminating the system's steady-state error. As a result, it's only reasonable to utilize a PI controller that ultimately has the following transfer function:

$$C(s) = K_p(1 + K_I\frac{1}{s}) \quad (6.17)$$

Where: K_P and K_I are the controller regulation parameters demonstrating the controller gain constant and the integral gain constant respectively. The pole placement design technique purely attempts to find controller settings that give the desired closed-loop poles. The arrangement is built in such a way that the control strategy originates from the desired system response, making it simple to find the controller gains mathematically (Tshemese-Mvandaba et al., 2021). The closed-loop poles can be

freely selected by adjusting the controller's gains K_P and K_I. As a result, the system's controller transfer matrix ***C(s)*** is:

$$C(s) = \begin{bmatrix} C_1(s) & 0 \\ 0 & C_2(s) \end{bmatrix} = \begin{bmatrix} K_{p1}(1 + K_{I1}\frac{1}{s}) & 0 \\ 0 & K_{p2}(1 + K_{I2}\frac{1}{s}) \end{bmatrix} \quad (6.18)$$

The PI controllers' parameters for the process's individual loops are designed, using Equations (6.16 and 6.18) for ***M(s)*** and ***C(s)*** respectively. Thus, the decoupled system is built by including the two diagonal PI controllers. Equation (6.19) is the indication of ***M(s)*C(s)***, which is the decoupled model to be used further for the controllers' parameter design:

$$M(s)C(s) = \begin{bmatrix} \frac{-873.68e^{-6}K_{P1}\left(1+K_{I1}\frac{1}{s}\right)}{s+0.000402} & 0 \\ 0 & \frac{6.6057e^{-5}K_{P2}\left(1+K_{I2}\frac{1}{s}\right)}{s+0.00781} \end{bmatrix} = \begin{bmatrix} h(s) \\ \varepsilon_g(s) \end{bmatrix} = \begin{bmatrix} Y_1(s) \\ Y_2(s) \end{bmatrix} \quad (6.19)$$

Therefore;

$$\begin{bmatrix} h(s) \\ \varepsilon_{gcz(s)} \end{bmatrix} = \begin{bmatrix} Y_1(s) \\ Y_2(s) \end{bmatrix} = M(s) \times \begin{bmatrix} C_1(s) & 0 \\ 0 & C_2(s) \end{bmatrix} \quad (6.20)$$

For complete decoupling or decouples, $Y_1(s)$ is assumed to be impacted by the control signal $C_1(s)$, and the control signal that has an impact on $Y_2(s)$ is assumed to be $C_2(s)$. Figure 6.4 is a block diagram representation of the closed-loop system incorporating the decouplers and the controllers.

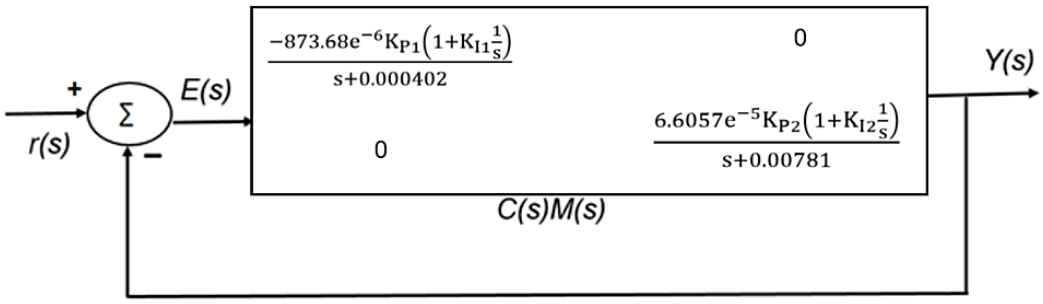

Figure 6.4: **Decoupled closed-loop system illustrated as a block diagram.**

It is noted from Figure 6.4 that the general representation of this closed-loop system is

$$Y(s) = M(s) \cdot C(s) \cdot E(s) \quad (6.21)$$

$$E(s) = r(s) - Y(s) \quad (6.22)$$

From the general closed-loop system and using the decoupled ***M(s)*** the outputs are expressed one by one, separating the froth layer height and decoupled Air hold up zone, (Y_1 and Y_2):

$$h(s) = Y_1(s) = M_{11}(s)C_1(s) \times (r_1(s) - Y_1(s)) \quad (6.23)$$

$$Y_1(s) = M_{11}(s)C_1(s) \cdot r_1(s) - M_{11}(s)C_1(s) \cdot Y_1(s) \quad (6.24)$$

$$Y_1(s) = \frac{M_{11}(s) \cdot C_1(s)}{1 + M_{11}(s) \cdot C_1(s)} \times r_1(s) \quad (6.25)$$

Substituting the transfer functions for $M_{11}(s)$ and $C_1(s)$ is obtained:

$$Y_1(s) = \frac{-0.00087368(K_{P1}s + K_{P1}K_{I1})}{s^2 + (0.000402 - 0.00087368K_{P1})s - 0.00087368K_{P1}K_{I1}} \times r_1(s) \quad (6.26)$$

Similarly, for the Air hold-up zone it is obtained:

$$\varepsilon(s) = Y_2(s) = M_{22}(s)C_2(s) \times (r_2(s) - Y_2(s)) \quad (6.27)$$

$$Y_2(s) = M_{22}(s)C_2(s)r_2(s) - M_{22}(s)C_2(s)Y_2(s) \quad (6.28)$$

$$Y_2(s) = \frac{M_{22}(s) \cdot C_2(s)}{1 + M_{22}(s) \cdot C_2(s)} * r_2(s) \quad (6.29)$$

$$Y_2(s) = \frac{6.6057e^{-5}(K_{P2}s + K_{P2}K_{I2})}{s^2 + (0.00781 + 6.6057e^{-5}K_{P2})s + 6.6057e^{-5}K_{P2}K_{I2}} * r_2(s) \quad (6.30)$$

The obtained transfer functions are given by Equations (6.26) and (6.30), which are used to define the parameters of PI controllers. This design procedure is based on the pole placement method (Ogata, 2002).

6.2.3 Controller design for the froth layer height

This subsection presents the PI controller design for the layer height $h(s)$. To achieve this, the second-order polynomial of the denominator of the obtained above transfer function (6.26) is considered, as follows:

$$s^2 + (0.0004002 - 0.00087368K_{P1})s - 0.00087368K_{P1}K_{I1} \quad (6.31)$$

The closed-loop system poles are determined by properly setting the controller parameters K_{P1} and K_{I1} to the suitable values. If the desired values of the closed-loop system's poles are specified, the suitable values of the controller parameters can be set based on this dependence. Then the desired closed-loop characteristic equation can be written in the following form:

$$s^2 + 2\zeta\omega_n s + {\omega_n}^2 \quad (6.32)$$

Where ζ and ω_n are the damping factor and un-damped natural frequency respectively. They specify the values of the desired poles. Comparison of Equations (6.31) and (6.32) allows the desired values of the controller parameters to be calculated.

$$s^2 + (0.0004002 - 0.00087368K_{P1})s - 0.00087368K_{P1}K_{I1} = s^2 + 2\zeta\omega_n s + {\omega_n}^2 \quad (6.33)$$

Through evaluation of the coefficients in front of the same powers of the variable *s* in Equation (6.33), the parameters of the PI controller are expressed by Equations (6.34) and (6.35), as follows:

$$K_{P1} = \frac{2\zeta\omega_n - 0.0004002}{-0.00087368} \tag{6.34}$$

$$K_{P1}K_{I1} = \frac{{\omega_n}^2}{-0.00087368} \tag{6.35}$$

The desired values of un-damped natural frequency have to be specified for the given froth layer height and air holdup transition behaviour processes to be capable to calculate the parameters of the controllers. Data for the transition behaviour of the industrial froth layer height and the air holdup processes are taken from the publications (Persechini et al., 2000), (Persechini et al., 2004), and (Calisaya et al., 2012). The characteristics of the open-loop behaviour as shown in Table 4.4 in chapter 4 are used as necessary to calculate the control parameters of the designed PI controller. The settling time (maximum and minimum), and overshoot percentage must be defined for the system's damped/ Un-damped natural frequency to be calculated correctly.

Using the data in Table 4.4, the desired damping factor and un-damped natural frequency values are calculated below, and the designed closed-loop system obtained the desired industrial process behavior. The peak value of the height is recorded as 0.67 cm. It is desired that the allowed overshoot of the closed-loop system is between 5% and 15 % from the peak value p_v of the open-loop process behaviour. In this case the percentage overshoot M_{pmax} = *15%* is equivalent to 0.10 cm and M_{pmin} = 5% is equivalent to 0.03 (cm). The damping factor (ζ) can be calculated using Equations (6.36 and 6.37)

The maximum value of the damping factor is calculated through Equation 6.36 (Ogata, K., 2002); (Nalan-Ahmadabad & Ghaemi, 2017).

$$\zeta_{M_{p\max}} = \sqrt{\frac{\left(\ln\frac{M_{p\max}}{100\%}\right)^2}{\pi^2 + \left(\ln\frac{M_{p\max}}{100\%}\right)^2}} = \sqrt{\frac{\left(\ln\frac{0.10}{100\%}\right)^2}{\pi^2 + \left(\ln\frac{0.10}{100\%}\right)^2}} = 0.91 \tag{6.36}$$

The minimum value of the damping factor is:

$$\zeta_{M_{p\min}} = \sqrt{\frac{\left(\ln\frac{M_{p\min}}{100\%}\right)^2}{\pi^2 + \left(\ln\frac{M_{p\min}}{100\%}\right)^2}} = \sqrt{\frac{\left(\ln\frac{0.03}{100\%}\right)^2}{\pi^2 + \left(\ln\frac{0.03}{100\%}\right)^2}} = 0.93 \tag{6.37}$$

As a result, the damping factor limitations are set as shown in Equation (6.38) for each value of the allowable overshoot.

$$M_{p\max} = 15\% \rightarrow \zeta_{p\max} = 0.91$$
$$M_{p\min} = 5\% \rightarrow \zeta_{p\min} = 0.93 \quad (6.38)$$

To calculate the controller parameters given by Equations (6.34) and (6.35) it is necessary to specify where closed-loop poles must lie. Equation (6.39) is used to calculate the un-damped natural frequency.

Generally, it is necessary to specify where closed-loop poles must lie, to calculate the controller parameters given by Equations (6.34) and (6.35), the value of the damping factor is selected to be 0.92, based on Equation (6.38). The next design specification is to determine the un-damped natural frequency (ω_n) to complete the second-order system's conditions. The following Equation (6.39) relates the settling time and oscillation frequency, (Ogata, K., 2002).

$$T_s = \frac{4}{\zeta\omega_n}; \quad (6.39)$$

The value of the settling time is selected from Table 4.4 to be equal to 116.1 seconds. Then the un-damped frequency is:

$$\omega_n = \frac{4}{\zeta T_s} = \frac{4}{0.92 \times 116.1} = 0.037 rad/s$$

The procedure followed in the selection of the poles is illustrated in the flow chart shown in Figure 6.5 below.

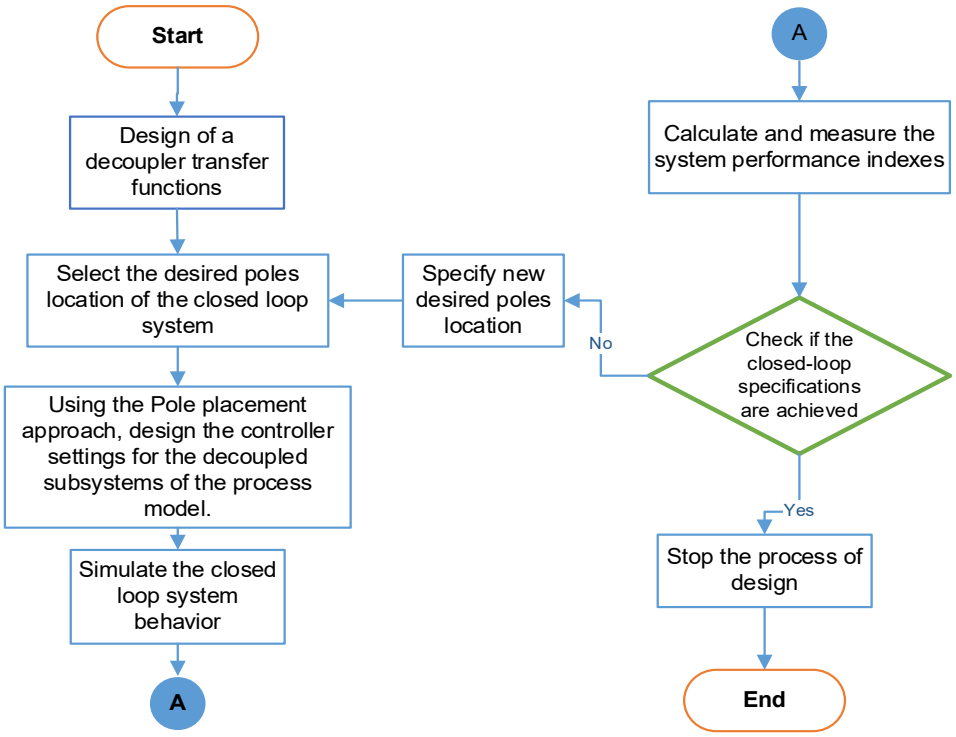

Figure 6.5: Flow-chart of the summary pole selection procedure

Therefore, the unknown controller parameter values are calculated as follows:

$$K_{P1} = \frac{2\zeta\omega_n - 0.0004002}{-0.00087368} = \frac{(2\times 0.92\times 0.037) - 0.000402}{-0.00087368} = -77.5 \quad (6.40)$$

$$K_{I1} = \frac{{\omega_n}^2}{-0.00087368 K_{P1}} = \frac{(0.037)^2}{(-0.00087368)\times(-77.5)} = 0.02 \quad (6.41)$$

6.2.4 PI Controller design for the Air holdup process

This subsection describes the PI controller design for the air hold-up process. To achieve this, it is required that the characteristic polynomial of the closed-loop transfer function given by Equation (6.30) is considered:

$$s^2 + (0.00781 + 6.6057e^{-5}K_{P2})s + 6.6057e^{-5}K_{P2}K_{I2} \quad (6.42)$$

The desired characteristic polynomial is:

$$s^2 + 2\zeta\omega_n s + {\omega_n}^2 \quad (6.43)$$

Comparison of the Equation (6.42) and (6.43) allows the desired values of the controller parameters to be calculated using Equation (6.44).

$$s^2 + (0.00781 + 6.6057e^{-5}K_{P2})s + 6.6057e^{-5}K_{P2}K_{I2} = s^2 + 2\zeta\omega_n s + {\omega_n}^2 \quad (6.44)$$

By means of comparison of the coefficients in front of the same powers of the variable ***s*** the control parameters of the PI controller are expressed by Equations (6.45) and (6.46), as follows:

$$K_{P2} = \frac{2\zeta\omega_n - 0.00781}{6.60557e^{-5}} \quad (6.45)$$

$$K_{P2}K_{I2} = \frac{{\omega_n}^2}{6.6057e^{-5}} \quad (6.46)$$

The same procedure used to design the control parameters for the first loop and calculations of the damping factor and un-damped natural frequency is then followed again for the second PI controller.

The peak value of the Air holdup is recorded as 0.248 in Table 4.4. The percentage overshoot of M_{pmax} = 15% of the peak value is equivalent to 0.0372 and M_{pmin} = 5% is equivalent to 0.0124. The maximum and minimum values of the damping factor (ζ) are calculated in Equation (6.47)

$$\zeta_{\max} = \sqrt{\frac{\left(\ln\frac{M_{p\max}}{100\%}\right)^2}{\pi^2 + \left(\ln\frac{M_{p\max}}{100\%}\right)^2}} = 0.93 \text{ and } \zeta_{\min} = \sqrt{\frac{\left(\ln\frac{M_{p\min}}{100\%}\right)^2}{\pi^2 + \left(\ln\frac{M_{p\min}}{100\%}\right)^2}} = 0.94 \quad (6.47)$$

As a result, the constraints are specified as shown in Equation (6.48)

$$M_{pmax} = 15\% \rightarrow 0.93$$
$$M_{pmin} = 5\% \rightarrow 0.94 \quad (6.48)$$

Now from Equation (6.48), an appropriate value of the damping factor of 0.93 is selected to specify the position of the closed-loop poles. The next design specification is to determine the un-damped natural frequency (ω_n) to complete the requirements of the second-order system for the second loop. The settling time is selected from Table 4.4 to be T_s = *116.08s*. Using the relationship of the settling time and frequency of oscillation as presented in Equation (6.49):

$$\omega_n = \frac{4}{\zeta T_s} = \frac{4}{0.93 \times 116.08} = 0.037 rad/s \tag{6.49}$$

As a result, the unknown PI controller parameters' values are calculated using Equations (6.47 and 6.48). After substituting the values of the damping factor and un-damped natural frequency, the PI controller parameters are:

$$K_{P2} = \frac{2\zeta\omega_n - 0.00781}{6.60557e^{-5}} = \frac{(2 \times 0.93 \times 0.037) - 0.00781}{6.60557e^{-5}} = 924$$

$$K_{I2} = \frac{{\omega_n}^2}{6.6057e^{-5} K_{P2}} = \frac{(0.037)^2}{6.6057e^{-5} \times 924} = 0.022 \tag{6.50}$$

The simulation and investigation of the closed-loop flotation column control system behavior are performed in the following section. The same set-point that were established in chapter 5 are used here again, for proper comparison of the techniques used to control the flotation system as presented in chapter 5 and chapter 6.

6.3 Simulation of the decoupled closed-loop system for the Froth layer height and Air holdup processes

A closed-loop system with the designed PI controllers is developed and modelled in MATLAB/SIMULINK to study the importance of decoupling multivariable systems. In a flotation system, it is important to monitor the froth height in the cleaning zone and the air holdup in the collection zone. This section concentrates on the investigation and analysis of the flotation process behaviour based on the Froth layer height and the air holdup for the case of the decoupled closed-loop control system. The designed parameters of the controllers are used in a closed-loop system control as presented in Figure 6.6. The same table that is introduced in Chapter 5 as Table 5.2 for set-point declarations is adopted at this point so that a proper performance comparison can be drawn between the two methods used in Chapter 5 and Chapter 6.

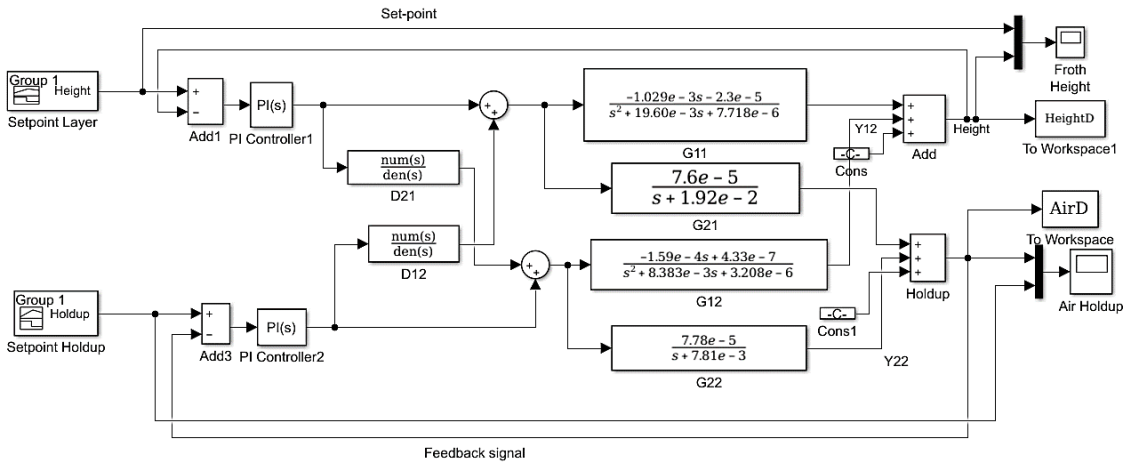

Figure 6.6: Simulink block diagram of the closed-loop 2x2 decoupled flotation system

Figures 6.7 to 6.10 present the transition behaviour of the decoupled closed-loop system under PI control for the study cases given in Table 5.2.

Case study 1: Start the process

Analysis based on set-point tracking for both air holdup and froth layer height is conducted, by initiating the system through an air injection at the bottom of the column. In Case study 1 the set-point of the froth layer height is established from 40 cm and increased to 60 cm, while the holdup is set to start at 10% and increase to 18% at 10s. The results for this case are presented in Figure 6.7 shown below.

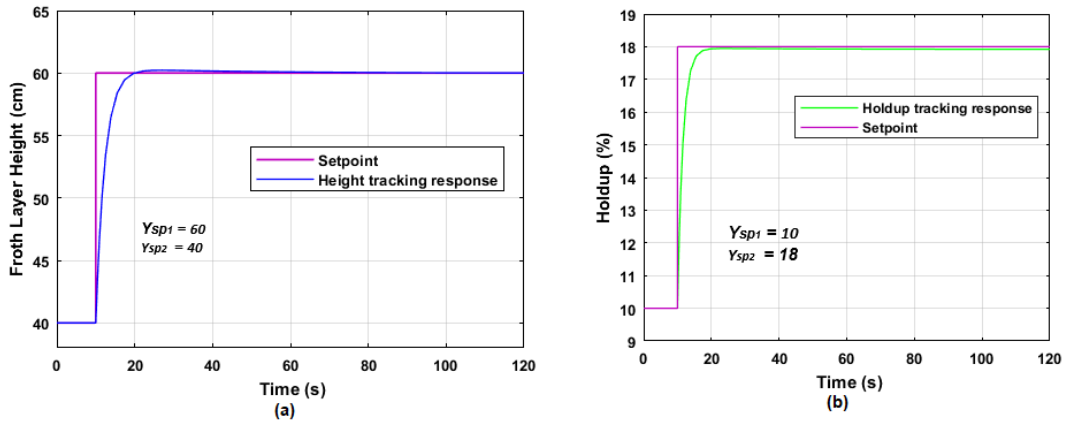

Figure 6.7: Case study 1: Closed-loop response of the Froth Layer Height and Air Holdup processes

Case study 2: Setpoint change applied on the Air holdup loop

Case study 2 presented in Figure 6.8 below the froth layer height is kept at the same set point as Figure 6.7, but the holdup step is changed to a pulse signal as presented. This is done to investigate the effect (influence) of air holdup set-point changes on the two loops (Froth layer height and holdup).

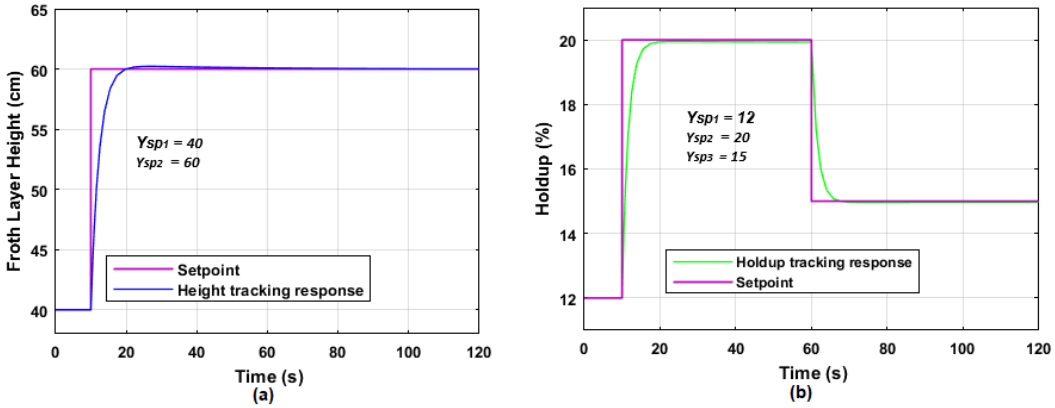

Figure 6.8: Case study 2: Closed-loop response of the Froth Layer Height and Air Holdup processes

As can be noted above both loops are not poorly influenced (in terms of rise-time, settling, and steady-state error) by the set-point changes applied to the holdup loop. Moving to the case study 3 changes are applied to the froth layer height only.

Case study 3: Air holdup remains the same and Froth layer height is changed

In Case study 3 the setpoint of the froth layer height is established to start at 50 cm, the set-point change is applied at 10 seconds to move the signal from 50 cm to 70 cm and decreased to 60 cm at 60 seconds, while the holdup is set only to start at 10% and increased to 18% at 10 seconds.

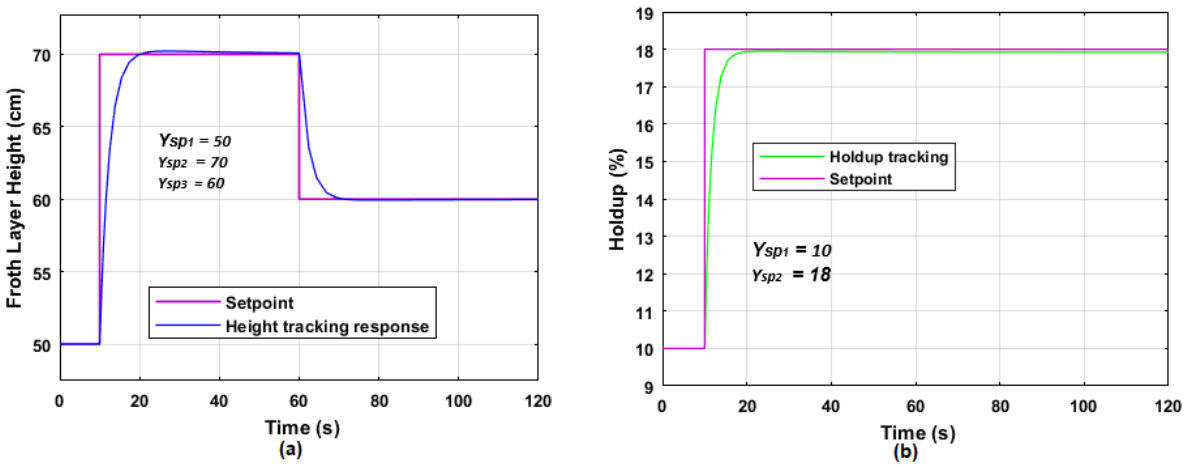

Figure 6.9: Case study 3: Closed-loop response of the Froth Layer Height and Holdup

The results shown in Figure 6.9 above represent a good setpoint tracking of froth layer height (Figure 6.9 (a)) and holdup (Figure 6.9 (b)) tracking any set-point change, to observe the effectiveness of the closed-loop flotation behaviour under the decoupled PI control. The set-point of the air holdup is returned to the same state as in case study 1, only to investigate the influence of the changes made in the cleaning zone or Froth layer height zone. The next case study demonstrates the effect of set-point changes applied on both loops at the same time.

Case study 4: Same time Regulation of Froth layer height and Air holdup

The effects of this last case for the two-input two-output (TITO) decoupled system are presented in Figure 6.10 presented below. In this case 4, the set-points of the Froth layer height and Air holdup altered their states at the same time, to observe the system's operational behaviour under this condition. The froth layer height in Figure 6.10 (b) is set to start at 80 cm, while the applied holdup starts at 4%.

This is done to see how well the closed-loop system tracks any set point or if the behaviour of the set-point tracking process is achieved in any circumstances.

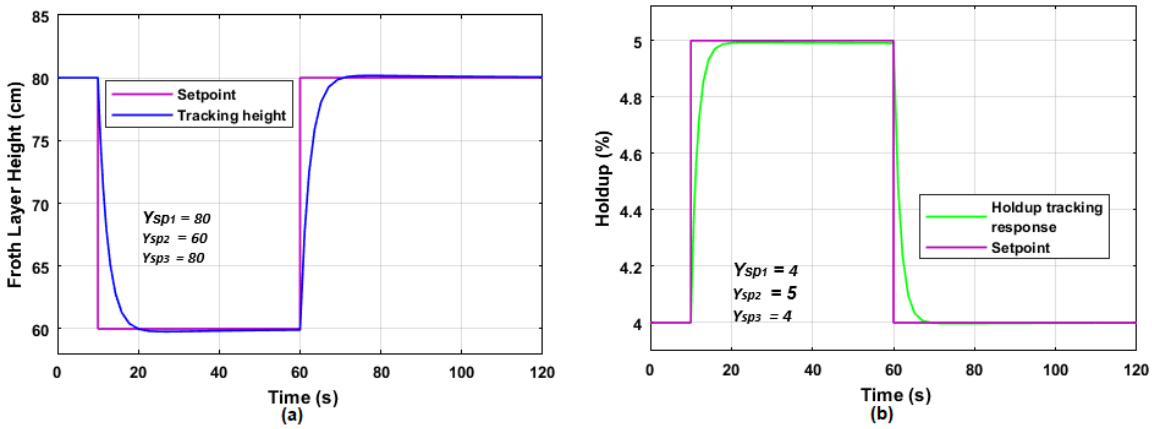

Figure 6.10: **Case study 4: Closed-loop response of the Froth Layer Height and Air Holdup processes**

The performances shown in Figure 6.7 and Figure 6.10 for the tracking of set-points and characteristics response are tabled in Table 6.2.

6.3.1 Performance indexes of the transition processes of the decoupled system

The transition behaviour characteristics of the processes as presented in Figure 6.7 to Figure 6.10 are measured and filled in Table 6.2. They are used to analyse the influence of the set-point changes of the decoupled system over the processes' behaviour. As it can be noted, the method of decoupling the system has minimized the overshoot and eliminated any steady-state error.

Table 6.2: **Transition processes performance indexes**

Case study	Set-point		Transition behaviour characteristics of the Decoupled Froth Layer Height and the Air Holdup				
			Rise time [sec]	Settling time [sec]	Peak time [cm] and [%]	Overshoot [cm] and [%]	Steady-state error [cm] and [%]
Case study 1	***h***	40-60 cm	4.91	18.05	26.9276	0.22	0
	ε_{gcz}	10-18 %	3.47	16.078	24.5276	0.05	0
	h	40-60 cm	4.908	18.05	26.9276	0.22	0

Case study	Set-point		Transition behaviour characteristics of the Decoupled Froth Layer Height and the Air Holdup				
			Rise time [sec]	Settling time [sec]	Peak time [cm] and [%]	Overshoot [cm] and [%]	Steady-state error [cm] and [%]
Case study 2	ε_{gcz}	12-20-15 %	0.59	66.17	24.5276	0.05%	0
Case study 3	***h***	50-70-60(cm)	1.25	68.75	26.9276	0.22	0
	ε_{gcz}	10-18(%)	3.47	16.078	24.5276	0.053%	0
Case study 4	*h*	80-60-80 cm	0.489	68.54	76.5187	0.17	0
	ε_{gcz}	4-5-4 (%)	0.51	66.25	24.9995	0.01%	0

6.3.2 Discussion of the simulation results

As it can be noted the closed-loop PI control system loops with a decoupler have a better response in terms of accomplishing all setpoint alteration with no overshoot or steady-state error for the closed-loop system with decouplers as compared with the one with no decouplers. Decoupling the multivariable system has proven to be an effective strategy to reduce interactions between the different loops. Table 6.2 gives the various performance characteristics for the Froth Layer Height and Air Holdup responses when the set points are varied. The investigation results show that the values of the indices of the Froth Layer Height and Air Holdup remain constant throughout the set-point variations, therefore this shows that the dynamic decoupling control design is an effective strategy to be used irrespective of the set-point variations. The next section presents the decoupling and controller design of the 3x3 multivariable flotation column system.

6.4 Development and decoupling of the flotation column 3x3 multivariable model

This section focuses on the decoupling, controller design, and simulation of the closed-loop system for the 3x3 multivariable flotation process model.

6.4.1 Design of decouplers for the 3x3 process model

From the general plant model presented in chapter 4, Equation (4.1) the 3x3 process transfer function $G_P(s)$ in Equation (6.51) requires the design of the transfer function matrix $D(s)$ for $G_P(s)D(s)$ to be a diagonal transfer function matrix $M(s)$,

$$G_P(s) = \begin{bmatrix} G_{11}(s) & G_{12}(s) & G_{13}(s) \\ G_{21}(s) & G_{22}(s) & G_{23}(s) \\ G_{31}(s) & G_{32}(s) & G_{33}(s) \end{bmatrix} \quad (6.51)$$

As it is shown previously the decoupler model for the 3x3 system is shown in Equation (6.52), which is introduced to eliminate complications in loop interactions for the changes in an individual process variable not to cause corresponding changes in another process variable.

$$D(s) = \begin{bmatrix} D_{11}(s) & D_{12}(s) & D_{13}(s) \\ D_{21}(s) & D_{22}(s) & D_{23}(s) \\ D_{31}(s) & D_{32}(s) & D_{33}(s) \end{bmatrix} \quad (6.52)$$

The diagonal transfer function matrix ***M(s)*** is*:*

$$M(s) = \begin{bmatrix} M_{11}(s) & 0 & 0 \\ 0 & M_{22}(s) & 0 \\ 0 & 0 & M_{33}(s) \end{bmatrix}$$

Then, the decoupled model is as shown in Equation (6.53):

$$M(s) = G_P(s) \times D(s) \quad (6.53)$$

Therefore;

$$\begin{bmatrix} h(s) \\ \varepsilon_{gcz(s)} \\ Q_B(s) \end{bmatrix} = \begin{bmatrix} Y_1(s) \\ Y_2(s) \\ Y_3(s) \end{bmatrix} = M(s) \times \begin{bmatrix} C_1(s) & 0 & 0 \\ 0 & C_2(s) & 0 \\ 0 & 0 & C_3(s) \end{bmatrix} \quad (6.54)$$

Where ***$C_1(s)$***, ***$C_2(s)$***, and ***$C_3(s)$*** are the controller's transfer functions for each of the three processes. For complete decoupling, it is assumed that ***$Y_1(s)$*** is affected by the controller ***$C_1(s)$***, ***$Y_2(s)$*** is only affected by the controller ***$C_2(s)$*** and ***$Y_3(s)$*** is only affected by the controller $C_3(s)$.

The strategy of setting the diagonal element of the decoupler to be 1 (Shen et al., 2010) and (Vhora & Patel, 2016) is followed in Equation (6.55).

$$D(s) = \begin{bmatrix} 1 & D_{12}(s) & D_{13}(s) \\ D_{21}(s) & 1 & D_{23}(s) \\ D_{31}(s) & D_{32}(s) & 1 \end{bmatrix} \quad (6.55)$$

Then the matrix *M(s)* is expressed as:

$$M(s) = \begin{bmatrix} G_{11}(s) & G_{12}(s) & G_{13}(s) \\ G_{21}(s) & G_{22}(s) & G_{23}(s) \\ G_{31}(s) & G_{32}(s) & G_{33}(s) \end{bmatrix} \times \begin{bmatrix} 1 & D_{12}(s) & D_{13}(s) \\ D_{21}(s) & 1 & D_{23}(s) \\ D_{31}(s) & D_{32}(s) & 1 \end{bmatrix} \quad (6.56)$$

$$M(s) = \begin{bmatrix} G_{11} + G_{12}D_{21} + G_{13}D_{31} & G_{11}D_{12} + G_{12} + G_{13}D_{32} & G_{11}D_{13} + G_{12}D_{23} + G_{13} \\ G_{21} + G_{22}D_{21} + G_{23}(s)D_{31} & G_{21}D_{12} + G_{22} + G_{23}(s)D_{32} & G_{21}D_{13} + G_{22}D_{23} + G_{23} \\ G_{31} + G_{32}D_{21} + G_{33}D_{31} & G_{31}D_{12} + G_{32} + G_{33}D_{32} & G_{31}D_{13} + G_{32}D_{23} + G_{33} \end{bmatrix}$$

$$M(s) = \begin{bmatrix} M_{11}(s) & 0 & 0 \\ 0 & M_{22}(s) & 0 \\ 0 & 0 & M_{22}(s) \end{bmatrix} \quad (6.57)$$

From Equations (6.56 and 6.57), for the matrix ***M(s)*** to be diagonal the following equations are written:

$$G_{11}D_{12} + G_{12} + G_{13}D_{32} = 0$$
$$G_{31}D_{12} + G_{32} + G_{33}D_{32} = 0 \quad (6.58)$$

$$G_{11}D_{13} + G_{12}D_{23} + G_{13} = 0$$
$$G_{21}D_{13} + G_{22}D_{23} + G_{23} = 0 \quad (6.59)$$

$$G_{21} + G_{22}D_{21} + G_{23}D_{31} = 0$$
$$G_{31} + G_{32}D_{21} + G_{33}D_{31} = 0 \quad (6.60)$$

From Equation (6.58), D_{12} and D_{32} can be expressed, as follows:

$$\mathrm{D}_{12} = -\left(\frac{\mathrm{G}_{12}+\mathrm{G}_{13}\mathrm{D}_{32}}{\mathrm{G}_{11}}\right) \quad (6.61)$$

Substitution of the above equation (6.61) into the second equation of Equation (6.58), D_{32} is obtained, as follows:

$$D_{32} = \frac{G_{31}G_{12}-G_{11}G_{32}}{G_{11}G_{33}-G_{31}G_{13}} \quad (6.62)$$

Substitute Equation (6.62) into Equation (6.61), then the final equation for D_{12} is:

$$D_{12} = -\left(\frac{G_{12}+G_{13}.\frac{G_{31}G_{12}-G_{11}G_{32}}{G_{11}G_{33}-G_{31}G_{13}}}{G_{11}}\right) = -\left[\frac{G_{12}}{G_{11}} + \frac{G_{13}}{G_{11}} \cdot \left(\frac{G_{31}G_{12}-G_{11}G_{32}}{G_{11}G_{33}-G_{31}G_{13}}\right)\right] \quad (6.63)$$

From Equation (6.59), D_{13} and D_{23} are expressed as follows

$$D_{13} = -\left(\frac{G_{13}+G_{12}D_{23}}{G_{11}}\right) = -\frac{G_{13}}{G_{11}} - \frac{G_{12}.D_{23}}{G_{11}} \quad (6.64)$$

Substitution of the above Equation (6.64) into the second equation of Equation (6.59), then D_{23} is:

$$G_{12}.\left(-\frac{G_{13} - G_{12}D_{23}}{G_{11}}\right) + G_{22}D_{23} + G_{23} = 0$$
$$\therefore D_{23} = \frac{G_{21}G_{13}-G_{11}G_{23}}{G_{11}G_{22}-G_{21}G_{12}} \quad (6.65)$$

Substituting D_{23} as presented above (Equation 6.65), into Equation (6.64), D_{13} is found

$$D_{13} = -\frac{G_{13}}{G_{11}} - \frac{G_{12}}{G_{11}}\left(\frac{G_{21}G_{13}-G_{11}G_{23}}{G_{11}G_{22}-G_{21}G_{12}}\right) \quad (6.66)$$

Using Equation (6.60), D_{31} and D_{21} are expressed as follows:

$$D_{21} = -\frac{G_{21}-G_{23}.D_{31}}{G_{22}} \quad (6.67)$$

$$D_{31} = \frac{G_{32}.G_{21}-G_{22}G_{31}}{G_{22}G_{33}-G_{32}G_{23}} \quad (6.68)$$

$$D_{21} = -\frac{G_{21}}{G_{22}} - \frac{G_{23}}{G_{22}} \cdot \left(\frac{G_{32}.G_{21} - G_{22}G_{31}}{G_{22}G_{33} - G_{32}G_{23}}\right) \quad (6.69)$$

The focus on simplifying the complex flotation system in Equation 4.1 and the steady-state gains ***G(t)*** as *t* turns to infinite will result in Equation (4.8). It can be noted that; as a result of the steady-state gains for the model in Equation (4.1) [***G(t)*** for $(t \to \infty)$] $G_{31} = 0; G_{32} = 0,$ and $G_{33} = 1$

After the decoupler design process has been completed, the solution to Equation (6.55) is as follows:

$$D(s) = \begin{bmatrix} 1 & -\frac{G_{12}}{G_{11}} & -\frac{G_{13}}{G_{11}} - \frac{G_{12}}{G_{11}}\left(\frac{G_{21}G_{13} - G_{11}G_{23}}{G_{11}G_{22} - G_{21}G_{12}}\right) \\ -\frac{G_{21}}{G_{22}} & 1 & \frac{G_{21}G_{13} - G_{11}G_{23}}{G_{11}G_{22} - G_{21}G_{12}} \\ 0 & 0 & 1 \end{bmatrix} \quad (6.70)$$

The diagonal parts of the matrix transfer function of *M(s)* as presented in Equation (6.57), after the solution of the decoupling process (Equation (6.70)) has been completed, the solution for the elements of the diagonal elements of the matrix M is as follows:

$$M_{11}(s) = G_{11} + G_{12}D_{21} + G_{13}D_{31} = G_{11} - \frac{G_{12}G_{21}}{G_{22}} \quad (6.71)$$

$$M_{22}(s) = G_{21}D_{12} + G_{22} + G_{23}D_{32} = G_{22} - \frac{G_{21}G_{12}}{G_{11}} \quad (6.72)$$

$$M_{33}(s) = G_{31}D_{13} + G_{32}D_{23} + G_{33} = G_{33} \quad (6.73)$$

The matrix form of the resulting *M(s)* transfer function is shown in Equation (6.74)

$$M(s) = \begin{bmatrix} G_{11} - \frac{G_{12}G_{21}}{G_{22}} & 0 & 0 \\ 0 & G_{22} - \frac{G_{21}G_{12}}{G_{11}} & 0 \\ 0 & 0 & G_{33} \end{bmatrix} \quad (6.74)$$

Now substitute Equation (6.74) for Equation (6.54), the transfer function of the decoupled open-loop system is

$$\begin{bmatrix} h(s) \\ \varepsilon_{gcz(s)} \\ Q_B(s) \end{bmatrix} = \begin{bmatrix} Y_1(s) \\ Y_2(s) \\ Y_3(s) \end{bmatrix} = \begin{bmatrix} G_{11} - \frac{G_{12}G_{21}}{G_{22}} & 0 & 0 \\ 0 & G_{22} - \frac{G_{21}G_{12}}{G_{11}} & 0 \\ 0 & 0 & G_{33} \end{bmatrix} \times \begin{bmatrix} C_1(s) & 0 & 0 \\ 0 & C_2(s) & 0 \\ 0 & 0 & C_3(s) \end{bmatrix} \quad (6.75)$$

The decoupled process has been done and the following Table 6.3 summarises the process completed.

Table 6.3: Expressions of the dynamics decoupling process applied

Decoupling Scheme	*D(s)*	*M(s)* $M(s) = G_P(s) \bullet D(s)$
Ideal	$D(s) = \begin{bmatrix} D_{11}(s) & D_{12}(s) & D_{13}(s) \\ D_{21}(s) & D_{22}(s) & D_{23}(s) \\ D_{31}(s) & D_{32}(s) & D_{33}(s) \end{bmatrix}$	$G_P(s) = \begin{bmatrix} G_{11}(s) & G_{12}(s) & G_{13}(s) \\ G_{21}(s) & G_{22}(s) & G_{23}(s) \\ G_{31}(s) & G_{32}(s) & G_{33}(s) \end{bmatrix}$
Dynamic Decoupling	$D(s) = \begin{bmatrix} 1 & -\frac{G_{12}}{G_{11}} & -\frac{G_{13}}{G_{11}} - \frac{G_{12}}{G_{11}}\left(\frac{G_{21}G_{13} - G_{11}G_{23}}{G_{11}G_{22} - G_{21}G_{12}}\right) \\ -\frac{G_{21}}{G_{22}} & 1 & \frac{G_{21}G_{13} - G_{11}G_{23}}{G_{11}G_{22} - G_{21}G_{12}} \\ 0 & 0 & 1 \end{bmatrix}$	$M(s) = \begin{bmatrix} G_{11} - \frac{G_{12}G_{21}}{G_{22}} & 0 & 0 \\ 0 & G_{22} - \frac{G_{21}G_{12}}{G_{11}} & 0 \\ 0 & 0 & G_{33} \end{bmatrix}$
Dynamics decoupled and Simplified model	$D(s) = \begin{bmatrix} 1 & -\frac{G_{12}}{G_{11}} & 0 \\ -\frac{G_{21}}{G_{22}} & 1 & 0 \\ 0 & 0 & 1 \end{bmatrix}$	$M(s) = \begin{bmatrix} \frac{-873.68 \times 10^{-6}}{\mathrm{s} + 0.000402} & 0 & 0 \\ 0 & \frac{6.6057 \times 10^{-5}}{\mathrm{s} + 0.00781} & 0 \\ 0 & 0 & 1 \end{bmatrix}$

As can be noted from above Table 6.3, the froth layer height and air hold-up model remain the same as in a 2x2 flotation system, since $G_{13}(s)$ and $G_{23}(s)$ are equal to zero. Therefore, the following subsection is based on the PI controller design only for the non-floated fraction (Bias).

6.4.2 PI Controller design for the Bias process

Persechini *et al*., (2004), present the dynamic behaviour of the bias, depending on all flow rates, and provided that both Q_T and Q_F are constant.

The dynamics of decoupled bias are shown in the 3rd loop of Equation (6.76). Recall from the general steady-state Equation (4.8) in chapter 4, to produce or form a closed-loop decoupled PI control design presented below Equation (6.76):

The closed-loop decoupled model resulted in Equation (6.76):

$$M(s)C(s) = \begin{bmatrix} \frac{-873.68e^{-6}K_{P1}(1+K_{I1}\frac{1}{s})}{s+0.000402} & 0 & 0 \\ 0 & \frac{6.6057e^{-5}K_{P2}(1+K_{I2}\frac{1}{s})}{s+0.00781} & 0 \\ 0 & 0 & (K_{P3}(1+K_{I3}\frac{1}{s}) \end{bmatrix} = \begin{bmatrix} h(s) \\ \varepsilon_g(s) \\ Q_B(s) \end{bmatrix} \quad (6.76)$$

Therefore, the closed-loop bias output is as follows:

$$Q_B(s) = Y_3(s) = M_{33}(s) \times C_3(s) \times E_3(s)$$

$$\Rightarrow E_3(s) = r_3(s) - Y_3(s) \quad (6.77)$$

The bias open-loop behaviour, as simulated in Chapter 4, gave the results shown in Table 4.4. Using the open-loop data information in Table 4.4, the PI control parameters are calculated following the same procedure as for the other two loops. The peak value of the bias is recorded as 7.34 cm^3/s, then the percentage overshoot of M_{pmax} = 15% is equivalent to 1.101 cm^3/s and M_{pmin} = 5% is equivalent to 0.367 cm^3/s. The damping factor (ζ) is then calculated using Equations (6.78 and 6.79).

The maximum value of the damping factor is

$$\zeta_{p\max} = \sqrt{\frac{\left(\ln\frac{M_{p\max}}{100\%}\right)^2}{\pi^2 + \left(\ln\frac{M_{p\max}}{100\%}\right)^2}} = \sqrt{\frac{\left(\ln\frac{1.101}{100\%}\right)^2}{\pi^2 + \left(\ln\frac{1.101}{100\%}\right)^2}} = 0.82 \quad (6.78)$$

The minimum value of the damping factor is calculated as:

$$\zeta_{p\min} = \sqrt{\frac{\left(\ln\frac{M_{p\min}}{100\%}\right)^2}{\pi^2 + \left(\ln\frac{M_{p\min}}{100\%}\right)^2}} = \sqrt{\frac{\left(\ln\frac{0.367}{100\%}\right)^2}{\pi^2 + \left(\ln\frac{0.367}{100\%}\right)^2}} = 0.87 \quad (6.79)$$

As a result, for each value of the acceptable maximum and minimum overshoot, the constrain of the damping factor are noted as follows:

$$M_{pmax} = 15\% \rightarrow 0.82$$
$$M_{pmin} = 5\% \rightarrow 0.87 \quad (6.80)$$

Use the open-loop settling time of 119.9 seconds as given in Table 4.4 and the selected damping ratio of 0.84 to find un-damped natural frequency using Equation (6.81).

$$T_s = \frac{4}{\zeta \omega_n}; \quad (6.81)$$

Thus;

$$\omega_n = \frac{4}{\zeta T_s} = \frac{4}{0.84 \times 119.9} = 0.04$$

6.4.3 Determination of the PI controller parameters of the Bias process

From the general closed-loop system in Equation (6.76), the decoupled transfer matrix M(s) is used, and the output of the bias only is expressed (separated from the froth layer height and decoupled Air hold-up zone).

The output of the Bias process $Y_3(s)$ as presented from Equation (6.77), is as follows:

$$Y_3(s) = \frac{C_3(s)M_{33}(s)}{1+C_3(s)M_{33}(s)} * r_3(s) \quad (6.82)$$

The part for the Bias from Equation (6.76) is substituted into Equation (6.82) and the expression of the closed-loop system for the Bias is obtained:

$$Y_3(s) = \frac{K_{P3}s+K_{P3}K_{I3}}{1+K_{P3}s+K_{P3}K_{I3}} \times r_3(s) \quad (6.83)$$

The closed-loop system in Equation (6.83) is not the second-order system and its characteristic polynomial equation cannot be compared with the desired standard dimensionless form as similarly performed in section 6.2 for froth layer height and the air holdup. Therefore, the PI controller parameters used for the 3rd controller loop of this 3x3 multivariable column flotation system are found through Matlab/Simulink PID tuner. Table 6.4 gives details of the steps followed in determining the PI controller parameters using the PID tuning toolbox. The process of determining the values of a proportional, integral, and derivative (PID) controller's gain to achieve desired performance and match design constraints is known as PID tuning.

Table 6.4: The PID tuner workflow process

Steps	Process	Description
1	In the SIMULINK Launch the PI Tuner	The software automatically calculates a linear plant model from the Simulink model and projects an initial controller.

2	Tune Controller	In the PID Tuner, manually alter design criteria in two design modes to tune the controller. The tuner calculates PI settings that ensure the system is stable.
3	Export parameters	Export the designed controller's parameters to the PI Controller block and test the controller's performance in Simulink.

The baseline controller can be defined, then by default **PID Tuner** displays both the responses using the current **PI Tuner** design and the responses using the baseline controller. In addition to the descriptions given in Table 6.4 above, the following Figure 6.11, shows how it is done in Simulink. There are two ways to define a baseline controller:

- Load a baseline controller when the **PID Tuner** is open, using the syntax "pidTuner" (sys).
- Make the current "**PID Tuner**" design the baseline controller at any time, by clicking the '**Export**' arrow and selecting "Save as Baseline or update Block".

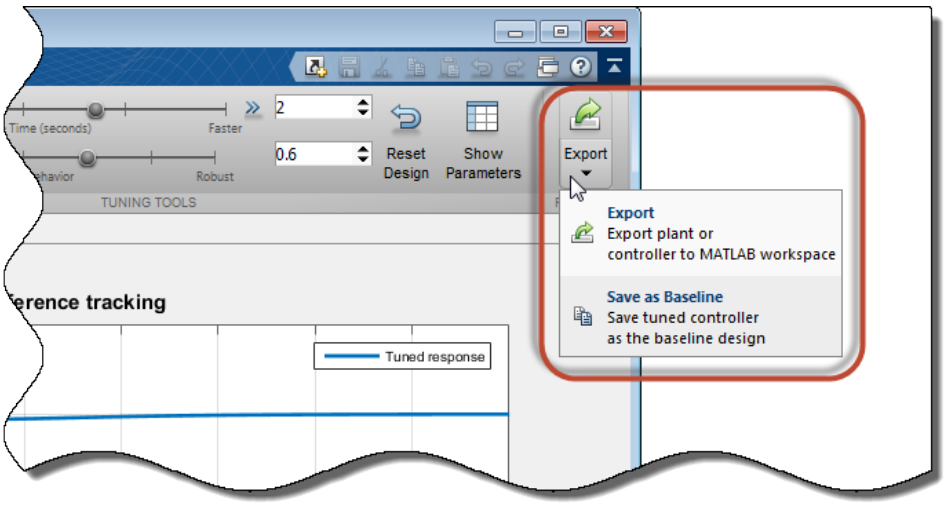

Figure 6.11: **Exportation of the tuned parameters for the PI controller**

After exporting the tuned parameters, the current transferred Tuned response becomes the Baseline response. A new Tuned response line is created by further adjusting the current design. Therefore, the control parameters for the third PI controller are $K_{P3} = 2$ and $K_{I3} = 0.55$, Figure 6.12, shows that the method described has been followed in Simulink and the control parameters used were exported using the PID tuner.

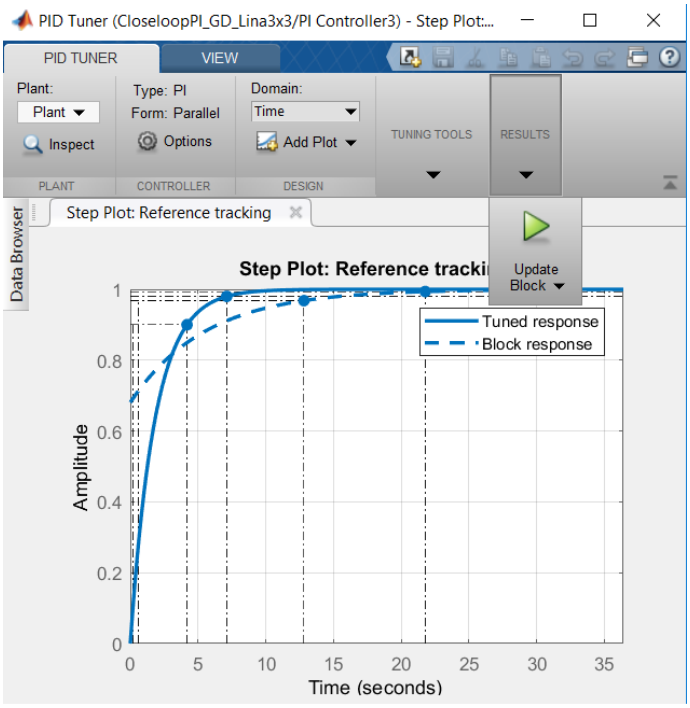

Figure 6.12: The baseline response becomes the Tuned response

The baseline response is an automatically tuned set of gains of the PID controllers. This is done with the aid of software tools to get the optimum system design and meet design objectives, even for plant models that traditional rule-based methods cannot manage. Traditionally or generally Figure 6.12 works in the following ways

- Identifying a plant model using data from input-output tests
- Model PID controllers, like in MATLAB using PID objects or in Simulink using PID Controller blocks.
- PID controller gains can be automatically adjusted, and the design can be fine-tuned interactively.
- Regulate multiple controllers in collection mode
- Tuning single-input single-output PID controllers as well as the structural design of multiloop PID controllers

The following section presents the simulation results of the closed-loop 3x3 multivariable closed-loop system.

6.4.4 Simulation of the Closed-loop 3x3 Column Flotation process

This section is based on the simulation of the multivariable system under study. The table introduced in Table 5.4 for set-point declarations is adopted at this point so that a proper performance comparison can be drawn between the two chapters (Chapter 5 and Chapter 6). From the simplified dynamic decoupled

model shown in Table 6.3, the following Simulink model shown in Figure 6.13, is produced. In the same way, as performed for the 2x2 closed-loop system in section 6.3, the simulation for the 3x3 multivariable closed-loop system is performed.

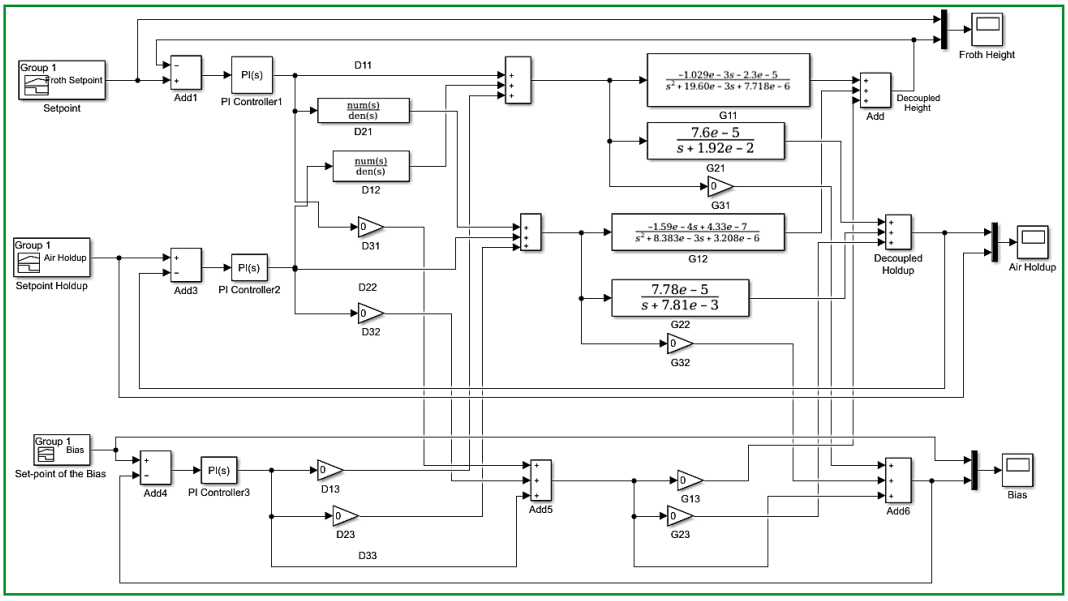

Figure 6.13: **Block diagram of the decoupled closed-loop system under PI control**

The following results demonstrate how the system in Figure 6.13 responds under different set-point changes. The aim is to observe the performance of the decoupled 3x3 closed-loop multivariable systems.

6.4.4.1 Simulation results of the 3x3 Multivariable closed-loop system

The model shown in Figure 6.13 is developed in Matlab/Simulink, with different set-points changes as defined in Table 5.4. To investigate and prove the efficiency of the designed controllers and the dynamic decoupling method used, the set points are randomly selected to prove the controller's abilities for set-point tracking and disturbance rejection of the closed-loop system. Figures 6.14 up to Figure 6.19 show that the controllers work well, and the decoupled closed-loop flotation system is successfully controlled. The results for the closed-loop system behavior with different set-point changes are presented through the following case studies (Figure 6.14 to Figure 6.19).

Case study 1: Starting the evaluation of the 3x3 process

The system shown in Figure 6.13 is used to implement Case study 1 as presented in table 5.4. the set-point of the froth layer height is established from 40 cm and increased

to 60 cm at 10 seconds, the holdup is set to start at 10% and increase to 18%, and the bias starts at 7.4 to 8 and changed back to 7.4 (cm^3/s) at 60 seconds.

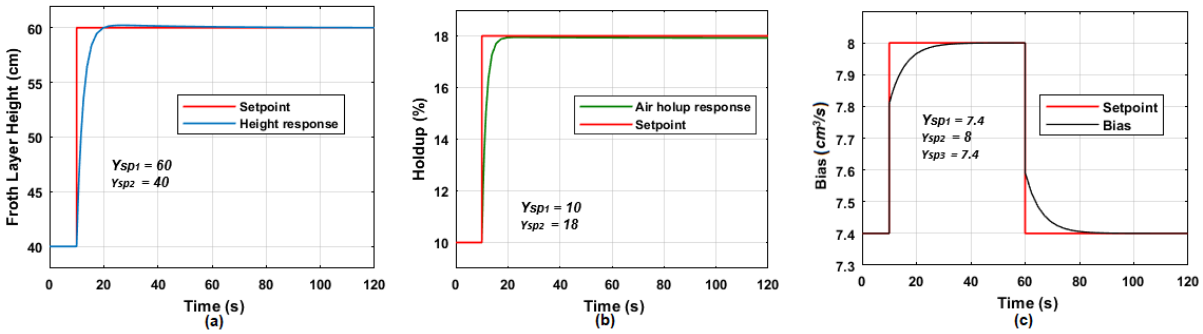

Figure 6.14: Case study1: Closed-loop response of the Froth Layer Height, Holdup, and Bias

Figure 6.14 (a) shown above presents the results of the froth layer height. As can be seen, the froth layer height responded according to the set point, its response started at 40cm, at the time of the 10-second change to 60 cm following the applied setpoint changes. Note that from Figure 6.14 (a), the blue response is the froth layer tracking the applied set-point change shown in red. Figure 6.14(b) presents the results of the air holdup in the collection zone, this response of the holdup within the air zone, effectively tracked the set-point that changed from 10% to 18%. Figure 6.14(c) presents the results of the bias at the setpoint of 7.4.

Case study 2: Set-point change applied on the Air holdup loop

In this case, the set-point changes are applied in the collection zone (gas holdup), to observe the closed-loop behaviour of the whole system and the tracking capabilities of all loops when one loop is under forced changes. Figure 6.15 shows the results based on the changes applied in the holdup Figure 6.15 (b).

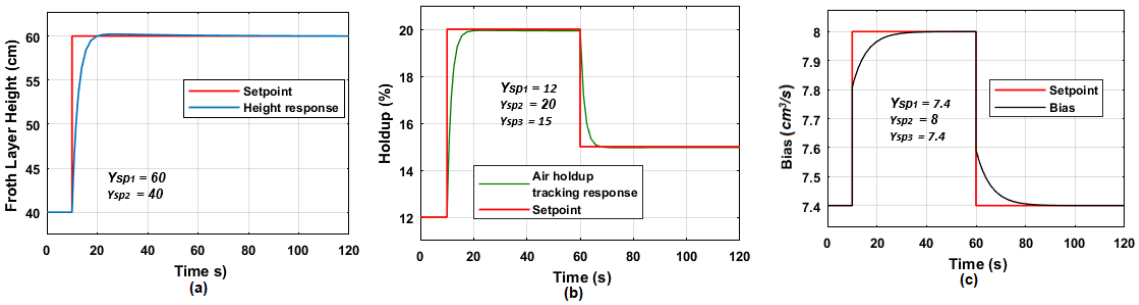

Figure 6.15: Case study 2: Closed-loop response of the Froth Layer Height, Holdup, and Bias

In the next case, Air holdup and the Bias remain the same as in case 1, while the froth layer height is changed. This is prepared to distinguish the capability of the designed controller to overcome the interconnections within the system.

Case study 3: Set-point change applied on the Froth layer loop

Now the set-point changes are applied in the cleaning zone (froth layer), to observe the closed-loop behavior of the whole system, the results are presented in Figure 6.16. Figure 6.16 (b) and Figure 6.16 (c) still accomplish their respective set-point although there is a reduction in the froth layer height at 60 sec (Figure 6.16 (a). As expected, once the system is decoupled the interactions are reduced in such a way that changes made in one loop should independently affect that specific loop only.

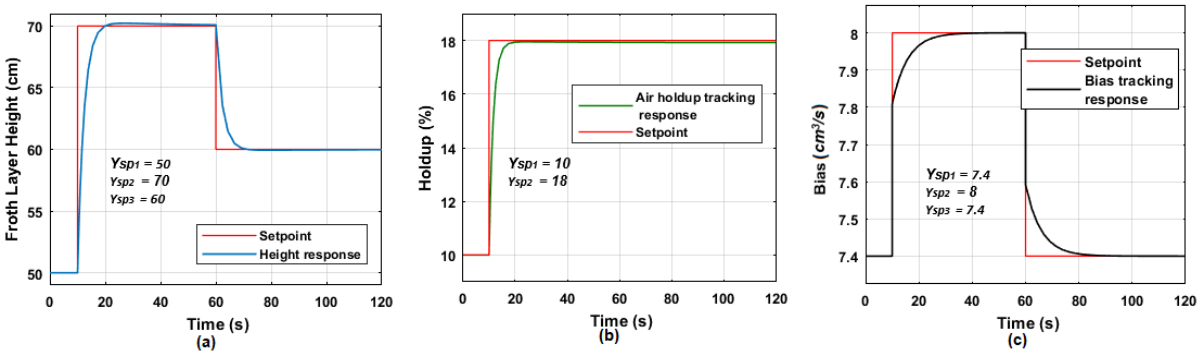

Figure 6.16: Case study 3: Closed-loop response of the Froth Layer Height, Holdup, and Bias

Case study 4: Set-point change applied on the Froth layer loop

Case study 4, presented in Figure 6.17 displays the results based on the set-point changes applied to the non-floated fraction. It can be noted that only the bias changed or followed the new set-point value with no negative effect on the froth height and holdup loops. Therefore, the set-point tracking is working successfully, as all the collection (the holdup) and the cleaning (froth height) zones still tracked their set-points while the non-floated rate is increased or changed from pulse to a step set-point.

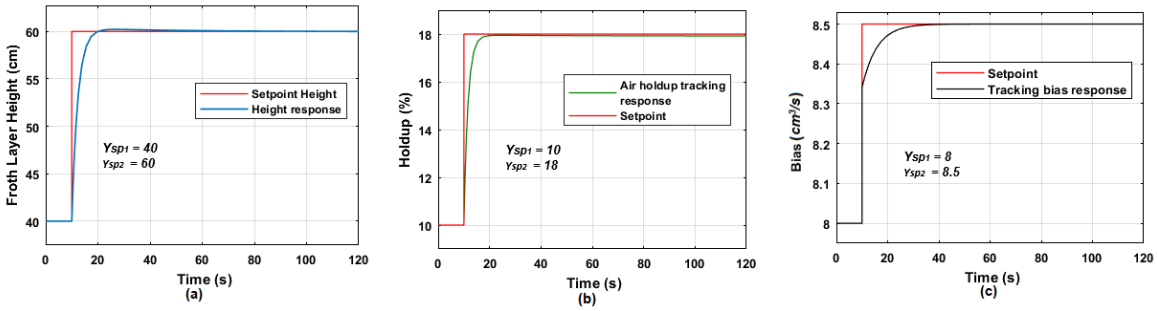

Figure 6.17: Case study 4: Closed-loop response of the Layer Height, Holdup, and Bias

Case study 5 & 6: Same-time Regulation of Froth layer height, Air holdup, and Bias

The real flotation plants may have many disturbances or set-point changes that may transpire even from the feed inflow or within the system. Figure 6.18 and Figure 6.19 (Case 5 and Case 6 respectively) represent the performance of the whole system under

different set-point changes that occur at the same time in all regions of the system. In these cases, the expectation is for each controller to show its ability to control and stabilize the section or zone connected.

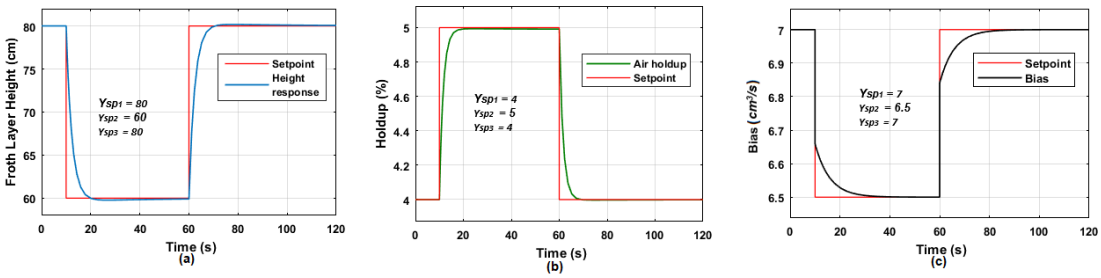

Figure 6.18: Case study 5: Closed-loop response of the Froth Layer Height, Holdup, and Bias

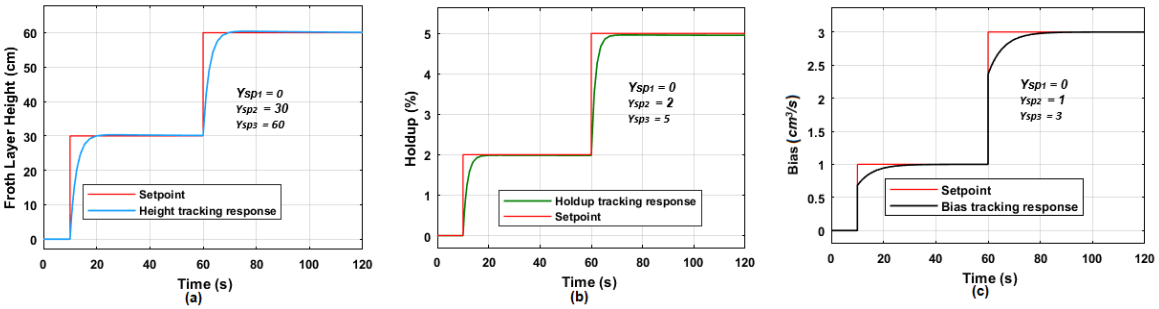

Figure 6.19: Case study 6: Closed-loop response of the Froth Layer Height, Holdup, and Bias

Table 6.6 shows the characteristic of the transition behaviour of the 3x3 multivariable closed-loop system. It can be noted that all the set points are tracked successfully for froth layer height, air holdup, and bias.

The next section (Section 6.5.5) aims to prove the system's capabilities for disturbance rejection.

Table 6.5: Transition behaviour characteristics for analysis of the different set-point influence over the height, air holdup, and bias closed-loop processes

Cases Study	Set-points		Decoupled Froth layer height under the designed PI controller				Decoupled Air hold-up under the designed PI controller				Decoupled Bias under the tuned PI controller			
			Rise time (s)	Settling time (s)	Overshoot	Peak Time	Rise time (s)	Settling time (s)	Overshoot	Peak time	Rise time (s)	Settling time (s)	Overshoot	Peak time
1	*h*	40-60(*cm*)	4.908	18.05	0.22	26.93	3.47	16.08	0.05	24.53	0	76.09	0	60
	ε_{gcz}	10-18(*%*)												
	Bias	7.4-8-7.4 (cm^3/s)												
2	*h*	40-60(*cm*)	4.908	18.05	0.22	26.93	0.59	66.17	0.05	24.53	0	76.09	0	60
	ε_{gcz}	12-20-15(%)												
	Bias	7.4-8(cm^3/s)												
3	*h*	50-70-60(cm)	1.25	68.75	0.22	26.93	3.47	16.08	0.05	24.53	0	76.04	0	60
	ε_{gcz}	10-18(%)												
	Bias	7.4-8(cm^3/s)												
4	*h*	40-60 cm	4.908	18.05	0.22	26.93	3.47	16.08	0.05	24.53	6.77	26.09	0	120
	ε_{gcz}	10-18 *%*												
	Bias	8-8.5 (cm^3/s)												
5	*h*	80-60-80(*cm*)	0.49	68.54	0.17	76.52	0.51	66.25	0.001	24.999	0	76.06	0	0
	ε_{gcz}	4-5-4 (%)												
	Bias	7-6.5-7(cm^3/s)												
6	***h***	0-30-60 cm	53.1	66.9	0.407	76.8	52.48	65.24	0.04	74.4	54.41	73.746	0	120
	ε_{gcz}	0-2-5 (***%)***												
	Bias	0-1-3(***cm^3/s***)												

6.4.4.2 Discussion of the simulation results for the Multivariable system

The simulation findings demonstrate that a decentralized PI control scheme based on dynamic decoupling is a good method to utilize regardless of set-point fluctuations or disturbance influence. Decoupling the process under investigation is a successful method for reducing the influence of interactions in closed-loop control even if the system model has been increased and it consistently kept the system stable as presented in Table 6.5. The set-point tracking results from the simulation of the closed-loop decoupled multivariable system were all successful. The obtained results will contribute to the motivation of the continued use of the existing PI controllers in the industry by enhancing the performance of multivariable systems using relevant design approaches and simple decouplers which can be programmed in the existing PLCs. The next section evaluated the performance of the system under random noise disturbances.

6.5 Investigation and Simulation of the closed-loop system under the influence of disturbances

The designed closed-loop decoupled system is tested when there are some disturbances. Different disturbances were added to the control loop signals of froth layer height, and air holdup control of the system, as presented in Figure 6.20. Figure 6.23 presents a closed-loop system Simulink model with disturbances applied at different positions (after decouplers and at the output) of the system's froth layer height. The aim of Figure 6.23 and Figure 6.29 is to evaluate the influence of an individual's loop on the whole system.

The following subsections demonstrate the results of the closed-loop system under disturbances. This is done to investigate the system's capabilities for disturbance rejection.

6.5.1 Process performance for disturbances applied at the control position

In the first case scenario, the investigation is done through the addition of random noise with two different noise magnitudes applied to the control loop signals of froth layer height (Loop 1), and air holdup control (Loop 2). The noise magnitudes of $9e^{-5}$ cm and $1e^{-3}$ cm, and noise magnitudes of $9e^{-5}$% and $1e^{-3}$ % are applied to loop 1, and loop 2, individually as shown in Figure 6.20.

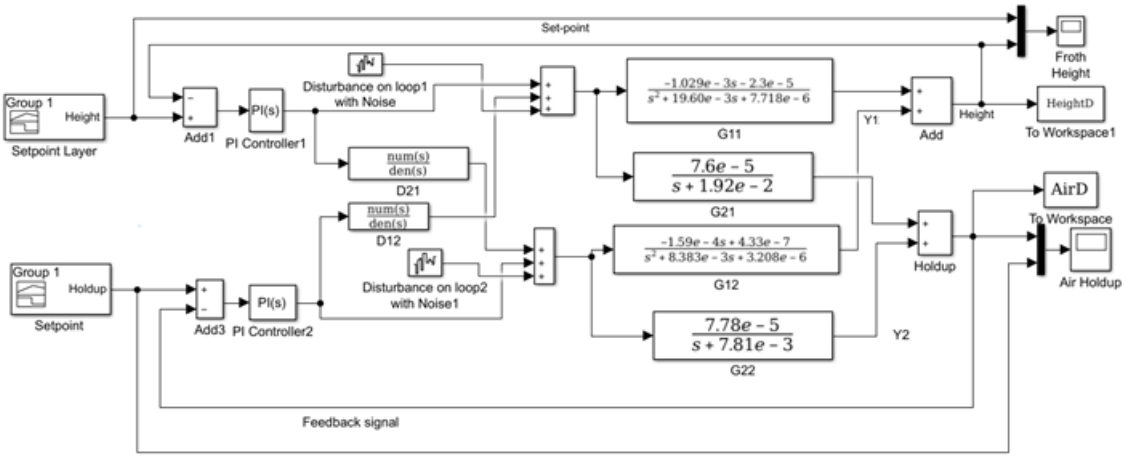

Figure 6.20: Dynamic decoupling controls subject to disturbances at the control signal interaction junction (u_1 and u_2)

Introducing the disturbance at the control interaction junction (u_1 and u_2) would affect the outputs (Y_2 and Y_1), but the results of the simulation show that the effects of this disturbance did not affect the set-point tracking and system stability as shown in Figure 6.21 and 6.22. Matlab simulation results are presented for two different values of random noise disturbance for the closed-loop column flotation processes with the disturbances applied at the interaction junction for the control signals.

Figures 6.21(a) presents the responses of the froth layer height and Figure 6.21(b) presents the results of the air holdup set-point tracking under the disturbances with a noise magnitude of 9e-5 for the considered case.

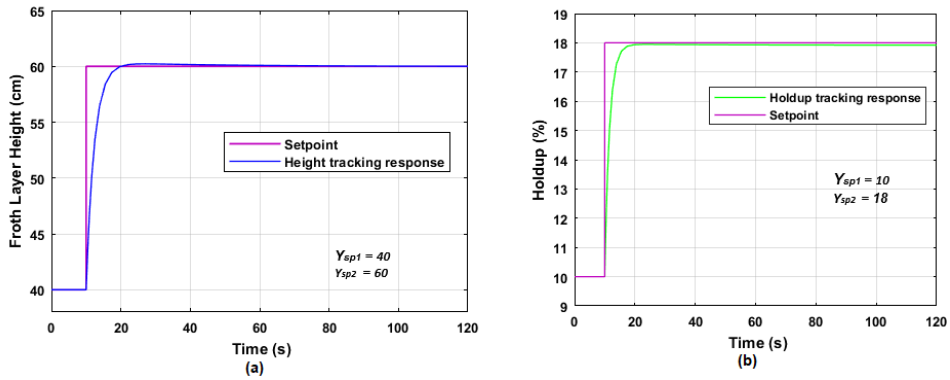

Figure 6.21: Closed-loop response of the Froth Layer Height and Air Holdup under disturbances 9e^{-5} noise magnitude

Figure 6.22 (a and b) shown below represent the responses for the froth layer height and air holdup set-point tracking under the disturbance of $1e^{-3}$. The set points in Figure 6.22 are changed at 10 and 60 seconds. Figure 6.22 (a) the setpoint is set to start at 50 cm, changed to 70 cm at time = 10s, and at time = 60 seconds, the setpoint is changed to 60 cm. According to the results, applying disturbance at the control interaction junction does not disturb the systems. Therefore, any noise disturbances applied at the control interaction junction don't affect or influence the outputs of the systems in both loops.

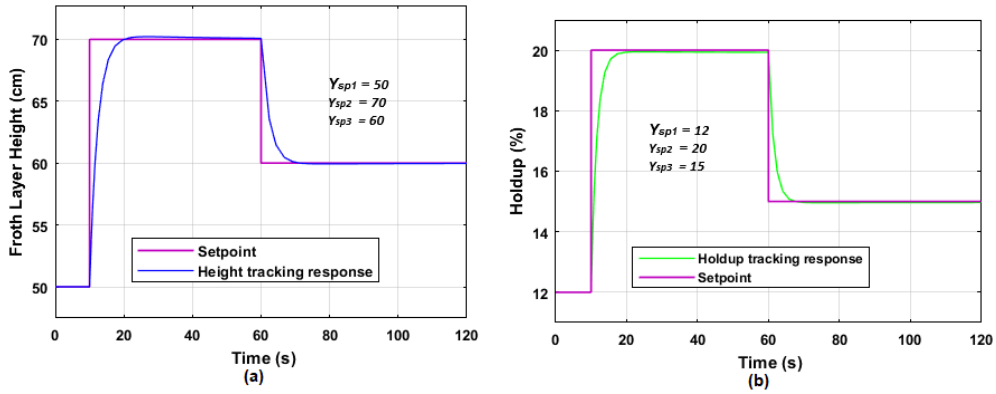

Figure 6.22: Closed-loop response of the Froth Layer Height and Air Holdup under disturbances $1e^{-3}$ noise magnitude

The results are an indication that the designed system can reject the disturbances and maintain any given set-point change with no noise.

In the second scenario, the disturbances were also injected at the output of the froth layer height (Y_1). At this stage no disturbance was applied at the air holdup loop (Y_2: loop2), the results of this scenario are presented in the following section.

6.5.2 Investigation of the disturbance influence applied on Loop 1 of the process

Decoupling the system aims at separating or removing the existence of the interconnections between loops. Using a random sequence with an association of time, the system is disturbed at the control interaction junction and the output by injecting a noise disturbance as illustrated in the Simulink block diagram of Figure 6.23. This is done to investigate the effects of the disturbances applied only in loop 1 froth height. The results of this investigation are shown in Figure 6.24 to Figure 6.28.

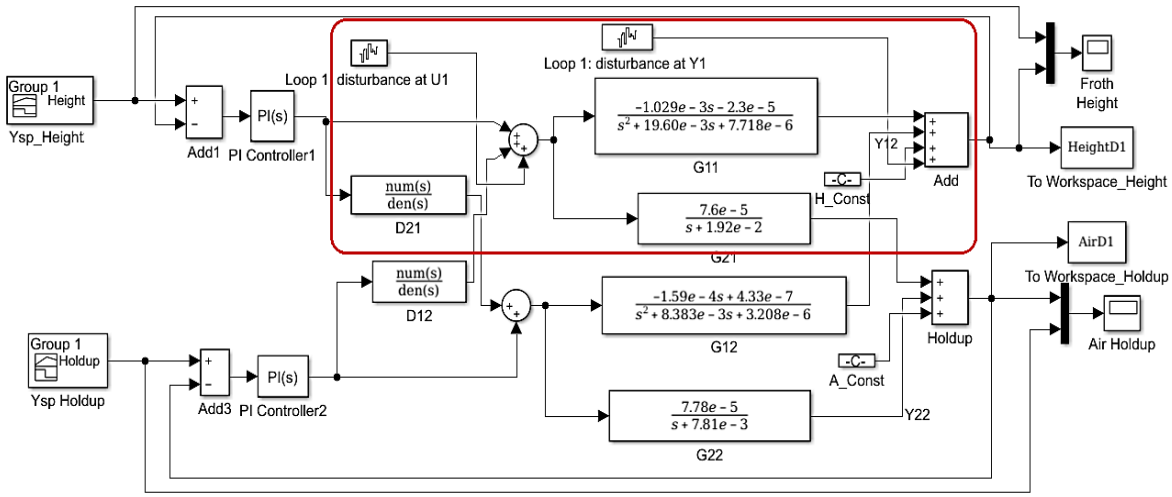

Figure 6.23: Dynamic decoupling controls subject to disturbances at the output (Y_1) and the interface junction (U_1)

The performance of the designed dynamic control system is investigated for various variables or random noise magnitudes added to the froth layer height loop (named

Loop 1). For the result in Figure 6.24, the noise magnitude applied is $2e^{-6}$ at the froth layer height (loop 1). Figure 6.24 (a) is the response of the froth layer height, notice that the noise presence is an indication of the applied disturbance. The result in Figure 6.24 (b) is the air holdup, as it can be noted there is no presence of noise, which means the disturbance in loop 1 did not disturb loop 2.

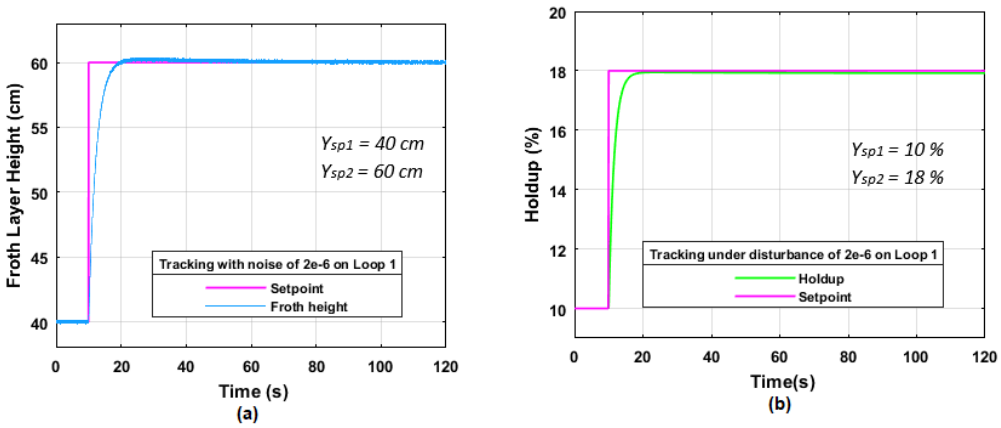

Figure 6.24: Closed-loop response of the Froth Layer Height and Holdup under disturbances of $2e^{-6}$ noise magnitude

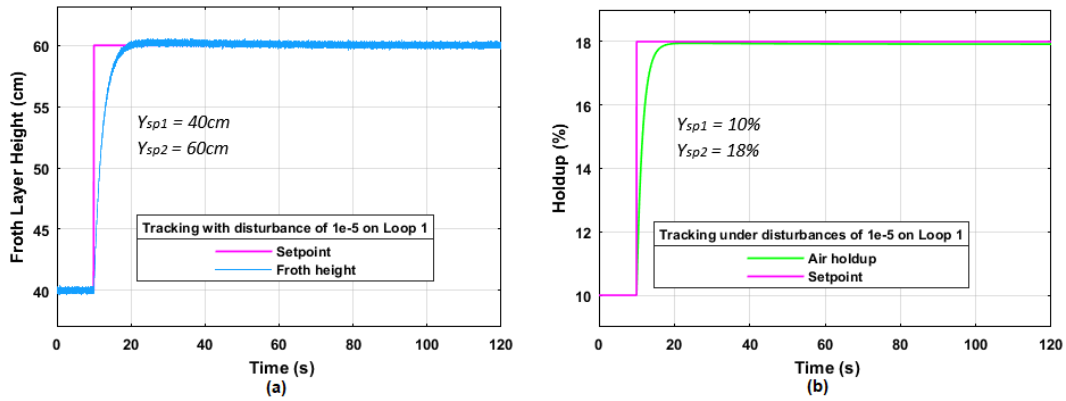

Figure 6.25: Closed-loop response of the Froth Layer Height and Holdup under disturbances of $1e^{-5}$ noise magnitude

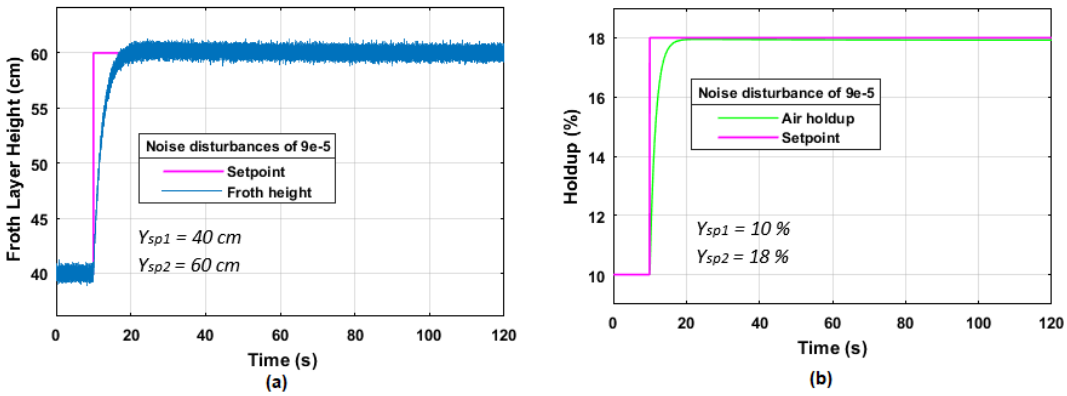

Figure 6.26: Closed-loop response of the Froth Layer Height and Holdup under disturbances of $9e^{-5}$ noise magnitude

The noise magnitude applied is increased to $1e^{-5}$ as indicated in Figure 6.25. A further increase to $9e^{-5}$ is applied in noise magnitude at the froth layer height loop as presented in Figure 6.26. Figure 6.25 (a) and Figure 6.26 (a) show the results of the changes made in noise magnitude.

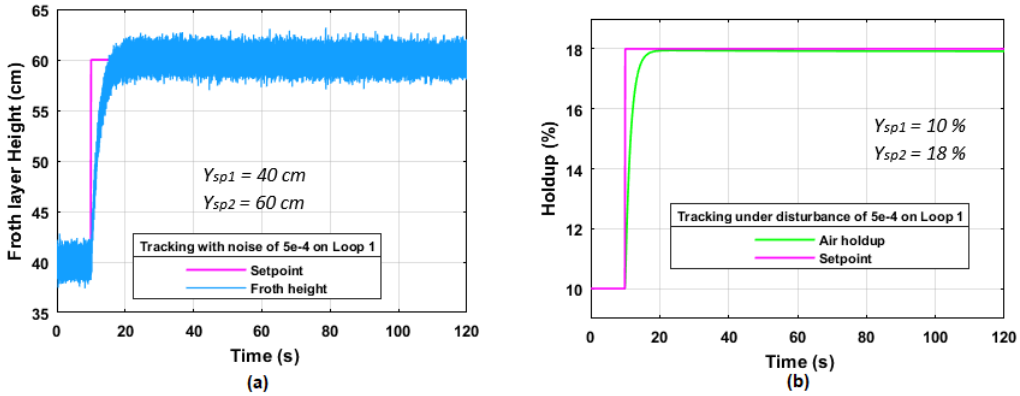

Figure 6.27: Closed-loop response of the Froth Layer Height and Air Holdup under disturbances $5e^{-4}$ noise magnitude

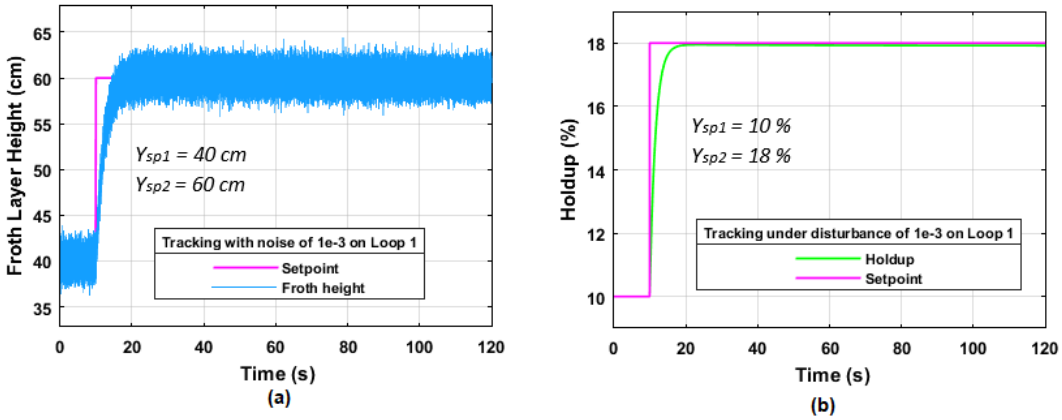

Figure 6.28: Closed-loop response of the Froth Layer Height and Air Holdup under disturbances $1e^{-3}$ noise magnitude

This investigation of increasing the magnitude of the added random noise continued to observe setpoint tracking under the influence of the disturbance and examine how this variation affected Loop 2.

All the result from Figure 6.24 to Figure 6.28 the air holdup, as it can be noted there is no presence of noise or any sign of disturbance due to loop 1. This means the disturbance in loop 1 did not disturb loop 2 anywhere. This has proven that decoupling these loops is accomplished. Similarly, the disturbances in the next section are applied at the interaction junctions of the air holdup zone (Loop 2).

6.5.3 Investigation on the disturbance influence applied on Loop 2 Air holdup

Decoupling the system aims at separating or removing the existence of the interconnections between loops. Using a random sequence with an association of time, the system is disturbed at the control interaction junction and the output by injecting a

noise disturbance as illustrated in the Simulink block diagram of Figure 6.29. This section loop 2 is the disturbance, this is done to investigate the effects of the disturbances applied on the air holdup zone.

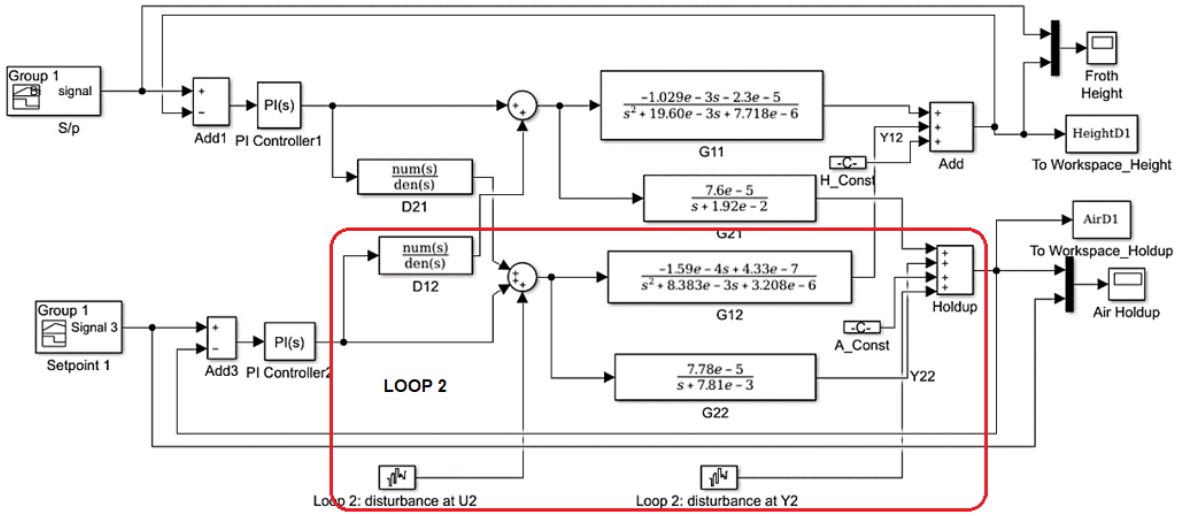

Figure 6.29: Dynamic decoupling controls subject to disturbances at the output (Y_2) and the interface junction (U_2)

The responses are represented in Figure 6.30 to Figure 6.34. In terms of the major performance indices, good tracking control is still accomplished. The response of the air holdup, on the other hand, gets noisier as the disturbance's noise magnitude increases. It is also noted that loop 1, for the froth layer height is not affected by the disturbance in loop 2. Therefore, both loops are fully decoupled from each other.

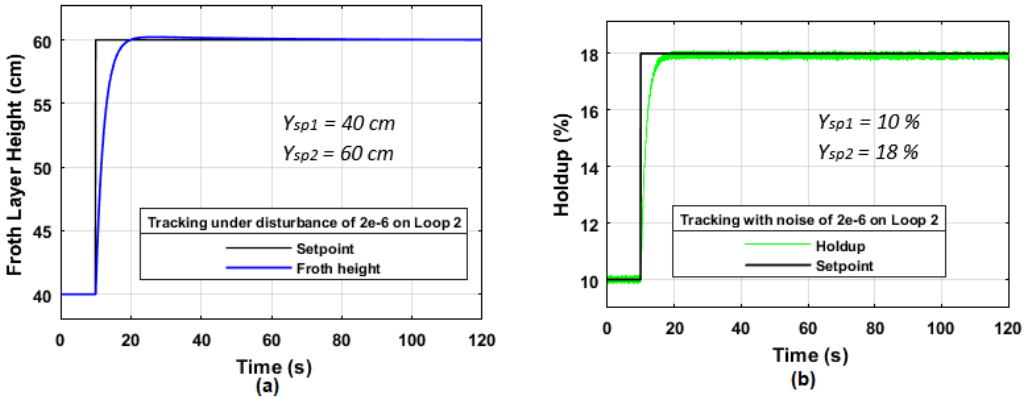

Figure 6.30: Closed-loop response of the Froth Layer Height and Holdup under disturbances of $2e^{-6}$ noise magnitude

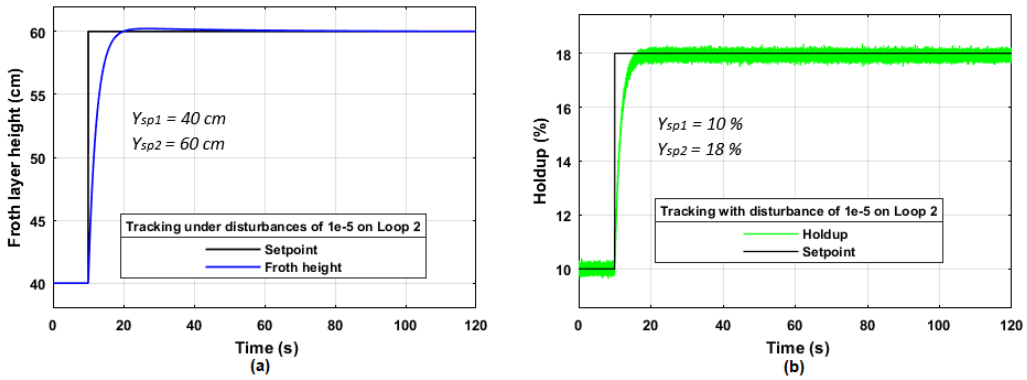

Figure 6.31: Closed-loop response of the Froth Layer Height and Holdup under disturbances of $1e^{-5}$ noise magnitude

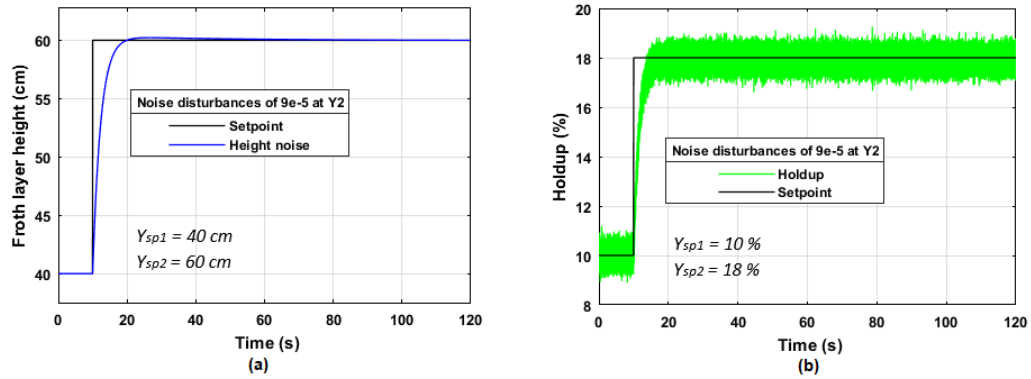

Figure 6.32: Closed-loop response of the Froth Layer Height and Holdup under disturbances of $9e^{-5}$ noise magnitude

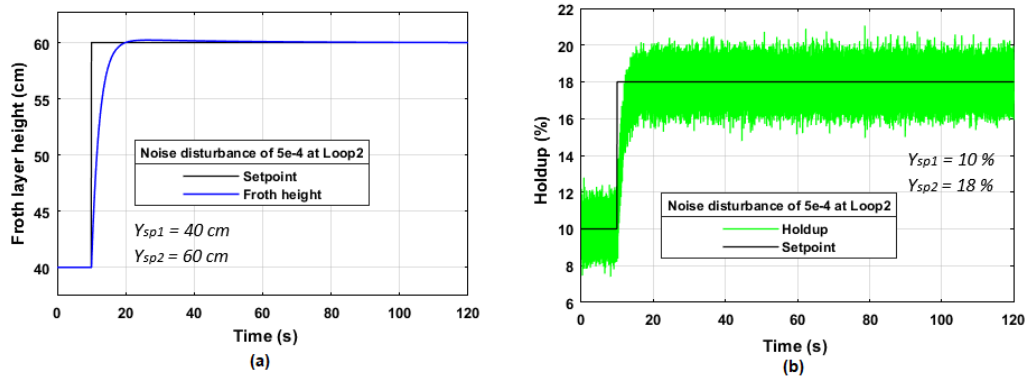

Figure 6.33: Closed-loop response of the Froth Layer Height and Air Holdup under disturbances $5e^{-4}$ noise magnitude

In the same way, the noise magnitude used for the investigation performed in section 6.5.2 (Loop 1: froth layer height) is considered for air holdup (loop 2). The results in Figure 6.30 to Figure 6.34 show that the disturbance and noise did not affect the froth layer height system. Table 6.6 presents various performance indices for the multivariable system response when the set points are varied, and unpredictable disturbance is applied.

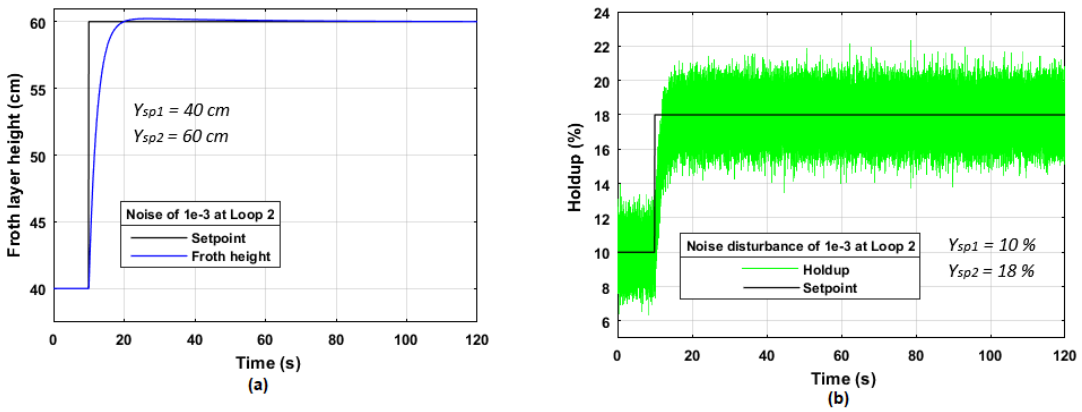

Figure 6.34: Closed-loop response of the Froth Layer Height and Air Holdup under disturbances $1e^{-3}$ noise magnitude

Table 6.6: Analysis of the disturbance effect over height, and air holdup

The position where the disturbance is applied	Noise magnitude	Decoupled Froth layer height under the designed PI controller					Decoupled Air hold-up under the designed PI controller				
		Rise time (s)	Settling time (s)	Overshoot	Peak time	Steady-state error	Rise time (s)	Settling time (s)	Overshoot	Peak time	Steady-state error
Loop 1	$2e^{-6}$	4.7567	113.3450	0.368	24.488	0	3.40	15.86	0.05	23.79	0
	$1e^{-5}$	4.5962	113.3450	0.56	24.488	0	3.40	15.86	0.05	23.79	0
	$9e^{-5}$	4.13	119.99	1.37	78.67	0	3.404	15.87	0.05	23.79	0
	$5e^{-4}$	13.595	119.999	3.17	78.67	0	3.40	15.86	0.05	23.80	0
	$1e^{-3}$	13.296	119.999	4.46	78.67	0	3.40	15.86	0.05	23.803	0
Loop 2	$2e^{-6}$	4.815	17.849	0.22	26.642	0	3.236	118.83	0.1228	78.67	0
	$1e^{-5}$	4.815	17.849	0.22	26.645	0	3.01	119.98	0.367	78.67	0
	$9e^{-5}$	4.815	17.849	0.22	26.646	0	12.205	119.999	1.25	78.67	0
	$5e^{-4}$	4.815	17.849	0.22	26.646	0	11.568	119.999	3.05	78.67	0
	$1e^{-3}$	4.8148	17.849	0.22	26.646	0	11.104	119.999	4.35	78.67	0

The investigation conducted shows that the closed-loop froth layer height and air holdup processes follow exactly the set-point variations. This shows that the dynamic decoupling and controllers designed presented a very effective strategy to be used regardless of the set-point variations or disturbances applied in a system under study. The results indicate that the elements of interactions in the system are eliminated.

6.5.4 Discussion of the results

Introducing a fully decentralized dynamic decoupled closed-loop control scheme for the multivariable column flotation systems has proven to be an effective strategy to eliminate the interactions and successfully reach all setpoint tracking sets for this system. All simulation results are utilized to check the effectiveness of the control strategies and to see if effective set-point tracking control and disturbance rejection can be achieved. The closed-loop simulation study for the froth layer height and air holdup are first investigated (section 6.3) for the ability to track the set point. This is accomplished by altering the setpoints from case study 1 to case study 4, and the results confirmed the designed control scheme's set-point tracking capabilities.

In the same way, the effects of disturbances are investigated to analyse the performance of the system under unusual conditions. For the first case scenario considered, the disturbances are applied at the interaction points of loop 1, (see Figure 6.23). This is examined by introducing various magnitudes of random noise to the froth layer loop, to investigate the capabilities of setpoint tracking and disturbance rejection abilities. The responses for both height and holdup loop set-point tracking with these disturbances for the considered scenario show that disturbance does not influence the performance of the air holdup zone (loop 2) while the disturbance is only applied to the froth height loop. In the second scenario, the investigation of the influence of the effect of disturbance is performed at the collection or air holdup zone as shown in Figure 4.29 (loop 2).

The tracking control is successfully performed for various noise variation magnitudes of random disturbances applied into the process, though it should be noted that as the magnitude of the disturbance increases, the holdup tracking response becomes noisier than the froth layer under the same noise magnitude. Comparing the results from Table 6.2 (case 1), and Table 6.5, it can be noted that the system’s responses, with and without disturbances have similar characteristic behavior.

It is necessary to perform some comparison analysis between the two methods used in this thesis. One method is based on the decentralized coupled system, as presented in chapter 5, and the second method is based on the decentralized dynamic decoupled system, as presented in chapter 6. The results of the comparison demonstrate that performance indices including rise-time, settling time, peak overshoot, and steady-state error performed much better for the dynamic decoupler system, see Table 6.8. This further shows that the use of the dynamic decoupling control design for the flotation system is much worth it regardless of the set-point value changes or disturbance tracking.

6.6 Comparison of the results between the decentralized coupler system and dynamic decoupler system

This subsection aims at comparing the results conducted based on the coupled decentralized method (chapter 5) and the dynamic decoupled technique used in chapter 6. A comparison between the characteristics behavior of the closed loop decentralized coupled column flotation system and dynamic decoupled column flotation system is presented in Table 6.7 below.

Table 6.7: Comparisons of the transition performance indexes between the decentralized coupler and decoupler system

Cases : refer to the Set-point used	Loop	Decentralized coupled approach				Dynamic decoupled scheme			
		Rise time [sec]	Settling time [sec]	Overshoot [cm] and [%]	Steady-state error cm] and [%]	Rise time [sec]	Settling time [sec]	Overshoot [cm] and [%]	steady-state error cm] and [%]
1	Height	5.48	18.73	0.36	0	4.91	18.05	0.22 cm	0
	Holdup	4.86	18.32	0.03	0	3.47	16.078	0.05 %	0
2	Height	5.43	68.32	3.68	0	4.91	18.05	0.22 cm	0
	Holdup	0.77	68.53	0.03	0	0.59	66.17	0.05%	0
3	Height	1.80	67.5	0.36	0	1.25	66.7	0.22 cm	0
	Holdup	4.84	64.5	0.21	0	3.47	16.078	0.05%	0
4	Height	0.49	66.1	0.11	0	0.489	66.0	0.17 cm	0
	Holdup	0.0044	68.56	0.26	0	0.51	66.25	0.01 %	0

Table 6.7 shown above compares the simulation results of the 2x2 model based on two techniques developed in chapter 5 (decentralized coupled approach) and chapter 6 (dynamic decoupled approach). Comparing the two methods, the dynamic decoupled technique provided the best results than the decentralized coupled approach. This was concluded when comparing the two chapters/ techniques /approach in terms of their response time, how long the system takes to settle, and most importantly the system's

steady-state error. Therefore, multivariable systems are recommended to use a decoupled decentralized approach to successfully eliminate the interactions within the system and have a process that can track all setpoint changes even if there's a big setpoint change in the system.

The following table, Table 6.8 presents the comparison results of the multivariable 3x3 flotation system model.

Table 6.8: Comparisons of the transition performance indexes between the decentralized coupler and decoupler system

Cases: refer to the Set-point used	Zones within the flotation	Decentralized coupled approach				Decentralized Dynamic decoupled approach			
		Rise time [sec]	Settling time [sec]	Peak time (s)	Overshoot cm] and [%]	Rise time [sec]	Settling time [sec]	Overshoot [cm] and [%]	Peak time (s)
1	Height	5.43	18.74	27.166	0.36	4.908	18.05	0.22 cm	26.93
	Holdup	4.91	18.35	27.166	0.03	3.47	16.078	0.05%	24.53
	Bias	1.1e-14	67.55	60	0	0	76.09	0	60
2	Height	5.38	68.32	61.92	3.68	4.908	18.05	0.22cm	26.93
	Holdup	0.77	68.53	27.166	0.03	0.59	66.17	0.05%	24.53
	Bias	1.1e-14	67.3	60	0	0	76.09	0	60
3	Height	1.78	67.49	26.99	0.36	1.25	67.1	0.22cm	26.93
	Holdup	4.89	64.53	62	0.21%	3.47	16.08	0.05%	24.53
	Bias	1.1e-14	67.46	60	0	0	76.04	0	60
4	Height	5.43	18.74	26.99	0.37	4.908	18.05;	0.22cm	26.93
	Holdup	4.91	18.35	26.99	0.03	3.47	16.08	0.05%	24.53
	Bias	4.12	17.35	74	0	6.77	26.099	0	120
5	Height	0.49	66.03	75.01	0.11	0.489	67.1	0.17cm	76.52
	Holdup	0.0044	68.56	12.51	0.26	0.51	66.25	0.001%	24.53
	Bias	7.6	67.37	7	0	0.01	76	6.94e-5	0

The same observation noted when simulating without the non-floated section (bias loop) is noted again in the overall results of the 3x3 model. In conclusion, the decentralized coupled approach as presented in chapter 5 has shown that the amount of change in the air holdup applied must not have a large gap of the changes, as this created overshoot on the other loop (height loop/ zone) and vice versa (see from Figure 5.7 – Finger 5.10). Given the obtained results of the transition performance of the closed-loop systems, the decentralized decoupled system has better performance when compared to the performance of the decentralized coupled method under the control of the PI and PID controllers' parameters as presented in Tables 6.6 and 6.7.

6.7 Conclusion

The controllers designed for MIMO systems have significant challenges due to the complexities induced by interacting loops. Interactions arise as a result of coupling between the control and process variables, which affects the states of the controlled variables. This chapter developed a basic dynamic decoupling technique to handle the problem of loop interactions, to disregard the interaction within the system. By using a pole placement technique to adjust the separate loops for tracking control of the output variables, PI controllers are created directly for the resulting decoupled system and independently.

In conclusion, it is noted that the designed controllers for the 2x2 and 3x3 multivariable systems performed according to the specifications. The dynamic decoupled flotation system considered here is controlled by PI controllers designed using the pole placement method. It should be clear that pole placement designs do allow a good closed-loop response, but require some experience to decide which pole locations are the best for any particular problem (Ogunnaike & Ray, 1994). All the results accomplished have proven to be successful in set-point tracking (Tables 6.2 and 6.5) and disturbance rejection (Table 6.6). The next chapter (Chapter 7) concentrates on the hardware implementation of the designed controllers under Chapter 5 and Chapter 6. Chapter 7 focuses on the real-time implementation of this study using a model transformation and the PLC environment for the real-time implementation of this flotation process.

CHAPTER SEVEN:
PRACTICAL IMPLEMENTATION OF THE CLOSED-LOOP COLUMN FLOTATION PROCESS, USING TWINCAT 3 SOFTWARE AND PLC

7.1 Introduction

The developed closed-loop model of the column flotation process is implemented in a real-time simulation platform using TwinCAT 3.1 Automation software and Beckhoff CX-5020 PLC through the model transformation method. The methodology is based on converting created continuous-time controllers and closed-loop system applications from Matlab/Simulink to Beckhoff Embedded PC-based PLC automation software using the TwinCAT 3.1 simulation environment for real-time control. The multivariable column flotation process is implemented in real-time in this chapter using real-time control techniques. This is done to demonstrate the effectiveness of the controllers developed in Chapters 5 and 6. The real-time control concept focuses on the creation of software algorithms for integrating a closed-loop control system application with a predetermined time window for gathering and processing data. The closed-loop real-time control system is executed on a Beckhoff CX5020 Programmable Logic Controller (PLC) with TwinCAT 3.1 software. Simulink control setup and configuration are possible with TwinCAT 3.1 software. However, successful code creation in Matlab/Simulink is required, followed by downloading the generated code to TwinCAT 3.1 software environments for real-time implementation. The EtherCAT communication protocol, an open real-time Ethernet designed by Beckhoff Automation, is used to communicate between the embedded PC and the Beckhoff CX5020 PLC.

Chapter 7 presents the Real-Time implementation results obtained and plotted in the TwinCAT 3 environment. This chapter is structured as follows, the overview and the novelty of Beckhoff CX5020 PLC are discussed in section 7.2. The approach for integrating TwinCAT 3.1 with Matlab/Simulink software is provided in section 7.3, along with methods for creating TwinCAT modules from a Simulink model to implement real-time control of the recommended control algorithms. Steps for real-time implementation are presented in section 7.4. Section 7.5 presents the module of the closed-loop control transformed from Matlab/Simulink to TwinCAT 3.1 and the results of the real-time implementation scheme are presented. Discussions of the real-time outcomes are offered in section 7.6. Section 7.7 concludes this chapter.

7.2 An Overview of Programmable Logic Controllers: Beckhoff CX50x0

Embedded devices, such as Programmable Logic Controllers, are used to create control algorithms for industrial process technologies (PLC). Machinery, material handling, packaging, and automation assembling are all examples of industrial PLC applications. Beckhoff CX50x0 is an embedded device that is used in industrial automation systems. According to the industrial needs, flexible and powerful PLCs like the Beckhoff CX5020 are used to deal with the rising complexity of the current automation industries. A PLC typically contains a Central Processing Unit (CPU), memory units such as Random Access Memory (RAM) and Read-Only Memory (ROM), a power supply unit, and other auxiliary devices such as I/O units. The CPU unit is at the core of the PLC. This unit contains a CPU (or microprocessors) that performs mathematical and logical operations, as well as links to local area networks, computer interfaces, and other peripherals. The CPU implements programs by verifying the input unit's states and sending data to external field devices through the output unit. The output unit communicates between the PLC's CPU and the outer field devices for which the PLC provides control signals.

Modern PLCs have proven particularly appealing for regulating real-time industrial activities due to their increased versatility in terms of standardization and performance. Some of the criteria of the International Electro-technical Commission (IEC) standards include real-time control software written in a variety of languages, as well as an embedded operating system capable of running a wide range of applications. The Beckhoff CX5020 PLC is used in this thesis to develop closed-loop real-time control for the column flotation process. The CX5020 is a DIN rail mountable, fan-less embedded PC with a direct connection for Beckhoff Bus Terminals or EtherCAT terminals, as shown in Figure 7.1. This industrial Embedded PC, such as the Beckhoff CX5020 PLC, is used for real-time control since it meets all of the requirements for implementation.

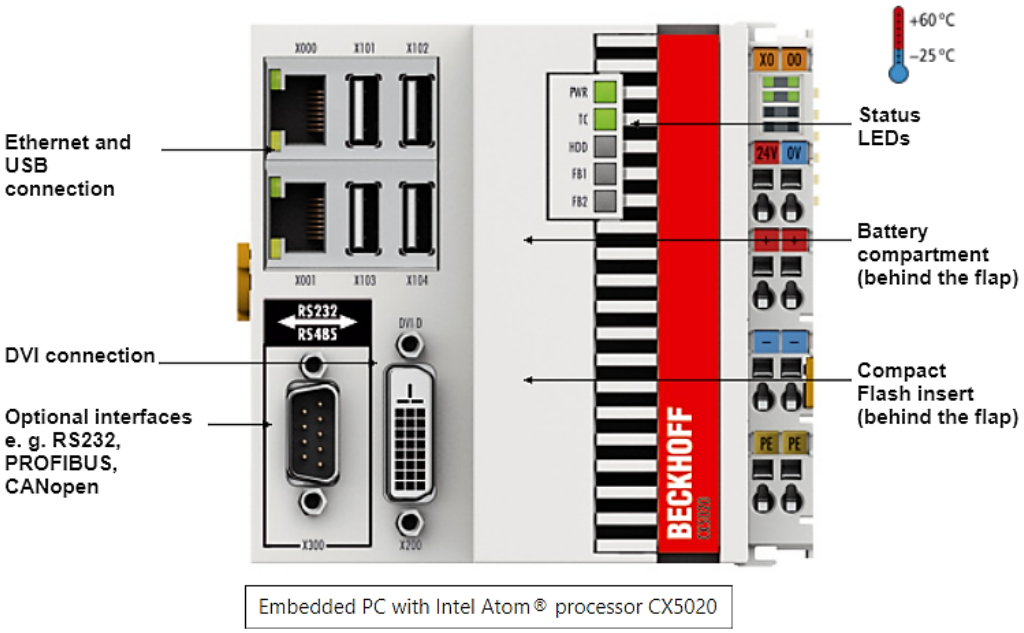

Figure 7.1: **Represents several features of the BECKHOFF CX5020 adopted from the Product manual of Beckhoff New Automation Technology. (www.beckhoff.com/CX5000)**

The CX5010 and CX5020 are Embedded PCs from the Beckhoff CX5000, and CX**5020** series based on intel atom processors, and they only differ by the CPU version. The CX5010 has a 1.1 GHz intel atom Z510 processor, while the CX5020 has a 1.6 GHz intel atom Z530 processor. Apart from the clock speed, the two processors also differ in the fact that the Z530 features hyper-threading technology because it has two virtual CPU cores for more effective execution of software. Depending on the installed TwinCAT runtime environment, the CX5010/CX5020 can be used for the implementation of PLC/Motion Control projects with or without visualization (Beckhoff, 2013). Beckhoff CX50x0 PLC is classified in different orders as presented in Appendix A. The basic configuration of the CX5020 includes a 128 MB Compact Flash card, two Ethernet RJ-45 interfaces, four USB-2.0 interfaces, and a DVI-D interface. This PLC has an almost unlimited number of input and output cards, which allows the user to decide the number of inputs and outputs required in any specific application.

As presented in Appendix B, the CX5020 is used in synchronicity with TwinCAT 3.1 software from Beckhoff and offers the same functionalities as large industrial personal computers (PCs). This Beckhoff PLC has up to four virtual IEC 61131 CPUs that can be programmed to four tasks, with a minimum cycle time of 12.5µs. It has a wide range of operating/storage temperatures that varies between -25 and 60ºC to enable applications in climatically challenging conditions. The operational software tool developed and used by Beckhoff is presented in the following section.

7.3 Matlab/Simulink integration through TwinCAT 3.1

Matlab/Simulink software may generate codes from Simulink models to multiple targets using the Embedded Simulink Coder, formerly known as "Real-Time Workshop". The Simulink Embedded Coder, in combination with Beckhoff Automation's TwinCAT 3.1 Target for Matlab/Simulink (TE1400), enables the development of C++ code, which is subsequently compressed into a standard TwinCAT 3.1 module format. Then, this code is loaded using the TwinCAT 3.1 development platform. The TE1400 software package is a user interface for developing real-time modules that run on the TwinCAT 3.1 runtime environment. Two licenses (TwinCAT 3.1 Target for Matlab/Simulink and TwinCAT 3.1 Interface for Matlab/Simulink) are generally required to complete the transformation from Matlab/Simulink to TwinCAT 3.1. TwinCAT 3.1 includes Matlab/Simulink coder system target files that can be utilized on the TwinCAT 3.1 target. TwinCAT targets allow the TwinCAT 3.1 runtime modules to be generated. The Matlab/Simulink, TwinCAT 3.1 Interface facilitates communication between Matlab/Simulink and the TwinCAT 3.1 runtime (Yang & Vyatkin, 2012). TwinCAT 3.1 delivers real-time parameter acquisition and visualization. The TwinCAT Component Object Model is the name of the real-time capable module (TcCOM). This module, which may be imported into the TwinCAT 3.1 environment, contains the Simulink model's input and output, as illustrated in Figure 7.2:

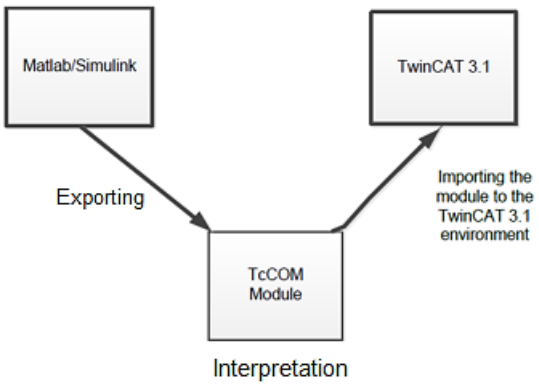

Figure 7.2: TcCOM module operation

TcCOM enables the interaction of modules written in multiple languages in a real-time setting. The transformation technique from Matlab/Simulink to TwinCAT 3.1 for implementation is shown as a block diagram representation in Figure 7.3.

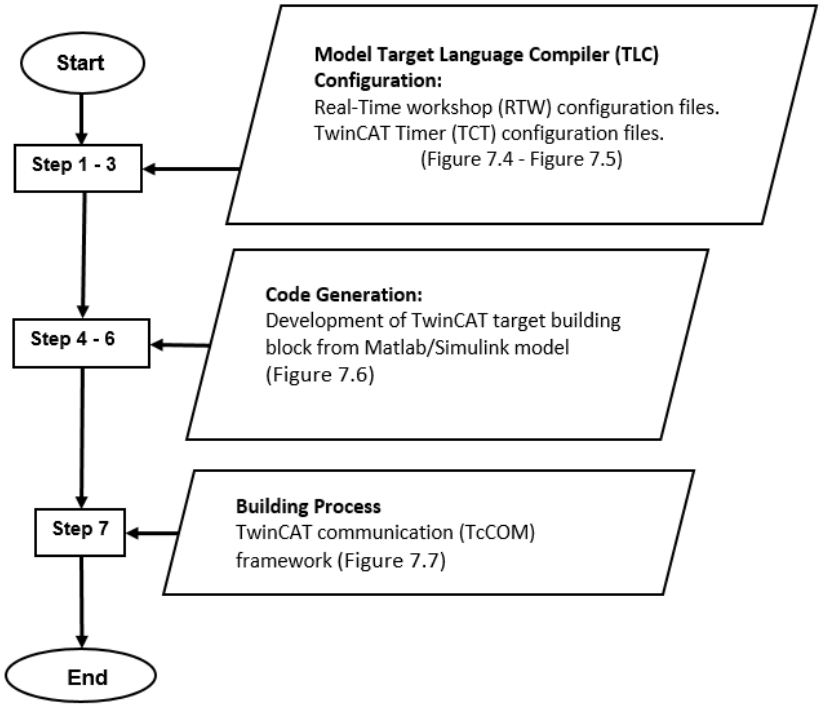

Figure 7.3: **Block diagram flow chart for Code Generation execution**

The Total Windows Control and Automation Technology, commonly known as the TwinCAT is a software platform developed by Beckhoff. To successfully export the model to the TwinCAT environment the steps presented below are applied:

Stages from Simulink to TwinCAT environment

Below are the steps for transforming a Matlab/Simulink model to a TwinCAT function block module for real-time control implementation.

1) In Simulink's main platform, the Simulink model is opened, and the model explorer tab is launched from the view menu, then the window in Figure 7.4 pop-up for Parameter Configuration. At this stage model Parameter Configurations such as simulation time, fixed-step time, and sample time are configured under step 1. To some extent, each computer-based model will have to use some discretization technique to reflect data flow in a physical system. Hence, it is important not to have variable step time, as this can create instability or error in the real-time mode of operation. The rate at which a physical device or development program checks its inputs and outputs is referred to as sampling time.

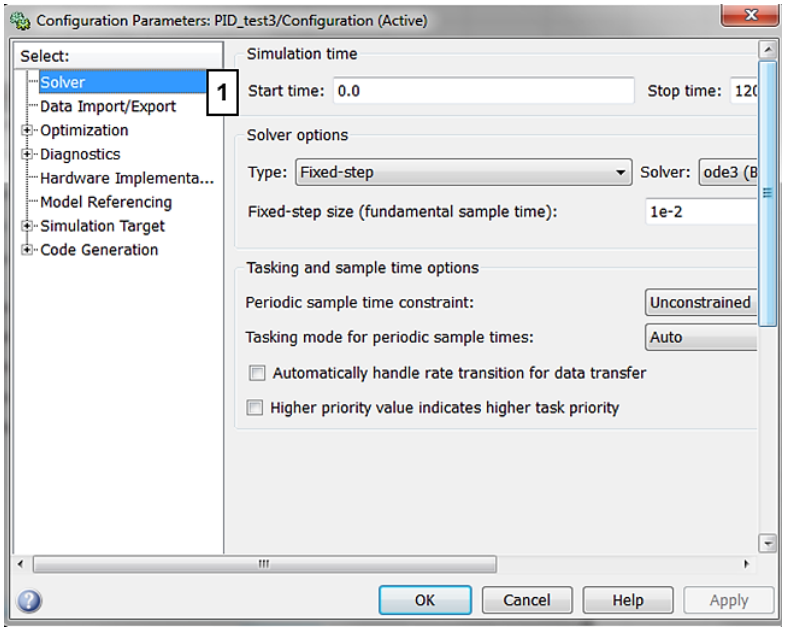

Figure 7.4: Parameter Configuration in Simulink Model Explorer

2) The model configuration is selected under the explorer pop-up window, then after, the generation code tub is activated.
3) A new pop-up window with the system target files will emerge. The TwinCAT system target is then selected from the TwinCAT.tlc file. The model explorer pop-up window is then closed. Figure 7.5 demonstrates the process of how the selection of the TwinCAT target file is completed. The model setup or configuration is selected, upon which the Code Generation tub is activated as shown in step 2, and the option for Target selection Browser will be available. Launching the system target browser resulted in another pop-up window appearing, having the system target files. Then, as shown in step 3 of Figure 7.5, the TwinCAT.tlc file for the TwinCAT target is selected and then press OK.

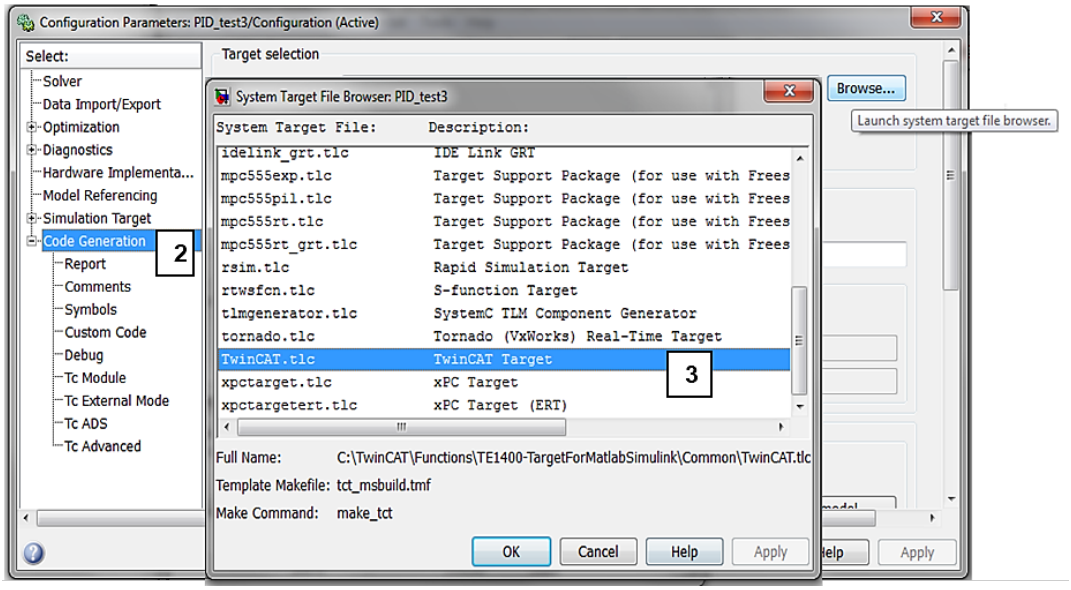

Figure 7.5: TwinCAT target file selection for code generation

4) The code generation and the building of the model process are then started via the Simulink menu, Tools, Code Generation, and Build Model in the order as presented in steps 4, 5, and 6 of Figure 7.6. At this stage, the TwinCAT target building block is developed from Matlab/Simulink model.

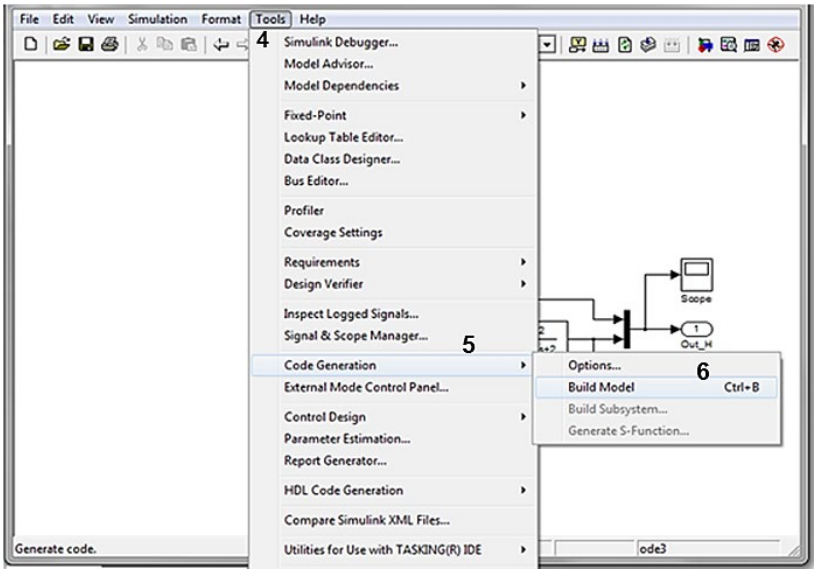

Figure 7.6: **Code generation and TwinCAT target building block from the Simulink platform**

5) The process initiated in Figure 7.6 is executed and recorded in step 7 of Figure 7.7. The building process can be monitored on the Matlab workspace as shown in the following Figure 7.7. The generated TwinCAT module indicated in a red rectangular area in Figure 7.7 can now be used to build the TwinCAT Object Model (TcCOM) module manually with Microsoft Visual Studio in a TwnCAT environment.

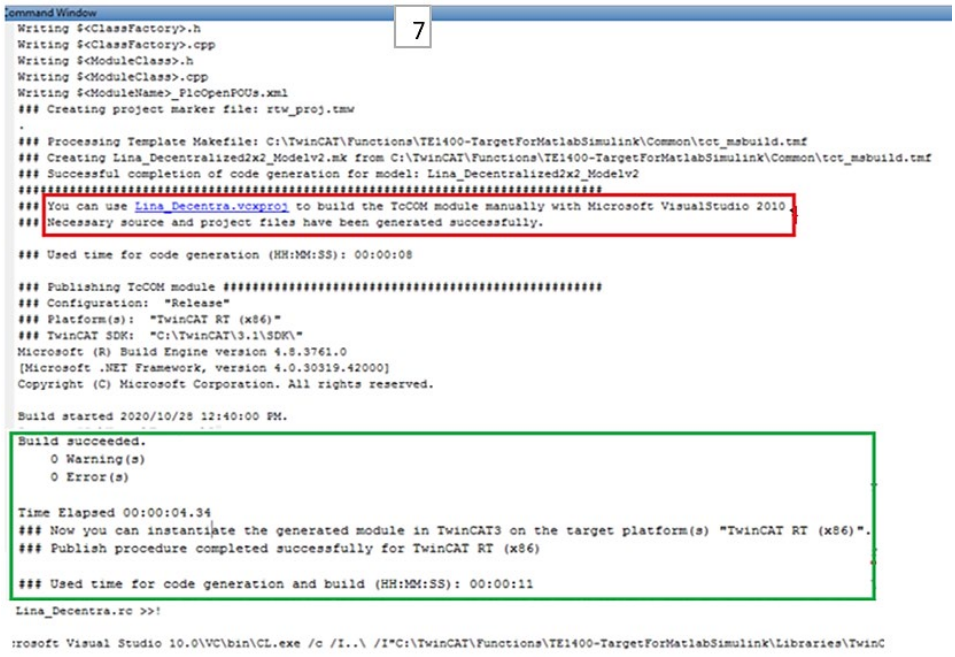

Figure 7.7: **Snapshot of the Code generated in the Simulink platform**

Building succeeded with no warning and zero errors as indicated in a green rectangular shape. All the model files required for transformation are ready at the end of the build process and may be used in the TwinCAT platform.

This code generator is used by the TwinCAT Target for MATLAB/Simulink. A TwinCAT Object Model known as TcCOM is built with the input and output terminals of the Simulink model if the code generator is configured correctly with TwinCAT Target. In the TwinCAT 3 development environment, this module class can be instantiated (TC3 XAE). If necessary, the module instance can be modified in the TC3 XAE. The module is executed in real-time once the TC3 runtime has been launched and may thus be integrated into a real-world control system machine. The application of TwinCAT 3 includes Real-time simulation, Rapid Control Prototyping, SiL (software-in-the-loop) simulation, Hardware in the Loop (HiL) simulation, and Model-based monitoring. The following section explains all the necessary steps for the implementation of the closed-loop column flotation system in the runtime PLC module.

7.4 Runtime implementation using Beckhoff TwinCAT 3.1 Software for Automation Technology

The TwinCAT runtime components are available for different platforms as presented by the TwinCAT 3 performance class of a Beckhoff PC and depend on the configuration and the technical data of the PC including the processor. In combination with the TwinCAT automation software, the CX Embedded PC has become powerful and compatible with IEC 61131-3 standard PLC. The greatest motivation behind this software is the integration of PLC, Motion Control (MC), and Human Machine Interface (HMI), in one software and on one CPU. The advantages are reduced interface complexity, PC-based control technology as an ‘open’ control concept, and one project storage place for hardware and software. The following sub-sections present how TwinCAT automation software platforms are used to develop the objectives of this research.

7.4.1 TwinCAT 3 Engineering

TwinCAT 3 is divided into components known as TwinCAT 3 engineering and TwinCAT 3 runtime. The TwinCAT 3 engineering components enable the configuration, programming, and debugging of applications. The TwinCAT 3 runtime consists of further components such as basic components and functions as shown in Figure 7.8.

Figure 7.8: Different platforms of TwinCAT 3 (www.beckhoff.com/CX5000)

TwinCAT Standard simply uses Visual Studio's foundational element, with all its advantages in terms of handling and connectivity to source code management tools. As the name suggests TwinCAT Integrated itself into Visual Studio. With support for the 3rd edition of IEC 61131-3, the C/C++, VB.NET programming languages, and links to Matlab/Simulink in Microsoft Visual Studio, it is possible to program automation objects in parallel. Independent of the language in which they were developed, the modules generated can exchange data and call each other. The MATLAB/Simulink connection allows TwinCAT modules created as models in the Simulink simulation environment to be executed.

The TwinCAT System Manager has been integrated into the development environment. To configure, parameterize, program, and troubleshoot automation devices, only one software is necessary, see Appendix C (TwinCAT transport layer and TwinCAT Module), and follow Figure 7.9 for possible TwinCAT runtime program modules in different languages.

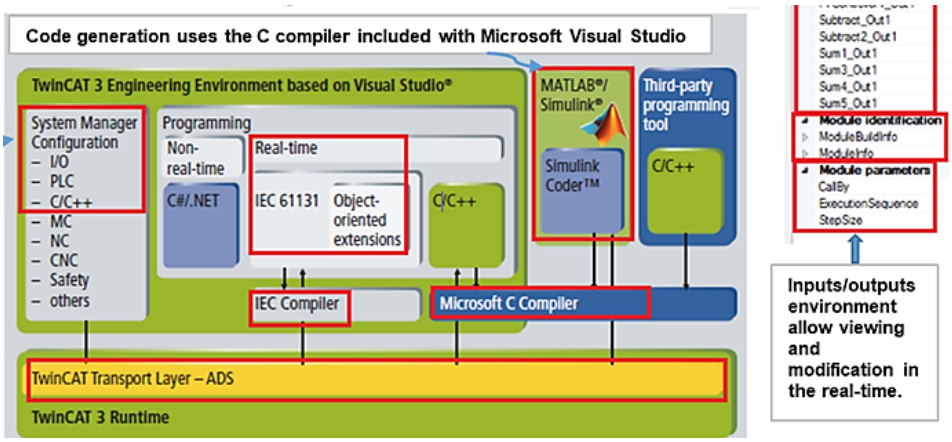

Figure 7.9: *eXtended Automation Engineering (XAE):* Language Support

The selected interfacing type displays the parameters and variables in TwinCAT 3's graphic interface, allowing real-time viewing and modification in runtime mode, as shown in Figure 7.9 above. The illustration of how each of the programming languages can be flexibly used to accomplish the eXtended Automation Engineering is presented in Appendix D. Figure 7.10 presents the process followed for successful real-time implementation of the controlled process using the TwinCAT 3 software and the Beckoff PLC hardware.

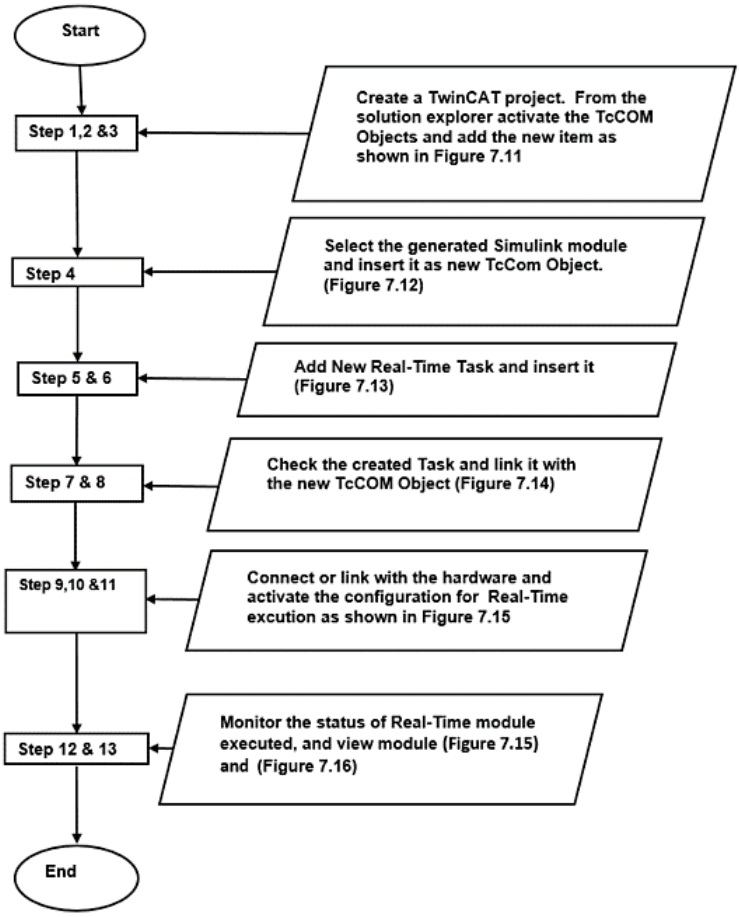

Figure 7.10: **The flow chart block diagram that represents the overall implementation of the closed-loop system under study**

7.4.2 TwinCAT environment

This section presents the steps applied within the TwinCAT environment for real-time purposes. The visual studio platform will pop up to create a new TwinCAT project when opening the TwinCAT Engineering platform (XAE). Create and save the project, step 1 in Figure 7.11 shows created and saved project. Now the solution explorer window pops up as shown in step 2 of Figure 7.11. Then through activation of the TcCOM Objects new item is added as shown in step 3 of Figure 7.11.

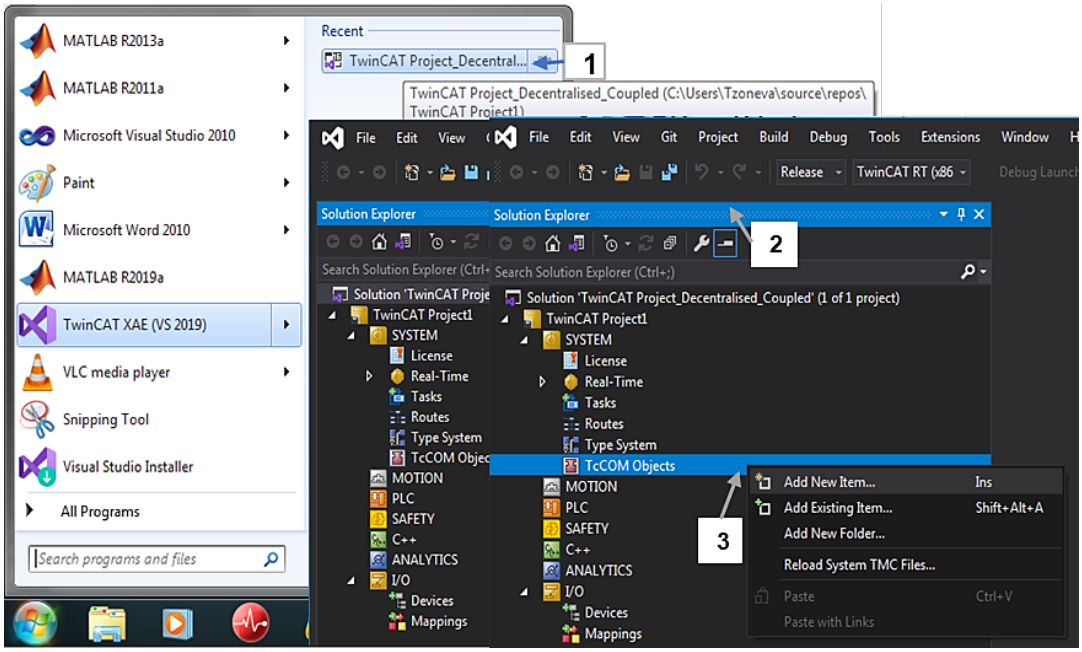

Figure 7.11: Create a new TwinCAT project

As a result, the created Simulink module is selected with its default defaults. The Simulink module was integrated with TwinCAT 3.1 via code generation, selecting and inserting the new Objects as shown in Figure 7.12. In step 4 of Figure 7.12, select the generated Simulink module and press OK to insert TcCom Object.

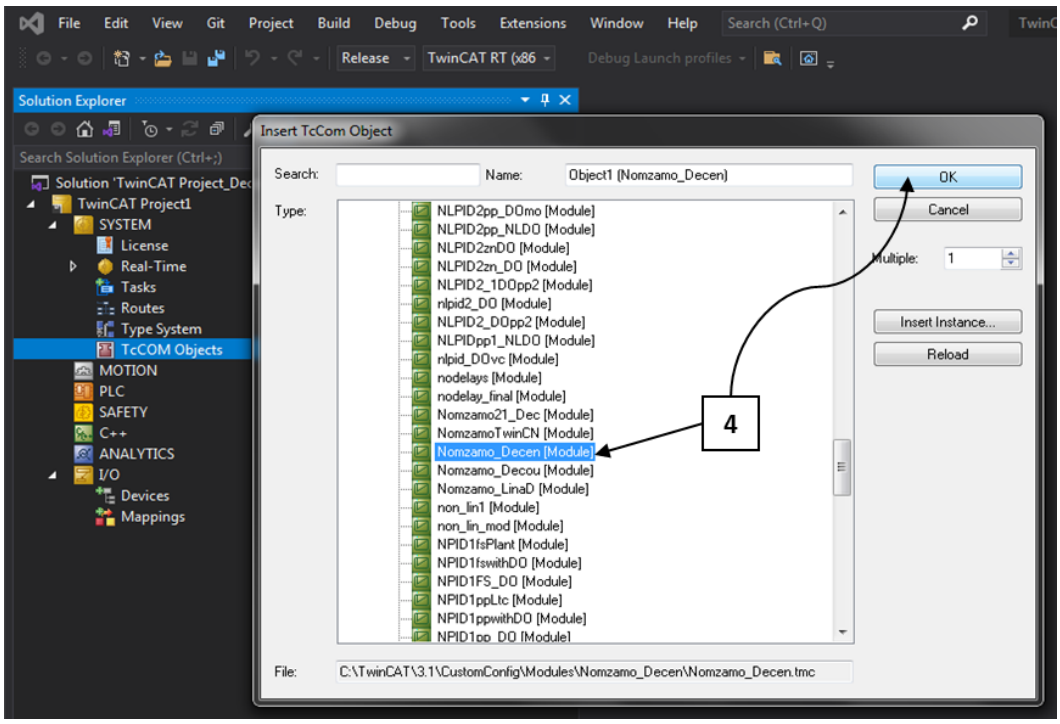

Figure 7.12: Adding new TcCOM object

In Figure 7.12 the module is added successfully, and it will then appear under TcCOM Objects. The next step is to create a Task and link it with the newly added Object. To

add a task right-click the Taskbar under the Real-Time tab and select Add New Item. Upon selection of Add New Item, an Insert Taskbar window will pop up, as shown in step 6 of Figure 7.13. Multicore Central Processing Unit (CPU) is supported by TwinCAT 3 XAR, which allows individual tasks to be allocated on the different cores of the CPU. This addition of the task is shown in the following Figure 7.13. Name the task and select OK, then the task will be successfully added as shown in Figure 7.14 step 7.

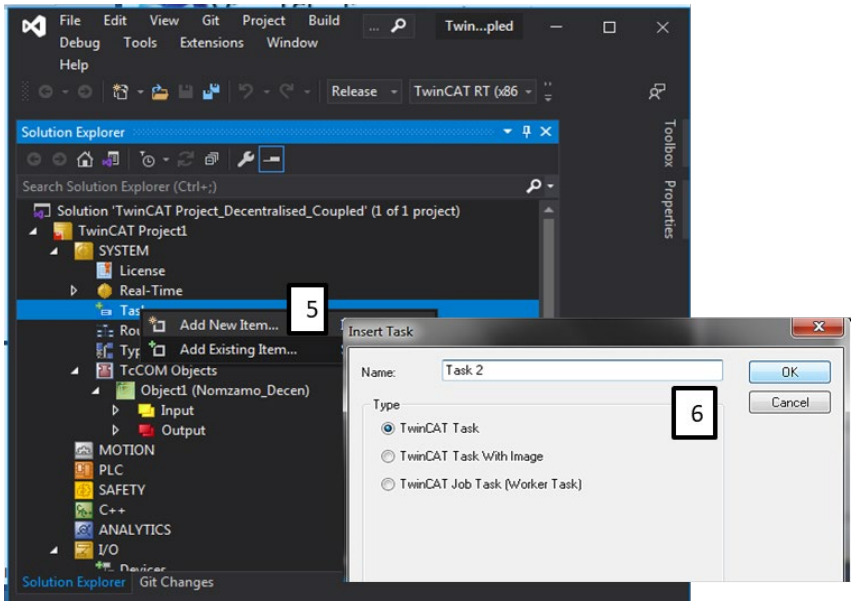

Figure 7.13: Add Task and linkage with the TcCOM object

In Figure 7.13, the real-time task was added, and the added task is shown in step 7 of Figure 7.14. To check this, select the Object node *of the module* and open the tab "*Context*". The resulting table contains the object ID and the object name of the task as shown in Figure 7.14 will pop up. Then browse under results to select the task to be linked with the TcCOM Object as presented in step 8 of Figure 7.14.

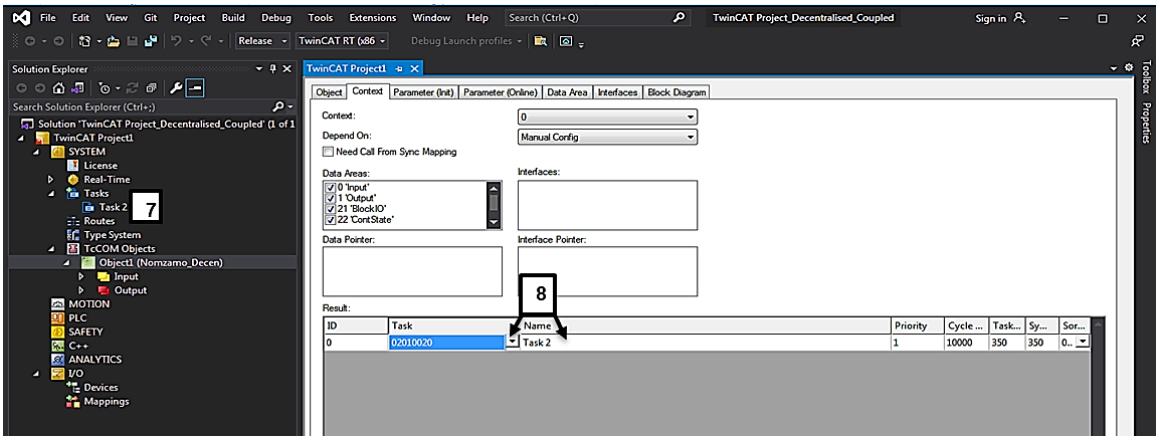

Figure 7.14: Link the TcCOM Object with real-time added Task

The model's configuration is now complete, and it may be used on the target system. Under step 9, browse the targeted scheme or device used for implementation. The PLC (target system) indicated using a red rectangle was selected as shown in the following Figure 7.15. Following the selection of the target system, step 10 in Figure 7.15 is used to activate the configuration for executing the created module on the target system. Step 11 of Figure 7.15 shows the physical appearance of the PLC hardware used for hardware implementation.

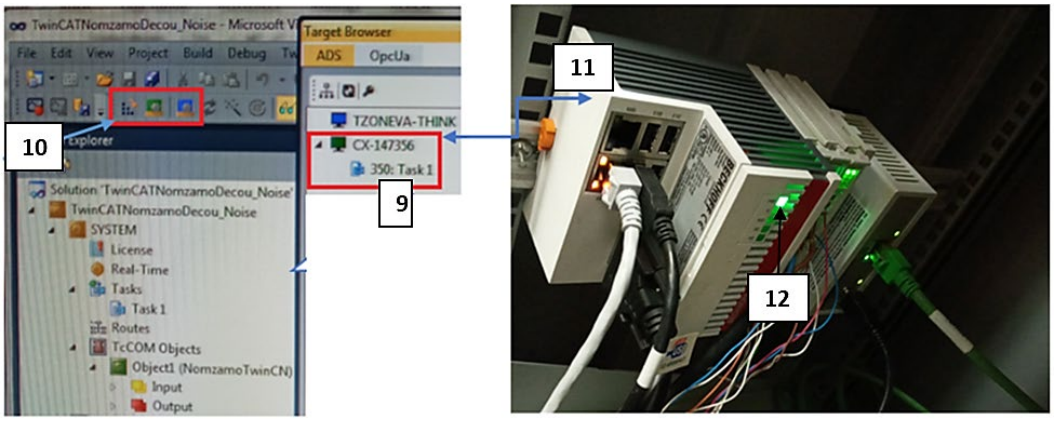

Figure 7.15: Linking the TcCOM object to the local PLC and activating the configuration

After activating the configuration on the target system, the TwinCAT system is launched, and the target status icon switches from blue to green, indicating that the system is functioning in real time, as illustrated in step 12.

The block diagram tab is selected within the software to display the system's function block diagram in run mode as shown in the following Figure 7.16.

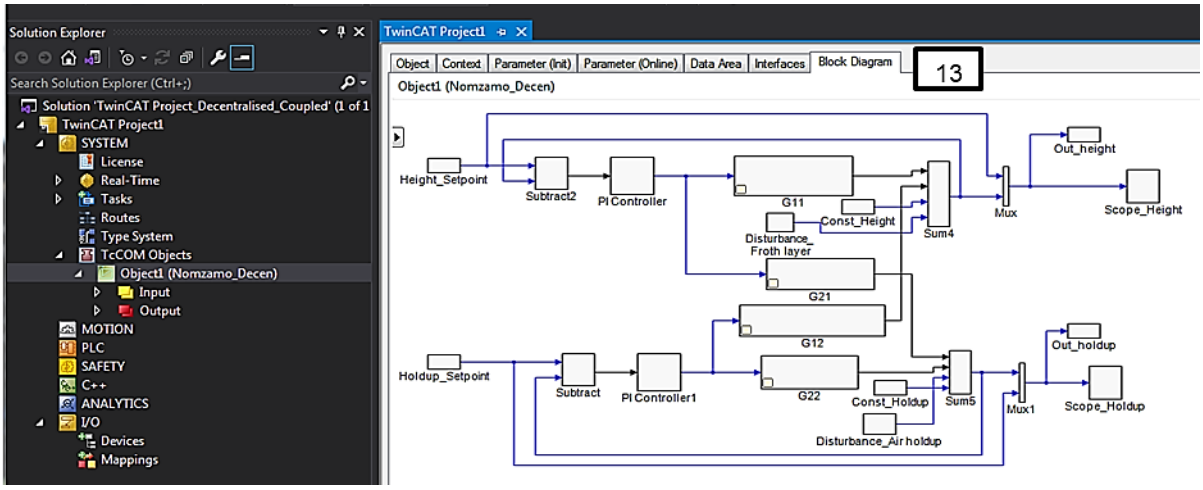

Figure 7.16: eXtended Automation Engineering (XAE): Language Support

The results of the system executed in an "*online*" environment or while the system status is activated are presented in the following section.

7.4.3 The Beckhoff CX5020 PLC Communication with Ethernet for real-time control

A communication connection between the PLC and the embedded PC is necessary to control a synthetic model from the Matlab/Simulink environment with a PLC. The Ethernet/IP communication protocol is used for that purpose. The CX5020 PLC is a real-time platform for executing applications downloaded from the TwinCAT 3.1 development environment using the Ethernet connection platform. Through this connection, real-time communication between the Matlab/Simulink, the TwinCAT 3.1 developed algorithms, and the PLC is provided. Therefore, the TwinCAT function block is online, it is now necessary to measure the real-time results using the *TwinCAT measurement project*. The following subsection clarifies how to create or import the system's output results from the PLC. Inserting the set-point values is achieved in run mode using the data input tab and then they are downloaded into the hardware to effectively make online changes on the PLC hardware in-loop scheme.

7.4.4 TwinCAT Measurement project

This section discusses the steps used to build a TwinCAT measurement project. The purpose of creating this measurement project is to be able to import or read the result from the PLC. Figure 7.17 presents the steps taken for the results to be successfully exported from the PLC and shown in the TwinCAT software environment.

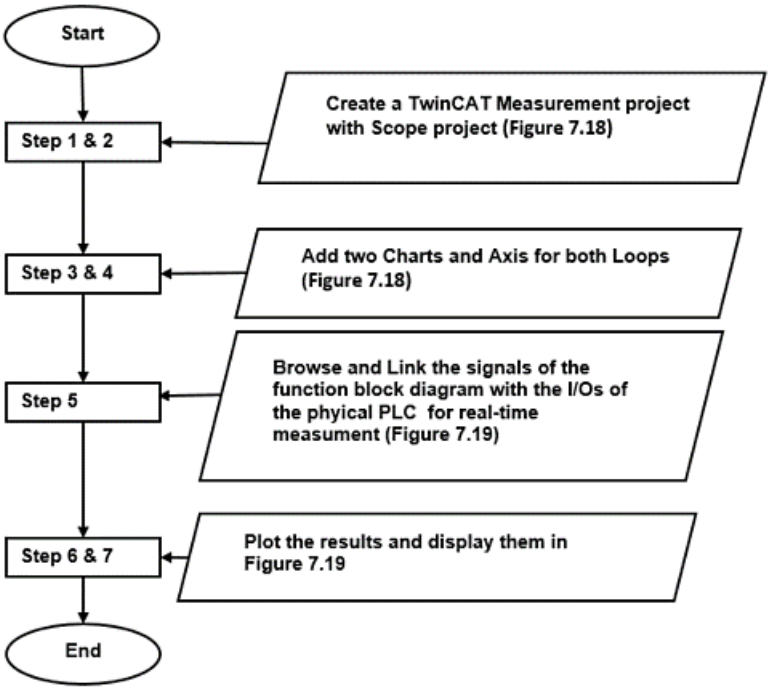

Figure 7.17: **Block diagram flow chart for real-time TwinCAT measurement implementation**

The real-time result presented throughout this Chapter are all measured via the process explained in Figure 7.18 below. To measure the online results, create a TwinCAT Measurement project, and add Scope Project as shown in steps 1 and step 2 of Figure 7.18. The Scope Project in step 2 is required to record the results of the system as imported from the hardware used for this implementation. Add a chart for each loop as shown in steps 3 and step 4 of Figure 7.18. Chart 1 displays measurements of the air holdup and Chart 2 displays measurements of the froth layer height.

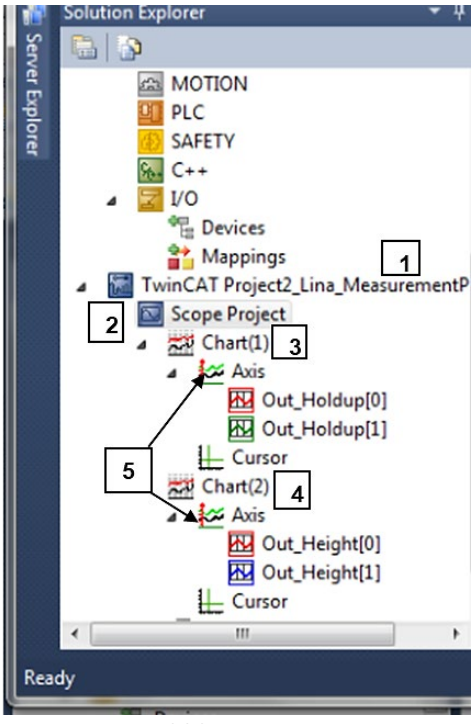

Figure 7.18: Real-time TwinCAT Measurement Project

To import the run-time results successfully link the Inputs and Output (I/O) of the PLC hardware and software, this action is only possible if the communication with the PLC is completed. Then the result of the implemented Task is displayed by the charts as shown in Figure 7.19 steps 6 and 7. Chart 1 indicated by an orange rectangle displays measurements of the air holdup and Chart 2 indicated by a purple rectangle displays measurements of the froth layer height.

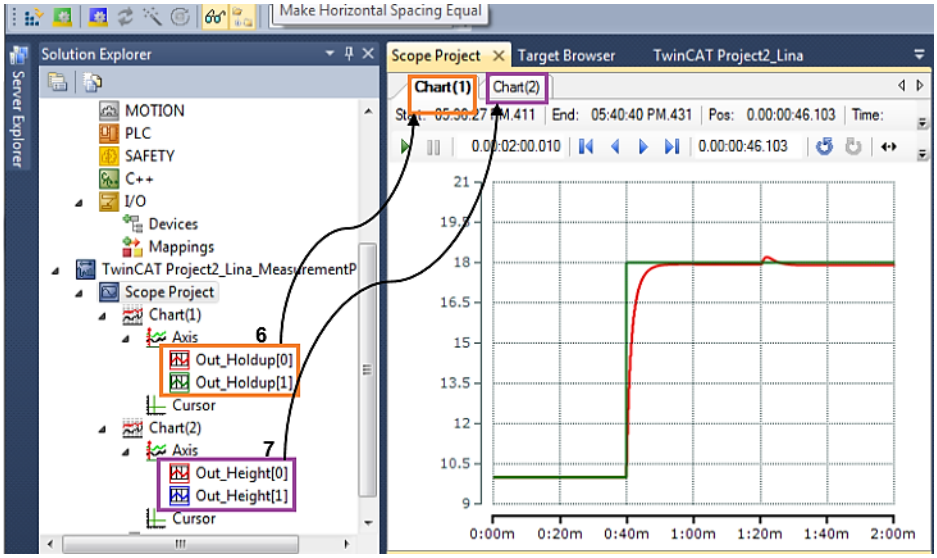

Figure 7.19: Real-time TwinCAT Measurement Project

The number of Charts to be added depends on how many variables are controlled or measured. For the 2x2 flotation system implemented in this study, it is enough to create or add two charts as shown in step 3 and step 4 of Figure 7.18. The TwinCAT measurement project section as indicated in Figure 7.18 is created to measure the real-time results from the PLC. The Axis within chart 1 presents air holdup results and the Axis within Chart 2 presents the online results of the froth layer height loop. Steps 6 and 7 of Figure 7.19 is to record the online results throughout this thesis. The following section executes the steps discussed in sections 7.3 and 7.4.

7.5 Real-time implementation of the closed-loop column flotation system

This section is based on the real-time implementation of the decentralized coupled and decoupled control system of the column flotation. The key to this section is to show the real-time results of the closed-loop control systems for the 2x2 model of the flotation plant under study as developed in Chapters 5 and Chapter 6 respectively. This section shows the transformed model deployed to the Beckhoff CX5020 Programmable Logic Controller (PLC) for real-time implementation under various set-point circumstances

and disturbances, using the TwinCAT 3.1 software environment. The results presented are used to demonstrate how well the developed controllers operate in real-time scenarios. First, the decentralized coupled system controllers' performance is evaluated. Then the performances of the decoupled decentralized controllers are tested and presented, and finally, the comparison of the two implemented methods versus the simulation results from Matlab is presented in various Tables.

To achieve the real-time implementation process followed by the program, and import the results from the PLC, the procedure presented in section 7.4 is followed. Figure 7.20 is a PLC presentation.

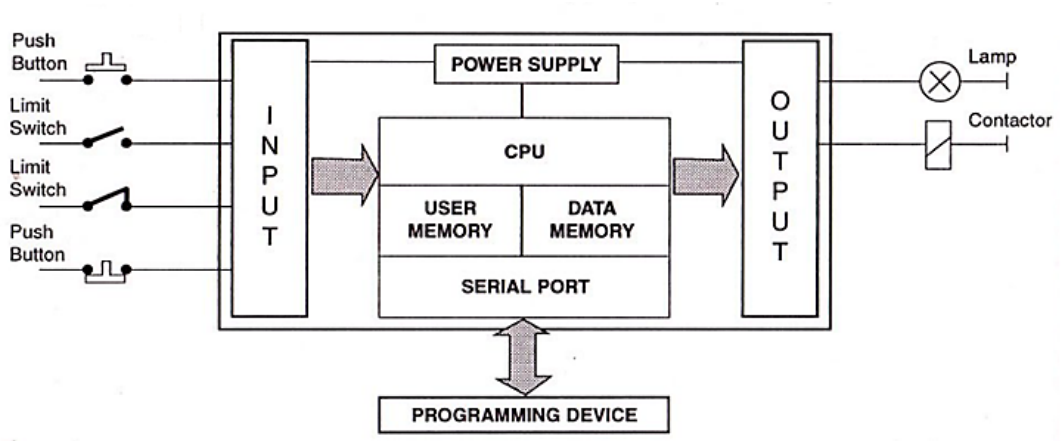

Figure 7.20: **Real-time TwinCAT Measurement Project**

Code configuration and calibration process had to be done so that the values read on the physical PLC followed the conditions prepared from the TwinCAT simulation environment. Once the PLC (external physical device) receives the variables, they go through the programmed logic and a decision is made and then sent back to TwinCAT run-time environment. All of the above is done while the simulation is running in real time. Figure 7.21 is a developed setup used for the implementation. The following components were used to develop the laboratory testbed:

- Programmable Logic Controllers (PLC)
- Power supply
- Industrial Computer
- Personal Computer x 1
- Matlab & TwinCat software tools

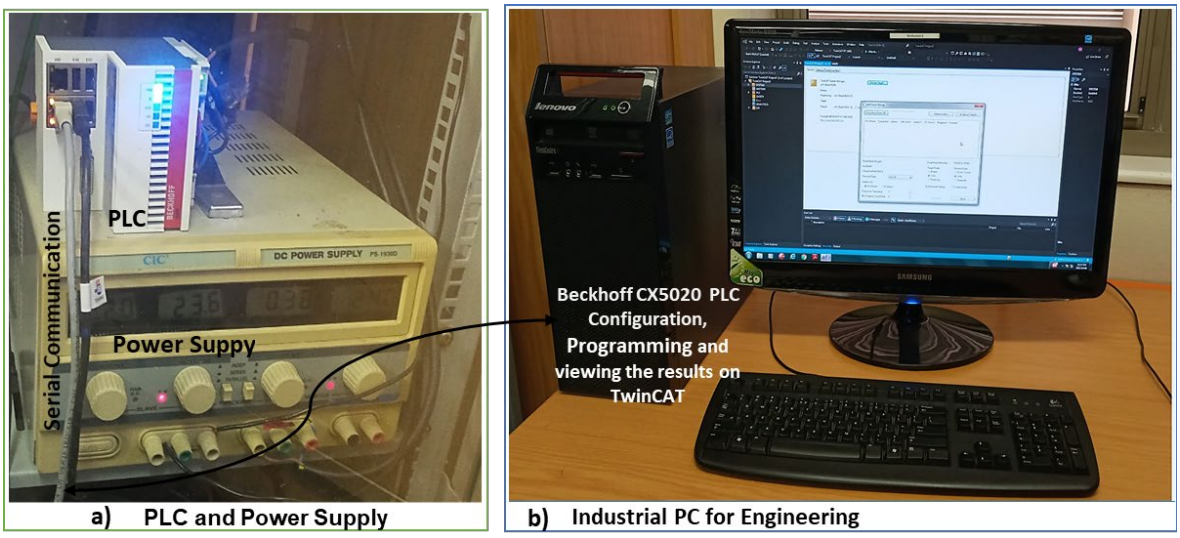

Figure 7.21: Implementation Testbed Scheme

Figure 7.21 (a) shows the power supply used to supply 24V power to the PLC. To be found on top of the power supply is the Programmable Logic Controller used to achieve hardware implementation for this project. The PLC is used as a physical control device to control the flotation system. All parameter setup and modifications are made on the device via the TwinCAT software and then sent or downloaded into the PLC using serial communication.

The investigations of real-time setpoint tracking control for both the froth layer height and air holdup are made respectively. Various responses are presented under this section with sub-section 7.5.1 for the decentralized coupled system and sub-section 7.5.2 for the decentralized decoupled system. The setpoint changes or different input signals are applied as covered in Chapter 5 and Chapter 6, the only difference now is that all the changes are made online as the implementation is in run mode.

7.5.1 A decentralized coupled system using closed-loop control

This section is based on the real-time implementation of the decentralized coupled flotation system model. The real-time execution process explained in sections 7.3 and 7.4 is followed in this investigation. The PLC configuration process is performed via the TwinCAT software environment as discussed in section 7.4. The set-point parameters are set and adjusted via model-specific parameters which are found in the property table of the block diagram, under the TwinCAT measurements project using the created test points for all scope input/output signals as discussed in section 7.4.4. Figure 7.22 presents the closed-loop function block model in TwinCAT environments.

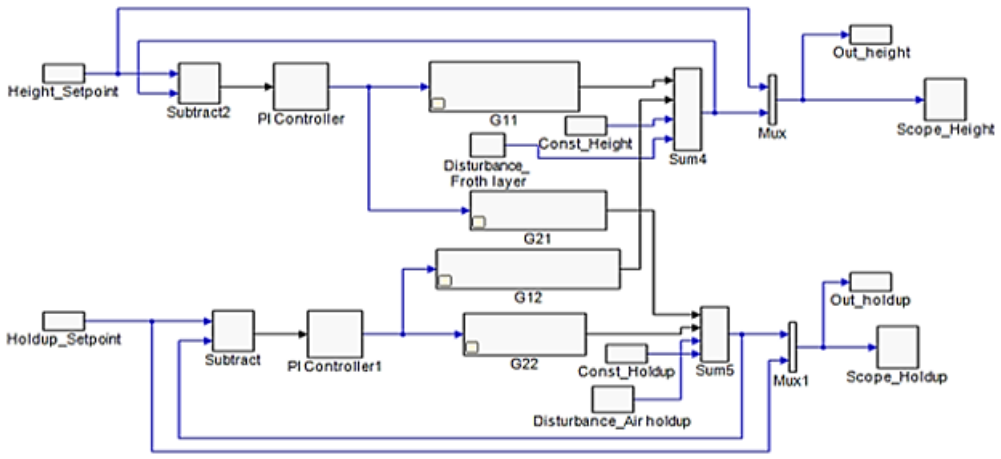

Figure 7.22: Decentralised TwinCAT real-time model

Figure 7.22 displays the TwinCAT 3 function block modules for the modified Simulink closed-loop multivariable process using the decentralized coupled approach. Through run-time execution, it is proven that there is a one-to-one correspondence of function blocks between Simulink and TwinCAT 3.1 since the data and parameter connections are the same in both systems. The following are the real-time implemented results from the investigations and experiments done for the decentralized coupled control scheme.

7.5.1.1 Runtime set-point tracking control for the decentralized closed-loop system

The case studies below are based on the run-time or online set-point tracking investigations for various step responses of the decentralized coupled model when the set-point is varied as presented in the following Table 7.1.

Table 7.1: Different Case Studies Implemented in Beckhoff PLC CX5020

Case study Set-points	Decoupled Plant with PI controller
	Froth Layer Height and Air holdup
h = 40-60(cm) ε_g =10-18(%)	Launch the process by setting the set point of the Air holdup (ε_g) to start at 10% and ends at 18%, while the set point of the Froth layer height (h) starts at 40 cm and ends at 60 cm.
h= 40-60(cm) ε_g =12-20-15(%)	The set-point of Air holdup is increased to observe the closed-loop behaviour of the system. While, the Froth layer height is kept at the same set point, to only investigate if the changes applied in one loop which is the Air holdup will influence that of the Froth layer height loop.
h=50-70-60(cm) ε_g =10-18(%)	The set-point of the Froth layer height is changed from the step to a pulse signal, this is done to observe the closed-loop behaviour of the system. The set-point of the Air holdup is returned to its initial value to only investigate the influence of the changes made in the froth height.
h=80-60-80(cm) ε_g = 4-5-4 (%)	Both set-points of the Air holdup and Froth layer height are changed, to observe the system's operational behaviour in case of unusual changes occur in the system. This case is done to observe the closed-loop behaviour of the Froth layer height and the Air holdup in abnormal conditions.

Different set-point changes were applied on the Property table of the function block diagram, and the results are presented for each case from Figure 7.23 up to Figure 7.26.

Case study 1: Start the process

To start the process, the air is injected at the bottom of the column. In case 1, as the amount of air is applied, the set-point of the air holdup (ε_g) in the collection zone is set to start from 10% - 18 %. At the same time, the set point of the Froth layer height (h) in the cleaning zone is set to start at start 40cm to 60cm. The designed controllers are implemented in the PLC for the control of the closed-loop system with the hardware environment. Figure 7.23 presents the result acquired online while the whole system is in runtime mode.

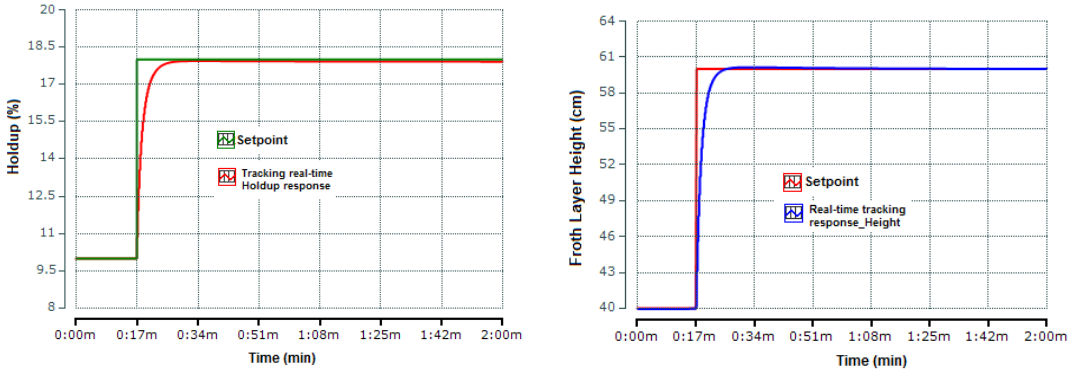

Figure 7.23: **Case 1: Real-time results of the Froth Layer Height and Air Holdup system**

With the observations of the results shown above, both reactions of the holdup and the Froth layer height have successfully tracked the desired input signal (Set-point). For further investigations, the set-points are changed in runtime mode, proving the possibilities of industrial or real-life usage of this experimentation.

Case study 2: Air holdup is changed and Froth layer height remains the same

In Case 2 the set-point changes are applied on the holdup loop to a pulse signal, and the set-point of the froth layer height is kept as in Case 1 with a step signal of 60 cm. When the holdup set point is dropped or changed from 20% to 15% at 1.08 minutes, the change created an overshoot on the froth layer height loop as presented in Figure 7.24.

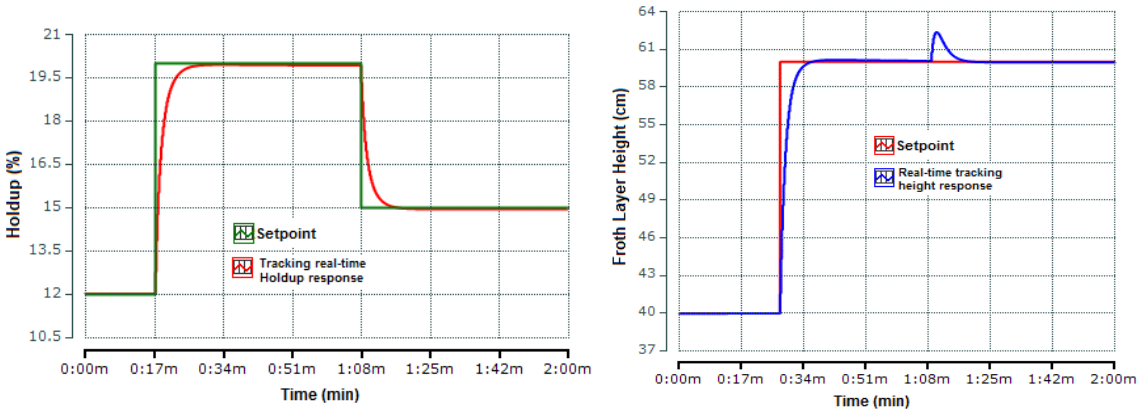

Figure 7.24: Case 2: Real-time results of the Froth Layer Height and Air Holdup system

In Figure 7.24 shown above, the response from the implemented closed-loop system successfully tracked both set-points for the two loops, which are the holdup and froth layer height respectively. Therefore, it is important to consider the amount of variation implemented at a time or the importance of the progressive variety of small changes in a flotation system.

Case study 3: Air holdup remains the same and Froth layer height is changed

The set-point of the Froth layer is changed from a step of 40 cm-60 cm to a pulse signal of 50 cm to 70 cm and from 70 to 60 cm. The set point for the holdup is taken back to the step signal as shown in Figure 7.25. When the set-point of the froth layer decreases from 70cm to 60cm at 1.20 minutes, the change created a small overshoot on the holdup loop as presented in Figure 7.25. This shows that dropping the froth layer height on the cleaning zone does affect the holdup on the collection zone.

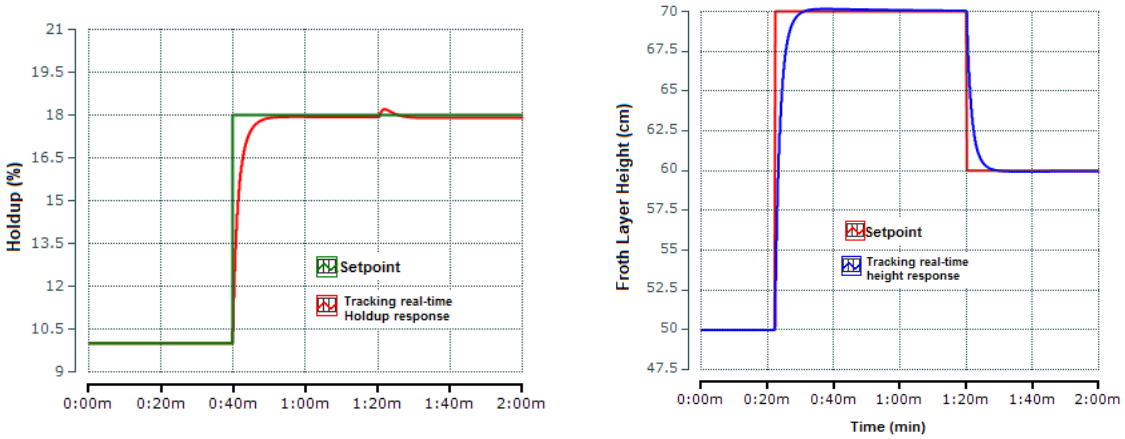

Figure 7.25: Case 3: Real-time results of the Froth Layer Height and Air Holdup system

Case study 4: Same time Regulation of Froth layer height and Air holdup

In case 4, the set-point changes are applied in both loops collection and cleaning zones (Holdup loop and Froth layer height loop) at the same time. The froth layer starts at 80cm and is decreased to 60 cm at 0.34 minutes, while the set-point of the holdup is set from 4% and increases to 5% at 0.34 minutes.

The results in Figure 7.26 indicate that when a sudden drop occurs on the froth layer height at 0.34 minutes, the change created an overshoot on the holdup response as presented in Figure 7.26. A set-point increase is applied on the froth layer height loop at 1.2 minutes, while a set-point decrease for the holdup is applied at 1.2 minutes also. Both zones followed the set-point changes, but the response of the holdup system in the collection zone is having a big overshoot as presented in Figure 7.26.

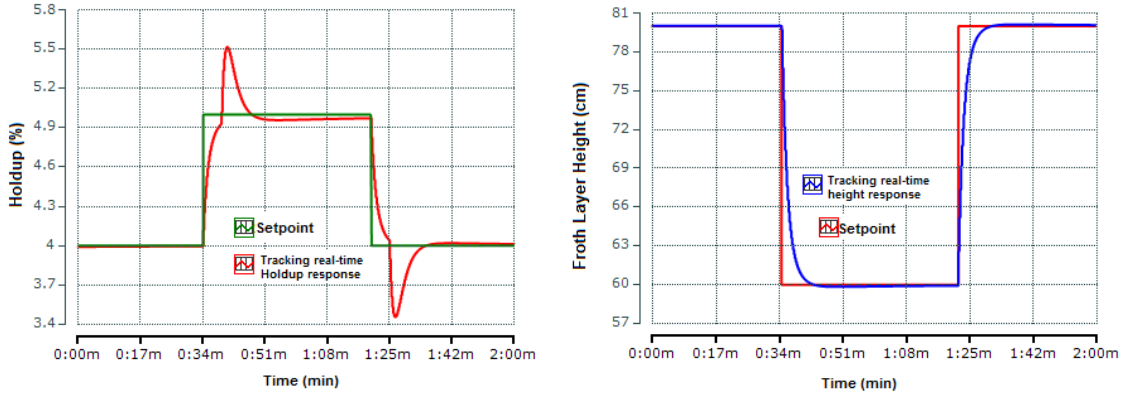

Figure 7.26: **Case 4: Real-time results of the Air Holdup and Froth Layer Height system**

This means although a decentralized controller is used for this flotation system, loop interactions still exist within this system. Hence, the significant online changes in the cleaning zone affect the collection zone reaction.

Summarising the above results

Investigations based on the online set-point tracking are conducted by applying different set-point changes in runtime mode. Runtime implementation results are shown in Figure 7.23 up to Figure 7.26. As analysed for each case study, the results show successfully set-point tracking indices apart from overshoots, as shown in case 2 and case 4. Therefore, the control of froth layer height and holdup loop is implemented successfully using TwinCAT 3 functional blocks and then downloaded to the Beckhoff CX5020 PLC for runtime implementation. The performance indices for the closed-loop system under decentralized control are similar when compared to the results provided in Chapter 5. The real-time characteristics behaviour of the decentralized coupled flotation system is presented in Table 7.2 below:

Table 7.2: Runtime characteristics of the decentralized Froth Layer Height and the Air Holdup Closed-loop system

Case study	Froth layer height performance indices				Air-holdup performance indices			
	Loop	Rise time (s)	Settling time (s)	Peak overshoot M_P (%)	Loop	Rise time (s)	Settling time (s)	Peak overshoot M_P (%)
1	Height	3	13.2	0	Holdup	5.1	15.3	0
2	Height	3	70	2	Holdup	5.1	70	0
3	Height	3	75	0	Holdup	5	72.6	0.3
4	Height	3.8	77.5	0	Holdup	5.1	80.1	0.5

The real-time PLC implementation of the decentralized 2x2 system is completed successfully. Then, the next step focuses on applying the disturbance to the system implementation model under study as simulated in chapter 5. It is also necessary to access how well can the designed controllers deal with the disturbance that is introduced while the system is in run-time mode. The following subsection presents the real-time implementation using the Beckhoff PLC.

7.5.1.2 Validation of the developed controller in a runtime environment

The transformation algorithm presented in section 7.4, is used for the implementation of the closed-loop column flotation algorithms using the Beckhoff PLC for the execution of the decentralized coupled control approach developed in Chapter 5. The aim is to verify the control method's effectiveness under varied disturbances in a hardware runtime environment system. Different disturbances are introduced as indicated in the following Figure 7.27.

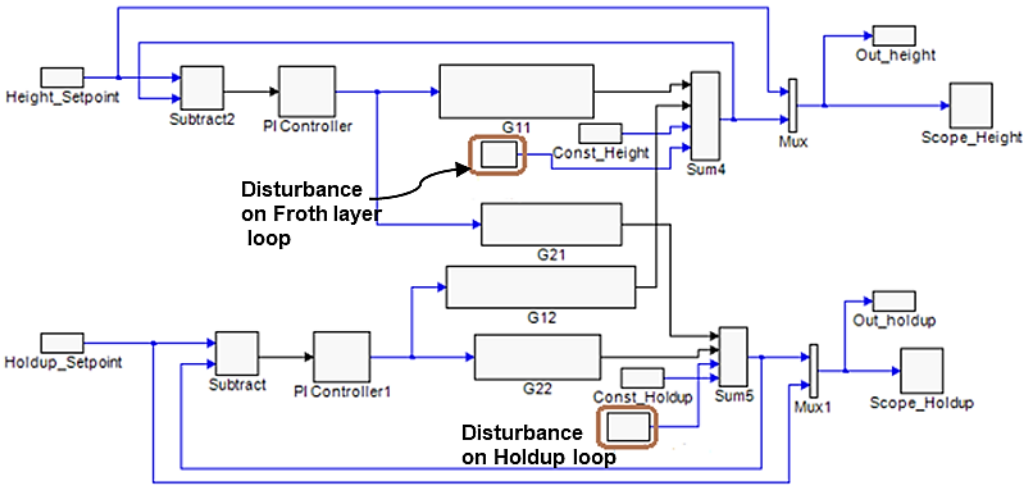

Figure 7.27: Real-time model of the Froth Layer Height and Air Holdup system

The system is disturbed by injecting a noise disturbance. A noise disturbance is injected at the output of the system as illustrated in the Function Block Diagram shown in Figure 7.27. The disturbances are created using a random sequence with an association of time. This is done to investigate the effects of the disturbance when either loop or zones of the system (froth layer height in the cleaning zone and air holdup in the collection zone) are experiencing disturbance at the same time. The real-time results of the froth layer height and the air holdup loop systems under the disturbance are respectively shown in Figure 7.28 up to Figure 7.31 with different case studies.

***Case study 1 F*roth Layer Height**

The behaviour of the designed dynamic control system is evaluated based on different disturbance variables. In this case, the random noise magnitudes are added to the froth layer height loop as a disturbance to the system. The first amount of disturbance applied is $9e^{-5}$ at the froth layer height, and the results are shown in Figure 7.24. Considering the obtained results, it is confirmed that the designed decentralized controller succeeded in keeping decent set-point tracking control under disturbance in a real-time environment. However, in this case, the presence of the disturbance is noticed through little noise within the actuary response.

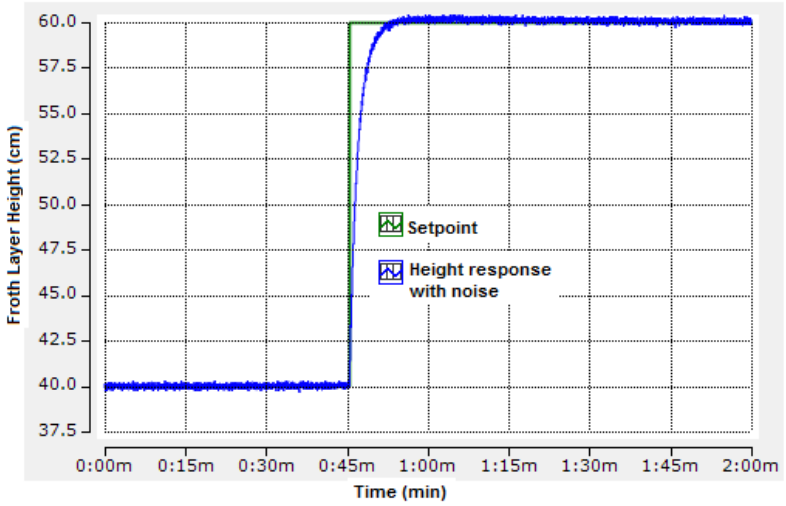

Figure 7.28: Case 1. Real-time results of the Froth Layer Height system under $9e^{-5}$ noise disturbance

***Case study 2 F*roth Layer Height**

In case 2 the applied amount of disturbance is increased to $1e^{-3}$=0.001, this is done to evaluate the effect of noise magnitude in the runtime environment. As may be seen in Figure 7.29, good tracking control is still possible. The reaction becomes noisier as the

amount of the disturbance grows larger. This is relating to what was discovered in Chapter 5.

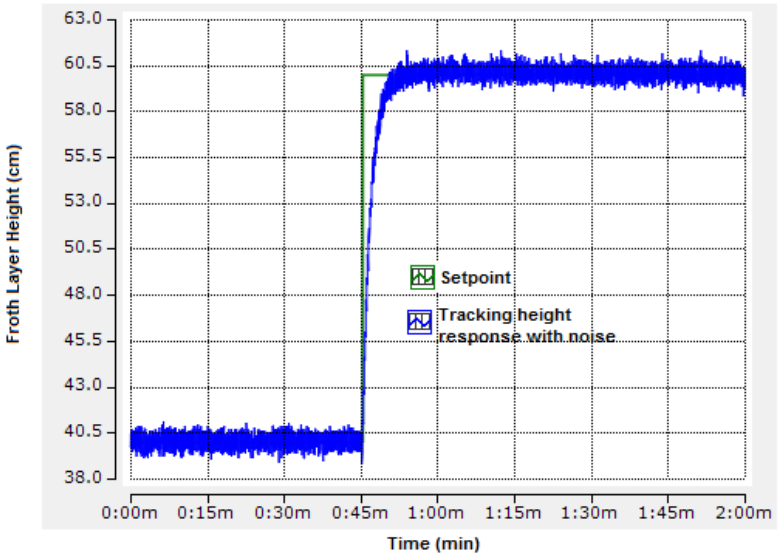

Figure 7.29: Case 2: Real-time results of the Froth Layer Height system under $1e^{-3}$ noise disturbance

From Figure 7.29 notice that the noise presence has increased, this is an indication of the applied disturbance, if the amount of applied disturbance increases the presence of noise at the system's output also increases. The next case considers the effect of disturbances on the Air holdup loop.

Case study 3 Air holdup

A step signal with a set point of 10%-18% is selected for further investigation. In case study 3 the magnitude of the applied disturbance is 0.00009 or $9e^{-5}$, this noise is applied in the air holdup loop of Figure 7.27. The results are shown in Figure 7.30 below. Seeing the obtained results, it is confirmed that the designed decentralized controller has been successful in keeping the selected set-point tracking control under disturbance in a real-time environment. However, the presence of disturbance is indicated by the noise that appears on the output response of the air holdup.

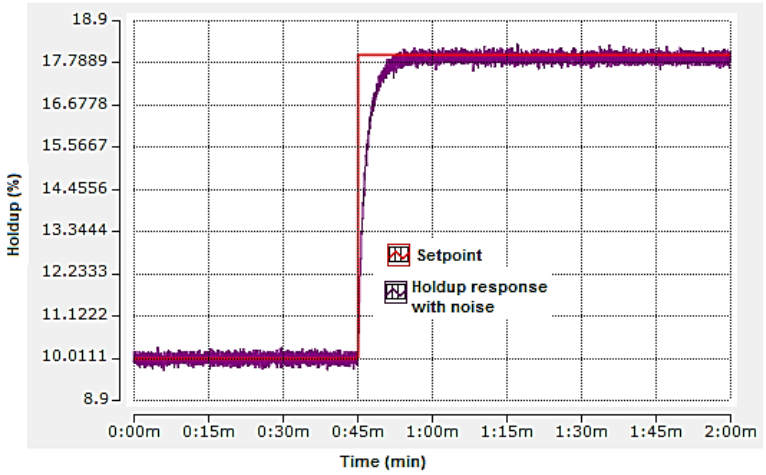

Figure 7.30: Case 3. Real-time results of the Air Holdup system under $9e^{-5}$ noise disturbance

In the next case, a disturbance is varied through adjustment of the noise magnitude applied on the Air holdup loop.

Case study 4 Air holdup

In this case 2, the aim is to evaluate how capable the designed controller is, in tracking the set-point when the applied amount of disturbance is increased to $1e^{-3}$. This online experiment is important to be performed because the flotation column is highly exposed to such industrial disturbance. As seen from the response in Figure 7.31, it is still possible to acquire strong set-point tracking control. The system's reaction grows noisier as the degree of the disturbance increases.

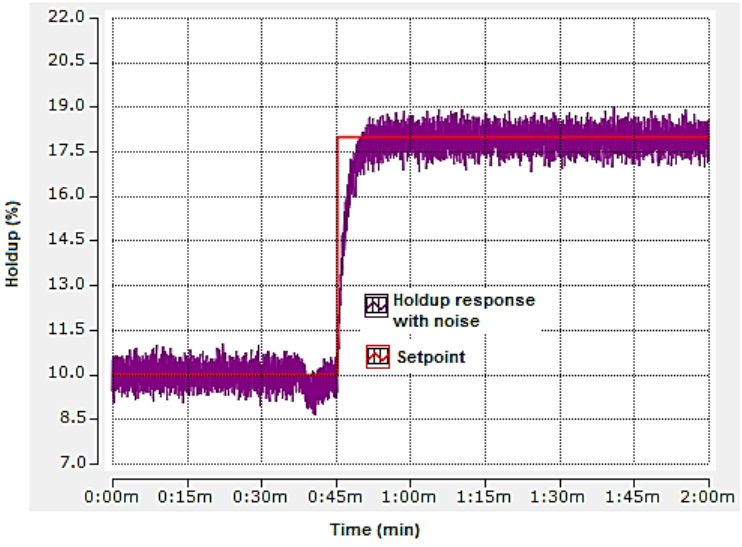

Figure 7.31: Case 1: Real-time results of the Air Holdup under the disturbance of $1e^{-3}$

Analyses of the obtained figures further confirm that the settings of the designed decentralized controller achieve set-point tracking control of the froth layer height and holdup in a real-time environment. Therefore, the designed controller has performed

well, but the more the noise magnitude increases the system response becomes noisily.

7.5.1.3 Summary of the runtime results based on the decentralized-coupled system in comparison with Matlab/Simulink results

The run-time PLC implementation based on decentralization of the flotation process has effectively proven to be one of the strategies that can be used for runtime minimization of the interactions that exist in any Multi-Input Multi-Output (MIMO) system. Figure 7.28 to Figure 7.31 show that the disturbance and noise did not affect the system's ability to maintain any set point in runtime mode. The investigation conducted using Beckhoff PLC as hardware integrated with industrial PC shows that the closed-loop system of the flotation system follows all the set-point variations in real time. Table 7.3 presents the various performance indices of the multivariable system response in runtime mode and compared with the result of the simulations conducted in Matlab/Simulation.

Table 7.3: Characteristics of the decentralized coupled Froth layer height and Air holdup performance

Performance indices of Closed-Loop decentralized-coupled for Column Flotation Process							
Case studies	**Loops**	**Matlab/Simulink**			**TwinCAT PLC real-time**		
		Rise time (s)	**Settling time (s)**	**Peak overshoot M_P (%)**	**Rise time (s)**	**Settling time (s)**	**Peak overshoot M_P (%)**
Case study 1	Height	5.48	18.73	0.36	3	13.2	0
	Air	4.86	18.32	0.03	5.1	15.3	0
Case study 2	Height	5.43	68.32	3.68	3	70	2
	Air	0.77	68.53	0.03	5.1	70	0
Case study 3	Height	1.80;	67.5	0.36	3	75	0
	Air	4.84	64.5	0.21	5	72.6	0.3
Case study 4	Height	0.49;	66.0	0.1	3.8	77.5	0
	Air	0.0044	68.56	0.27	5.1	80.1	0.5

As proven and stated in this section the coupled decentralized control method fails to eliminate the overshoot and keep any set point. Hence, it is important to implement another method that can overcome all the underperformances identified. This research aims at implementing an industrial column flotation process. Having said that, it is important to design a controller that handles nonlinearities and uses methods that can be conveniently used in industry. Therefore, the next section introduces the dynamic decoupling of the decentralized closed-loop control system intending to eliminate the overshoot and keep smooth setpoint tracking. The process of transformation, TwinCAT configuration, and the building of the TwinCAT measurement are arranged as discussed in sections 7.3 and 7.4. Implementation results are presented in the following section.

7.5.2 Decentralized dynamic decoupling closed-loop control transformations and the run-time results

This section demonstrates the implementation of the decentralized dynamic decoupled closed-loop flotation model. The implementation of this system in runtime mode is executed following the process algorithm as explained in sections 7.3 and 7.4. These sections discussed system model configuration, integration with TwinCAT, and Beckhoff PLC real-time implementation respectively. The closed-loop flotation process as developed in Chapter 6 is transformed into TwinCAT 3.1 software environment for hardware implementation. The Programmable Logic Control (PLC) configuration process is performed via TwinCAT software. The Beckhoff CX5020 PLC is then used to deploy the TwinCAT block diagram illustrated in Figure 7.32 for real-time control execution with various set-point conditions and disturbances. The following Figure 7.32 is captured while in real-time mode, hence numeric set-point values are displayed.

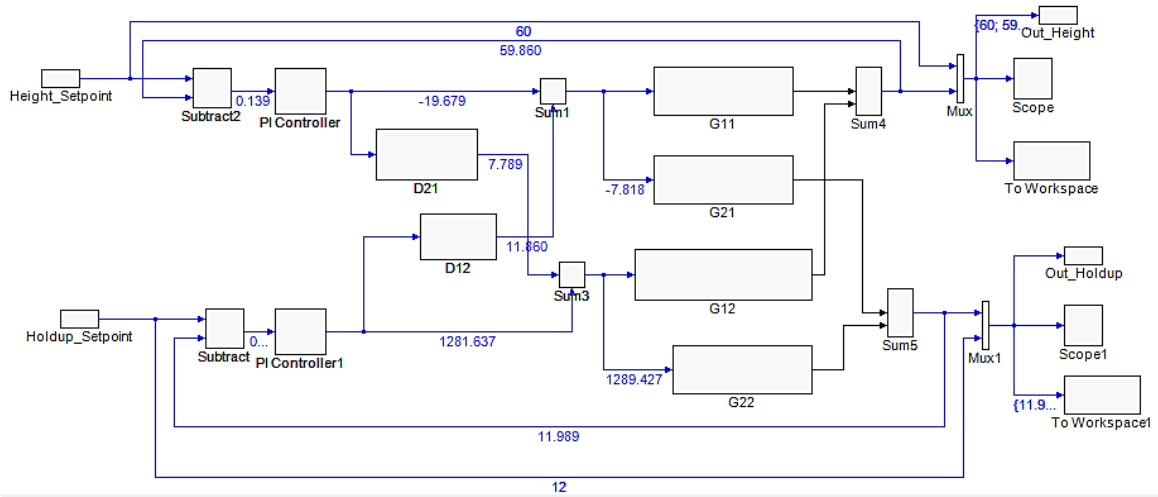

Figure 7.32: TwinCAT 3 function blocks representation of the decentralized dynamic decoupled system model

Because the data and parameter connections are the same in both platforms, there is a one-to-one correspondence of function blocks between Simulink and TwinCAT 3.1, according to the transformation approach. The following are the real-time simulation results from the investigations and experiments done for the dynamic decouple decentralized control scheme.

7.5.2.1 Runtime set-point tracking control for the decentralized dynamic decoupling control

The real-time implementation results from the investigation of the experiment conducted using Beckhoff CX5020 PLC are presented here. The developed control algorithms of the decentralized dynamic decoupled system are used for this implementation. This is done to verify the effectiveness of the control schemes in a real-time environment.

Several case studies shown below are based on online set-point tracking investigations for various set-point changes as defined in Table 7.1.

The performance of the flotation system under the designed dynamic decoupled control in a real-time environment is shown in Figure 7.33 to Figure 7.36.

Case study 1: Start the process

An investigation for setpoint tracking for both air holdup and froth layer height is conducted. The air is injected at the bottom of the column, and the set-point of the air holdup (ε_g) in the collection zone is set to start from 10% and increase to 18 % at 0.17 min. At the same time, the set-point of the Froth layer height (h) in the cleaning zone is set to start at start 40cm from 0 to 0.17 min and increase to 60cm from 0.17 to 2 minutes. As seen in Figure 7.33, the designed dynamic decoupled controllers can track the set point in runtime mode. Figure 7.33 presents the result acquired online while the whole system is in runtime mode.

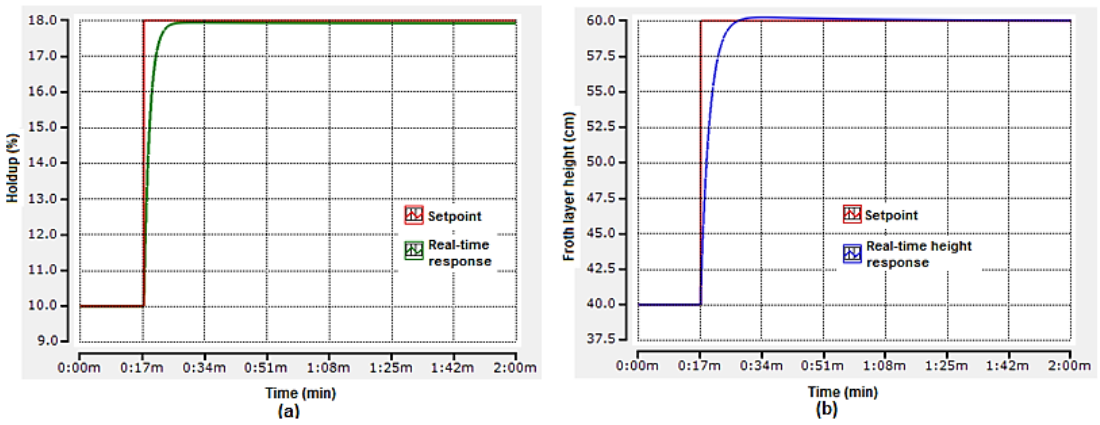

Figure 7.33: Case 1: Real-time results of the Froth Layer Height and Air Holdup system

In Case study 1 shown above the holdup is set to start at 10% and increase to 18% during run-time at 0.17 minutes (10.2s) as presented in Figure 7.33(a). Figure 7.33(b) presents the results of the system when the set-point of the froth layer height is set to start from 40 cm and increase to 60 cm at 0.17 minutes in a real-time environment.

Case study 2: Air holdup is changed and Froth layer height remains the same

In Figure 7.34 (b) the froth layer height is kept at the same set point as Figure 7.33 (b), on the other hand, to investigate the influence of air holdup set-point changes on the two loops (Froth layer height and holdup), the holdup step is changed to a pulse signal as presented in Figure 7.34 (a). As it can be noted on the real-time implemented results as shown below, the reduction of the amount of air applied on the collection zone (air holdup) at time 1.08 minutes, did not disturb or interrupt the behaviour of the system. This means the interactions within the system are eliminated, through the decoupling process.

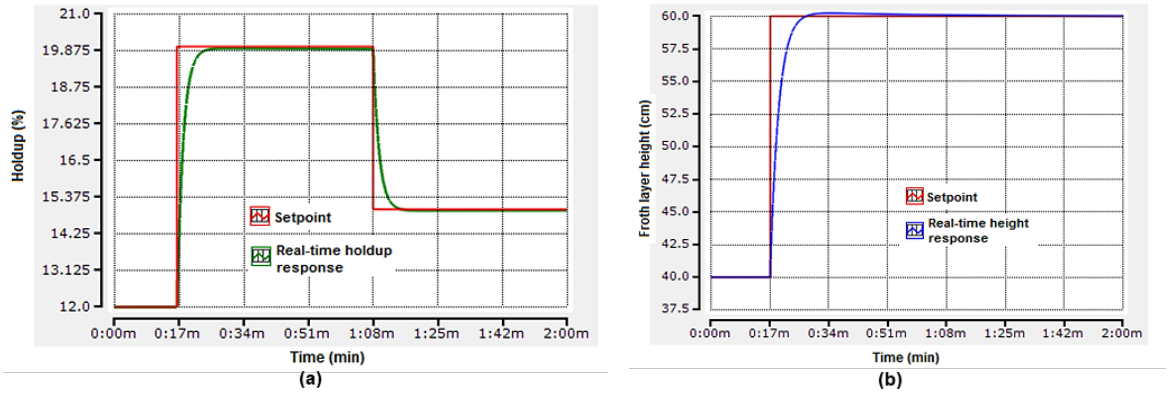

Figure 7.34: **Case 2: Real-time results of the Froth Layer Height and Air Holdup system**

Now, the next point is to adjust or change the set-point froth layer height and keep the original amount of air holdup.

Case study 3: Air holdup remains the same and Froth layer height is changed

Case **study** 3 in Figure 7.35 established the set-point of the froth layer height to start at 50 cm, the set-point change is applied at 0.17 minutes to move the signal from 50 cm to 70 cm and decreased to 60 cm at 1.08 cm, while the holdup is set to start at 10% and increased to 18% at 0.17 minutes. In real life, this is exercised by collecting a huge amount of mineral particles from the collection zone that would increase the froth layer. Then for Figure 7.35 (b), the drop of froth layer height at 1.08 min is made possible by adding wash water on the top of the column.

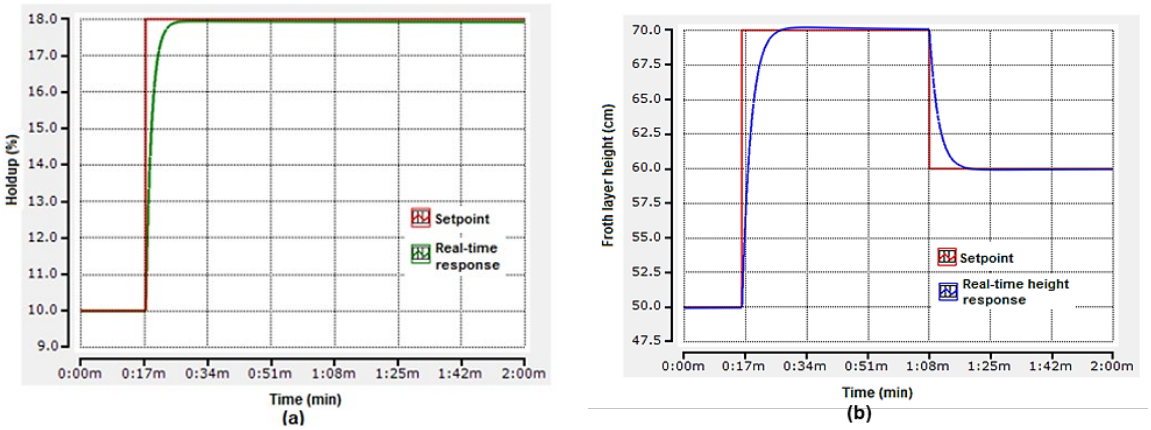

Figure 7.35: Case 3: Real-time results of the Layer Height and Holdup

The next Case study 4 in Figure 7.36 presents the results of the system when the set-point of the holdup and froth layer height are both changed at the same time.

Case study 4: Same time Regulation of Froth layer height and Air holdup

In Figure 7.36 below both set-points of the Froth layer height and Air holdup altered their states at the same time, to observe the system's operational behaviour. The froth layer height in Figure 7.36 (b) is 80 cm, while the applied holdup is 4%. Abnormal changes are applied at 0.17 minutes, where the set-point of the layer height is dropped to 60cm. In reality, adding the wash water on top of the column may result in a drop in froth layer height. Then again, the holdup set-point is changed from 4% - 5% at 0.17 minutes. In Figure 7.36 (a), the set-point of the air hold is decreased from 5% - 4%, which means the air applied is reduced at 1.08 minutes the set-point changes from 5% - 4%

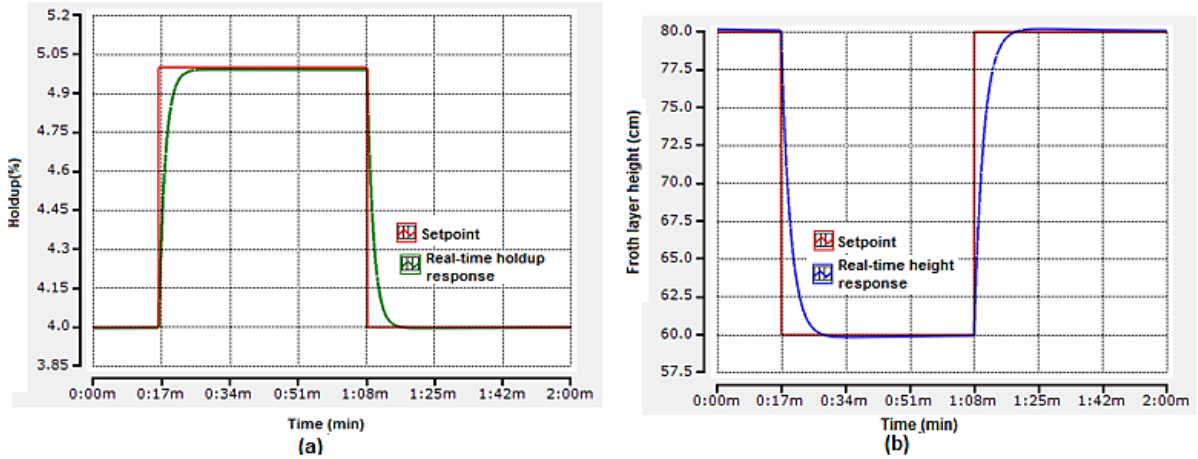

Figure 7.36: Case 4: Real-time results of the Froth Layer Height and Air Holdup processes

As it can be noted above both loops are not poorly influenced by the set-point changes applied in the holdup loop and froth layer height at the same times. In Figures 7.33-7.36 the real-time behaviour of the dynamic decoupled flotation system is presented, and the real-time characteristics of the results are presented in Table 7.4 as follows:

Table 7.4: Real-time characteristics of the decentralized decoupled system

Case study	Froth layer height performance indices				Air-holdup performance indices			
	Loop	Rise time (s)	Settling time (s)	Peak overshoot M_P (%)	Loop	Rise time (s)	Settling time (s)	Peak overshoot M_P (%)
1	Height	5.1	20.4	0.01	Holdup	2.55	15.3	0
2	Height	5.1	20.4	0.01	Holdup	2.55	69.9	0
3	Height	5.1	75	0.01	Holdup	2.55	15.3	0
4	Height	5	73.8	0	Holdup	2.55	69.9	0

The real-time characteristics and the analysis conducted using Beckhoff PLC as hardware integrated with industrial PC shows that the closed-loop system of the decoupled flotation system follows all the set-point variations in real-time with no overshoot. The effects of instabilities are investigated for the froth layer height control loop and air holdup loop in real-time using the developed dynamic decoupled process.

7.5.2.2 Validation of the developed dynamic decoupled process performance in a runtime mode

The procedure adopted is the same as that for the froth height and air holdup control loops in Chapter 6. The difference this time is that the research is carried out using real-time software and technology. At the output, the disturbances are forced into the primary froth height and air holdup control loops respectively. Figure 7.33 shows the TwinCAT functional block diagram with a disturbance at the outputs.

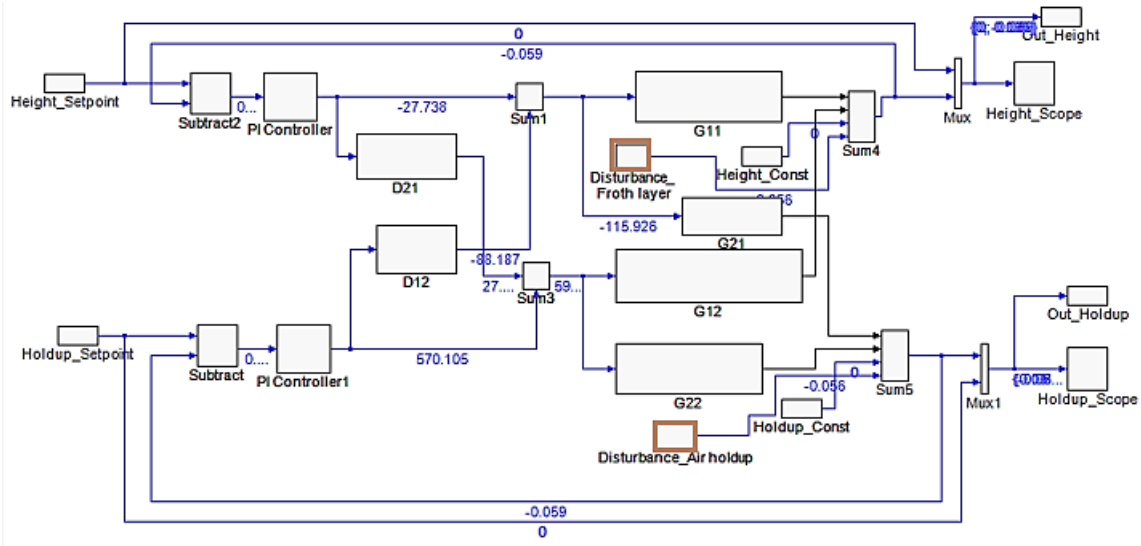

Figure 7.37: **Dynamic decoupled Closed-loop TwinCAT 3 function blocks under disturbance**

The following subsections aim to validate the performance of the designed controllers. It is well known that any given system needs to be controlled such that it keeps stability and set-point tracking even if the system experience unfocussed conditions.
To evaluate the influence of the disturbance, different amounts of the disturbance are applied. The magnitude of the disturbance applied in the system, or each loop is increased from $9e^{-5}$ (Figure 7.38), changed to $5e^{-4}$ (Figure 7.39), and $1e^{-3}$, as seen in Figure 7.36 the set-point tracking, is still successful.

***Case study 1:* Froth Layer Height**

The behavior of the designed dynamic control system is evaluated based on different disturbance variables. In this case, the random noise magnitudes are added to the froth layer height loop as a disturbance to the system. The first amount of disturbance applied is $9e^{-5}$ at the froth layer height, and the results are shown in Figure 7.38. Considering the obtained results, it is confirmed that the designed decentralized controller succeeded in keeping decent set-point tracking control under disturbance in a real-time environment. However, in this case, the presence of the disturbance is noticed through little noise within the actuary response.

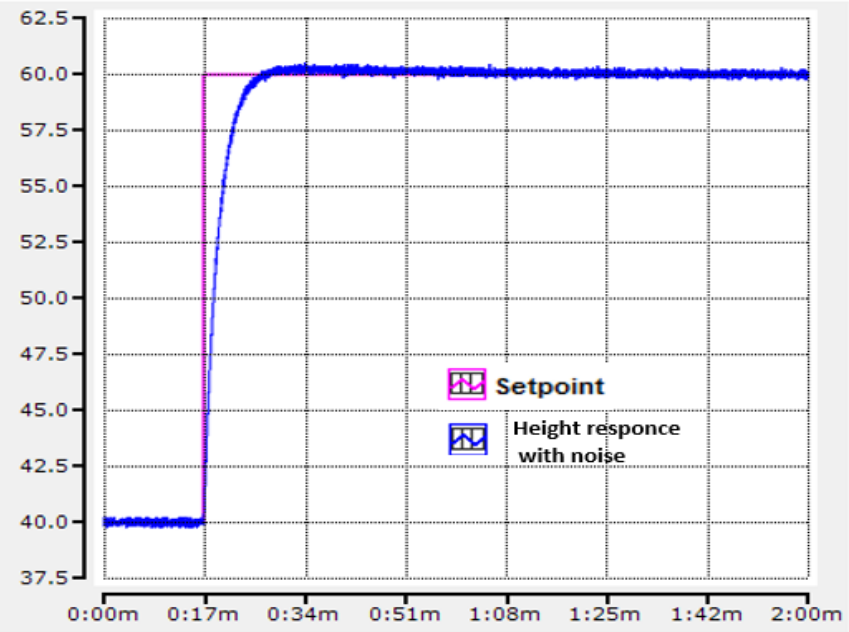

Figure 7.38: Closed-loop real-time response of the Froth Layer Height and Holdup Under noise disturbances of $9e^{-5}$ magnitude applied in loop 1

***Case study 2 F*roth Layer Height**

In case 2 the applied amount of disturbance is increased to $1e^{-3}$=0.001, this is done to evaluate the effect of noise magnitude in a runtime environment. As can be realized from the response in Figure 7.39, strong tracking control is still possible. The system's reaction becomes noisier as the amount of the disturbance grows larger. This is extremely similar to what was discovered in Chapter 5.

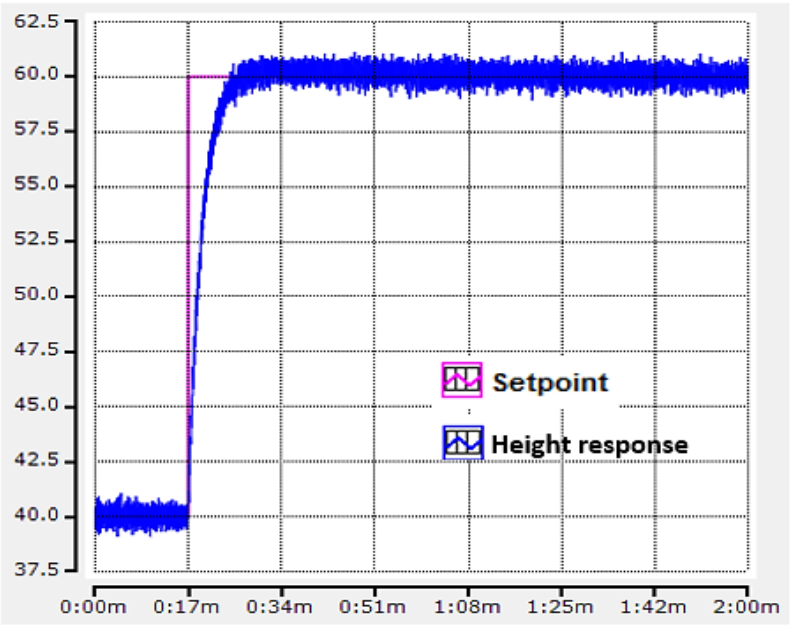

Figure 7.39: Closed-loop response of the Froth Layer Height and Air Holdup under disturbances $1e^{-3}$ noise magnitude

Case study 3 Air holdup

A step signal with a set point of 10%-18% is selected for further investigation. In case study 3 the magnitude of the applied disturbance is 0.00009 or $9e^{-5}$, this noise is applied in the air holdup loop of Figure 7.37. The results are shown in Figure 7.40 below. Seeing the obtained results, it is confirmed that the designed decentralized controller has been successful in keeping the selected set-point tracking control under disturbance in a real-time environment. However, the presence of disturbance indicated by the noise appears on the output response of the air holdup.

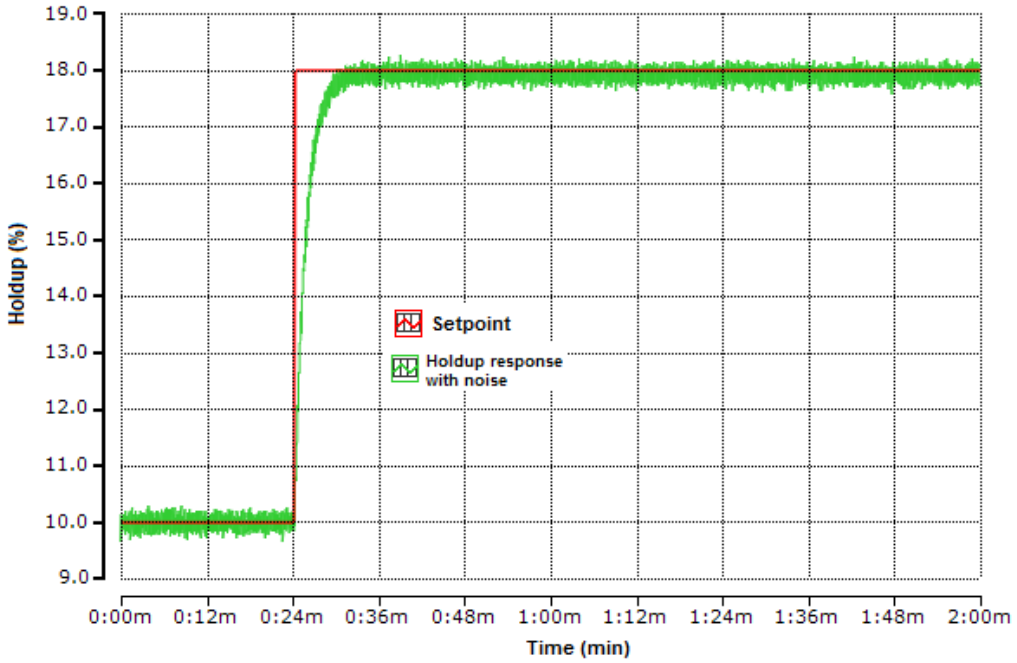

Figure 7.40: **Closed-loop real-time response of the Holdup Under noise disturbances of $9e^{-5}$ magnitude applied in loop 1**

Case study 4 Air holdup

In this case 2, the aim is to evaluate how capable the designed controller is, in tracking the set-point when the applied amount of disturbance is increased to $1e^{-3}$. This online experiment is important to be performed because the column flotation column is highly exposed to such industrial disturbance. As seen from the response in Figure 7.41, the closed-loop system's reaction still achieved a decent set-point tracking control.

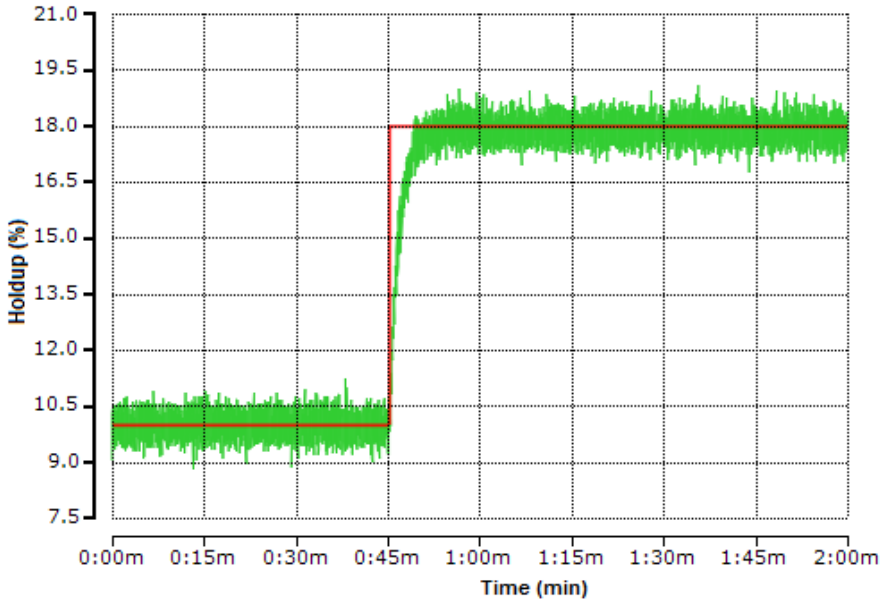

Figure 7.41: **Closed-loop response of the Froth Layer Height and Holdup Under noise disturbances of 1e^{-3} magnitude applied in loop 1**

The results indicate that the effects of the disturbance applied do not quite affect set-point tracking. The characteristics of the system transition behavior under the applied disturbances are observed for each case. Good tracking control is still accomplished, as evidenced by the results. The reaction becomes noisier as the amount of the disturbance grows larger. This relates to the findings reported in Chapter 6. In some cases, the system controlled can be bigger or more complex than the 2x2 model, but the principle or the process for real-time implementation using the Beckhoff PLC is the same. The next section is based on the comparisons of the run-mode results as per the implementation results conducted.

7.5.2.3 Summary of the case studies

The algorithms of the control design techniques that are developed and simulated in Chapters 5 and 6 are implemented using the Beckhoff CX5020 PLC to verify the industrial suitability of the controller design, model transformation, and real-time execution. The effectiveness of set-point tracking control and disturbance rejection is evaluated using the procedures necessary for the model transition from Matlab/Simulink to TwinCAT 3 functional blocks. The TwinCAT 3 functional blocks model is used to accomplish the desired variables in run-time, and then the data is downloaded to the Beckhoff CX5020 PLC for real-time execution. Based on the examined scenarios of decentralized-coupled and decentralized dynamic decoupled control, good set-point tracking control is realized for the MIMO closed-loop Column Flotation process.

The responses of the closed-loop decentralized coupled flotation algorithm for set-point tracking of the froth layer height and air holdup loops are recorded. Through these results it is noted that the algorithm based on a decentralized-coupled system has limitations in terms of variations that can be applied, random variation resulted in several overshoots. Hence, the dynamic decoupling of the flotation was introduced and implemented. Runtime implementation results of the closed-loop decentralized dynamic decoupled system as presented in section 7.5.2 have accomplished all set-point tracking with no limitations in terms of variations. In runtime mode, set-point tracking under the influence of disturbances for the studied situations was also tested. The online or real-time results demonstrate that for smooth set-point tracking, the amount of disturbance is critical. The decentralized decoupled control system, on the other hand, can nevertheless follow set-point variations without overshooting. The following Table 7.5 is based on the comparisons of the results simulated in Matlab/Simulink and the real-time implementation results from the TwinCAT 3 environment.

Table 7.5: Comparison characteristics of the decentralized decoupled Froth layer height and Air holdup performance

Case studies	Loops	Performance indices of closed-loop decentralized dynamic decoupled for Column Flotation Process					
		Matlab/Simulink			TwinCAT PLC real-time		
		Rise time (s)	Settling time (s)	Peak overshoot M_P (%)	Rise time (s)	Settling time (s)	Peak overshoot M_P (%)
Case study 1	Height	4.91	18.05	0.22	5.1	20.4	0.01
	Air	3.47	16.078	0.05	2.55	15.3	0
Case study 2	Height	4.908	18.05	0.22	5.1	20.4	0.01
	Air	0.59	66.17	0.05%	2.55	69.9	0
Case study 3	Height	1.25	68.75	0.22	5.1	75	0.01
	Air	3.47	16.078	0.053%	2.55	15.3	0
Case study 4	Height	0.489	68.54	0.17	5.1	73.8	0.01
	Air	0.51	66.25	0.01%	2.5	69.9	0

Table 7.5 presents the characteristic index of Matlab/Simulation results vs with PLC runtime results. As can be seen from the responses presented from 7.38 up to Figure 7.41, good tracking control is still achieved. This relates well with the findings reported in Chapter 4 about the normal behavior or functionality of the column flotation systems. However, the findings and all the achievements in this chapter can add valuable contributions if they can be industrially implemented.

This indicates that the decentralized decoupled systems are a good option for the rejection of the random variations that might occur in the control signal when the column flotation system is implemented in runtime mode. These results also agree with results obtained from the Simulink environment. This implies that industrial usage of this method can be highly recommended.

7.6 Discussion

The control algorithms developed in chapters 5 and 6 using different control design methodologies are used for real-time implementation in this chapter. This is done to verify whether the designed controllers can be effective when they are used in a hardware environment or real-world scenarios. The TwinCAT module is successfully created within the TwinCAT environment based on the processes required for model transformation between Matlab/Simulink and TwinCAT 3 functional blocks. This was completed after the code generation was achieved as discussed in section 7.3. The build TwinCAT project data is subsequently transferred to the Beckhoff CX5020 PLC for real-time processing. TwinCAT measurement project as discussed under section 7.4, is built and used to display the real-time results executed within the PLC.

To evaluate the operation and reliability of the designed controllers, the set-point tracking control and the effects of the disturbance rejection are evaluated via a real-time environment as presented in section 7.5.1. For the situations investigated, good set-point tracking control is accomplished for the MIMO closed-loop flotation process of the decentralized-coupled control and decentralized dynamic decoupling control approach as presented in section 7.5.1. Also, the effects of disturbances are explored, and the system's performance with numerous disturbances placed on the considered scenario achieved good performance.

The setpoint for real-time control for the particular loop is not realized smoothly in the case of the decentralized closed-loop coupled control. As a result, more research into the control design for specific loops is required, hence the calculated set-point adjustments are prepared and used in this thesis. But it is expected to have any random

setpoint, hence it is necessary when designing a controller to use a technique suitable to handle any abnormal situation. Therefore, the development of the decentralized dynamic decoupled control scheme is introduced and implemented in section 7.5.2. Even when the real-time implementation is conducted, designed decentralized dynamic decouple controllers have proven to be an effective algorithm to be used for the flotation process, regardless of the set-point variations or disturbances applied in a system. The results of real-time implementation in both control techniques show that the output signal can follow the input signal and achieve stable results.

7.7 Conclusion

In this chapter, the general introduction of Programmable Logic Controllers (PLC), and the model transformation technique to achieve real-time implementation of the flotation process system are discussed. The technique used in this study is selected because it suits real-life industrial needs. The model transformation procedure has proven capabilities of integrating Matlab/Simulink control function blocks into TwinCAT 3.1 function blocks for real-time implementation based on the inquiry done between Simulink and TwinCAT 3 software platforms. Because of the significant capabilities that such integration provides, the current software and software components can be reused.

Beckhoff CX5020 PLC together with TwinCAT 3 software was used for the implementation of the decentralized coupled and decentralized dynamic decoupled model-based controllers. The technique used and implemented using Beckhoff PLC CX5020 in this chapter can be adopted and implemented in an industrial environment, because it allows easy model transformation from a well-known and used software of Matlab/Simulink. Set-point tracking control and disturbance rejection were evaluated for effectiveness. The TwinCAT 3 functional blocks module is used to achieve the desired variables in run-time, after which it is downloaded to the Beckhoff CX5020 PLC for real-time execution. It is possible to establish good set-point tracking control for this Multi-Input Multi-Output (MIMO) closed-loop Column Flotation process based on the considered cases of the decentralized-coupled and decentralized dynamic decoupled control.

Through these results it is noted that the algorithm based on a decentralized-coupled system has limitations in terms of variations that can be applied, random variation resulted in several overshoots. Hence, the dynamic decoupling of the flotation was introduced and implemented. Runtime implementation results of the closed-loop

decentralized dynamic decoupled system as presented in section 7.5.2 have accomplished all set-point tracking with no limitations in terms of variations. For the circumstances under consideration, the effectiveness of set-point tracking control and set-point tracking under the influence of disturbances was also evaluated in runtime mode. The online results demonstrate that the size of the disturbance affects the amount of noise and smooth set-point tracking. Though, the decentralized dynamic decoupled control system is still capable of tracking the set-point variations with no overshoot. If one needs to extend the system to implement a 3x3 or 4x4 model, the same algorithm/principle as presented in this Chapter 7 must be used.

The selection of Beckhoff PLC CX5020 as an implementation environment is motivated by the reliability of this platform and Beckhoff CX5020 is built according to new industry standards. Allowing transformation makes it more advantageous to use than any other Programmable Logic Controller. The next chapter presents, a review of the deliverables of the thesis, and the future directions of research are outlined.

CHAPTER EIGHT:
CONCLUSION, DELIVERABLES, AND RECOMMENDATION

8.1 Introduction

This chapter provides a summary of the thesis deliverables, established approaches, areas applicable to the thesis deliverables, future work that could be done to improve the thesis, and current publications based on the studies. The focus of the study is on flotation process control design methodologies. Because of the complexities, loop interaction, and potentially unstable dynamics, a careful design technique is essential to control such a process. Pure linear control methods alone may not be adequate in these systems. The Matlab/Simulink environment is utilized to evaluate and test the efficiency of the developed models and methodologies in understanding and assessing the thesis objectives' possibilities. Comparative performance assessments, such as reconfigurability and decentralization assessment, are carried out utilizing the two platforms (Matlab/Simulink and TwinCAT 3.1).

Using the Beckhoff PLC TwinCAT 3.1 run-time (Beckhoff Automation) environment, the thesis discusses the developed methods for the design and implementation of the closed-loop system. Also, different controller design approaches are investigated followed by the selection of decentralization and dynamic decoupled controller design techniques. The thesis contributions are designed to give a foundation for understanding the principles of the TwinCAT 3.1 software environment, runtime Programmable Logic Control (PLC) implementation, and its application to industrial distributed control systems. The combination of the Beckhoff PLC and TwinCAT 3.1 has opened more possibilities for the industry to implement beneficial academic findings, through the integration of Simulink and TwinCAT 3.1 software.

The suitability of closed-loop control systems following functional block programming concepts is demonstrated through simulations. The model transformation between the two environments (Matlab/Simulink and TwinCAT 3.1) was created in this thesis based on modeling, data analysis, and runtime implementation that can be useful for more research investigations and implementation of industrial engineering projects. The ability to combine the Matlab/Simulink control function blocks into the TwinCAT 3.1 function blocks for real-life industrial implementation has been demonstrated by the real-time implementation outcomes of the closed-loop process for all the investigated situations.

The structure of this chapter reviews all the findings, results achieved, and thesis deliverables. The deliverables of the thesis are covered in section 8.2. The possible

academic, research, and industrial applications of the thesis's deliverables are described in section 8.3. Section 8.4 delivers possible future research work and possible solutions in the field of industrial control, automation, and implementation. Section 8.5 gives reference to the papers that are published and submitted to journals.

8.2 Thesis Deliverables

The need for controlling and monitoring the Column flotation process has been emphasized in this thesis. Chapter one has indicated the usefulness of this process, and the fact that it is widely used in the concentration of low-grade ores. It is indicated that the concentrate is the last product of a complex circuit, and hence control performance of the flotation system has a direct impact on the plant behaviour. Therefore, the project's deliverables are based on the aim and objectives as outlined in Chapter one.

8.2.1 Literature review

The literature review is covered in Chapter two. The review covers the general introduction and the history of the column flotation system with relevant problems. Under the review of the flotation process, different control approaches with different control variables were investigated. Review of existing literature based on process control theory, flotation system modeling, model-based control methods, and identification of the key variables that need to be manipulated and controlled. Different control strategies such as Model Predictive Control, Neural network-based controller design, different geometric concepts, linear and nonlinear Proportional-Integral-Derivative, and different multivariable control concepts existing in the literature are discussed in Chapter two. From the literature, various flotation models have been developed based on the processes and sub-processes occurring in flotation. An overview of the literature indicates that various approaches have been adopted for the extraction and measurement of valuable minerals within the flotation system. The need for minimization or elimination of the existing interactions, optimization of the process, and automation of this system is noticed. Therefore, the literature review Chapter is constructed in this thesis with a focus put on different angles of mineral processes.

8.2.2 The Theoretical Features of Flotation and System Modeling

The steady-state and dynamic performance or features of the column flotation process model are analysed to develop a clear knowledge of the system's steady-state and dynamic behavior for various changes in the input circumstances, as discussed in

Chapter 3 and Chapter 4. Chapter 3 mainly focuses on the Flotation schemes in the mining industry, wastewater treatments, paper recycling, and different mathematical models of the column flotation systems.

Using the online digital library, books, and other sources, the modeling of flotation has been reviewed to identify significance, usefulness, as well as limitations within this field of study as presented in Chapter 4. Through various investigations and experimentation, It has been noticed that the best pairing of controlled and manipulated variables is a deciding factor in grade prediction and control performance in the Column Flotation process.

8.2.3 Decentralization of the Model, Controller design, and simulation of the closed-loop system on Matlab/Simulink

Models and simulations of different cases were conducted for normal operation, and when the system undergoes challenges in terms of flow stability was investigated by increasing and decreasing the flow rates. The decentralization Controller design technique used lowers the impact of interactions between processes, through Relative Gain Array (RGA). The adopted design procedure is using Internal Model Controller-based (IMC) Proportional-Integral-Derivative (PID) feedback control for set-point tracking and disturbance rejection. The capabilities of the decentralized controller are accomplished for the system under study. The basic principle of this method is discussed first, followed by the details of the design procedure described in Chapter 5. Because it follows the principles of functional block programming and the model transformation method, MATLAB/Simulink is utilized as a simulation environment to test the closed-loop system under the designed controllers. Simulation results of the closed-loop column flotation processes based on 2x2 and 3x3 Multi-Input and Multi-Output (MIMO) models are presented in this report.

8.2.4 Modeling and simulation of the dynamic decoupled system on Simulink

Investigations and developments of the decoupled multivariable models of the column flotation process are conducted in this thesis. Modeling of the column flotation process and design of the controllers for the decoupled flotation system are described in Chapter 6 of this report. Different case studies based on the closed-loop dynamic decoupled system are outlined in Chapter 6. Simulations of the 2x2 and 3x3 models of the column flotation are performed using Matlab/Simulink environment with different set-point tracking control and disturbance, as presented in Chapter 6. This Chapter aims at improving the flotation system behaviour, through reduction of the process interactions and the design of convenient controllers. Through controller design and

decoupling of the flotation process, a controllable closed-loop system where the changes on one loop do not affect or change the state of the other loop is achieved. The decentralized dynamic decoupled technique worked in achieving the objective of this research and can be recommended for many complex industrial processes because it is capable of decreasing interaction within the process. The major objective of this thesis was to find ways of implementing the closed-loop column flotation process with the designed controllers. Through literature review, it has been found that the real-time implementation of these processes such as flotation control is required, hence Chapter 7 was done.

8.2.5 Runtime Implementation

This thesis develops an algorithm that specifies the processes of the software transformation from the Matlab/Simulink platform to the TwinCAT 3 runtime environment. This development can be utilized as a starting point for subsequent research. The findings of the runtime simulation and the results produced using the Beckhoff PLC have demonstrated the appropriateness and possibility of integrating Matlab/Simulink work into the TwinCAT 3.1 platform. The benefits of such integration mean that software component interchange and portability are conceivable. This is proven in this thesis by implementing the multiple-input and multiple-output (MIMO) flotation process.

The generated software model from Matlab/Simulink environment to TwinCAT 3 simulation environment is utilized to perform the real-time execution of the closed-loop flotation process with different control conditions to demonstrate the effectiveness of the transformation. Software integration of Simulink and TwinCAT 3 gives possibilities of implementing linear or nonlinear controllers with MIMO processes in a runtime mode of operation. The application of PC and PLC technologies produces better runtime results in comparison with the manual or classical control methods as presented in this thesis. These results are used to motivate industrial use of the developed algorithm, other than classical control methods only. The good thing about model transformation applied in this thesis, it automatically translates each state flow block into customized basic function blocks with the inputs, outputs, and parameters as their Simulink counterparts. This technique can also be advantageous to be used for the industrial implementation of different processes. Further, clarification of this implementation is discussed in Chapter 7.

8.3 Academic/Research and Industrial Application

The algorithms resulting from this thesis may be used for:

- Engineering project implementation in industry, and additional research investigations.
- As a step-by-step guide or algorithm for transforming produced software from Matlab/Simulink to the TwinCAT 3.1 simulation environment,
- Real-life industrial implementation can be used in the automation industry,
- Educational purposes and training institutions in the fields of engineering and run-time automation.

The massive importance of the column flotation process to the economy of the whole industrial world can be informally expressed through further research.

8.4 Future work

The future work will concentrate on the following research directions:

- Development of new logic algorithms and controller design based on an industrial process such as a flotation process to use or design adaptive controllers towards harshness of real-world conditions.
- Develop algorithms and controllers for hardware in loop implementation schemes for the cases when controller hardware (PLC) and hardware plant communication (Compact-RIO) are used for the implementation.
- Implementation of the developed schemes in runtime, real-life environments, on pilot plants, from the mineral or mining industry.

8.5 Publication

N. Tshemese-Mvandaba, R. Tzoneva, and M. E. S. Mnguni. "Decentralised PI controller design based on dynamic interaction decoupling in the closed-loop behaviour of a flotation process", International Journal of Electrical and Computer Engineering (IJECE), December 2021

N. Tshemese-Mvandaba, and M. E. S. Mnguni. “Design and implementation of decentralized PI controller based on dynamic decoupling flotation process using Beckhoff PLC TwinCAT 3.1 environment”, International Journal of Electrical and Computer Engineering (IJECE), (Accepted)

N. Tshemese-Mvandaba, and M. E. S. Mnguni. “Modelling and controller design based on decentralised coupled flotation process”, Submitted to IEEE Access, November 2022

N. Tshemese-Mvandaba, and M. E. S. Mnguni. “Model transformation and real-time implementation of a decentralised coupled process”, International Journal of Modelling and Simulation, (A manuscript submitted for review)

BIBLIOGRAPHY/REFERENCES

Abankwa, N.O., Bowker, J., Johnston, S.J., Scott, M. & Cox, S.J. 2018. Estimating the Longitudinal Center of Flotation of a Vessel in Waves Using Acceleration Measurements. *IEEE Sensors Journal*, 18(20): 8426–8435.

Astrom, K.J. & Hagglund, T. 1995. *PID Controllers : Theory, Design, and Tuning*.

Bahadori, A., Zahedi, G., Zendehboudi, S. & Bahadori, M. 2013. Estimation of air concentration in dissolved air flotation (DAF) systems using a simple predictive tool. *Chemical Engineering Research and Design*, 91(1): 184–190.

Behin, J. & Bahrami, S. 2012. Modeling an industrial dissolved air flotation tank used for separating oil from wastewater. *Chemical Engineering and Processing: Process Intensification*, 59: 1–8.

Bergh, L.. & Yianatos, J.. 1993. Control Alternatives for Floatation Columns. , 6(6): 631–642.

Bergh, L.., Yianatos, J.. & Leiva, C.. 1998. Fuzzy Supervisory Control of Floatation Columns. , 103(8): 1679–1689.

Bergh, L.G. & León R, A. 2005. Simulation of monitoring and diagnosis of flotation columns operation using projection techniques. *Proceedings of the 44th IEEE Conference on Decision and Control, and the European Control Conference, CDC-ECC '05*, 2005: 7680–7685.

Bergh, L.G. & Yianatos, J.B. 2003. Flotation column automation: State of the art. *Control Engineering Practice*, 11(1): 67–72.

Blahous, L. & Marx, T. 2009. Control of Flotation and Acquisition of the Key Control Variables. *IFAC Proceedings Volumes*, 42(23): 73–78.

Bouchard, J., Desbiens, A., del Villar, R. & Nunez, E. 2009. Column flotation simulation and control: An overview. *Minerals Engineering*, 22(6): 519–529. http://dx.doi.org/10.1016/j.mineng.2009.02.004.

Bristol, E.H. 1966. On a new measure of interaction for multivariable process control. *IEEE Transactions on Automatic Control*, 11(1): 133–134.

Calisaya, D., Poulin, E., Desbiens, A., Del Villar, R. & Riquelme, A. 2012. Multivariable predictive control of a pilot flotation column. *Proceedings of the American Control Conference*: 4022–4027.

Carvalho, M.T. & Durão, F. 2002. Control of a flotation column using fuzzy logic inference. *Fuzzy Sets and Systems*, 125(1): 121–133.

Castro, C., Vargas, H., Farias, G., Fabregas, E., Aracena, A. & Morales, J. 2018. Modeling and multivariable analysis of a flotation column system. *IEEE ICA-ACCA 2018 - IEEE International Conference on Automation/23rd Congress of the Chilean Association of*

Automatic Control: Towards an Industry 4.0 - Proceedings: 1–7.

Chen, D. & Seborg, D.E. 2002. Relative Gain Array Analysis for Uncertain Process Models. *AIChE Journal*, 48(2): 302–310.

Engineering, M. 1992. Keywords. , 5(6): 685–693.

Finch, J.A. & Dobby, G.S. 1990. Column flotation. : 1–12.

Guang, H., Jie, L. & Peng, C. 2015. Decoupling control design for the module suspension control system in maglev train. *Mathematical Problems in Engineering*, 2015.

Hernandez-Alcantara, D., Amezquita-Brooks, L. & Morales-Menendez, R. 2017. Decentralized Controllers for the Steering and Velocity in Vehicles. *IFAC-PapersOnLine*, 50(1): 3708–3713. https://doi.org/10.1016/j.ifacol.2017.08.566.

Horn, Z.C., Auret, L., McCoy, J.T., Aldrich, C. & Herbst, B.M. 2017. Performance of Convolutional Neural Networks for Feature Extraction in Froth Flotation Sensing. *IFAC-PapersOnLine*, 50(2): 13–18.

Jain, A. & Babu, B. V. 2016. Sensitivity of relative gain array for processes with uncertain gains and residence times. *IFAC-PapersOnLine*, 49(1): 486–491. http://dx.doi.org/10.1016/j.ifacol.2016.03.101.

Li, Z., Huang, M., Gui, W., Hua, Y. & Zhu, J. 2019. Optimal Reagents Control for Flotation Processes: An Adaptive Dynamic Programming Approach. *Proceedings - 2019 Chinese Automation Congress, CAC 2019*: 73–78.

Liuyuan, LiZheKum, Fujunyu & WangFeng. 2011. The Study of Detecting and Controlling System of Mineral Pulp Level. In *Proceedings of the 2011 IEEE International Conference on Cyber Technology in Automation, Control, and Intelligent Systems*. 195–200.

Lundh, M., Gaulocher, S., Pettersson, J., Lindvall, H. & Gallestey, E. 2017. MODEL PREDICTIVE CONTROL FOR FLOTATION PLANTS. : 6.

Maldonado, M., Desbiens, A., Poulin, Del Villar, R. & Riquelme, A. 2010. Automatic control of bubble size in a laboratory flotation column. *International Journal of Mineral Processing*, 141(1): 27–33.

Maldonado, M., Desbiens, A. & del Villar, R. 2009. Potential use of model predictive control for optimizing the column flotation process. *International Journal of Mineral Processing*, 93(1): 26–33.

Mohanty, S. 2009. Artificial neural network based system identification and model predictive control of a flotation column. *Journal of Process Control*, 19(6): 991–999. http://dx.doi.org/10.1016/j.jprocont.2009.01.001.

MUGA, J.N. 2015. DESIGN AND IMPLEMENTATION OF IEC 61499 STANDARD-BASED

NONLINEAR CONTROLLERS USING FUNCTIONAL BLOCK PROGRAMMING IN By JULIUS N ' GON ' GA MUGA Thesis submitted in partial fulfilment of the requirements for the degree Doctor of Technology : Electrical Engin. , (December).

Nadda, S. & Swarup, A. 2018. Decoupled control design for robust performance of quadrotor. *International Journal of Dynamics and Control*, 6(3): 1367–1375. https://doi.org/10.1007/s40435-017-0380-0.

Nakhaei, F., Sam, A., Mosavi, M.R. & Zeidabadi, S. 2010. Prediction of copper grade at flotation column concentrate using Artificial Neural Network. *International Conference on Signal Processing Proceedings, ICSP*: 1421–1424.

Nalan-Ahmadabad, S. & Ghaemi, S. 2017. The Design of Pole Placement With Integral Controllers for Gryphon Robot Using Three Evolutionary Algorithms. *International Journal of Materials, Mechanics and Manufacturing*, 5(2): 127–131.

Núñez, F., Tapia, L. & Cipriano, A. 2010. Hierarchical hybrid fuzzy strategy for column flotation control. *Minerals Engineering*, 23(2): 117–124.

Ogunnaike, B. & Ray, H. 1994. *Process Dynamics, Modeling, and Control*.

Persechini, M.A.., Jota, F.. & Peres, A.E.. 2000. Dynamic Model of a Floatation Column. *Science*, 13(14): 1465–1481.

Persechini, M.A.M., Peres, A.E.C. & Jota, F.G. 2004. Control strategy for a column flotation process. *Control Engineering Practice*, 12(8): 963–976.

Pujol, G., Rodellar, J., Rossell, J.. & Pozo, F. 2007. Decentralised Reliable Guaranteed Cost of Uncertain Systems: an LMI Design. *IFAC Proceedings Volumes (IFAC-PapersOnline)*, 16: 263–268.

Riquelme, A., Desbiens, A., Del Villar, R. & Maldonado, M. 2016. Predictive control of the bubble size distribution in a two-phase pilot flotation column. *Minerals Engineering*, 89: 71–76.

Ross, C.C., Smith, B.M. & Valentine, G.E. 2000. 2000 WEF and Purdue University Industrial Wastes Technical Conference. *Industrial Wastes*, (c): 1–24.

Sastri, S.R.. 1998. Column floatation: Theory and practice. *IMPC 2018 - 29th International Mineral Processing Congress*: 44–63.

Shean, B.J. & Cilliers, J.J. 2011. A review of froth flotation control. *International Journal of Mineral Processing*, 100(3–4): 57–71.

Shen, Y., Cai, W.J. & Li, S. 2010. Multivariable process control: Decentralized, decoupling, or sparse? *Industrial and Engineering Chemistry Research*, 49(2): 761–771.

Sobhy, A. & Tao, D. 2013. Nanobubble column flotation of fine coal particles and associated

fundamentals. *International Journal of Mineral Processing*, 124: 109–116. http://dx.doi.org/10.1016/j.minpro.2013.04.016.

Tang, Y., Peng, C., Yin, S., Qiu, J., Gao, H. & Kaynak, O. 2014. Robust model predictive control under saturations and packet dropouts with application to networked flotation processes. *IEEE Transactions on Automation Science and Engineering*, 11(4): 1056–1064.

Thulasi Dharan, S., Kavyarasan, K. & Bagyaveereswaran, V. 2017. Tuning of PID controller using optimization techniques for a MIMO process. *IOP Conference Series: Materials Science and Engineering*, 263(5): 0–17.

Tshemese-Mvandaba, N., Tzoneva, R. & Mnguni, M.E.S. 2021. Decentralised PI controller design based on dynamic interaction decoupling in the closed-loop behaviour of a flotation process. *International Journal of Electrical and Computer Engineering*, 11(6): 4865–4880.

Veselý, V. & Thuan, N.Q. 2011. Robust decentralized controller design for large scale systems. *Proceedings of the 2011 12th International Carpathian Control Conference, ICCC'2011*: 425–428.

Vhora, H. & Patel, J. 2016. Design of Static and Dynamic Decoupler for Coupled Quadruple Tank Level System. *Nirma University Journal of Engineering and Technology*, 5(2): 8–12.

Vhora, H., Patel, J., Systems, T., Thulasi Dharan, S., Kavyarasan, K., Bagyaveereswaran, V., Garrido, J., Morilla, F., Vazquez, F. & Edgar, T. 2017. Design of Static and Dynamic Decoupler for Coupled Quadruple Tank Level System. *2009 European Control Conference, ECC 2009*, 5(5): 4007–4012. https://pdfs.semanticscholar.org/6e20/a49dae324247c625fc014e1d572ee4c83477.pdf.

Vieira, S., Sousa, J.M.C. & Durão, F.O. 2007. Fuzzy predictive control of a column flotation process. *IFAC Proceedings Volumes (IFAC-PapersOnline)*, 38(1): 127–132.

Vieira, S.M., Sousa, J.M.C. & Durão, F.O. 2004. Combination of fuzzy identification algorithms applied to a column flotation process. *IEEE International Conference on Fuzzy Systems*, 1: 421–426.

Vieira, S.M., Sousa, J.M.C. & Durão, F.O. 2005. Fuzzy modelling strategies applied to a column flotation process. *Minerals Engineering*, 18(7): 725–729.

Weimeng, H. 2014. Flotation Circuit Optimisation and Design. , (September): 1–150.

Yahui, T., Maryam, A., Xiaoli, L., Fei, L. & Stevan, D. 2018. Three-Phases Dynamic Modelling of Column Flotation Process∗. *IFAC-PapersOnLine*, 51(21): 99–104. https://doi.org/10.1016/j.ifacol.2018.09.399.

Yang, C.H. & Vyatkin, V. 2012. Transformation of Simulink models to IEC 61499 Function Blocks for verification of distributed control systems. *Control Engineering Practice*, 20(12): 1259–1269. http://dx.doi.org/10.1016/j.conengprac.2012.06.008.

Yang, H. & Fan, M. 2012. The mathematical model for natural settling classification of flotation tailings. *Proceedings - 2012 International Conference on Computer Distributed Control and Intelligent Environmental Monitoring, CDCIEM 2012*: 754–758.

Yianatos, J.B., Bergh, L.G., Díaz, F. & Rodríguez, J. 2005. Mixing characteristics of industrial flotation equipment. *Chemical Engineering Science*, 60(8-9 SPEC. ISS.): 2273–2282.

Zoitl, A. & Lewis, R. 2014. *Modelling control systems using IEC 61499, 2nd edition*.

APPENDICES

The list of the appendices are as follows

- **APPENDIX A:** The order identifier for CX5000 devices
- **APPENDIX B:** Technical datasheet representation of the Beckhoff CX5020
- **APPENDIX C:** TwinCAT transport layer and TwinCAT Module
- **APPENDIX D:** Flexible use of programming languages

Appendix A: The order identifier for CX5000 devices

Beckhoff CX50x0 PLC is classified in different orders as presented in Appendix A

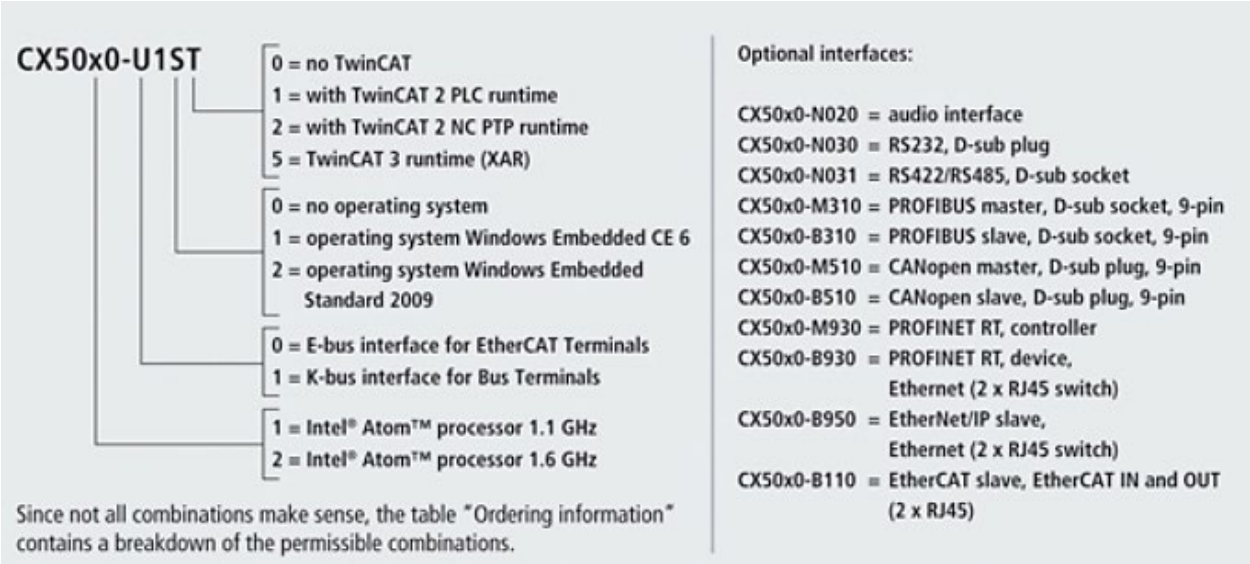

Appendix B: Technical datasheet representation of the Beckhoff CX5020

Technical data	CX5020
Processor	Intel® Atom™ Z530 processor, 1.6 GHz clock frequency
Internal Flash memory	128 MB Compact Flash card (optionally extendable)
Internal main memory	512 MB RAM (optionally 1 GB installed ex factory)
Interfaces	2 x RJ 45, 10/100/1000 Mbit/s, DVI-D, 4 x USB 2.0
Diagnostics LED	1 x power, 1 x TC status, 1 x flash access, 2 x bus status
Clock	Internal clock with battery backup for time and date (battery replaceable)
Operating system	Microsoft Windows CE or Microsoft Windows Embedded Standard
Control software	TwinCAT PLC runtime or TwinCAT NC PTP runtime
Power supply	24 V DC (-15 %/+20 %)
Current supply	I/O terminals 2 A
Max. power loss	12.5 W (including system interfaces)
Dielectric strength	500 Veff (supply/internal electronics)
Dimensions (H x W x D)	100 mm x 106 mm x 92 mm
Weight	approx. 575 g
Operating/storage temperature	-25 °C ... +60 °C / -40 °C ... +85 °C
Relative humidity	95 % no condensation
Vibration/shock resistant	conforms to EN 60068-2-6/EN 60068-2-27/ 29
EMC immunity/emission	conforms to EN 61000-6-2 / EN 61000-6-4
Protection class	IP 20

Appendix B presents all the important fixtures within CX5020. It gives an illustration of how CX5020 is used with TwinCAT 3.1 software from Beckhoff to offer the same functionalities as large industrial personal computers (PCs).

Appendix C: TwinCAT transport layer and TwinCAT Module

TwinCAT transport layer and TwinCAT Module are modules that have fixed object IDs and are accessible from each module.

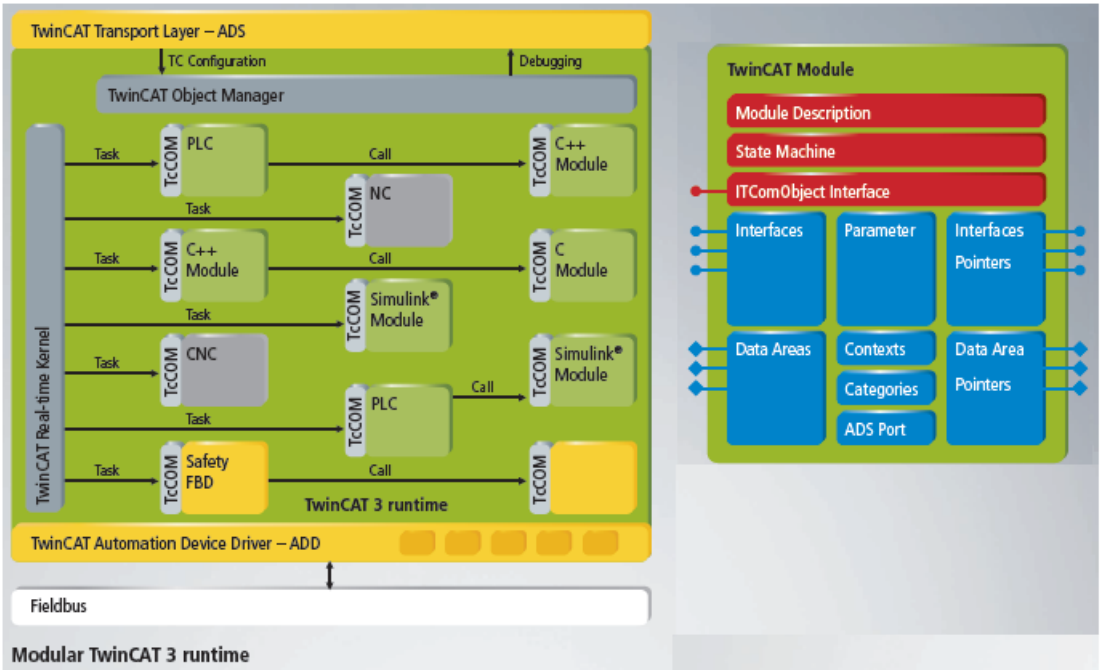

Figure C: TwinCAT Modular

Appendix D: Flexible use of programming languages

Appendix D display how each of the programming languages can be flexibly used to accomplish the eXtended Automation Engineering.

Table D: Flexible use of programming languages

Flexible use of programming languages	
C and C++ programming languages	**. NET programming languages**
▪ standardised ▪ widely used programming languages ▪ very powerful programming languages ▪ run under the same runtime as PLC programs ▪ for the implementation of drivers	▪ used for non-real-time-programming (e.g.: HMI) ▪ source code management in the same project
Extended debugging of C++ programs	**Link to Matlab/Simulink**
▪ debugging of C++ programs that run in real-time ▪ use of breakpoints ▪ use of watch lists ▪ use of call stacks	▪ great variety of toolboxes ▪ possibilities for use: ▪ building of control circuits ▪ in simulation ▪ in optimisation ▪ automatic code generation ▪ debug interface between Matlab®/Simulink® and TwinCAT